

Open Research Online

The Open University's repository of research publications and other research outputs

N and C isotropic composition of different varieties of terrestrial diamonds and carbonado

Thesis

How to cite:

Shelkov, Denis Alexander (1997). N and C isotropic composition of different varieties of terrestrial diamonds and carbonado. PhD thesis The Open University.

For guidance on citations see [FAQs](#).

© 1997 The Author



<https://creativecommons.org/licenses/by-nc-nd/4.0/>

Version: Version of Record

Link(s) to article on publisher's website:

<http://dx.doi.org/doi:10.21954/ou.ro.0000d550>

Copyright and Moral Rights for the articles on this site are retained by the individual authors and/or other copyright owners. For more information on Open Research Online's data [policy](#) on reuse of materials please consult the policies page.

oro.open.ac.uk



UNRESTRICTED

N and C isotopic composition of different varieties of terrestrial diamonds and carbonado.

by

Denis Alexander Shelkov

Graduated in Lomonosov Moscow State University 1993

A thesis submitted for the degree of Doctor of Philosophy.

July 1997

Planetary Science Research Institute

The Open University

Author no: M7164563
Date of submission: 10th July 1997
Date of award: 9th December 1997

To my wife Maria and my parents.

Acknowledgements.

First of all I would like to thank Prof. Colin Pillinger for his supervision, critical discussions and editing the manuscript; I appreciate in particular the freedom research I have had throughout the course of the research and the opportunity to attend a number of important international conferences. I would also like to express my special thanks to Dr Alexander Verchovsky and Dr Judith Milledge who have contributed a lot of their time to this work and Prof. Yu.A.Shukolukov for his recommendation to do this PhD project.

The results of the research were directly dependant on usage and ability of the experimental equipment and in this respect I am most grateful to the people who gave me my first lessons in mass-spectrometry in Moscow: Dr S.Yu.Sokolov and Dr Yu.A.Kostitsin, and also to Dr A.B.Verchovsky who taught me and developed my skills in the PSRI. Since the instrument mainly used for the research was built by Dr I.A.Franchi and initially used and calibrated by D.Brilliant I have often relied on their advice and expertise. The instrumental chapter in particular presents a result of collaborative work from a number of people: D.Brilliant (first stages of development of the instrument), G.Rooke (the latest stages) and Dr A.B.Verchovsky. I would also like to thank here technicians J.Gibson and M.Higgins for their help in using carbon mass-spectrometers. Without above mentioned people neither instrumental chapter, nor the research in general could be feasible.

In selecting and obtaining sample material a number of people have also been involved: Dr H.J.Milledge, Dr G.P.Bulanova, Dr F.V.Kaminsky, Dr W.R.Taylor, Dr G.B.Smelova, Dr S.R.Tal'nikova, Dr O.D.Zakharchenko and Dr V.I.Vaganov. I have also discussed the results with them and I am most grateful for their remarks and comments.

During writing and editing the manuscript many people have helped me, however, I would like express my special thanks to Dr H.J. Milledge and Dr S.Kelley.

I am also most grateful to the management of DeBeers Industrial Diamond Division Ltd for providing financial support for my research in the field of diamond geochemistry and also attendance at the Annual Diamond Conferences. In particular I would like to thank Dr R.J.Caveney for his interest in my study and my performance during the period of my research.

There are also many others who directly or indirectly have influenced on the completion of this thesis, but unfortunately I do not have enough space here to mention everyone. However, there are still a few whom I would like particularly to thank: my wife Masha who, I believe, put a lot of effort and patience into keeping me going all these years; my parents who always encouraged and supported me over these four years; students and staff of PSRI and Earth Science Department whom I have found most friendly and helpful in many different ways.

Probable impossibilities are to be preferred to improbable possibilities.

Aristotle

Abstract.

During the course of this research an instrument utilising combustion as a means of gas extraction capable of N, C, Ar and He analysis has been developed and the entire analytical procedure has been automated.

N and C isotopic analysis has been performed on eclogitic and peridotitic diamonds (mainly from Yakutian kimberlites and the Roberts Victor kimberlite pipe). Diamonds with unusual (light and heavy relative to the peak of $\delta^{13}\text{C}$ distribution of mantle diamonds) carbon isotopic signatures were considered for the research so that diamonds in the range of $\delta^{13}\text{C}$ from -30‰ to +2.8‰ were characterised for $\delta^{15}\text{N}$. The results together with data obtained previously by the others define fields for eclogitic and peridotitic diamonds on a plot of $\delta^{15}\text{N}$ vs. $\delta^{13}\text{C}$. The model of mantle nitrogen and carbon evolution is discussed.

A comprehensive comparison between carbonado and other known forms of microcrystalline diamond (framesites and shock diamonds) has been made for a number of parameters: N and C isotopic composition and N content; ^4He content; morphology of the inner structure of diamond aggregates. It can be concluded that carbonado is generally similar to framesites and all facts known about carbonado can be explained on the grounds of common mantle origin involving subducted carbon and nitrogen. Since extremely high ^4He concentrations are encountered in carbonado this parameter is considered to be the most singular feature of this diamond variety and the radial distribution of ^4He in single diamond crystals has been studied. A ^4He content comparable with that in carbonado was found in the 30 μm skin of diamond crystals (up to 1.4×10^{-2}) suggesting that carbonado could acquire high ^4He concentration in the same geological processes as single diamond crystals and making carbonado indistinguishable from mantle diamonds in terms of He content. An additional result of the investigation is that the maximum of ^4He diffusion coefficient for diamond at mantle P,T conditions can be

estimated ($\approx 4 \times 10^{-21}$) from the ^4He zoning identified in the interior of a diamond crystal from the Finsch kimberlite.

A number of diamonds of impact origin from Popigai crater and Ebeliak river placer deposits were studied for N, C and Ar isotopic compositions. It was concluded that diamonds from these two localities have resulted from separate impact events and that diamond aggregates studied are most probably consist of a mixture of different Ar and N carriers (e.g. two types of diamond grains).

Table of contents.

Chapter 1. Introduction.	1
1.1. General.	1
1.2. Short review on diamond properties.	3
1.3. Nitrogen impurity in diamonds.	6
1.4. Morphological varieties of diamond crystals (after Orlov, 1973 and Vladimirov et al., 1989).	8
<i>Single diamond crystals.</i>	8
<i>Polycrystalline aggregates of diamond.</i>	9
1.5. Diamonds in relation to kimberlites.	9
1.5.1. Kimberlites.	11
1.5.2. Xenoliths (after Dawson, 1980).	14
<i>A. The peridotite-pyroxenite suite.</i>	16
<i>B. The eclogite-grospydite suite</i>	17
1.5.3. Diamonds.	18
1.6. Polycrystalline varieties of diamonds (see also chapters).	19
1.6.1. Carbonado.	19
1.6.2. Yakutites (diamonds of shock origin).	22
1.6.3. Framesites.	23
1.7. Brief review of N and C isotopic geochemistry of the crust and the mantle.	23
1.7.1 C and N isotopic composition of crustal material.	24
<i>Carbon.</i>	24
<i>Nitrogen</i>	26
1.7.2. Carbon and nitrogen isotopic composition of the mantle.	30
1.7.2.1. Carbon and nitrogen isotopic compositions of basalts.	30
<i>Carbon.</i>	30
<i>Nitrogen.</i>	30
1.7.2.2. Isotopic composition of C and N in diamonds of mantle origin.	31
<i>Carbon.</i>	31
<i>Nitrogen.</i>	36
1.7.2.3. C and N isotopic geochemistry of the mantle.	37
1.8. The source material for the Earth's formation.	37
1.9. Aims of the study.	39
1.9.1 C and N of subcontinental mantle.	39
1.9.2 Carbonado and other polycrystalline forms of diamond.	40

1.9.3 Analytical technique development.	41
Chapter 2. High precision nitrogen stable isotope analysis combined with He, Ar and C isotope measurements performed in the automated mode.	43
<i>Abstract.</i>	43
2.1. Introduction.	44
2.1.1 Nitrogen isotopic analysis.	44
2.1.2. Overview of methods used for stable isotope analysis.	44
2.1.3. N isotopic studies and the advantages of combined analysis of isotopic ratios of N with that of other gases.	46
2.1.4. Aims of this work.	47
2. 2. General overview of the instrument.	47
2.2.1. The overview of the inlet system.	47
2.2.2. Pumping systems.	48
2.3. Loading system.	51
2.3.1 Overview.	51
2.3.2 Sample preparation.	52
2.3.3 Loading procedure.	52
2.4. Extraction system.	54
2.4.1. Overview.	54
<i>Simple combustion section.</i>	54
<i>Horizontal combustion section.</i>	55
<i>High temperature combustion section.</i>	55
<i>Combustion section used for combined N, C and noble gas analysis in diamonds.</i>	56
2.4.2 Gas extraction	57
2.5. Purification system.	57
<i>Stage 1.</i>	57
<i>Stage 2.</i>	58
<i>Stage 3.</i>	58
2.6. Isotopic measurement.	58
2.6.1. Isotopic analysis of the gases extracted from samples.	58
2.6.2. Quadrupole static mass spectrometer.	59
2.6.3. Nitrogen static mass spectrometer.	60
2.6.3.1. The ionisation source.	60
2.6.3.2. The collector assembly	60
2.7. Carbon abundance measurements	61
2.8. Reference gas aliquotting systems.	61

2.8.1 Nitrogen reference gas aliquotter.	61
2.8.2 Noble gas reference gas aliquotter.	62
2.9. Automation of the analysis.	63
2.9.1. Inlet system.	63
2.9.2 Control of temperature.	64
2.9.3. QMS control.	65
2.9.4. Nitrogen MS control.	65
2.9.5. Pressure and temperature monitoring.	66
2.10. Instrumental appraisal and calibration	66
2.10.1. Instrumental appraisal	66
2.10.1.1.Nitrogen.	66
2.10.1.2. "Mass 30" effect on nitrogen isotope measurements and correction of nitrogen isotopic composition.	68
2.10.1.3.Mass 30 correction.	69
2.10.1.4. He and Ar measurements.	71
2.10.2. Instrumental calibration	72
2.10.2.1. AIR standard.	72
2.10.2.2. Diamond standard.	73
2.10.2.3 Biotite standard.	75
2.10.2.4. Baratron calibration	76
2.11. Blank measurements.	76
2.12. Concluding remarks and further developments.	77
Chapter 3. Carbon and nitrogen isotopic composition of mantle diamonds and their implications for the Earth's evolution model.	79
<i>Abstract.</i>	79
3.1. Introduction.	80
3.1.1. $\delta^{13}\text{C}$ in diamonds.	80
3.1.2. $\delta^{15}\text{N}$ in diamonds.	81
3.1.3. Interpretations of $\delta^{13}\text{C}$ and $\delta^{15}\text{N}$ variations in diamonds.	82
3.1.4. Aims of the study.	83
3.2. Samples.	84
3.2.1. Diamonds with known paragenesis.	84
3.2.2. Diamonds with unusual $\delta^{13}\text{C}$ and $\delta^{15}\text{N}$ isotope signatures.	85
3.3. Experimental technique.	86
3.4. Results.	86
3.5. Discussion.	89
3.5.1. $\delta^{15}\text{N}$ and $\delta^{13}\text{C}$ in diamond of peridotitic and eclogitic paragenesis.	89
3.5.2. Eclogitic diamonds in relation to the carbon and nitrogen in the	

subducted slab.	96
<i>Subduction of carbon and nitrogen into the mantle.</i>	96
<i>Eclogitic diamonds.</i>	98
3.5.3. Peridotitic diamonds.	100
3.5.4. Fibrous diamonds.	101
3.5.5. Earth's origin as deduced from carbon and nitrogen isotope variations in diamonds.	102
3.6. Conclusions.	105
Chapter 4. The radial distribution of implanted and trapped ^4He in single diamond crystals and implications for the origin of carbonado.	107
<i>Abstract.</i>	107
4.1. Introduction.	108
4.2. Samples and experimental technique.	109
4.3. Results.	110
4.4. Discussion.	114
4.4.1. Bulk concentrations of implanted ^4He and the ^4He implantation profiles.	114
4.4.2. Implications of the results for the origin of carbonado.	116
4.4.3. Variations of ^4He content in the interior of the diamonds and He diffusion coefficient.	118
4.5. Conclusions.	119
Chapter 5. Carbonado origin: a comparison with other forms of microcrystalline diamond based on C, N, He data and inner morphology.	121
<i>Abstract.</i>	121
5.1. Introduction.	123
5.2. Samples.	125
5.3. Experimental technique	125
5.4. Results	127
4.4.1. N abundance and N and C isotopic composition	127
4.4.2. Morphology and inner structure of carbonado	130
4.4.3. IR study of carbonado	131
4.4.4. He abundances.	132
5.5. Discussion.	133
5.5.1. Carbonado and diamonds of impact origin	133
5.5.2. Relations to the diamonds derived by kimberlites	134
<i>Helium</i>	134

<i>Carbon and nitrogen isotopic composition</i>	136
5.6. Is carbonado an exceptional type of terrestrial diamonds?	137
5.7. Conclusions.	138
Chapter 6. C, N, Ar and He study of shock diamonds from Ebeliakh alluvial deposits and Popigai crater.	139
<i>Abstract.</i>	139
6.1. Introduction.	140
6.1.1. Properties of diamonds formed in the impact craters.	140
6.1.2. Formation of shock diamonds.	141
6.1.3. Noble gases in shock produced diamonds.	141
6.1.4. Aims of the study.	142
6.2. Samples.	142
6.3. Experimental technique.	143
6.4. Results	144
6.4.1. N, C, He and Ar in the bulk experiments.	144
6.4.2. N and Ar release patterns and correlations.	147
6.4.3. Ar components.	147
6.5. Discussion.	151
6.5.1. Two component mixture.	151
6.5.2. The model.	153
6.5.3. Sample Y7	154
6.6. Conclusions.	155
Chapter 7: Conclusions and further research.	157
7.1. Conclusions.	157
7.1.1. C and N systematics of terrestrial diamonds and their implications.	157
7.1.2. The origin of carbonado.	159
7.1.3. ⁴ He content in the single diamond crystals.	160
7.1.4. C, N, Ar and He in diamonds of shock origin.	160
7.1.5. Experimental technique.	161
7.2. Suggestions for further research.	162
7.2.1. C and N isotope study of diamonds.	162
7.2.2. Diamonds formed by an impact.	162
7.2.3. Applications of step combustion technique for the study of mantle diamonds.	163
Appendices.	165
Appendix 1: Accuracy of nitrogen and noble gas reference aliquotting system.	165
Appendix 2: Precision of the nitrogen isotopic analysis.	168

Appendix 3: Precision of the Ar isotopic analysis based on the measurements of different aliquots of reference gas.	172
Appendix 4: Calibration of the nitrogen mass spectrometer.	176
Appendix 5: Experimental reproducibility for N and C.	177
Appendix 6: Tables of sample descriptions for Chapter 3.	178
Appendix 7: Data tables for Chapter 3.	180
Appendix 8: Data table for Chapter 4.	182
Appendix 9: Calculation of U-Th content in diamond host rock.	184
Appendix 10: Calculation used to provide theoretical implantation profiles for sample F4.	185
Appendix 11: Data tables for Chapter 5.	189
Appendix 12: Data tables for Chapter 6.	191
Appendix 13: Statistical parameters of linear correlations used in Chapter 6.	193
References.	194

List of figures.

Figure 1.1 Carbon P-T phase diagram.	3
Figure 1.2 Infrared absorption spectra of type Ia diamonds.	6
Figure 1.3. Major original habits of diamond.	9
Figure 1.4. Generalised model of kimberlite diatreme and its sub-diatreme dykes (Dawson, 1980).	11
Figure 1.5. Initial $^{87}\text{Sr}/^{86}\text{Sr}(\text{a})$ and initial $^{207}\text{Pb}/^{204}\text{Pb}(\text{a})$ ratios plotted against initial $^{206}\text{Pb}/^{204}\text{Pb}$ for Group I and II kimberlites (Smith, 1983).	13
Figure 1.6. Group I and II kimberlites together with mid-oceanic ridge basalts, oceanic island basalts and diopsides from peridotite xenoliths.	14
Figure 1.7. Classification of ultramafic rocks according to International Geological Union.	15
Figure 1.8. Plot of $\delta^{13}\text{C}$ of reduced carbon in sedimentary rocks of Precambrian to Middle Cambrian versus the rank of organic.	24
Figure 1.9. Variations of $\delta^{15}\text{N}$ in coal as a function of the concentration of volatiles.	28
Figure 1.10. Carbon isotopic composition of yellow, pink-brownish, green, grey, black and colourless diamonds.	33
Figure 1.11. Carbon isotopic composition of different diamond varieties.	34
Figure 1.12 Coanjula fibrous microdiamonds.	35
Figure 1.13. Isotopic composition of diamonds of eclogitic and peridotitic suites.	35
Figure 1.14. $\delta^{17}\text{O}$ - $\delta^{18}\text{O}$ relationships among Earth-Moon and chondrites.	38

Figure 2.1. "Main" line schematic.	49
Figure 2.2. "Back" line schematic.	50
Figure 2.3 Loading section and horizontal combustion system.	53
Figure 2.4. Extraction sections used for experiments involving noble gases.	56
Figure 2.5. Configuration of the computer communications.	64
Figure 2.6. Variations of error in $\delta^{15}\text{N}$ against reference gas aliquot size.	68
Figure 2.7. Reference gas calibration line: 28/29 vs. 30/29.	69
Figure 2.8. Geometrical illustration of "mass" 30 correction.	71
Figure 2.9 and 2.10. Reproducibility of experiments in terms of N and C isotopic composition, based on measurements of laboratory standard diamond.	74
Figure 2.11. Ar calibration line	75
Figure 2.12. Calibration of capacitance manometer (Baratron) using diamond.	76
Figure 3.1. Results of experimental study of C and N in diamonds of different paragenesis and diamonds with C and N isotopic extremes.	88
Figure 3.2. The $\delta^{13}\text{C}$ - $\delta^{15}\text{N}$ plot for diamonds of different paragenesis and fibrous diamonds. We should note that N and C isotopic data obtained by Boyd, 1988 would be plotted within the fields determined.	90
Figure 3.3. N vs. $\delta^{15}\text{N}$ plot for octahedral diamonds having $\delta^{13}\text{C}$ in the range from -3‰ to -9‰ and fibrous diamonds.	93
Figure 3.4. Distribution histogram for $\delta^{15}\text{N}$ (A) and $\delta^{13}\text{C}$ (B) in octahedral diamonds.	94
Figure 3.5. Distribution histograms for $\delta^{15}\text{N}$ of: A — eclogitic diamonds with $\delta^{13}\text{C}$ of ca. -5‰; B — eclogitic diamonds with $\delta^{13}\text{C}$ lower than -10‰, including carbonado and framesites; peridotitic diamonds.	95
Figure 3.6. Schematic $\delta^{13}\text{C}$ vs. $\delta^{15}\text{N}$ diagram indicating different diamond fields and possible reservoirs which mixing can provide diamonds with variations of C and N isotopic composition.	97
Figure 3.7. Schematic $\delta^{13}\text{C}$ vs. $\delta^{15}\text{N}$ diagram showing different diamond fields along with CI, CM, EH and EL chondrites.	104
Figure 4.1. Complete ^4He content depth profiles for two diamond crystals.	111
Figure 4.2. Detailed ^4He content profiles for the samples F4, F1 and A1 corresponded to the skins of the samples only.	112
Figure 4.3. A comparison between theoretical and experimentally obtained ^4He implantation depth profiles.	115
Figure 4.4. ^4He concentrations of mantle diamonds, carbonado and different zones of diamond crystals of mantle origin.	117
Figure 5.1. N-C isotope plot for different types of polycrystalline diamonds.	127
Figure 5.2. Carbon isotopic composition of carbonado, framesites and shock	

produced diamonds.	128
Figure 5.3. Distribution of N content in carbonado.	129
Figure 5.4. Distribution of N content in framesites.	129
Figure 5.5. IR spectra of carbonado (CB20) crystallite indicating IaA aggregation state of N.	132
Figure 5.6. Distribution of ^4He concentrations in diamonds.	133
Figure 5.7. N and C isotope variations in diamonds.	136
Fig.6.1 C and N isotopic composition of shock diamonds.	145
Fig.6.2. Carbon isotopic composition of diamonds and graphites from impactites.	146
Fig.6.3. Step combustion experiment Y18(2).	148
Fig.6.4. $^{40}\text{Ar}/^{36}\text{Ar}$ - $1/^{36}\text{Ar}$ correlations based on results of step combustion experiments Y18(2) (solid line) and Y14 (dashed line).	149
Fig. 6.5. Comparison of N— ^{36}Ar correlations of samples from Ebeliak deposits with lonsdaleite and samples from Popigai crater.	150
Fig. 6.6. Comparison of Ar in shock diamonds from Popigai and Ebeliak with kimberlitic diamonds.	155

List of tables.

Table 1.1. Methods used to synthesise diamond at low pressures and low temperatures (from Bachman, 1994).	5
Table.1.2. Composition of inclusions in carbonado samples from different localities.	21
Table 1.3 Properties of shock diamonds suggesting two types of source material (Veshnevsky et al., 1995).	22
Table 1.4. Chemical composition of baddingtonite.	27
Table 1.5. Nitrogen isotopic composition of some components of the oceanic reservoir.	29
Table 1.6. Nitrogen isotopic composition of different crustal materials.	29
Table. 1.7. N isotope data that have been obtained from oceanic basalts and a harzburgite.	31
Table 2.1. Standard deviations for nitrogen isotopic measurements of different aliquots of reference gas.	67
Table 2.2. Precision, sensitivity and blanks of Ar and ^4He measurements	72
Table 4.1. ^4He concentrations in the diamonds studied and U-Th concentrations in the host rocks required to produce excess of ^4He .	113
Table 5.1. Methods involved in the research.	126

Chapter 1. Introduction.

1.1. General.

Understanding of the processes of Earth's formation and its evolution is one of the main goals of geochemistry. Mid oceanic ridge (MOR) basalts are accessible, providing us with information about modern mantle and hence about its current stage of evolution; crustal rocks of different ages and mantle rocks brought to the surface at different geological times can in theory provide us with information about the evolution of the crust and of the mantle. However, most of the geochemical signatures of the minerals can have been modified due to secondary processes during their residence in the crust, and therefore original geochemical and isotopic signatures of rocks and minerals of considerable age are not normally well preserved. It is generally accepted that most diamonds are xenocrysts in kimberlites and lamproites, having merely been transported by kimberlitic melts to the Earth's crust. Hence they may contain isotopic and geochemical signatures acquired during their growth in the mantle, because they have the ability to preserve these signatures due to high resistance to secondary processes. It is also accepted that diamonds were formed in the mantle, and some of them may be as old as 3.3 Ga (Richardson, 1993), as revealed from the studies of radiogenic isotope systematics in diamond inclusions; estimations of diamond ages based on noble gas studies have been taken to suggest that some diamonds are almost as old as the Earth (Ozima and Zashu, 1983). Hence, studying of diamond is one of the few direct methods (possibly the only one) providing information about the ancient mantle.

Whereas C isotopes have already been studied in different types of diamond and a significant number of data have been acquired for diamonds from kimberlitic rocks, only preliminary attempts have been made to understand N isotopic variations in diamonds although N is known to be a major impurity in terrestrial diamonds. The first systematic study of both N and C isotopic composition in diamonds has been made by Boyd, 1988;

diamonds from various localities and of different morphologies (octahedra, fibrous and coated diamonds) were analysed. The second study (Van Heerden, 1994) made an attempt to investigate N isotopic composition in diamonds in relation to eclogitic and peridotitic inclusion classification. No systematical study of polycrystalline diamonds (framesites, carbonado and diamonds formed in the shock processes) have yet been carried out. Knowledge about N and C isotopic variations in these diamonds may provide additional information helping us to understand the reasons for the existing of large isotopic variations of C and N observed in previous works.

Diamonds can often be found in placer deposits because kimberlitic rocks are eventually decomposed by secondary processes, whereas diamond, being a resistant phase, survives to be re-deposited in alluvia. However, some polycrystalline diamonds from placers, often referred as carbonado, have exhibited some properties which were not usual for diamonds from kimberlitic rocks, leading to controversy about the process of their formation. The controversy is generally based on the occasional observations made by several scientists on few samples but nevertheless some of these observations were considered completely unexplainable from the traditional stand point involving the mantle origin of diamonds. However, none of the researches on carbonado had included complementary studies involving different methods applied to the same samples, and only few of them had tried to compare carbonado with other types of polycrystalline diamond of known origin. Such specimens include framesites and the shock-formed diamonds which were recently discovered in impact craters, adding even more uncertainty to the understanding of the nature of polycrystalline diamonds from placers, since impact rocks bearing diamonds can be also decomposed, leading to the re-deposition of the diamonds. It is worth noting that the most unusual features of carbonado are the high concentrations of radiogenic noble gases such as ^4He produced by U-Th fission (Ozima *et al.*, 1991), and the light isotopic composition of the carbon (Vinogradov *et al.*, 1966; Galimov *et al.* 1985; Ozima *et al.*, 1991, Kaminsky, 1991). The understanding of the nature of these features is closely related to more fundamental questions of diamond geochemistry than to the origin of one diamond variety. Knowledge of the possible extent of ^4He implantation

in diamonds during their residence in the crust is essential to the estimation of the original isotopic composition of He trapped in diamonds, while the carbon isotopic composition of carbonado may indicate the existence of a phase depleted in ^{13}C isotope that was involved in the mantle processes, if carbonado could be proved to be of mantle origin. Therefore, if any conclusions could be reached on the subject, they may have effect on the understanding of C, N and noble gas systematics of diamond in general.

1.2. Short review on diamond properties.

Diamond is a fcc crystal, space-group Fd3m and thus has a centre of symmetry, which is important because defects which destroy the local centro-symmetry, can be analysed by a number of techniques and their development is P/T dependant, so that mantle history can be postulated. Other structural varieties of carbon are amorphous carbon, α - and β - graphite (layered hexagonal structure), lonsdaleite (hexagonal wurtzite structure), chaoite (Goresy and Donnay, 1968) recently the carbon allotrope C_{60} was discovered (Kroto *et al.*, 1985) and a number of other kinds of carbon has been postulated; some of them can coexist with diamond, and are of interest in this context.

Sixty eight elements have been found in diamond (Sellschop, 1979) and it is these impurities which provide much of the knowledge regarding processes of diamond formation now available. However, most effort has been concentrated on N, H and noble gas impurities.

What is more important is that isotopic variations have been found within and between diamonds, and as analytical techniques became more sensitive, the detailed distribution of such variations can be analysed in relation to geological provenance.

Diamond is exceptionally hard (diamond much harder than any other natural mineral) and chemically stable (except to oxygen at temperatures greater than $\approx 600^\circ\text{C}$) making it resistant to secondary alteration, the low diffusion rates of nitrogen and noble gases in diamonds means they are likely to retain their mantle record for Ga time scales and may therefore act as a “bottle” for storing and transporting gases to the Earth’s surface. This, together with the great antiquity (>3 Ga) of some diamonds makes them a

mineral of considerable importance for understanding the geochemistry of the early mantle of the Earth.

Among chemical properties of diamond the oxidation in the vacuum at temperature above $\approx 600^{\circ}\text{C}$ is the most important for our study, since this allows us to extract gases trapped in diamond structure at relatively low temperatures and simultaneously analyse chemical and isotopic composition of noble gases, nitrogen and CO_2 .

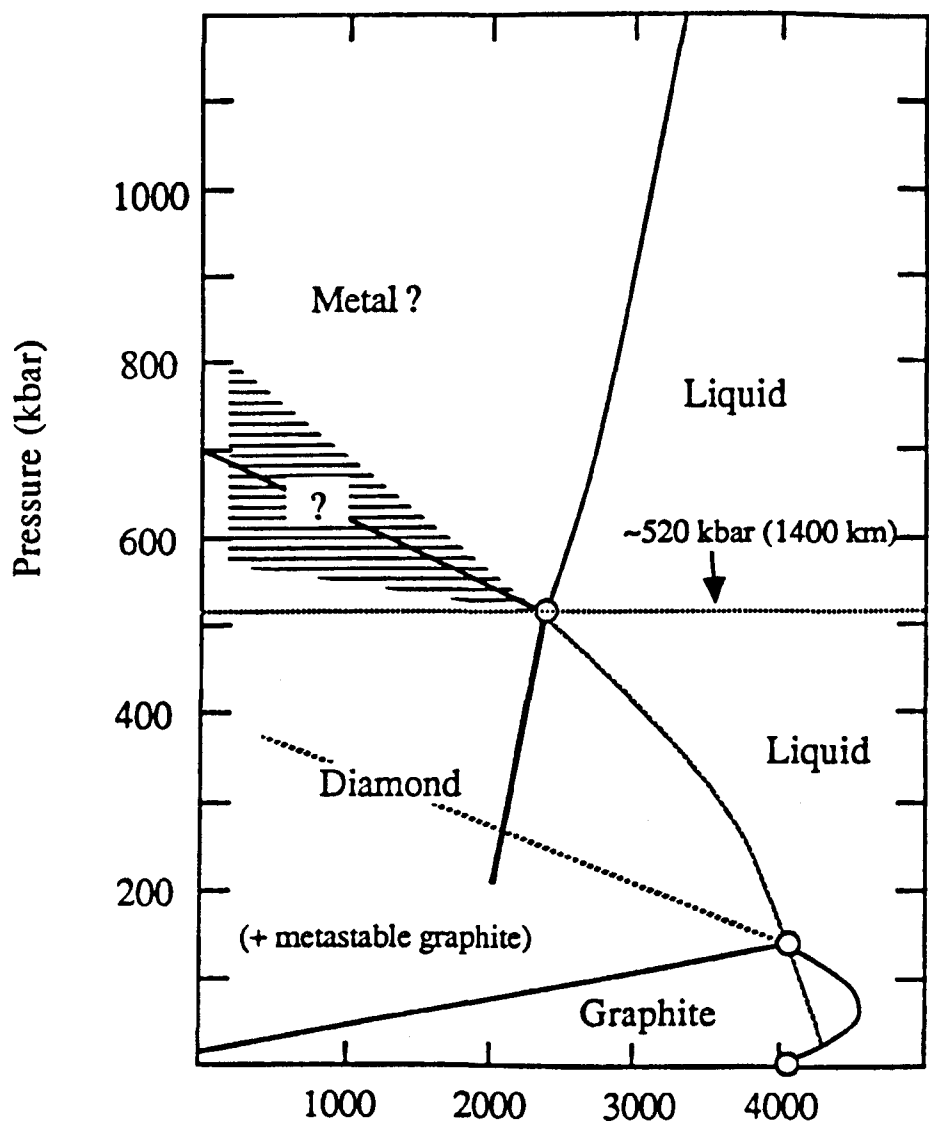


Figure 1.1. Carbon P-T phase diagram (Bundy, 1980)

Diamond-graphite thermodynamic system was originally studied by Berman and Simon(1955), who calculated the PT equilibrium curve. Then it was developed by Bundy

(1980) for C transformation in wide range of PT conditions(fig 1.1). Petrologic studies of mineral inclusions in natural diamond and diamond-bearing xenolithic rocks (Meyer, 1968; Sobolev, 1974; Sobolev *et al.*, 1986; Tsai *et al.*, 1979; Gurney *et al.*, 1979; Vaganov and Sokolov, 1988) confirmed ultra-high pressure and temperature conditions involved in diamond formation.

Although formation of diamonds in equilibrium conditions was well understood, physicists kept searching for metastable conditions leading to the diamond formation. As a result two general processes were discovered to be able to generate diamonds: shock and chemical vapour deposition (CVD) processes(table 1.1). Whereas natural examples of shock synthesised diamonds were discovered in meteorite impact structures, diamonds formed in CVD processes have not so far been recognised in nature unambiguously. However, CVD processes were proposed to explain several unusual diamond occurrences such as diamonds in ureilites, the Kokchetav metamorphic complex and Ries crater diamonds(Hough *et al.*, 1995).

Table 1.1. Methods used to synthesise diamond at low pressures and low temperatures (from Bachman, 1994).

<u>Thermal CVD</u> thermal decomposition chemical transport reaction (CTR) hot filament technique oxy-acetylene torch halogen-assisted CVD	<u>Microwave Plasma CVD</u> 915 MHz plasma 9.45 GHz low pressure plasma 2.45 GHz thernal plasma torch 2.45 GHz magnetised (ECR) plasma 8.2 GHz plasma
<u>DC Plasma CVD</u> low pressure DC plasma medium pressure DC plasma hollow cathode discharge DC arc plasmas and plasma jets	<u>Other (Non-CVD) Methods</u> C-implantation with laser treatment laser-conversion of amorphous carbon
<u>Radiofrequency Plasma CVD</u> low pressure RF glow discharge thermal RF plasma CVD	

1.3. Nitrogen impurity in diamonds.

At the beginning of the twentieth century most of the diamonds were discovered to have certain optical absorption features which were absent in the other rarer species (see Woods, 1994). The diamonds with those features were classified as type I and others as type II (Robertson *et al.*, 1934). Later it was realised that the type I diamonds are the ones which contain nitrogen whereas type II diamonds contain only a few ppm.

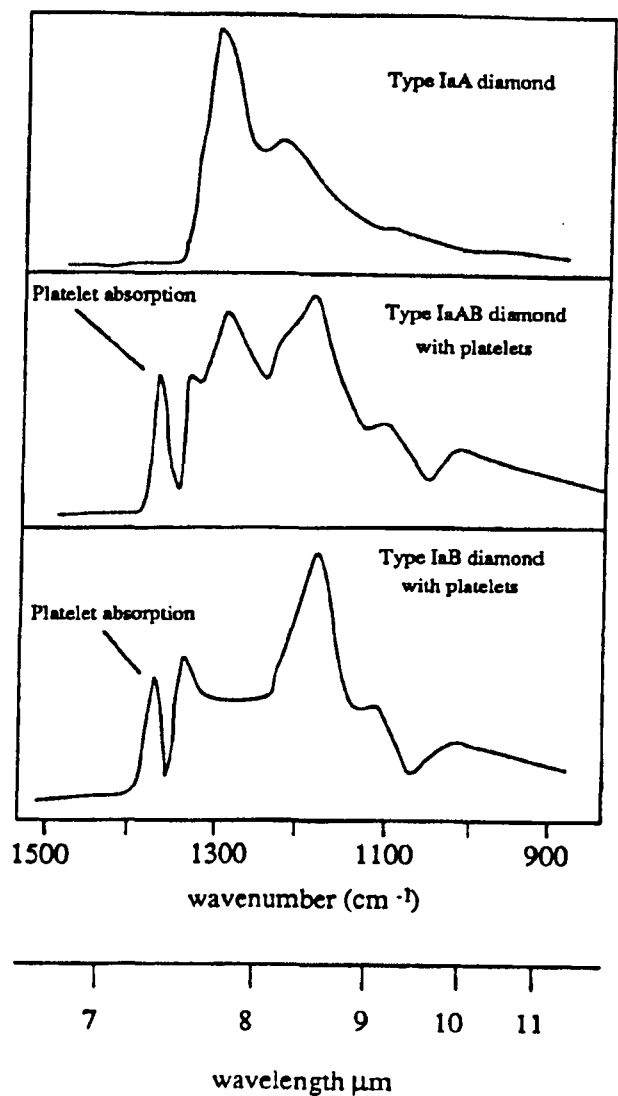


Figure 1.2 Infrared spectra of type Ia diamonds (After Davies, 1984)

Further spectroscopic investigation proved that nitrogen in the majority of natural type I diamonds is partially aggregated and these diamonds subsequently were referred to type Ia. On the contrary diamonds, where nitrogen is found as single substitutional atoms, known as Ib; Ib type is normal for synthetic diamonds but exceptionally rare for natural ones. Type Ia in its turn was subdivided accordingly to the major two types of aggregates (A and B) into IaA and IaB. They could be easily recognised by IR spectra (fig. 1.2.). Both these defects could be often present together in diamonds. It has been found that the A centre has trigonal symmetry, and this and other considerations suggest the structure to be a pair of adjacent N atoms. According to the evidence from EPR studies (see for reference Woods, 1994), the B centre consist of four substitutional N atoms tetrahedrally sited about a vacancy. Although the A and B aggregates contain the bulk of the nitrogen in natural diamonds, other aggregates of less importance occur in the diamond structure, such as N3 centre, voidites etc. Platelets are another type of defect in diamonds, for which the relation to nitrogen is still not understood, however, their formation has been found to be related to the presence of nitrogen and the process on its aggregation from A centres to B centres.

Laboratory experiments in which diamonds are treated at high temperatures, under high pressure to prevent conversion to graphite, have thrown light on the interrelationships between the various states of nitrogen in diamond and the sequence of its aggregation in nature. Heating type Ib diamonds (with single N atoms) with concentrations between 10^{19} and 10^{20} cm⁻³ (560-5600 ppm) at temperatures 1700°C — 1900°C, under stabilising pressure in the range 5.5—6.5 GPa, brings about substantial aggregation to form N pairs (A centres) (Chrenko *et al.*, 1977; Taylor *et al.*, 1995). Conversely, heating natural type IaA/B specimens containing predominantly A centres for 30 min at 1850°C, produces no changes, however at 1960°C, 2040°C and 2240°C produces some disaggregation (see Woods, 1994). These results imply that nitrogen atoms, taken up by the growing diamond in the form of single N defect at supersaturated concentrations, undergo the reaction



with the forward reaction strongly dominant. Typical experimental results are: a composite heat treatment of a type IaA natural diamond comprising 3 hr at 2500°C, 1 hr at 2600°C and 30 min at 2700°C resulted in conversion to B centres such that the final B: A concentration ratio reached around 3:1 (e.g. Evans and Qi, 1982).

The observed dependence of the aggregation process on HP/HT conditions has been successfully applied to the interpretation of the geological history of natural diamonds (Taylor and Milledge, 1995; Taylor *et al.*, 1995). It has confirmed long residence times for the majority of diamonds in the mantle, since they are usually contain nitrogen in an aggregated form.

1.4. Morphological varieties of terrestrial diamonds (after Orlov, 1973 and Vladimirov *et al.*, 1989).

It is accepted that the most comprehensive classification of the terrestrial diamonds was originated by Orlov in 1973. The classification is based on the differences in the primary growth forms of the diamond crystals, since growth of diamond under different conditions of crystallisation provides variable morphology. Secondary morphological features resulting from processes subsequent to diamond crystallisation are disregarded in this classification .

Single diamond crystals.

Variety I. Octahedral {111} shapes (fig. 1.3) are the most abundant among monocrystals of diamond. Octahedral crystals occur both with mirror-smooth, even faces and sharp edges, and with stepped development of the {111} planes.

Variety II. The growth form of this variety is cube {100} (fig. 1.3). Plane-faced crystals of this variety are found only as cubic polyhedra. These include crystals with even faces, and also with concave, negative faces, as on skeletal forms.

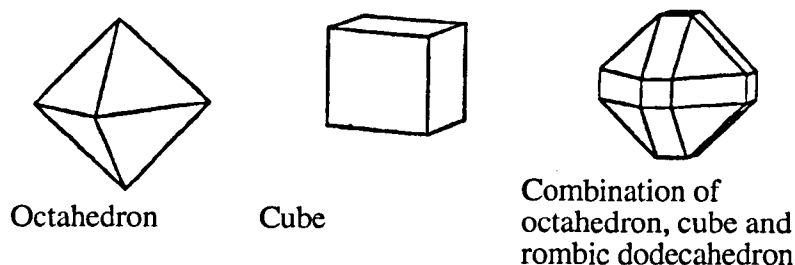


Figure 1.3. Major original habits of diamond

Variety III. This variety consist of cubic diamonds characterised by features of fibrous growth. They could be either semitransparent and colourless or greyish or almost black and non transparent. They can appear in the parallel aggregates and spinel twines.

Variety IV. This group consist of octahedra, cubes and combinations of octahedron-cube-rhombic dodecahedron shapes. The diamonds of the group have a “coat” and consequently called "coated stones". The cores of these crystals are octahedrons of variety I, which covered by a fibrous coat of yellowish or greenish colour, sometimes dull due microscopic inclusions. Microscopic inclusions are most abundant on the core-coat boundary.

Variety V. Octahedra with syngenetic graphite inclusions. Diamonds of this variety are dark or even black due to high graphite impurity in the outer part of the crystals. Cores are commonly transparent and colourless.

Variety VI. Spherocrystals which are shaped as spheroid, octahedra, dodecahedra or cuboid. These crystals were formed by fibrous growth from single centres similar to the growth of spherolites, but fibres develop parallel to the direction of growing forming monocrystals.

Polycrystalline aggregates of diamond.

Variety VII(ballas) The term ballas describes diamond spherolites of radial fibrous structure. They are usually perfectly spherical but drop- and pear-shaped specimens are

also known. Ballas may be colourless, greyish or black. The dark colour is due to microscopic black impurities, possibly graphite, common for outer part of spherulites.

Variety VIII(boart). Characteristic of this variety are aggregates of large number of small euhedral crystals, more or less uniform in size. The aggregates are oval or globular in shape, while individual crystallites show octahedral habit, often with stepped development of faces.

Variety IX(boart). This variety of distinctly granular diamond aggregates has the appearance of irregular lumps. The individual grains are easily distinguishable but show not regular crystal form. The aggregates are opaque, dark-grey or black. Boart of irregular shape coloured from grey to black, formed by diamond grains of crystallographic shapes. The aggregates could be unequally grained.

Variety X. Carbonado (see chapter 1.6.1 for details).

Variety XI. Yakutite (impact diamonds, see chapter 1.6.2 for details).

The classification was originally developed for diamonds occurred mainly on the territory of former Soviet Union, therefore polycrystalline aggregates such as framesites and stewartites (see chapter 1.6.3 for details) were not taken into account due lack of the samples from South Africa. However, it seems that they could be related to the variety IX of diamonds in general.

1.5. Diamonds in relation to kimberlites.

Most of the diamonds found on Earth, without doubt, originate in kimberlites or lamproites, or are related to them in some way, e.g. most of the diamonds extracted from placers are originally brought to the surface by kimberlites. Therefore much research has been concentrated on kimberlitic diamonds and associated rocks, which are a valuable source of knowledge about mantle geochemistry and petrology. There follows a short review of available literature on the subject.

1.5.1. Kimberlites (fig.1.4).

Kimberlites were the first rocks in which diamonds were found and still remain the main target (together with lamproites) of diamond exploration. Therefore we need to consider this particular rock to evaluate the connection between diamonds and the diamond bearing assemblage.

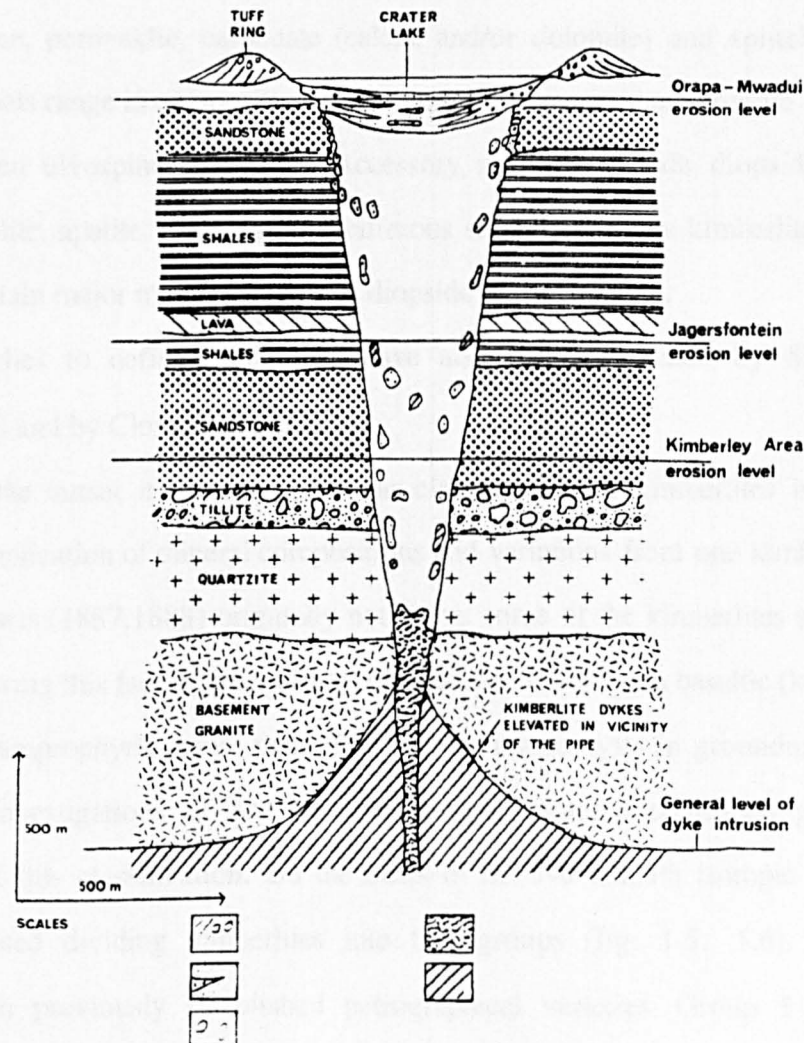


Figure 1.4. Generalised model of kimberlite diatreme and its sub-diatreme dykes (Dawson, 1980).

The term “kimberlite” appeared when Henry Carvill Lewis described the diamond bearing rock from Kimberley (South Africa) as a porphyritic mica-bearing peridotite and recognised that it was a type of volcanic breccia (Lewis, 1887), and the rock was named

kimberlite after geographical locality. Since then, a lot of effort has been made by petrologists to understand the complex nature of this alkali ultramafic rock and to arrive at a comprehensive definition of it. Mitchell (1979) defines kimberlites as follows:

Irregular alkalic peridotites containing rounded and corroded megacrysts of olivine, phlogopite, magnesian ilmenite and pyrope set in a fine-grained groundmass of second generation euhedral olivine and phlogopite, together with primary and secondary (after olivine) serpentine, perovskite, carbonate (calcite and/or dolomite) and spinels. The spinels range in composition from titaniferous magnesian chromite to magnesian ulvospinel-magnetite. Accessory minerals include diopside, monticellite, apatite, rutile and nickeliforous sulphides. Some kimberlites may contain major modal amounts of diopside or monticellite.

Other approaches to define kimberlites have also been advocated by Skinner and Clement(1979) and by Clement *et al.*(1984).

From the outset it became clear that classification of kimberlites is necessary owing to complication of mineral compositions and variations from one kimberlite body to another. Lewis (1887,1888) originally noted that some of the kimberlites are enriched in mica. Following this fact Wagner (1914) divided kimberlites into basaltic (less than 5% of mica) and lamprophyric (more than 50% of mica phenocrysts in groundmass) types. More recent investigations of Sr, Nd, Pb isotopic systems confirmed geochemical significance of this classification. On the basis of Sr, Nd and Pb isotopic data Smith (1983) suggested dividing kimberlites into two groups (fig. 1.5, 1.6), essentially consistent with previously established petrographical varieties. Group I kimberlites possess isotopic characteristics similar to those of many ocean island basalts (OIB) and are believed by some geologists to have been derived from sources in the asthenosphere. Group II kimberlites have higher abundances of potassium and are characterised by time-averaged enrichment of light rare earth elements and elevated Rb/Sr ratios. They are thought to be produced by partial melting within the sub-continental lithosphere. Groups I and II correspond to basaltic and lamprophyric types respectively. Because it was

considered inappropriate and misleading to use terms such as basaltic kimberlite (Mitchell 1970, Skinner and Clement 1979) it is better for classification purpose to divide kimberlites into Groups I and II without petrographical specification in the names.

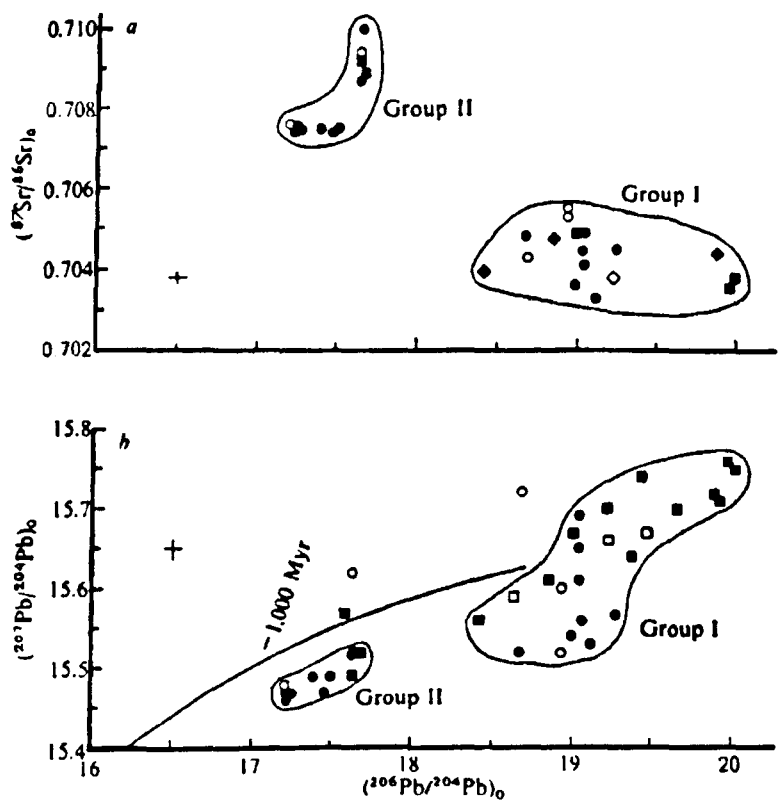


Figure 1.5. Initial $^{87}\text{Sr}/^{86}\text{Sr}$ (a) and initial $^{207}\text{Pb}/^{204}\text{Pb}$ (a) ratios plotted against initial $^{206}\text{Pb}/^{204}\text{Pb}$ for Group I and II kimberlites (Smith, 1983).

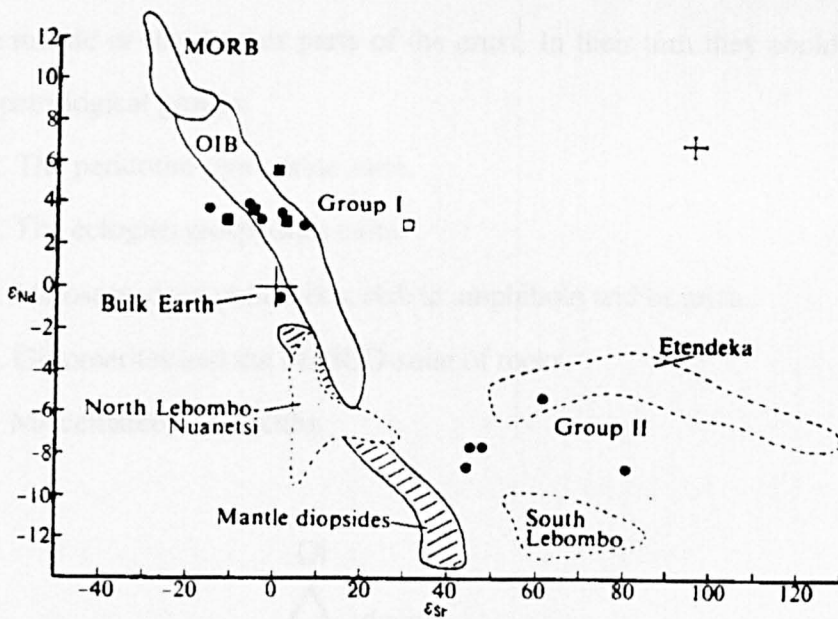


Figure 1.6. Group I and II kimberlites together with mid-oceanic ridge basalts, oceanic island basalts and diopsides from peridotite xenoliths (Smith, 1983).

1.5.2. Xenoliths (after Dawson, 1980).

Kimberlite intrusions contain fragments of a wide variety of rock types. Minerals derived from their disintegration are incorporated into the host kimberlite, thereby resulting in an extremely complex and hybrid mineralogy. Some types of xenoliths could often contain diamonds.

Xenoliths from five different sources may be recognised:

1. Fragments of the immediate wall-rock of the intrusion.
2. Fragments derived from earlier formations, existing at the time of kimberlite emplacement, but subsequently removed by erosion.
3. Blocks from buried formations.
4. Granulites derived from deep seated metamorphic terrains.
5. Xenoliths of rock-types believed to derive from the Earth's upper mantle.

The last type of xenoliths possesses the high density and specific mineralogy which indicate the high pressure and temperature conditions of formation normally associated with the mantle or the deepest parts of the crust. In their turn they could be divided into several petrological groups:

- A. The peridotite-pyroxenite suite.
- B. The eclogite-grospydites suite.
- C. Metasomatised peridotites, rich in amphibole and/or mica.
- D. Glimmerites and the MARID-suite of rocks.
- E. Miscellaneous xenoliths.

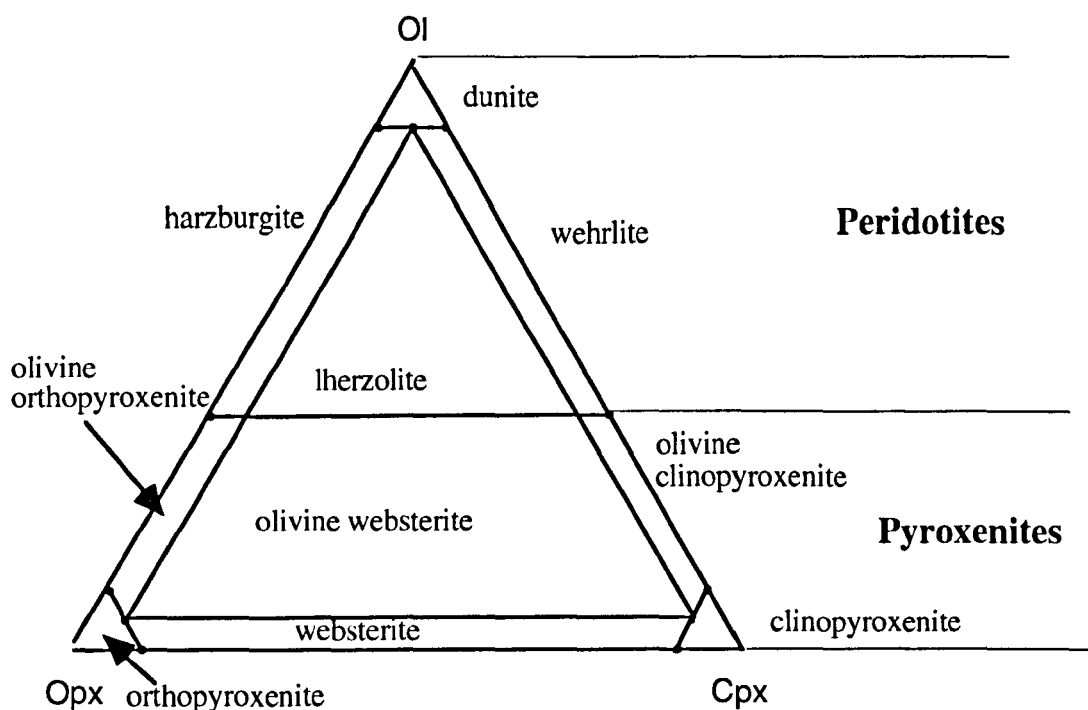


Figure 1.7. Classification of ultramafic rocks according to International Geological Union.

Representatives of A-E groups vary in volume in different kimberlite bodies. Usually they comprise no more than 2% of the bulk rock (Davidson 1967, The kimberlites of USSR), but in a few exceptional cases such as Matsoku and Lesotho the xenoliths form 20-30% of the rock (Dawson, 1968). In general, xenoliths of peridotites are predominant, though occasionally pyroxenites are relatively common (Matsoku,

Lesotho); in Roberts Victor, Bobbejaan, Rietfonten (S.Africa), Orapa (Botswana), Zagadochnaia (Yakutia) eclogites comprises a high proportion. Groups A and B will be discussed further, as their parageneses is generally known to be linked with diamonds.

A. The peridotite-pyroxenite suite.

The rocks of the peridotite-pyroxenite suite are lherzolites, harzburgites, dunites, websterites and pyroxenites. The nomenclature, based on the modal proportion of olivine, orthopyroxene and clinopyroxene according to the International Union of Geological Sciences suggested classification which is shown in the fig. 1.7. The pressure and temperature limits of formation of the rocks of peridotite-pyroxenite suite may be deduced from the stability fields of individual minerals or assemblages, these fields being based upon current experimental data (see Dawson, 1980). In the case of garnet lherzolites, these have been shown to have formed over a wide PT regime. Taken as a group, garnet lherzolites have formed at temperatures varying from approximately 900°C to almost 1400°C and have apparently been derived from the depths of between 120 and 210 km.

The rock series garnet lherzolite- garnet harzburgite-harzburgite-dunite has been linked together as being a sequential series: the garnet lherzolite is the most fertile and the dunite is the most barren in the sense that dunite is the end member after complete extraction of basaltic liquids from parental garnet lherzolite (O'Hara *et al.* 1975; Carswell *et al.* 1979). Whilst this model is essentially correct, there are other alternative explanations for the genesis of some of these rocks. For example Dawson *et al.* (1980) have shown that some garnet lherzolites may be derived by exsolution of small amounts of garnet and diopside from harzburgites; some garnet harzburgites are the result of pro-graded metamorphism of orthopyroxene-olivine-chromite rock, and there are several instances of garnet-bearing rocks in which the garnet is seen replacing spinel.

The more iron rich garnet websterites and garnet pyroxenites are believed to have originated by partial fusion of garnet lherzolites to form liquids relatively rich in iron; these liquids did not migrate far from the site of origin, and consolidated under essentially

the same pressure/temperature conditions as the rock from which they were derived (Gurney et al 1975).

B. The eclogite-grospydite suite

Nodules of eclogite are much rarer in kimberlites than those of peridotites with very few exceptions, however eclogitic xenoliths bear diamonds more frequently.

The term eclogite was first introduced by Haüy (1882) and applied to the metamorphic rock from the Fichtelgebirge, Bavaria, consisting of green omphacite and pink pyrope. In the early days of diamond mining in South Africa the term was introduced as the name of the rock composed of garnet-pyroxene nodules in kimberlite. Smulikowski (1972) and Coleman *et al.*, (1965) have shown that the garnets in the kimberlite eclogites are relatively rich in the pyrope molecule, and that clinopyroxene has a relatively high diopside/jadeite ratio; in addition Banno (1970) has shown, on the basis of Fe-Mg partitioning between coexisting garnets and clinopyroxene, that kimberlite eclogites have equilibrated at high temperature. Grospydites are a special type of peraluminous eclogite. The principal difference between grospydite and kyanite eclogite is that garnet in the grospydite contains more than 50% of grossular molecule.

The origin of eclogites in kimberlites remains a controversial topic in mantle geochemistry because of their great antiquity (e.g. Jacob and Jagoutz, 1991) and the vigorous debate about whether they represent either oceanic crust recycled by subduction or crystallised high pressure melt. The question is relevant to the interpretation of the isotopic composition of carbon in diamonds, since diamonds of the eclogitic suite are characterised by wide variations of $\delta^{13}\text{C}$ and hence could be related to the crustal material.

Convincing evidence from oxygen isotope measurements (Garlick *et al.* 1971), showing a range of $\delta^{18}\text{O}$ values similar to those observed in ophiolites (Gregory and Taylor, 1981; McCulloch *et al.* 1981) gave rise to the models which suggests the origin of eclogites as subducted oceanic crust. Taking into account radiogenic isotope studies of eclogites from South Africa which gave evidence of late Archean age (Jacob and Jagoutz, 1991; Jagoutz *et al.*, 1984; Manton and Tatsumoto, 1971, Pearson *et al.* 1995), mantle

eclogites are very likely to represent the only accessible relicts of the Archean oceanic crust. Jacob *et al.* (1994) showed that the genetic model developed on the basis of South African eclogites is also applicable to mantle eclogites from Siberia. Some Udachnaya eclogites have trace element concentrations similar to mid-oceanic ridge basalts though many are more depleted in light rare earth elements (Jerde *et al.*, 1993, Ireland *et al.*, 1995). Ireland *et al.* (1995) attributed this feature to the extraction of tonalitic/trondhjemitic melt during subduction of oceanic crust.

Petrogenetic models postulating a magmatic origin for eclogites as mantle melts or cumulates were popular early in the intensive study of eclogites from the kimberlites of South Africa (e.g. Hatton, 1978; MacGregor and Carter 1970). Sobolev *et al.* (1994) also argued quite recently for a mantle origin of eclogites, denying any connection with subduction for the majority of eclogites from Udachnaya:

"..the best evidence for their mantle origin is an absence of any firm evidence for a crustal origin"

1.5.3. Diamonds.

After the first discovery of diamonds in kimberlite (Lewis, 1887), it was believed that they had been formed in the rock itself and until recently kimberlite was considered to be the only primary source of diamonds. The association therefore suggested a phenocrystal relationship, and accordingly Harte *et al.* (1980), Mitchell and Crochet (1971) and Dawson (1971) supposed diamonds to be one of the early crystallisation products of kimberlite within the upper mantle. Other versions of phenocrystal hypotheses maintain that diamond grew in an explosion chamber at high levels in the crust (Leontyev and Hadenskii, 1957, Trofimov 1971). The discovery of diamondiferous xenoliths of mantle rocks such as eclogites and peridotites made it obvious that some diamonds were formed in the mantle from a primary source other than kimberlites. The connection with mantle xenoliths was supported by different features e.g. similarity between composition of diamond inclusions and that of mantle xenoliths (see below); diamonds in kimberlites are usually resorbed which shows that they are unlikely to be in

equilibrium with other kimberlite crystallisation products; the age of diamonds is usually greater than the emplacement age of the corresponding kimberlite. Hence, current opinion on the subject claims the majority of diamonds to be xenocrysts in kimberlites, they are just passengers travelling using kimberlite as transport.

Paragenetic assemblages of diamond inclusions were originally studied by Meyer (1968 a,b) and by Sobolev *et al.* (1969). The researches were carried out generally on the basis of a comparison of syngenetic inclusions within diamonds and coexisting minerals in the diamondiferous xenoliths. Two major parageneses were recognised: peridotitic and eclogitic, — they correspond to two types of mantle xenoliths (both of which could be diamondiferous) often found by kimberlites. A summary of recognised paragenetic varieties, including subtypes of the peridotitic and eclogitic suites are shown in Bulanova *et al.*, 1993.

1.6. Polycrystalline varieties of diamonds.

Polycrystalline diamonds have not been studied extensively as compared with single diamond crystals due to their unimportance for diamond exploration, and hence no systematic research was carried out to establish geochemical methods of distinguishing between the different varieties such as carbonado, yakutites and framesites. However, several investigations using different methods were made for each variety separately, suggesting some differences between them.

1.6.1. Carbonado.

Carbonado can be described as a polycrystalline aggregate of diamond with crystallites ranging from 10 μm to 95 μm (Fettke and Sturgis, 1933 and Kerr, 1948) and having a significant number of pores, often rounded, incorporated in these diamond aggregates (Trueb and de Wys, 1969; Trueb and Buttermann, 1969). The largest carbonado was found in 1895 being of 3167 ct (Westman, 1982), which is slightly larger than the largest diamond ever found (Cullinan 3106 ct - itself fragment of a cleavage a

single diamond crystal), although the size of most carbonados varies from less than 1 ct to 40 ct. It has been known as a polycrystalline form of diamond at least since the 1840's (Trueb and de Wys, 1971), when it was first discovered and mined as a placer mineral in Sincoro county in Brazil. Subsequently it has been found in the States of Bahia, Parana and Minas Gerais (Trueb and de Wys, 1969; Kaminsky, 1991) and at time mining of such diamonds accounted for 60-70% of all diamond production in Brazil (Sturzer, 1931) and up to 0.1% of the world production of industrial diamonds (Trueb and de Wys, 1969). It is also known from other areas particularly in Venezuela (Gran Sabana region) and from Ubangui region (Berberati, Carnot, Nola (West Ubangui) and Ouadda, N'Dele (East Ubangui)) of the Central African Republic, where the name "carbon" (Trueb and de Wys, 1971) is more common. Finds of carbonado were also reported in Western Australia and Russia (Kaminsky *et al.*, 1978) but no special research was undertaken to confirm them as carbonado. Even though carbonado finds have been widely reported from the alluvial deposits, they have never been described in primary rocks so that their origin is uncertain.

In the first studies Roth *et. al.* (1926) and Gerlach (1924) postulated the presence of amorphous carbon or graphite as a colouring and binding agent between diamond crystallites but Brandenburg (1930) found no such evidence in X-ray diffraction diagrams. Certain differences have been detected between carbonados from Brazil and from Ubangui. Crystallites in Brazilian carbonado were found to be between 1 μm and 4 μm in diameter (total range 0.5-20 μm) and appear to be either octahedra or anhedral (Trueb and de Wys, 1969). The samples from Ubangui have crystallites of size 5-10 μm (ranging from 2 to 100-250 μm , although the latter are rare), and octahedral and cubic morphology of the crystallites was observed (Trueb and de Wys, 1971). The density of carbonado from Brazil, on account of variable number of pore space, is 3.326-3.434g/cc (Trueb, de Wys, 1969) but 3.176-3.301g/cc in Ubangui specimens (Trueb, de Wys, 1971) (the density of pure diamond is 3.511g/cc). The composition of mineral inclusions in carbonados (table. 1.2.) was found to be quite different as compared to these that occurred in kimberlite diamonds. However, the inclusions in carbonado were mainly

observed in pores and cracks occurring frequently in the diamond aggregates, suggesting a secondary nature (Trueb and Buttermann, 1969; Trueb and de Wys, 1969, Kerr, 1948). Differences between the compositions of inclusions in carbonado from Brazil, Venezuela and Central Africa could also be observed.

Table. 1.2. Composition of inclusions in carbonado samples from different localities (Kerr, 1948; Trueb and de Wys, 1969; Trueb and de Wys, 1971; Trueb and Buttermann, 1969).

CARBONADO FROM BRAZIL	CARBONADO FROM UBANGUI	CARBONADO FROM VENEZUELA
orthoclase(80%) hematite gehlenite allanite perovskite zircon rutile corundum cassiterite graphite quartz magnetite chalcedony chloritoid pseudomalachite covellite anhydrite	Al-serpentine clorite chromite florencite ilmenite magnetite perovskite quartz olivine rutile	quartz

The range of C isotopic composition for carbonados from Brazil and Central Africa was found to be from -23‰ to -31‰ (Vinogradov *et al.* 1966; Galimov *et al.* 1985; Ozima *et al.*, 1991, Kaminsky, 1991), which is unusual for diamonds from kimberlitic sources. Hence it was suggested that an unusual process or source material was necessary to explain the existence of carbonado. Recent data for noble gases in carbonado added even more controversy concerning the geological history of carbonado. Concentrations of radiogenic isotopes of noble gases (excluding ^{40}Ar) in carbonados had appeared to be much greater than in any other terrestrial diamonds studied, for example, ^4He concentrations could be several orders of magnitude higher than that found in any other diamonds (Ozima *et al.*, 1991). The isotopic composition of He, Xe, Ne, Kr shows that fission of U and Th had a major influence on the noble gas isotopic system of carbonado (Ozima *et al.*, 1991) which was considered to be impossible in the mantle environment, due to the low U-Th concentrations expected there.

1.6.2. Impact diamonds.

Yakutites were first recognised as a variety of diamond in 1966, when polycrystalline diamonds of unusual morphology were discovered in alluvial deposits of Northern Yakutia. Being anhedral and of dark-brown to steel-grey colour, they were often confused with carbonado in the literature. Similar polycrystalline diamond aggregates were also encountered in alluvial deposits in the Ukraine (Polkanov *et al.*, 1973, 1978). During mineralogical studies of yakutites, the hexagonal modification of carbon (lonsdaleite) was recognised to be contained in the polycrystalline aggregates (Krajnyuk and Bartoshinsky, 1971; Kaminsky *et al.*, 1978, 1985; Klyuev *et al.*, 1978). Since lonsdaleite is a high pressure modification of carbon, having already been recognised in meteorites (Hanneman *et al.*, 1967), the formation of yakutites appeared to be linked with meteorite impact events. In 1972 Masaitis *et al.* reported first finds of polycrystalline diamonds with lonsdaleite in impactites from the Popigai crater, confirming an impact origin for yakutites. Recently the impact produced diamonds were reported in deposits of the KT-boundary (Gilmour I. *et al.* 1992), and from the Ries crater (Hough *et al.*, 1995, ref).

Table 1.3 Properties of shock diamonds suggesting two types of source material (Veshnevsky *et al.*, 1995).

Properties of diamonds	Type I	Type II
density, g/cm ³	3.44 — 3.55	2.5 — 3.1
colour of photoluminescence	yellow-orange/brick-red	yellow-green/light-blue
combustion temperatures	580°C — 760°C	520°C — 650°C
$\delta^{13}\text{C}, \text{‰}$	-9.9 — -20.1	-22.3 — -24.6
source material	graphite	organic matter

Impact diamonds recovered from impactites are mainly 0.1—0.5 mm in size, but specimens from placers up to 1—5 mm have been found; their colours are variable from colourless through yellow to grey and black (yellow and black are the most usual). The size of crystallites usually varies in the range 0.1-1 μm and specimens show strong preferred orientation. Carbon isotopic composition ranges from -9‰ to -21‰ (Kaminsky

et al., 1977; Galimov *et al.*, 1978; Kaminsky 1991). Several features of the diamonds suggested two types of source material (table 1.3).

1.6.3. Framesites.

Framesite is a commonly used term for polycrystalline diamonds from Orapa and Jwaneng kimberlite pipes where polycrystalline diamonds constitute a substantial proportion of the total diamond population. Terms like boart and stewartite are more or less synonymous with framesite, and in different geographical areas different names are in use. The colour of the aggregates is usually from white to dark grey and single crystallites are often smaller than 100 μm in diameter. The mineral composition of inclusions in the aggregates resembles those described for single diamonds crystals, and inclusions of both eclogitic and peridotitic types of assemblages can be recognised in the framesites (Kirkley *et al.* 1991 and McCandless *et al.*, 1989). Although, carbon isotopic composition in framesites was found to vary from -3.8‰ to -23.5‰ the diamonds enriched in ^{12}C isotope were encountered more often for framesites from Orapa and Jwaneng than for single diamond crystals. The only difference which could be observed between framesites from Orapa and from Jwaneng is the appearance of magnetism in the framesites from Orapa, resulting from the presence of magnetite in the interstitial space.

1.7. Brief review of N and C isotopic geochemistry of the crust and the mantle.

Carbon and nitrogen belong to the group of the most abundant elements in the solar system. They play the significant roles in the geochemistry of the Earth, especially in the biosphere. Both elements have accumulated on the Earth's surface during geological history. Their major reservoirs are the atmosphere for N, and the biosphere and carbonaceous sediments for C. Carbon occurs in the reduced form in organic matter and hence in coal. It also occurs in the oxidised state primarily as carbon dioxide, as carbonate ions in aqueous solution, and as carbonate minerals. Nitrogen forms only a

small number of minerals all of which are uncommon. Perhaps, the most abundant are the nitrides (K and Na), which can usually be found in non-marine evaporate deposits in arid regions of the Earth. Natural occurrences of other nitrates are also known. In igneous rocks N occurrence primarily in the form of ammonia, which replaces potassium in silicate minerals. Nitrogen in soils and aqueous environments on the surface of the Earth appears in the form of nitrate, nitrite, ammonium, ammonia, oxides and in amino acids and other organic matter (Faure, 1986).

1.7.1 C and N isotopic composition of crustal material.

Carbon.

Among the rocks constituting the Earth's crust carbon is largely confined to those of sedimentary nature. A significant part of Earth's carbon is fixed in carbonates and in reduced forms of biogenic origin.

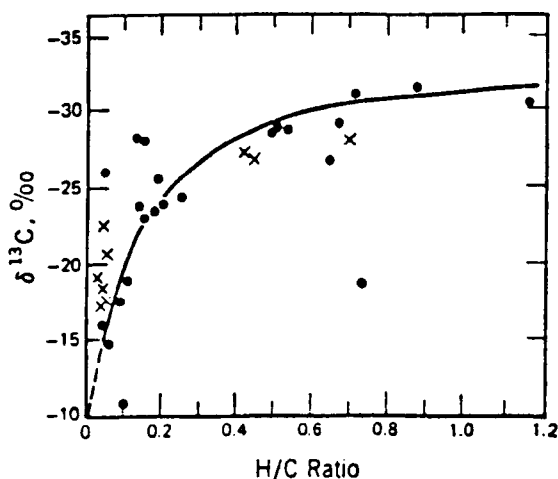
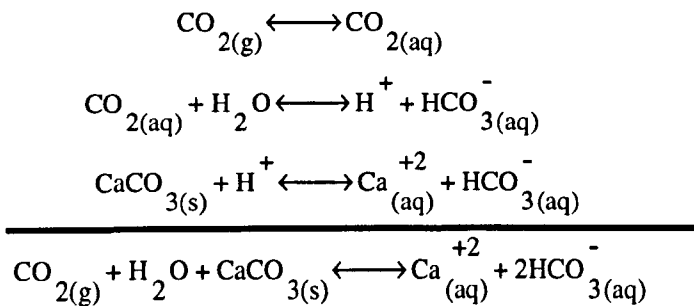


Figure 1.8. Plot of $\delta^{13}\text{C}$ of reduced carbon in sedimentary rocks of Precambrian to Middle Cambrian versus the rank of organic (McKirdy and Powell, 1974).

The carbon contained in fossil fuels (coal, petroleum, natural gas etc.) is strongly enriched in ^{12}C , which is consistent with the view that those materials have biogenic origin. The $\delta^{13}\text{C}$ of fossil fuels falls into range -20‰ – -40‰ , with exception for natural gas which may be as light as -70‰ . Progressive metamorphism of kerogens leads to enrichment by ^{13}C due to the formation and loss of methane, which concentrates ^{12}C (fig.

1.8). On the other hand the effect could be explained by an isotopic exchange between carbonates and graphite during metamorphism (Kreulen and van Beek, 1983)

Carbon isotopic composition in sedimentary carbonates is noticeably different from the carbon of fossil fuels, since fractionation processes have taken place during carbonate precipitation. The fractionation of carbon isotopes between CO₂ gas and carbonate species in aqueous solution has been studied by Deuser and Degens (1967), Wendt (1968), Vogel *et al.*, (1970) and Emrich *et al.*, (1970), among others. The carbonate equilibrium can be represented by the following equations:



The fractionation factors for carbon isotopes in this system reported by Emrich *et al.* (1970) are:

	$\alpha, 20^\circ\text{C}$
Calcium carbonate-bicarbonate =	1.00185
Bicarbonate-carbon dioxide gas =	1.00838
Calcium carbonate-carbon dioxide gas =	1.01017

These results indicate that calcium carbonate precipitated in isotopic and chemical equilibrium with CO₂ gas is enriched in ¹³C by about 10‰. The δ¹³C values of carbonates of marine origin of Cambrian to Tertiary age are virtually constant and have values close to zero on the PDB scale., average value obtained for 321 samples of marine sediments being of +0.56±1.55‰(Keith and Weber, 1964). Freshwater carbonates are more variable in isotopic composition and more enriched in ¹²C, the average value being of -4.93±2.75‰ for 183 samples (Keith and Weber(1964). The isotopic composition of carbon in the shells of modern marine molluscs ranges from +4.2 to -1.7‰ and in freshwater species from -0.6 to -15.2‰, reflected in similar variations to that of corresponded carbonates.

Banded iron-formations containing deposits of laminated chert, iron oxides, silicates and carbonates are an important object of carbon geochemistry, since they carry information about the Precambrian environment and contain significant amounts of carbonaceous material. Siderite from this formation have carbon with isotopic composition in the range from $-9.0 \pm 1.7\text{‰}$ and for ankerite the range is $-9.6 \pm 1.6\text{‰}$ (Becker and Clayton, 1972). Similar results were observed for the banded iron-formation of Krivoi Rog (Russia) (Galimov, 1968). The formations often contain graphite, sometimes up to 3% of the rock, which has $\delta^{13}\text{C}$ value ranging from -20‰ to -36‰ , thus undoubtedly of organic origin.

Nitrogen.

Generally speaking the highest concentrations of nitrogen are observed in fossil fuel deposits connected with organic matter. Coal can contain up to 3% of nitrogen, while marine sediments contain only a few thousand ppm, and most other rocks contain of much less than 1000 ppm of nitrogen.

Organic matter contains a significant part of the fixed nitrogen, although some of it is in minerals in the form of ammonia, and occasionally forms nitrates. The abundance of nitrates, however, is low among rocks, since nitrates can easily be dissolved in water at normal temperatures.

The appearance of ammonia ions in silicates is of great interest because they are more stable. The size of the ammonia ion is almost the same as that of potassium ion, therefore the highest concentration of nitrogen could be expected in potassium silicates. Among these the most interesting are feldspar, which has an ammonium species buddingtonite containing of about 5 weight percent of ammonia (table 1.4). Buddingtonite was discovered in 1964 in the ores of "Sulphur Bank", California as a pseudomorph of plagioclase in andesitic rocks transformed by hydrothermal solution high ammonia (Erd *et al.*, 1964). Buddingtonite is the hydrated ammonium feldspar with formula $\text{NH}_4\text{AlSi}_3\text{O}_8 \cdot 1/2\text{H}_2\text{O}$. Afterwards it was recognised in the ore deposits of "Phosphoria Formation", Idaho where it consist of 50% of the rock, and is associated with albite, illite

and montmorillonite (Gulbrandsen, 1974). It has been suggested that buddingtonite originated as a result of the diagenesis of volcanic glasses. In 1982 the mineral was found in ores of "Condor", Australia in concentrations of 10% in the 600m thick layers of bitumenised rock (Loughnan, Roberts,1983). The authors concluded from their research that the mineral was formed at significant depth in a high ammonium environment.

Table 1.4. Chemical composition of buddingtonite.

	1	2
SiO ₂	63.80	67.97
Al ₂ O ₃	19.16	18.02
Fe ₂ O ₃	1.88	0.42
TiO ₂	0.99	—
MgO	0.21	0.14
CaO	0.04	0.31
BaO	0.26	—
Na ₂ O	0.06	0.04
K ₂ O	0.62	1.03
(NH ₄) ₂ O	7.95	7.92
S	1.59	—
H ₂ O	3.28	3.31
H ₂ O	0.88	0.83
Sum	100.69	99.99

1— buddingtonite from "Sulphur Bank" (Erd *et al.*,1964); 2— buddingtonite from "Condor" (Loughnan, Roberts,1983).

Other silicates do not exceed ppm levels of nitrogen concentration. According to Wlotzka (1972) the majority of them contain 10-70 ppm of nitrogen. However, based on more recent researches, nitrogen proved to be more abundant than that in minerals from some crustal rocks e.g. Honma and Itihara (1981) and Duit *et al.*(1986) who reported that biotites in igneous and metamorphic rocks commonly contain >250 ppm of [NH₄]⁺, Boyd *et al.*(1993) reported concentrations up to 900 ppm for orthoclase and 691 ppm for muscovite. For biotite up to 5000 ppm of ammonia has been reported by Darimont *et al.* (1988).

In order to understand the isotopic geochemistry of nitrogen in crustal rocks, it is necessary to know the nitrogen isotopic composition in biogenic matter, as it is subsequently involved in sedimentation and then in diagenesis.

In general, nitrogen in animal tissue is enriched in ¹⁵N relative to the atmosphere, whereas plants tissue might be slightly depleted in ¹⁵N. However, a wide range of δ¹⁵N

values occurs in plant tissues when the nitrogen was derived from nitrate or ammonia that had been isotopically fractionated before being absorbed by the plants. As a result the $\delta^{15}\text{N}$ values of "total soil nitrogen" range widely in 176 soil analyses from -4.4‰ to +17‰, according to Letolle (1980). The ground water $\delta^{15}\text{N}$ value varies from 0‰ to 25‰ depending on the sources that may locally dominate the inputs of N (Letolle, 1980).

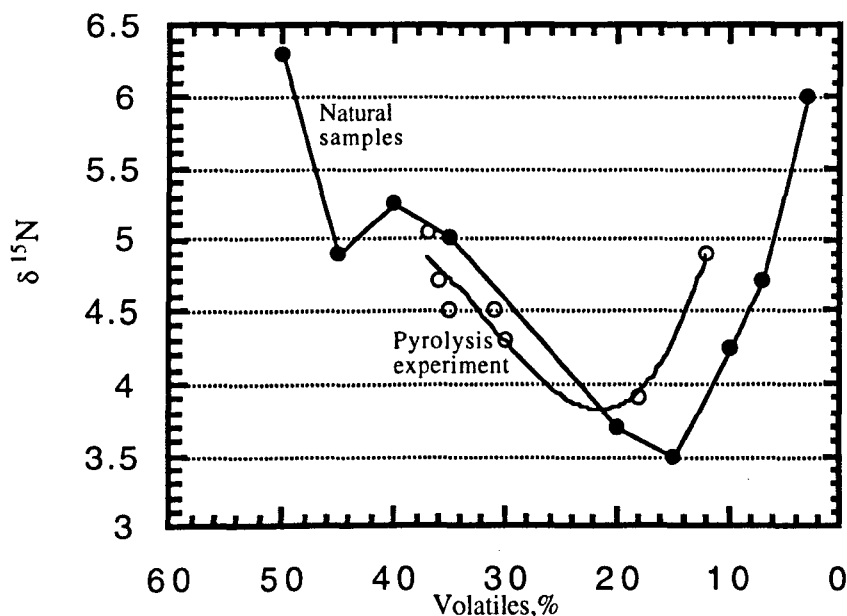


Figure 1.9. Variations of $\delta^{15}\text{N}$ in coal as a function of the concentration of volatiles (Data from Drechsler and Stiehl 1977; Stiehl and Lehmann, 1980)

The isotopic composition of N in coal varies from -2.5 to +6.3‰ and seems to depend on the origin of the organic material and on the rank of the coal. Drechsler and Stiehl (1977) and Stiehl and Lehmann (1980) concluded from their measurements that "humid" coal, derived from terrestrial plants, has lower $\delta^{15}\text{N}$ values than "bituminous" coal formed from zoo-plankton and phyto-plankton. The volatile N compounds released during thermal maturation of coal are initially enriched in ^{15}N , which causes the $\delta^{15}\text{N}$ value of the coal to decrease. This phenomenon is demonstrated by the $\delta^{15}\text{N}$ values of coal ranging in rank from lignite to anthracite (fig. 1.9). The trend was duplicated by stepwise pyrolysis of a sample of bituminous coal heated from 225°C to 400°C (Drechsler and Stiehl, 1977; Stiehl and Lehmann, 1980).

Table 1.5. Nitrogen isotopic composition of some components of the oceanic reservoir (Cline and Kaplan, 1975)

	Range of $\delta^{15}\text{N}$	Mean $\delta^{15}\text{N}$
Organisms		
Phytoplankton	+5.2‰ to 9.7‰	+7.5
Zooplankton	+12.8‰	+12.8
Fish	+9.9‰ to 20.5‰	+15.9
Dissolved component		
Nitrate	+4.8‰ to +7.5‰	+6.2
Ammonia	+6.5‰ to +7.5‰	+7.0
Dissolved N ₂	-0.2‰ to +0.7‰	+0.4
Sediments		
Ammonia	+2.9‰ to +5.3‰	+4.1
Organic	+4.7‰ to +6‰	+5.4
Total Nitrogen	+5.3‰ to +13.4‰	+5.7
Rain		
Nitrate	-7.3‰ to +3.4‰	-1.7
Ammonia	-0.1‰ to 9.0‰	+4.6

The ocean reservoir includes several components containing nitrogen, their $\delta^{15}\text{N}$ value variations were reported by Cline and Kaplan, 1975 (table 1.5.).

Table 1.6. Nitrogen isotopic composition of different crustal materials.

Type of material	$\delta^{15}\text{N}$, ‰	Reference
total soil nitrogen	-4.4 to +17	Letolle, 1980 (176 samples)
ground water	+0 to +25	Letolle, 1980
lacustrine sediments	+2.7 to +5.6	Pang and Nriagu, 1976
Coal	-2.5 to +6.3	Foure, 1986
Petroleum	+0.7 to +8.3	e.g. Wlotzka, 1972
Particulate organic from sedimentation traps	+2.9 to 4.4	Saito and Hattori, 1980
terrestrial particles of organic matter	+2.5(av.)	Sweeney <i>et al.</i> , 1978
marine sediments	+6.8±4.1	Wada <i>et al.</i> , 1975
granites	+5.1 to +10.2	Boyd <i>et al.</i> , 1993
mineral separates from granites	+2 to +15.9	Boyd <i>et al.</i> , 1993
metasediments	+1 to +5.9	Bebout and Fogel, 1992

The isotopic composition of nitrogen for granites and metamorphic rocks lies in a similar range of $\delta^{15}\text{N}$ to that discussed above for sediments and organics (table 1.6). The $\delta^{15}\text{N}$ values for granites from the Cornubian batholith vary from +5.1 to 10.2‰, whereas the mineral separates of these rocks show variations from +2 to +15.9‰ (Boyd *et al.*, 1993). The highest values were observed for biotite. Studies of nitrogen in metasedimentary rocks in the Catalina Schist, California yielded values of $\delta^{15}\text{N}$ between +1‰ and +5.9‰, with systematic increases of $\delta^{15}\text{N}$ with increasing metamorphic grade.

1.7.2. Carbon and nitrogen isotopic composition of the mantle.

In order to evaluate C and N isotopic variations in the mantle several types of rocks and minerals can be used. Studies of basalt glasses or gas vesicles in the basalts provide isotopic characteristics of C and N in the modern sub-oceanic mantle, while studies of carbonates in carbonatites and kimberlites provide a way of characterising C isotopic composition. For investigations of the N isotopic composition of sub-continental mantle, the most suitable material is diamond, the mineral which contains higher concentrations of N and C than any other phases formed in the sub-continental mantle.

1.7.2.1. Carbon and nitrogen isotopic compositions of basalts.

Carbon.

Carbon isotope signatures of oceanic basalt glasses provide an important means of probing the geochemistry of mantle carbon. The abundance and isotopic composition of carbon in basalt glasses have generally been determined by stepped combustion to separate indigenous and non-indigenous carbon components (Mattey *et al.*, 1984; Exley *et al.*, 1986a; Exley *et al.*, 1986b; DesMarais, 1986; Sakai and DesMarais, 1984) and $\delta^{13}\text{C}$ range from $\approx -4\text{‰}$ to $\approx -8\text{‰}$ with few exceptions was obtained. Some of the data on marginal basin basalts, though, provide lower $\delta^{13}\text{C}$ values, sometimes as low as -16.5‰ (Mattey *et al.*, 1984; Exley *et al.*, 1986; Macpherson and Mattey, 1993). Two explanation have been suggested to explain this phenomenon. According to the first, light carbon in these basalts is a result of subduction of sedimentary carbon with further mobilisation due progressive metamorphism and dissolution in the basalt melt (Mattey *et al.*, 1984). The second explanation proposes that the fractionation is caused by degassing of the magma (Macpherson and Mattey, 1994).

Nitrogen.

Until recently nitrogen isotope data on basalts were rather too complex to be interpreted in terms of relation to certain reservoirs of mantle nitrogen; the summary of

previous studies, after Boyd and Pillinger (1994), is presented in table 1.7. However, the scatter of the data from +12‰ to -4.5‰ can be understood assuming contamination of indigenous mantle by crustal nitrogen; the contamination effect is already well known for Ar in basalts. Results obtained by Marty *et al.*, (1995) confirms the suggestion showing the mixing lines between Ar and N of MORB and those of AIR. In their study, the gas from fluid inclusions from several MORB samples was analysed and it appeared to be that fluid inclusions contains almost an order of magnitude more nitrogen than glasses, and therefore contamination effect is less noticeable in case of gas in vesicles than in case of gas dissolved in glasses. On the basis of combined Ar and N isotopic study Marty *et al.*, 1995 have concluded that $\delta^{15}\text{N}$ of MORB fluid is $\approx -4\text{‰}$.

Table. 1.7. N isotope data that have been obtained from oceanic basalts and a harzburgite (after Boyd and Pillinger, 1994).

Sample	[N],ppm	$\delta^{15}\text{N}$, ‰	References
OIB(Hawaii)	1	+17	Becker and Clayton, 1977
OIB(Hawaii)	0.4	-0.4	Sakai <i>et al.</i> , 1984
MORB(n=2)	0.9,1.4	-0.1,-0.8	Sakai <i>et al.</i> , 1984
OIB(Hawaii)	0.2-1.2	+12.8 to +15.5	Exley <i>et al.</i> , 1987
MORB(A,P)(n=6)	0.2-2.1	+7.5	Exley <i>et al.</i> , 1987
MORB(I.O.)(n=2)	0.3,0.4	-4.5,-1.9	Exley <i>et al.</i> , 1987
OIB(Hawaii)	6	-1.1	Javoy <i>et al.</i> , 1986
MORB(A)	12	-3.5	Javoy and Pineau, 1991
Harzburgite	8	-5.0	Nadeau <i>et al.</i> , 1990

1.7.2.2. Isotopic composition of C and N in diamonds of mantle origin.

Carbon.

The first C isotopic data was reported by Craig (1953), who analysed six octahedral diamonds from the South African kimberlite mines and obtained values between -2.4‰ and -4.7‰ except for one value of +2.4. Then Wickman (1956) analysed 37 diamonds mainly from Africa and obtained the range -3.2‰ to -9.6‰, with one sample having a $\delta^{13}\text{C}$ value -13.9. These results suggested that diamonds were isotopically homogeneous. However, further research revealed a wider range of $\delta^{13}\text{C}$ (Vinogradov *et al.*(1966)

obtained values of $\delta^{13}\text{C} = -27.8\text{‰}$ to -28.4‰ for carbonado diamonds, Kovalskiy *et al.* 1972 have reported $\delta^{13}\text{C}$ values of -21.4‰ to -22.2‰ for four diamonds from the Ebelyakh placers and $\delta^{13}\text{C}$ values of -32.2 for one from Mir pipe). Systematic studies of diamonds localities world wide established a wider range of $\delta^{13}\text{C}$ from -34.4‰ to $+2.8\text{‰}$ (Galimov *et al.* 1978; Sobolev *et al.* 1979; Smirnov *et al.*, 1979; Milledge *et al.*, 1983; Deines *et al.* 1984, 1987, 1991, 1992; Kirkley *et al.*, 1991; Boyd *et al.*, 1987; 1988, 1994) than had been suggested by the pioneering works of Craig (1953) and Wickman (1956).

Diamonds derived from kimberlites and lamproites have been studied systematically. There have been some attempts to find correlations between $\delta^{13}\text{C}$ and different properties of diamonds, such as colour, inclusions, and morphologies (summarised in Vladimirov *et al.*, 1989). Colour of diamonds seems to have no obvious connection with the isotopic composition of carbon (fig. 1.10). However, some differences in $\delta^{13}\text{C}$ value distributions were observed for different morphological varieties (fig. 1.11). These analyses refer mainly to diamonds from areas of the former Soviet Union. However, the similar ranges of $\delta^{13}\text{C}$ were reported for fibrous cubes (variety III) and coated diamonds (variety IV) by Boyd and Pillinger (1994), and $\delta^{13}\text{C}$ variations of cubic microdiamonds from the Northern Territory of Australia (Lee *et al.*, 1991) were found to be similar to those for diamonds of variety II (fig. 1.12). Relationship between carbon isotopic composition and the paragenesis of mineral inclusions (fig. 1.13) was first identified by Sobolev *et al.* 1979: the $\delta^{13}\text{C}$ value for most diamonds containing peridotitic inclusions or obtained from peridotitic xenoliths range between -1‰ and -10‰ (peak $\approx -5\text{‰}$), in contrast to the diamonds of eclogitic suite which show $\delta^{13}\text{C}$ variations from -35‰ to $+2.5\text{‰}$ (major peak $\approx -6\text{‰}$), covering the whole range of $\delta^{13}\text{C}$ for diamonds (such variations were also observed for Type II diamonds (Milledge *et al.*, 1983)). However, diamonds with websteritic inclusions, which are variety of peridotitic diamonds, were found to be enriched in ^{12}C relatively to the majority of P-type diamonds, having $\delta^{13}\text{C}$ in the range from -6‰ to -23‰ , with the peak of the distribution -18‰ (Deines *et al.* 1993; van Heerden *et al.*, 1995).

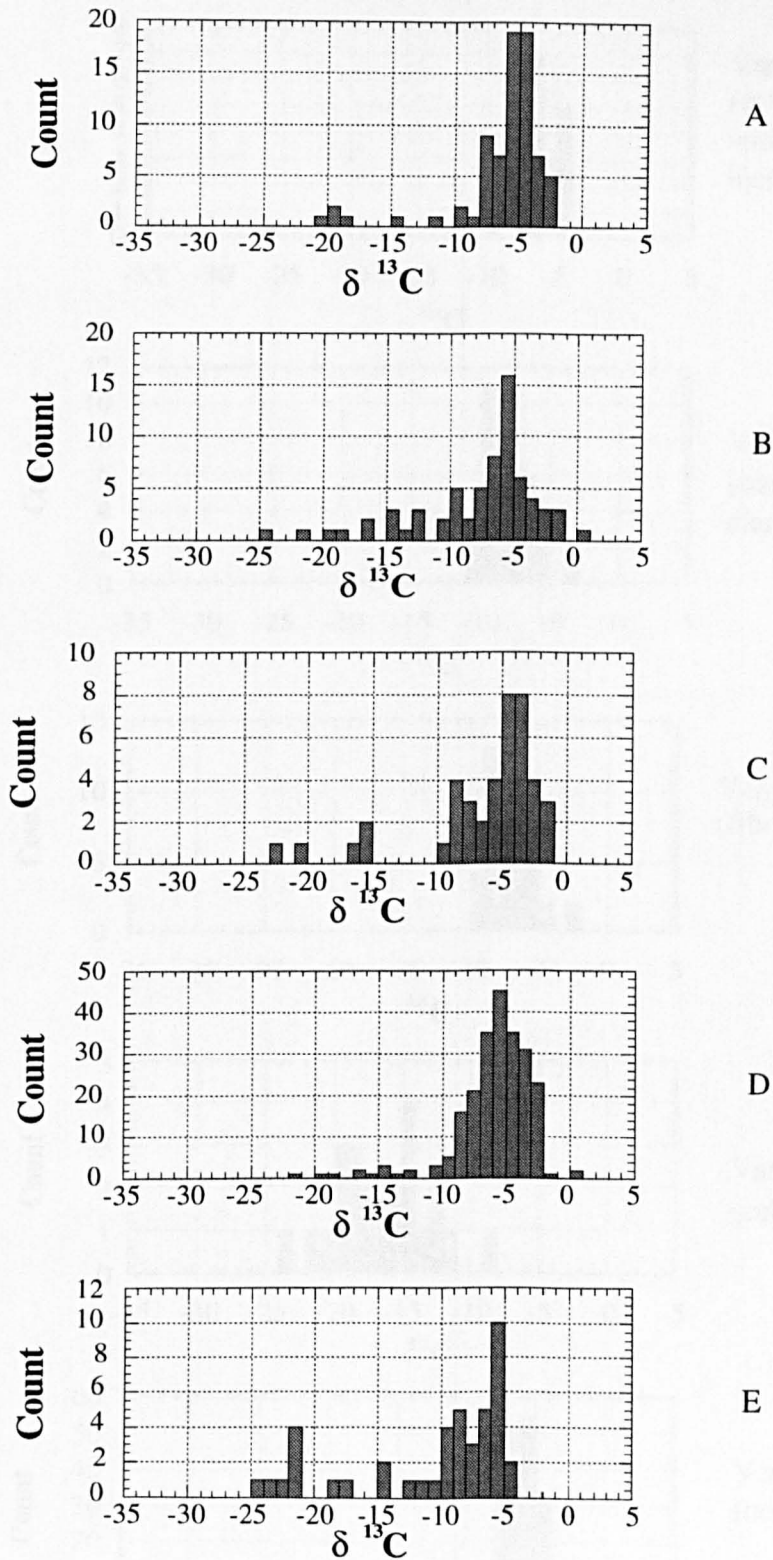


Figure 1.10 Carbon isotopic composition of yellow (A), pink-brownish (B), green (C), grey and black (D), and colourless (E) diamonds (Vladimirov et al., 1989).

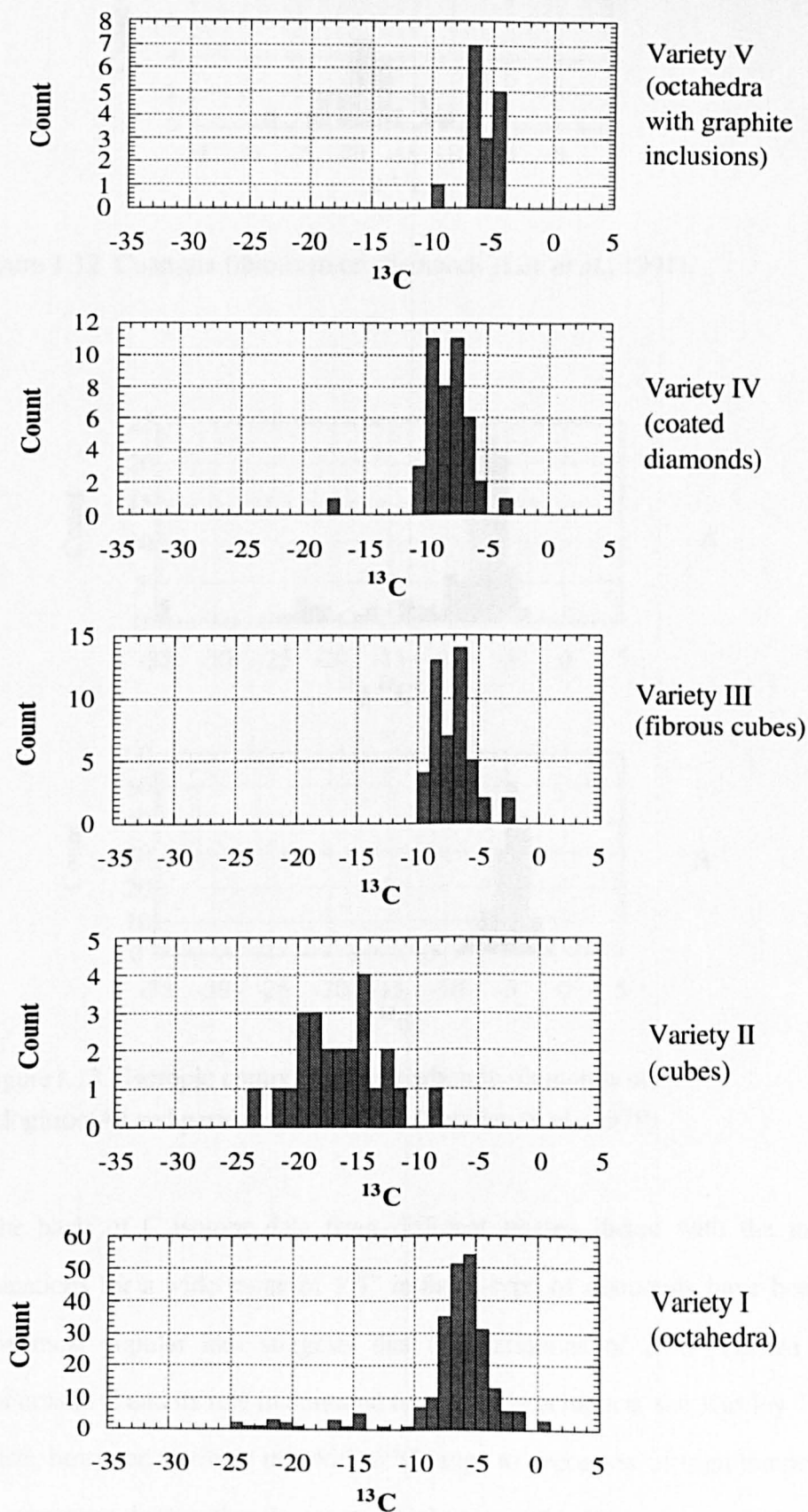


Figure 1.11 Carbon isotopic composition of different diamond varieties (Vladimirov et al., 1989).

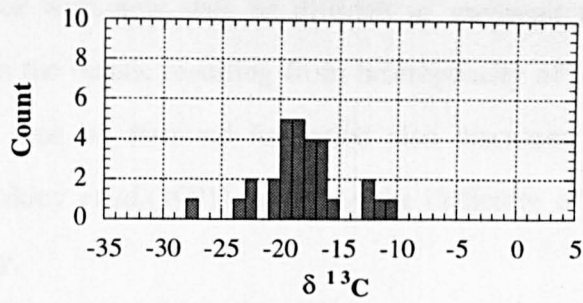


Figure 1.12 Coanjula fibrous microdiamonds (Lee *et al.*, 1991).

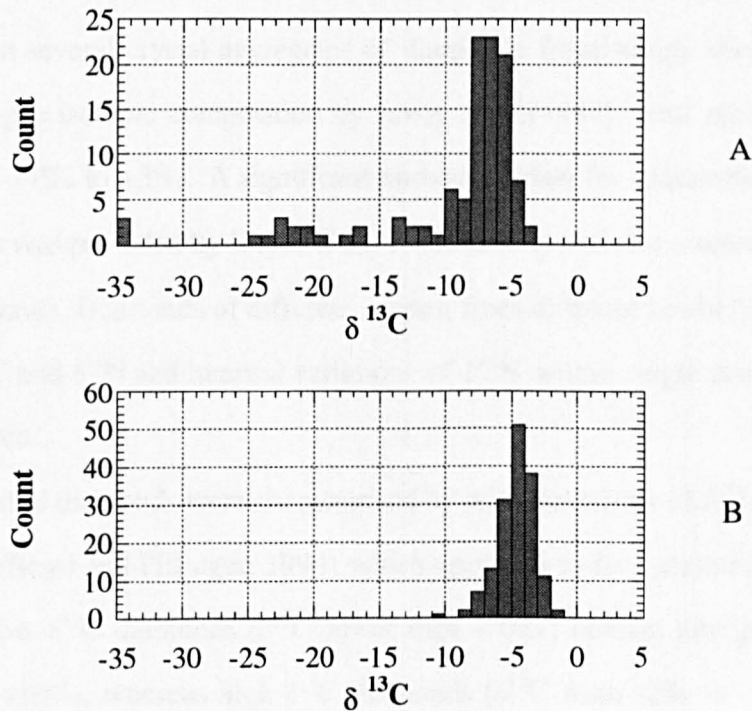


Figure 1.13 Isotopic composition of carbon in diamonds of eclogitic(A) and peridotitic suites (B) (Sobolev *et al.*, 1979)

On the basis of C isotope data from different phases linked with the mantle, several explanations for a wide range of $\delta^{13}\text{C}$ in the E-type of diamonds have been put forward. The most popular idea suggests that the variations of $\delta^{13}\text{C}$ resulted from subduction of crustal C and its role in diamond formation in eclogites(see Kirkley 1991). Some scientists, however, attribute this wide $\delta^{13}\text{C}$ range to processes of high temperature fractionation occurring deep within the mantle (Galimov, 1984, 1991; Javoy *et al.* 1986). There have been several approaches which generally invoke Rayleigh distillation, which

are either at variance with new data or difficult to envisage (Kirkley *et al.* 1991). Variations of $\delta^{13}\text{C}$ in the mantle resulting from heterogeneity of the Earth from the very beginning until the time of diamond formation also discussed (Deines *et al.* 1987). Boyd(1988) and Kirkley *et al.*(1991) point out the difficulty of preserving primordial isotope heterogeneity.

Nitrogen.

The first six analyses of nitrogen isotopic composition in diamonds were reported by Wand *et al.*(1980) and Becker and Clayton. (1977): $\delta^{15}\text{N}$ was found to be in the range 0 — +5‰. Then several crystal aggregates of diamonds from Mbuji Mayi, Zaire were studied for nitrogen isotopic composition by Javoy *et al.*(1984), who recognised wider variations from -11‰ to +5‰. A significant number of data for diamonds from world-wide kimberlites was provided by Boyd(1988) in the first systematic research of nitrogen isotopes in diamonds. Diamonds of different shapes, from different kimberlite pipes were analysed for $\delta^{13}\text{C}$ and $\delta^{15}\text{N}$ and internal variations of $\delta^{15}\text{N}$ within single diamond crystals were demonstrated.

The octahedral diamonds were characterised by wide variations of $\delta^{15}\text{N}$ values from +16‰ to -11‰ (Boyd and Pillinger, 1994) which appeared to be correlated with $\delta^{13}\text{C}$ in some respects: low $\delta^{13}\text{C}$ diamonds ($\delta^{13}\text{C}$ lower than -10‰) contain nitrogen within the range -2.5‰ to +16‰, whereas high $\delta^{13}\text{C}$ diamonds ($\delta^{13}\text{C}$ from -2‰ to -10‰) contain nitrogen ranging from +6‰ to -11‰ (Boyd and Pillinger, 1994).

Nitrogen isotopic composition of fibrous diamonds (coats and fibrous cubic diamonds of IV variety by classification of Orlov(1973)) were found to lie in a rather narrow range of $\delta^{15}\text{N}=-5\pm4\text{‰}$ and $\delta^{13}\text{C}=-6.5\pm3\text{‰}$ (Boyd *et al.* 1994). Based on these data, Boyd *et al.*(1994) suggested a model for the formation of that particular type of diamond. According to this model, the growth of fibrous diamonds resulted when kimberlitic magma invaded continental lithosphere, but failed to move the whole way up to the surface. The magma released a significant amount of fluid saturated with carbon so that rapid crystallisation of diamond could occur (Boyd *et al.* 1994).

1.7.2.3. C and N isotopic geochemistry of the mantle.

It is generally accepted that isotopic composition of the carbon reservoir in the Earth's mantle is about -5‰. This became evident when statistically representative dataset of $\delta^{13}\text{C}$ values for different mantle phases became available. Peaks of $\delta^{13}\text{C}$ distribution for diamonds, carbonatites, carbonates from kimberlites and MOR along with OI basalts are in good agreement with each other, and point out on the existence of a homogeneous reservoir of carbon; no difference was observed for suboceanic (basalts) and subcontinental (kimberlites, carbonatites) mantle. However, the reason for rather wide variations of $\delta^{13}\text{C}$ within diamonds of the eclogitic suite still give rise to discussion. The situation as regards the understanding of the isotopic geochemistry of nitrogen within the mantle remains obscure and puzzling owed to the lack of adequate data. On the basis of $\delta^{15}\text{N}$ values for fibrous diamonds and high- $\delta^{13}\text{C}$ octahedral diamonds, Boyd and Pillinger (1994) concluded that nitrogen in diamonds with $\delta^{13}\text{C} \approx -5\text{‰}$ represents the subcontinental mantle nitrogen reservoir, which is in agreement with the earlier suggestion of Javoy *et al.*, (1986), based on the study of diamonds and basalts. However, the whole range of variations indicated in diamonds from -11‰ to +16‰ could not be explained unambiguously.

1.8. The source material for the Earth's formation.

Since the first steps in development of planetology it is believed that carbonaceous chondrites are the best candidates for the role of source material for the Earth's formation. Relative composition of the major petrological elements of the CI chondrites proved the best match to the bulk Earth, but volatiles could give to rise problems if they could not be removed from the early Earth by degassing process. However, the questions as to how far the process could go and whether it is possible for 99% of volatiles to be removed, are remains without a clear answer.

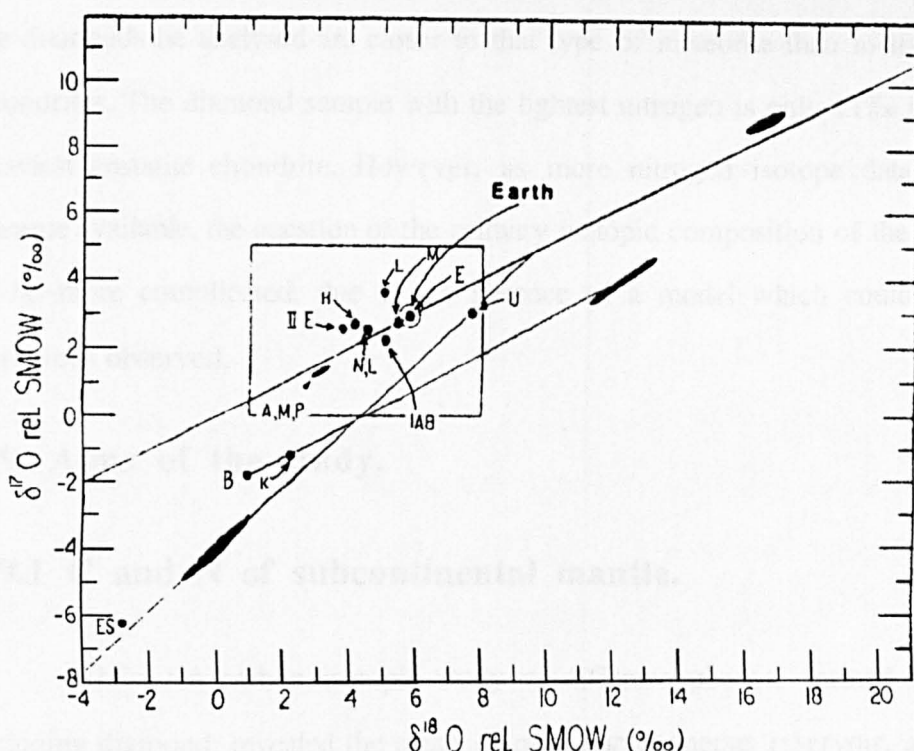


Figure 1.14. $\delta^{17}\text{O}$ - $\delta^{18}\text{O}$ relationships among Earth-Moon and chondrites. H,L -ordinary chondrites; E- enstatite chondrites; A,M,P- eucrites, howardites, diogenites, mesosiderites and pallasites; N, L - Nakhla and Lafayette; U - ureilites; I AB, II E - iron meteorites; B - Bencubbin and Weatherford; ES - Eagle Station, Iizawisis; M - moon; K - Kakangari. (after Clayton *et al.*, 1976)

The revolutionary work of the Chicago group (Clayton *et al.*, 1976) raised the question of the Earth's source material once again when oxygen isotope analysis was introduced to a study of meteorites. They demonstrated remarkable similarity between the isotopic composition of oxygen in the enstatite chondrites and that of the Earth and the Moon, which could not be said for the other types of meteorites (fig. 1.14). Considering hydrogen isotopic composition, the enstatite chondrites appear again to provide the best fit to that of the Earth as compared with our meteorites. However, carbon isotopes do not provide useful way of distinguishing CI, CM and enstatite chondrites, since all of them, together with Earth's bulk carbon, are in the same range of $\delta^{13}\text{C}$ values. Nitrogen, on the contrary, discriminates very strongly between carbonaceous and enstatite chondrites. The $\delta^{15}\text{N}$ of the former ranges from +20‰ to +40‰ whereas for the latter it is from -22‰ to -42‰. Therefore, primary nitrogen of the Earth could be the distinguishing feature in the discussion. According to Javoy *et al.* (1986), the original isotopic composition of the

Earth's nitrogen could be matched with that of enstatite chondrites, since the $\delta^{15}\text{N}$ value of the diamonds he analysed are closer to that type of meteorite than to the carbonaceous chondrites. The diamond sample with the lightest nitrogen is only 11‰ heavier than the heaviest enstatite chondrite. However, as more nitrogen isotope data for diamonds became available, the question of the primary isotopic composition of the Earth appeared to be more complicated, due to the absence of a model which could explained the variations observed.

1.9. Aims of the study.

1.9.1 C and N of subcontinental mantle.

Whilst the carbon isotopic study of different phases, formed in the mantle, including diamond, revealed the presence of a homogeneous reservoir, a more detailed view of diamonds, as representing carbon in sub-continental mantle, indicates the existence of a certain heterogeneity reflected by wide $\delta^{13}\text{C}$ variations in the eclogitic diamonds. Combined C and N isotopic studies undertaken to shed some light on the nature of the heterogeneity of C in diamonds have already indicated certain differences in the distribution of $\delta^{15}\text{N}$ for isotopically light and isotopically heavy $\delta^{13}\text{C}$ diamonds. However, N isotope data for diamonds with heavy carbon ($\delta^{13}\text{C}$ -2‰ — +2.5‰) and with very light C ($\delta^{13}\text{C}$ -15‰ — -35‰) are either not statistically representative or absent which might be explained by the rarity of such specimens as compared with the majority of diamonds which have $\delta^{13}\text{C}$ -5±4‰. Previous C and N studies of diamonds also revealed the fact that N and C isotopic compositions of fibrous diamonds show a very restricted range, whereas octahedral diamonds have wide variations of both C and N isotopic compositions. The reasons for the presence of N isotopic variations in octahedral diamonds is also disputed, and interpretations generally invoke subduction, N evolution from primitive isotopic composition of enstatite chondrite type material to the modern isotopic composition of N reflected by some diamonds, and/or fractionation processes. Octahedral diamonds are known to be associated with two types of paragenetic

assemblages (peridotitic and eclogitic) which supposedly reflect different environments of diamond formation, hence understanding of N isotopic variations of these subtypes can reveal some information on the reasons for the total variations.

Having as the main objective of the research, the further development of C and N isotopic systematics of diamonds hopefully leading to better understanding of the geochemistry of sub-continental mantle, I set our intentions to:

1. Characterising for N isotopic composition diamonds having unusual ranges of C isotopic composition ($\delta^{13}\text{C}$ of 0 — +2.5‰ and $\delta^{13}\text{C}$ of -15 — -30‰);
2. Investigation of N isotopic variations in diamonds of known paragenetic types;
3. Comparison of diamonds formed in the mantle with other types of terrestrial diamonds such as yakutites and carbonado, in terms of C and N geochemistry.

The research is intended to answer the following questions:

1. Do C and N isotopic systematic of diamonds support the subduction influence on the C and N isotope geochemistry of the sub-continental mantle?
2. Is enstatite chondrite type of material a suitable starting point for the Earth's mantle evolution, and can the signs of N evolution of the Earth's mantle be identified?

1.9.2 Carbonado and other polycrystalline forms of diamond.

Carbonado diamonds remain a highly controversial topic in diamond mineralogy and geochemistry, due mainly to absence of a co-ordinated approach to the study of this type of diamond and a comprehensive comparison with other types of polycrystalline diamonds. Two main geochemical distinguishable features of carbonado (extremely light carbon isotopic composition and the presence of highly radiogenic noble gases) may have a significant influence on the understanding of C and N isotopic variations in the diamonds of defined mantle origin, and the significance of possible variations of radiogenic noble gases in diamonds. Therefore, by combining C, N isotopic analysis and N, He content measurements, with IR and internal structure investigations of carbonado diamonds from Brazil and Central Africa, I seek to provide a comprehensive characterisation of these carbonado populations. The comparison of the geochemistry of

carbonado with that of yakutites and framesites may lead either to developing means of separating these diamond groups, or to the similarity with one of them, thereby suggesting the origin of carbonado. The existence of the specific noble gas isotope signature of carbonado is linked to the more fundamental questions of noble gas geochemistry in diamonds, since none of the previous studies of noble gases in single diamond crystals was able to identify the contribution of components of different origin, thus leaving significant uncertainty in the interpretation of data, for example as regards He. Hence, to clear this up, the ^4He zoning could be investigated, since ^4He can characterise the extent of post-growth modification of the radiogenic noble gas isotopic signature due to the implantation as a result of U-Th decay in surrounding environment.

Thus, in respect of carbonado origin the objectives are as follow:

1. To characterise the geochemical and mineralogical properties of carbonado on the basis of the combined study of two sample sets (Brazil and Central Africa);
2. To compare carbonado with other types of polycrystalline diamonds of known origin, and to identify possible links between them;
3. To investigate the possible extent of He concentrations resulted from natural α -particle implantation effect on single diamond crystals from kimberlitic rocks, and to test the necessity of invoked an unusual processes of carbonado formation to explain its noble gas content.

1.9.3 Analytical technique development.

Simultaneous analysis of N and C in samples of terrestrial diamonds was successfully introduced by Boyd *et al.*, (1988) and therefore the principles of nano-mole analysis in a static mass-spectrometer, as well as the gas purification and the gas handling system were adopted for this study from previous works (Wright *et al.*, 1988; Boyd *et al.*, 1988). Even though this research was not targeted at the introduction of new analytical techniques, many developments and improvements were investigated in order to reach the goals on which the research was targeted:

1. It is well known that atmospheric N contamination may have a tremendous effect on the correct interpretation of N isotopic measurements, especially for the samples containing low N contents. Using a combination of step heating and step combustion techniques, the most satisfactory form of temperature treatment of diamond samples prior to analysis to remove any possible N contamination was devised;
2. To increase effectiveness of sample throughput, further improvements of the loading and extraction techniques were achieved;
3. The effect of non-nitrogen contribution on the small gas aliquots (less than 1.5 ng of nitrogen) in the gas handling system was investigated, and an efficient correction procedure was introduced;
4. The performance of simultaneous N, C and noble gas analysis of diamond using the same extraction, gas handling and purification systems requires modification of some units, as well as the introduction of an additional mass-spectrometer and reference system;
4. To increase the effectiveness of the instrument, a fully automated system was developed to perform the whole analysis from the extraction to the isotopic measurements; this was especially important for high resolution step heating and combustion experiments.

Chapter 2. High precision nitrogen stable isotope analysis combined with He, Ar and C isotope measurements performed in an automated mode.

Abstract.

This chapter details the design, calibration and operating protocol for a new automated instrument designed for N, C and noble gas analysis. The instrument includes a gas source static-vacuum mass spectrometer utilised for abundance and stable isotope analysis on picomole quantities of nitrogen gas, a quadrupole static mass spectrometer utilised for analysis of some noble gases and nitrogen content, and a capacitance manometer for the quantitative measurements of carbon yields. The original design of the instrument is similar to that described by Wright et al. (1988) but has been modified to enable analysis of noble gases and to automate the entire analytical procedure.

This instrument is capable of analysing less than 0.1 nmol of nitrogen and about 3×10^{-10} cc of Ar and of 3×10^{-9} cc of ^4He , and is routinely used for stepped heating (pyrolysis and combustion) experiments performed in relation to different geochemical studies. The precision of the $\delta^{15}\text{N}$ measurements range from $\pm 0.2\%$, for 0.1 nmol to $\pm 3.5\%$ for 10 pmol from repeated zero enrichment reference measurements. However, the reproducibility of measurements of standards involving extraction and purification has a standard deviation of $\approx 1\%$. The precision of $^{40}\text{Ar}/^{36}\text{Ar}$ is $\approx 3\%$ $^{38}\text{Ar}/^{36}\text{Ar}$ is $\approx 4\%$ for Ar aliquot of 1.8×10^{-7} cc.

2.1. Introduction.

2.1.1. Nitrogen isotopic analysis.

When compared to the advances made in the high-precision measurement of stable isotopes of light elements such as carbon, hydrogen, sulphur and oxygen in geological specimens, the study of nitrogen isotopes have progressed at a considerably slower rate. One explanation, suggested by Kaplan (1975), is the difficulty in the measurement of an element of low abundance in geological specimens but which constitutes almost 80% of the Earth's atmosphere.

The magnitude of this problem has been reduced by the application of "stepped" heating (pyrolysis) techniques (Chang *et al.*, 1974; Becker and Clayton, 1975). This involves heating the sample in discrete temperature increments under vacuum in order to resolve the various sources of nitrogen within the sample. Further developments were instigated by heating a sample in a pressure of a few torr of oxygen in a stepped combustion extraction (Frick and Pepin, 1981; Lewis *et al.*, 1983), which in conjunction with pyrolysis techniques increased the chance of separating gas from different carriers. However, only the introduction of static mass spectrometers for nitrogen isotopic analysis has really allowed the progress in the understanding of nitrogen isotopic geochemistry (Wright *et al.*, 1988).

2.1.2. Overview of methods used for stable isotope analysis.

Conventional gas source mass spectrometers operating in the dynamic vacuum mode and consistent with early designs (Nier, 1947) are traditionally used for stable isotope analysis. During analyses the mass spectrometer is left open to the pumping system and rapid and repeated comparisons of sample and reference gas are measured by means of a 4-way "changeover" valve. Both are bled consecutively through two capillaries, each from its own reservoir. Although the precision of the $\delta^{15}\text{N}$ values is high, approximately +0.026‰ (e.g. Mariotti, 1984), this method requires relatively large

samples to be used, as the majority of sample gas does not contribute in any way to the analysis. For one analysis, a typical sample size of $>0.1 \mu\text{mol}$ s nitrogen would be required. Assuming an average geological sample contains a few tens of ppm of nitrogen, then the initial sample size would be in the order of 1g . This is impractical with samples that are in limited supply or of a valuable nature such as extraterrestrial material (i.e. lunar samples, meteorites), diamonds and some mineral separates. Application of step heating techniques to separate gases released from different carriers present within the sample would require even larger sample sizes depending on the number of steps needed for resolution of the components.

The advent of static vacuum mass spectrometers began to resolve this problem. Initially developed for noble gas analysis (Reynolds, 1956), static mass spectrometry was suggested as a technique for the measurement of nitrogen abundances (Irako et al., 1975 and later Gardiner and Pillinger, 1979) and then for nitrogen isotopic analysis (Fallick et al., 1980), before finally being developed by Brown and Pillinger (1981) and Frick and Pepin (1981). Static vacuum mass spectrometers resulted in an increase in sensitivity of about 3 orders of magnitude compared to dual inlet dynamic vacuum instruments. The major reason for this improvement was that the mass spectrometer was isolated from the pumps prior to the gas being admitted and hence acted as its own sample reservoir. The huge increase in sensitivity which allowed a corresponding decrease in sample size was achieved at a cost of only a factor of 10 loss of precision for the isotopic measurements (Wright *et al.*, 1988). An extensive discussion of static versus dynamic mass spectrometers has been detailed elsewhere with reference to carbon isotopic analysis (Wright et al., 1983; Wright, 1984; Pillinger, 1984; Carr et al., 1986).

Another instrument commonly used for elemental analysis in industry has recently been introduced for isotopic analysis (Hashizume and Sugiura, 1990). The Quadrupole Mass Spectrometer (QMS) is a device based around a quadrupole mass filter. It is possible to tune the quadrupole to filter out all but specific ions by means of manipulating the “path stability”. Practically, this means that only ions of a certain range of charge/mass combination can pass through the radio frequency (r.f.) electric field generated between

the four poles of the filter (Todd and Lawson, 1975). By tuning this r.f. field it is possible to select charged ions with a small mass range effectively limited to a single atomic mass. Using parameters for the ion source and detector it is then possible to optimise the detection of these ions. The ease, with which a radio frequency can be allocated (scanned) to tune different masses, enables the QMS to acquire data more rapidly than a sector type mass spectrometer. The only drawback with the system is that inaccuracies in the measurements made it very difficult to study of N, Ne and Ar abundances together with isotopic composition. Hashizume and Sugiura (1990), however developed the QMS for use in static mode eliminating inaccuracies with alterations in experimental technique and statistical analysis of large numbers of measurements.

2.1.3. N isotopic studies and the advantages of combined analysis of isotopic ratios of N with other gases.

The static mass spectrometry technique applied to the isotope analysis of nitrogen in geological samples has successfully been introduced in many fields of geochemistry. While important results for understanding the subcontinental mantle geochemistry have been obtained by systematic study of diamonds (Boyd, 1988), many encouraging data have been obtained for extraterrestrial materials such as meteorites, lunar soils and interstellar grains (see for reference Pillinger, 1992). Although many researches have been carried out on nitrogen geochemistry of suboceanic mantle (Sakai *et al.*, 1984; Exley *et al.*, 1987; Javoy and Pineau, 1991), only simultaneous analysis of N and Ar isotopes have led to the significant progress in the understanding of N and Ar isotopic variations of MOR basalts (Marty, 1995, Marty *et al.*, 1996). Many other studies have also pointed out the importance of conjoined N, C and noble gas analysis with step combustion-pyrolysis technique due to the heterogeneity of most natural samples. Therefore, development of an instrument working automatically and capable of the analysis of N, C and noble gases seems to be essential for understanding terrestrial and extraterrestrial geochemistry of volatiles.

2.4. Aims of this work.

Here in I discuss operation procedures and the design of extraction and purification systems, reference gas systems, for two static mass spectrometers (a magnetic sector gas source static vacuum mass spectrometer routinely used for nitrogen isotope measurements and quadrupole static mass spectrometer used for noble gas measurements). Both instruments were built with a view to being used in automatic mode. The design of this instrument is developed from that described previously by Wright et al . (1988) and utilises the principles of the extraction and purification techniques described by Boyd et al . (1988). However, major modifications have been made to the inlet section and pumping systems, and to the operation of the instrument, which have improved the precision and accuracy of the nitrogen isotope measurements by a factor of 10 and hence led to a further reduction in the sample size required for analyses of nitrogen abundances and isotopic composition. Using a highly sensitive quadrupole mass spectrometer enables simultaneous analysis of nitrogen and noble gases in the same samples. Automation of the entire procedure from extraction to the isotopic analysis has simplified and regulated usage of the instrument and is a step forward in respect of standardisation of the step heating technique, whilst freeing the operator from tedious instrument minding over extended (many hours) periods.

2.2. General overview of the instrument.

2.2.1. The overview of the inlet system.

The inlet system with exception of parts of the combustion section, purification volumes and loading section is constructed in stainless steel 3/8 inch and 3/2 inch diameter pipework as opposed to the pyrex glass-line technology previously employed; various parts of pipeline are joined together by VCR type of fittings (Valve and Fitting Co, U.K.), and by FC flanges (Vacuum Generator Co, UK) The advantages of this are that the inlet is more robust and less prone to breakages, and that a cleaner vacuum can be

maintained as the metal system can easily be baked at 100-150°C to reduce contamination on the inner surfaces of the pipework. The sample gas is manipulated around the inlet by the use of two types of BK series air-actuated valves (Nupro, Valve and Fitting Co, U.K.), CR38 valves (VG Hastings, Sussex, U.K.) and pneumatic right-angle valves (AV150M-P, MDC). The configuration of the inlet is illustrated in Figure 2.1 and 2.2.

2.2.2. Pumping systems.

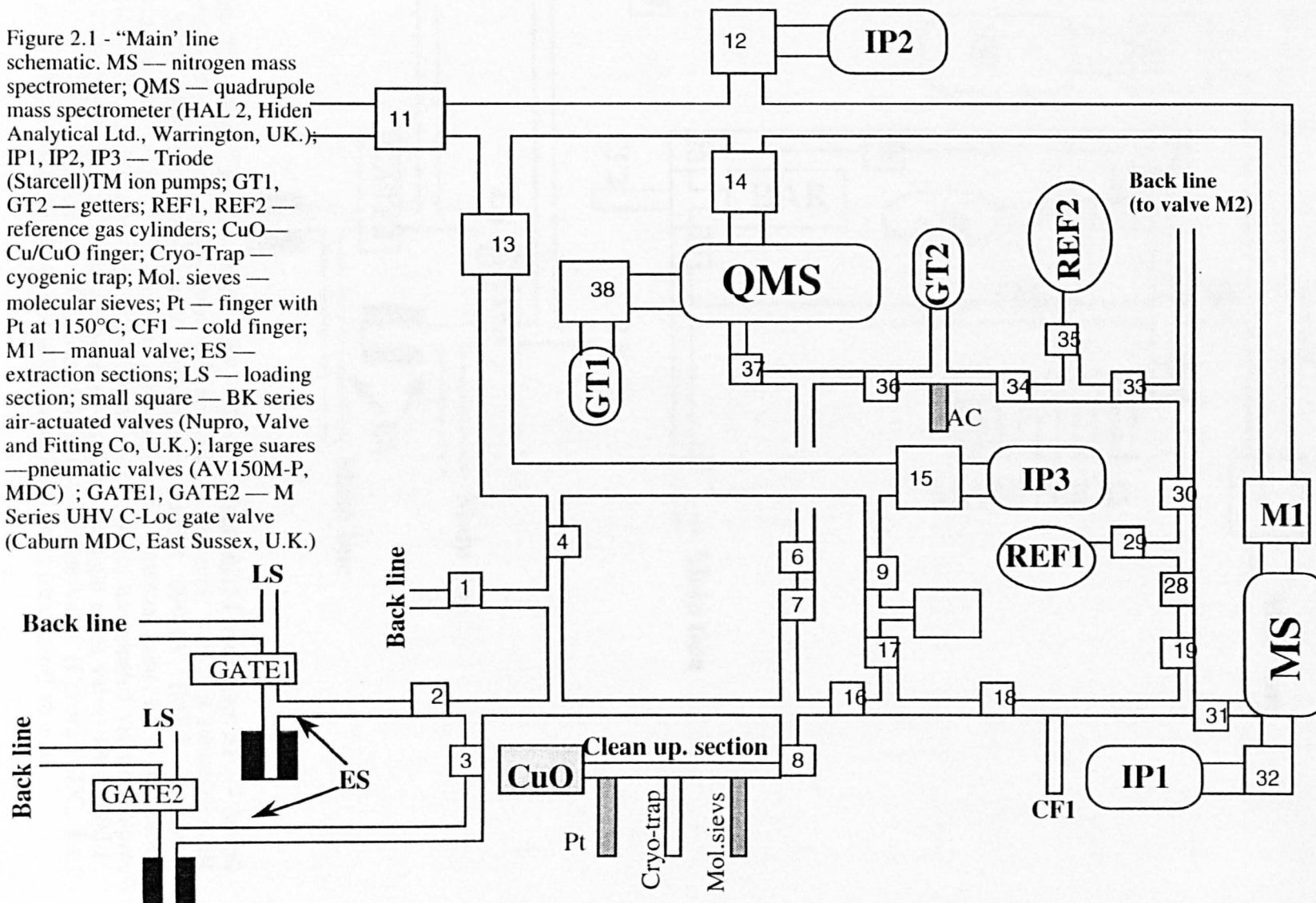
There are two separate vacuum systems for the inlet:

- i) The "main" line (fig. 2.1) which evacuates the combustion section, purification sections and the sample split volumes (i.e. the line routinely used during sample analysis).
- ii) The "back" line (fig. 2.2.) which pumps out the sample loading and standard loading section, the capacitance manometer, CO₂ split volumes, manifold and the N and noble gas reference gas aliquotting systems.

Both of these lines are maintained at high vacuum by two Triode (Starcell)TM ion pumps (IP3 and IP4) in conjunction with IPS60 power supplies (VG Hastings, Sussex, U.K); ion pumps are separated from the pipe line by pneumatic right-angle valves (AV150M-P, MDC). These can monitor pressures in the range of 10⁻⁴ mbar to 10⁻⁹ mbar. The main line is usually maintained at a pressure of <10⁻⁸ mbar, whereas the back line operates at ≈10⁻⁷ mbar.

Rough pumping for inlet pressures of >10⁻³ mbar (e.g. after loading a sample) is achieved using a model MS50 sorption pump (VG Hastings, Sussex, U.K) packed with 50 nm molecular sieve. The combination of sorption pump and ion pump provides a completely oil-free pumping system and hence a greatly reduced hydrocarbon background.

Figure 2.1 - "Main" line schematic. MS — nitrogen mass spectrometer; QMS — quadrupole mass spectrometer (HAL 2, Hiden Analytical Ltd., Warrington, UK.); IP1, IP2, IP3 — Triode (Starcell)™ ion pumps; GT1, GT2 — getters; REF1, REF2 — reference gas cylinders; CuO — Cu/CuO finger; Cryo-Trap — cryogenic trap; Mol. sieves — molecular sieves; Pt — finger with Pt at 1150°C; CF1 — cold finger; M1 — manual valve; ES — extraction sections; LS — loading section; small square — BK series air-actuated valves (Nupro, Valve and Fitting Co, U.K.); large squares — pneumatic valves (AV150M-P, MDC) ; GATE1, GATE2 — M Series UHV C-Loc gate valve (Caburn MDC, East Sussex, U.K.)



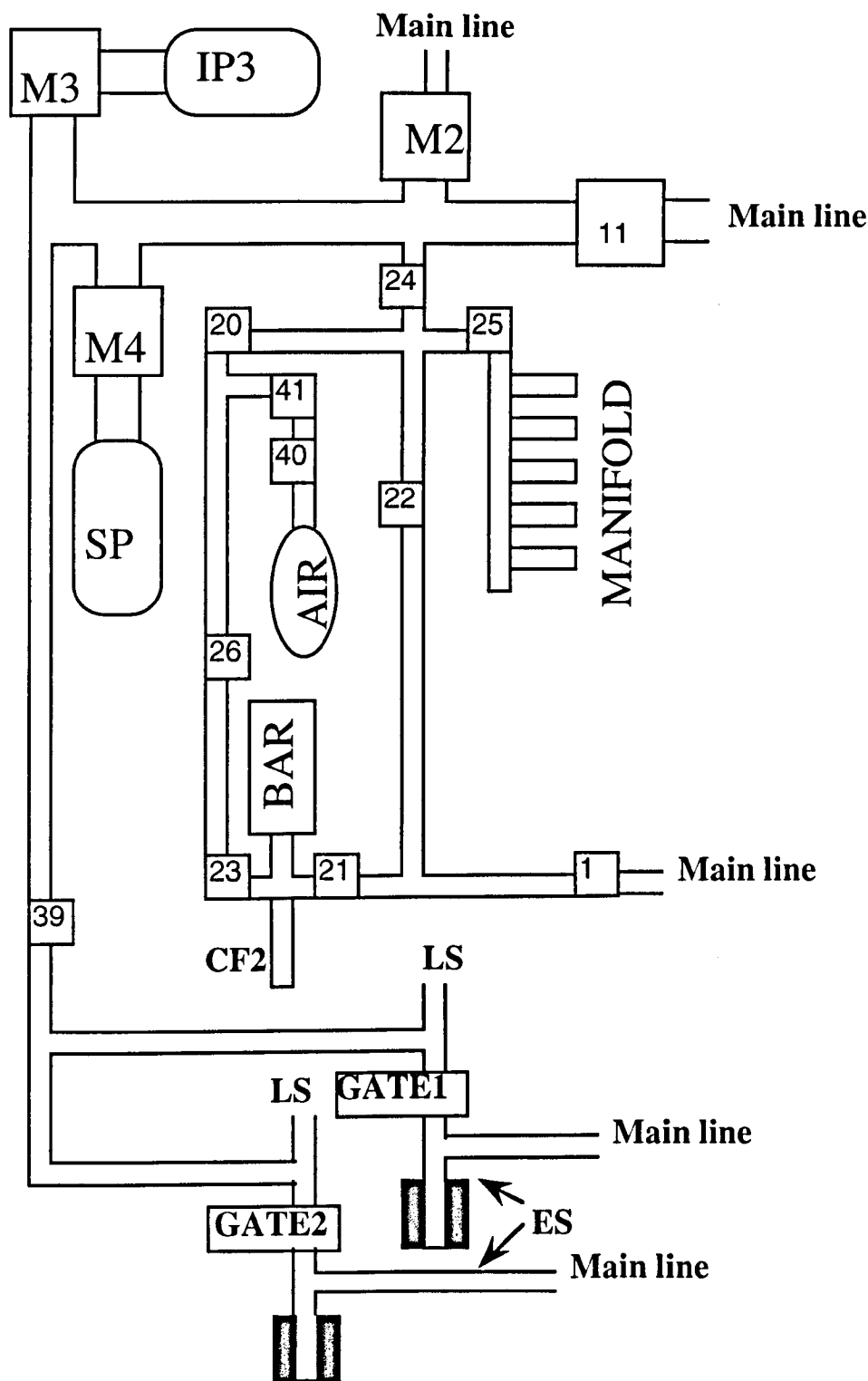


Figure 2.2. "Back" line schematic. IP4 — Triode (Starcell)™ ion pump; SP — MS50 sorption pump (VG Hastings, Sussex, U.K.); AIR — reservoir with AIR standard; BAR — MKS Baratron capacitance manometer, model 390HA (MKS Baratron, Massachusetts, U.S.A.); CF2 — cold finger; M2; M4 — manual valve; ES — extraction sections; LS — loading section; small square — BK series air-actuated valves (Nupro, Valve and Fitting Co, U.K.); large squares — pneumatic right-angle valves (AV150M-P, MDC); GATE1, GATE2 — M Series UHV C-Loc gate valve (Caburn MDC, East Sussex, U.K.); MANIFOLD — manifold including 5 ports for take off vessels.

The nitrogen analyser is connected to a Triode (Starcell)™ ion pump (IP1 fig. 2.1), in conjunction with a VPS60 power supply (VG Hastings, Sussex, U.K.), by a CRP38 high vacuum, bakeable stainless steel valve (VG Hastings, Sussex, U.K.) and to the inlet section via a modified NUPRO 4BK all metal bellows valve (NUPRO, Oxford Valve and Fitting Co, Oxon, U.K.). These valves are shown in Fig. 2.1. as 32 and 31 respectively. If the mass spectrometer is at atmospheric pressure (i.e.. after filament replacement or vacuum loss), it can be evacuated to a pressure of 10^{-3} mbar via a manual valve M1 (CR38, VG Hastings, Sussex, U.K.) and valve 11 to a sorption pump situated in the inlet (Fig. 2.1 and 2.2).

The vacuum in the QMS (HAL 2, Hiden Analytical Ltd., Warrington, UK) is maintained via valve 14 by a Triode (Starcell)™ ion pump (IP2 fig. 2.1), in conjunction with a VPS60 power supply (VG Hastings, Sussex, U.K.) In order to decrease hydrocarbon background in the QMS it is also connected to the Ti-Al getter (GT1, fig. 2.1) via valve 38, allowing separation of the QMS from the getter when nitrogen analysis performed.

2.3. Loading system.

The two similar loading systems are attached to the inlet of the “back” line and are designed with several objectives in mind: (i) high sample throughput; (ii) ability to perform thermal treatments of the samples prior to analysis to remove gas components which are not of interest (e.g. atmospheric and organic contamination).

2.3.1 Overview.

The samples can be sequentially placed in the loading volume situated between a M Series UHV C-Loc gate valve (Caburn MDC, East Sussex, U.K.) and valve 39 (fig. 2.3). The gate valve (GATE, fig. 2.3) is a manual valve with a Viton O-ring seal which separates the high vacuum combustion section from the back line. The loading volume consists of a glass section, where up to 10 samples can be held, attached to a metal-glass connection (Valves and Fittings Co., UK). The glass section contains a quartz tube joined

with a pyrex tube by quartz-pyrex connection (Cambridge Glassblowing Co., UK) and two Young valves (H Young, Scientific Glassware Ltd., UK), one of which is used for sample introduction and another to separate the loading volume from the inlet of the back line to decrease the size of the volume which is necessarily exposed to atmosphere. A schematic of the loading system is illustrated in Fig. 2.3.

2.3.2 Sample preparation.

Several ways of sample preparation for nitrogen isotopic analyses have been suggested in the previous studies (e.g. Boyd, 1988). Perchloric acid, for example, oxidises all forms of carbon except diamond therefore treatment with HClO_4 were applied in order to remove organic contamination from samples. In addition combustion in the atmosphere, at 500°C for 3-4 hours as suggested by Boyd (1988) was applied for diamond samples prior to analysis. In order to optimise the above treatments pyrolysis at $1100\text{-}1200^\circ\text{C}$ prior to combustion of diamond was investigated. The loading section has been designed so that samples can be pre-pyrolised before the actual experiment (fig. 2.3).

2.3.3 Loading procedure.

The loaded samples are evacuated overnight with the back line ion pump (IP4, fig. 2.2) after pumping on the - sorption pump (SP, fig. 2.2) . To drop the sample into the extraction section, the gate valve is opened and the sample can be moved into the combustion tube using the metal magnet (fig. 2.3.). After the sample is loaded the gate valve is then closed and the extraction can commence.

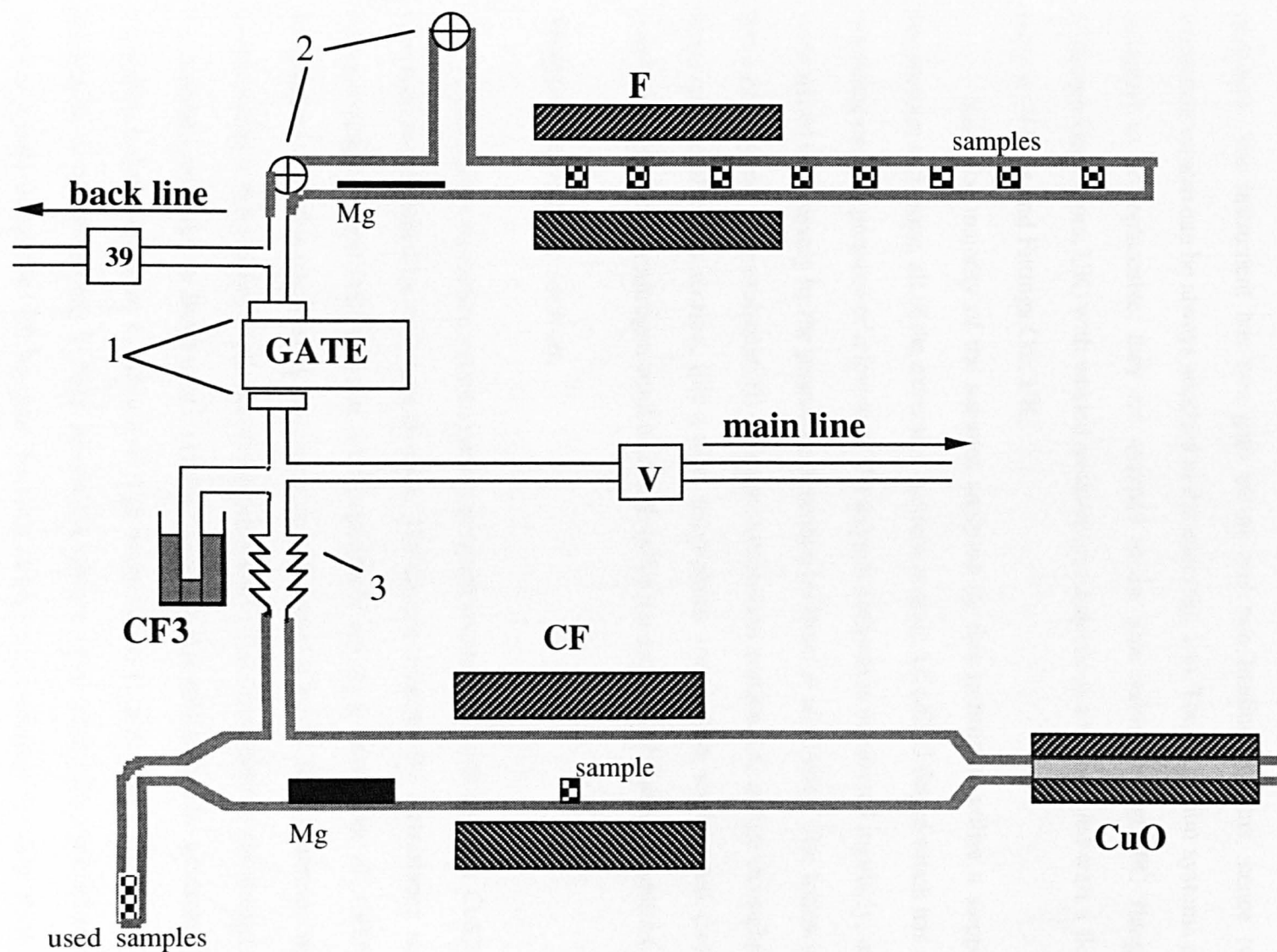


Figure 2.3 Loading section and horizontal combustion system. F — furnace; CF — combustion furnace; CuO — Cu/CuO reservoir and furnace; CF3 — cold finger; GATE — M Series UHV C-Loc gate valve (Caburn MDC, East Sussex, U.K.); V — valve 2 or 3 see fig. 1; Mg — magnet; 1 — flanges (Valves and Fittings Co, UK); 2 — Yuong valves; 3 — flexy section (G321-6-GX-3, Cajon Co., UK); plain lines — metal pipework; grey lines — pyrex or quartz pipes.

2.4. Extraction system.

2.4.1. Overview.

Several extraction systems of different design were investigated for experimental purposes. The instrument has two gate valves and two loading systems, hence two extraction system can be always attached to the inlet (fig. 2.1). The extraction systems are designed to be replaceable; they are attached to the gate valve through FC flanges (Vacuum Generators, UK) with welded metal-glass connections accompanied with a flexi section (Valves and Fittings Co., UK).

Since the majority of the samples analysed by this instrument utilise a stepped combustion technique, all of the extraction sections contain a Cu/CuO finger which has an operating oxygen pressure of a few torr. The oxygen pressure is monitored regularly, and replenished if necessary by the procedure described by Boyd *et al.* (1988). The following types of systems were evaluated: (i) a simple combustion section, (ii) a high throughput horizontal combustion section, (iii) a high temperature combustion section and (iv) a combustion section for nitrogen combined with noble gas analysis of diamond samples.

Simple combustion section.

The simple extraction system consists of quartz reactor tube with attached Cu/CuO reservoir accompanied by resistance furnace. The sample is heated by a resistance wire furnace designed and built on site for temperatures up to a maximum of 1300°C; temperature control is obtained by the use a chromel-alumel (Cr Ni / AlNi) thermocouple connected to a temperature controller (Eurotherm 808). The description of the design of the furnaces are given by Boyd *et al.* (1988). Although this system has an advantage of simplicity it does not allow: 1) safe use of high temperatures (higher than 1200°C) due to collapsing of quartz reactor; 2) high sample throughput since after each experiment the sample should be touched off by glass blowing leading to an increase in blank level; 3) limited ability to combust large samples (diamonds in particular) due to absence of the

oxygen flow in the reactor; 4) use for a He analysis due to a high He blank (He easily diffuses through quartz).

Horizontal combustion section.

In order to analyse samples (especially diamonds) routinely using bulk combustion technique a horizontal combustion section has been designed (fig. 2.3). It has Cu/CuO reservoir on the one side of the quartz reactor tube and on the other side a cold finger and a finger used for storage of analysed samples. Using such a design CO₂ is continuously frozen down giving the oxygen better access to the sample, this results in increase of a size of diamond which can be combusted in one step. Since furnaces can be moved, the spent sample can be removed by the metal magnet from the reactor straight after the sample gas transferred in the purification section. Therefore, blank between different samples does not change considerably. This design allows analysis of up to 7-8 diamond samples over a day, however the temperature ranges used and noble gas blanks are similar to those associated with type of extraction system described above.

High temperature combustion section.

In order to increase the range of extraction temperatures and to decrease noble gas blanks an extraction system having the space surrounding the reactor tube and Cu/CuO reservoir maintained at low vacuum (Fig.2.4,b) has been investigated. The supplementary vacuum is achieved by surrounding each with a jacket (alumina for the reactor and quartz on the Cu/CuO reservoir) and evacuating the space between by rotary pump. The main reasons for this are that it prevents internal quartz reactor tube from collapsing at temperatures of 1500°C and also dramatically decreases noble gas blanks due to reduced exposure to atmospheric diffusion.

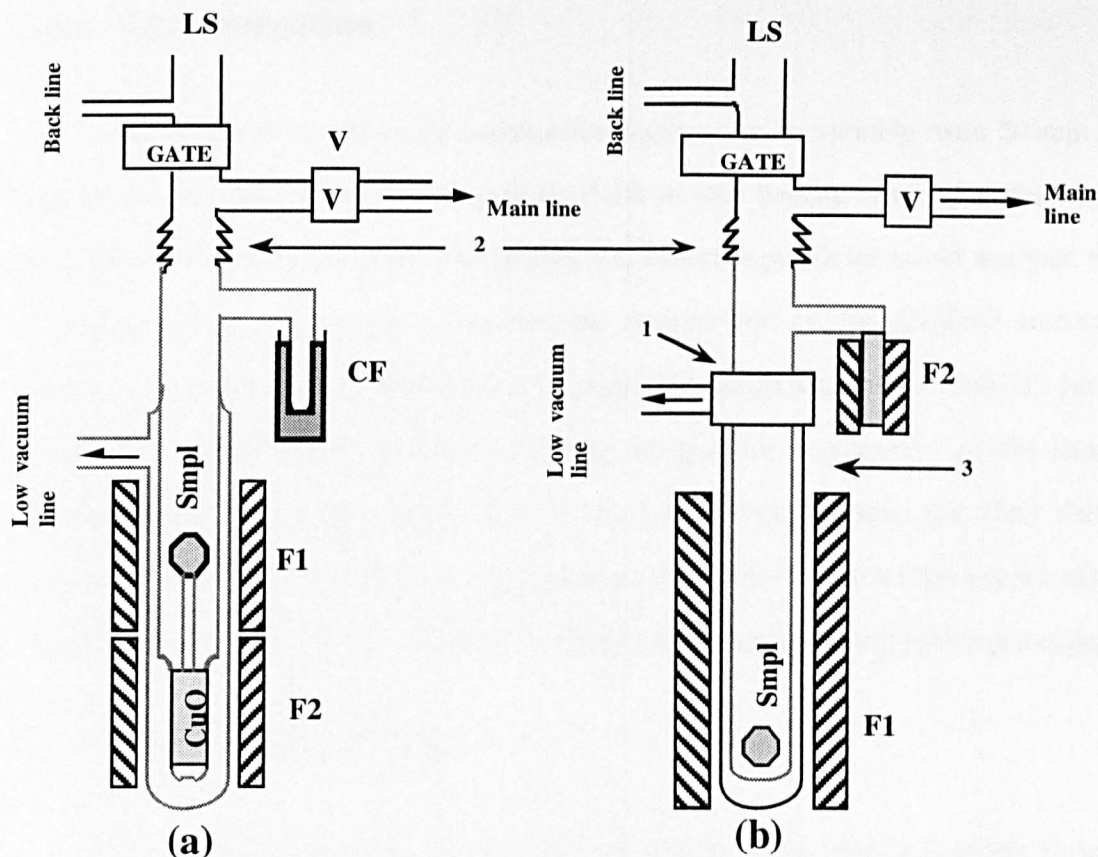


Figure 2.4. Extraction sections used for experiments involving noble gases. (a) — combustion section used for combustion of large samples; (b) — high temperature section. F1 — sample furnace; F2 — Cu/CuO furnace; CF — cold finger; CuO — Cu/CuO reservoir; GATE — M Series UHV C-Loc gate valve (Caburn MDC, East Sussex, U.K.); V — valve 2 or 3 see fig. 2.1; 1 — flanges (Valves and Fittings Co, UK); 2 — flexy section (); 3 — alumina tube; plain lines — metal pipework; grey lines — pyrex or quartz pipes.

Combustion section used for combined N, C and noble gas analysis in diamonds.

The last extraction system described here provides low noble gas blanks and also an ability to combust large diamond samples. This system has a Cu/CuO reservoir and cold finger split at different ends of the reactor tube (fig. 2.4a) and quartz jacket is attached to the reactor and the Cu/CuO reservoir (the space inside the jacket is held at the low vacuum). However, this design does not allow samples to be removed from the reactor and each new experiment can only be started after entire combustion or degassing of the previous one.

2.4.2 Gas extraction

The length of a step in the combustion section can be variable from 20 min to 1 hour, depending on: (i) the type of analysis (bulk or step heating types of extraction; (ii) the number of constituent gases to be analysed as different purification and analysis times are required. For a pyrolysis extraction the temperature of the Cu/CuO furnace is maintained at 450°C. For a combustion extraction, the temperature of the Cu/CuO furnace is increased to 850-920°C in order to liberate oxygen for combustion of the sample. Before transferring of the sample gas in the purification section, the CuO furnace temperature is reduced to 600°C for 5-10 minutes, to reabsorb most of the excess oxygen and then reduced to 450°C for a further 5-10 minute to reabsorb any remaining oxygen.

2.5. Purification system.

The purification section consists of a molecular sieve trap, a Cu/CuO finger, a platinum finger and a variable cryogenic trap (temperatures on all traps are controlled by Eurotherm temperature controllers (see 2.9.2)). The original design of this section has been described in some detail by Boyd et al . (1988). The aim of this section is to collect the sample gas from a temperature step and purify it prior to its analysis in the mass spectrometer. The purification procedure was originally designed to remove any species which could ultimately interfere with the m/z 28 and 29 i.e. CO, CO₂ , dimerised CH₄ etc. and to reduce any nitrogen oxide species to N₂ gas. Since the instrument can perform sequential analysis of He content and Ne, Ar, N and C isotopic compositions and contents the purification procedure is not exactly the same as was used for N analysis (Boyd, 1988).

Stage 1.

After the extraction stage, the sample gas is transferred to the molecular sieves kept at the liquid nitrogen temperature with an exception of He and Ne which can not be trapped by molecular sieves. To avoid mainly He contamination through single walled

glass, the Cu/CuO finger is held at room temperature. Subsequently an appropriate aliquot of He and Ne can be taken and analysed by QMS.

Stage 2.

This stage of purification is equivalent to that described by Boyd, (1988) used for N analysis. At the end of this stage CO₂ is frozen down on the cryogenic trap while N and Ar are in the gas phase available for the analysis. For most of the samples the N and Ar mixture is split in approximately equal volumes: 50% for Ar analysis and 50% for N are taken separately for analysis of their isotopic compositions and abundances.

Stage 3.

The carbon dioxide frozen on the cryogenic trap is released while temperature on the trap is increased up to -120°C and then it is frozen down again on to the capacitance manometer (baratron) cold finger. Then, after the CO₂ is released from the baratron cold finger, it can be appropriately split and measured by the baratron (see section 2.7).

2.6. Isotopic measurement.

2.6.1. Isotopic analysis of the gases extracted from samples.

Currently the QMS is used for (i) quantitative simultaneous analysis of ⁴He content and Ne isotopes; (ii) isotopic analysis of Ar in half of the Ar-N mixture; (iii) measurement a small aliquot of N to estimate N abundance and select an appropriate proportion of sample gas to be let in to the MS.

QMS measurements are performed in static mode with background data taken prior to sample analysis. The background is measured while the QMS is connected to the ion pump (IP2, fig. 2.1). After background measurements the QMS is separated from the ion pump (IP2 fig. 2.1) by closure of the valve 14 and a sample gas is let in to the chamber through the valve 6. If necessary the small aliquot of sample gas can be taken using volume between valves 6 and 7 to be analysed to give an indication of total

abundance; according to the size of this aliquot the instrument chooses an appropriate proportion of the sample gas to be let into the mass spectrometer for maximum accuracy without saturating the system. Following 20 seconds of equilibration, the acquisition of data starts. The number of performed scans can be variable from 50 to 200 depending on the purpose of analysis.

Measurement of the small nitrogen aliquot is performed in a similar mode to noble gas measurements except for the fact that for nitrogen analysis the getter is separated from the QMS by closure of valve 38 (fig. 2.1). Ions of m/z 14 and 29 are measured in the aliquot to give a guide to the abundance of nitrogen and its isotopic composition (measurement of m/z 29 is especially important for exotic extraterrestrial samples (e.g. Franchi *et al.*, 1986) which contain extremely heavy nitrogen ($\delta^{15}\text{N} > +350\text{‰}$)).

Once the nitrogen aliquot is analysed by QMS, a splitting sequence can be selected to take an appropriate aliquot for nitrogen isotopic analysis proceeded using the MS. The analysis is performed in static mode with zero data taken prior to sample measurements. After the background measurements, the chamber is separated from the ion pump and the nitrogen aliquot can be let in to the MS. Data acquisition starts following equilibration between the aliquot volume used and the MS chamber (20 seconds). Since the MS contains three collectors, intensities of m/z 28, 29 and 30 are simultaneously acquired. Final data are presented as intercepts of 28/29, 30/29 ratios and 28 intensity corrected for background measurements.

2.6.2. Quadrupole static mass spectrometer.

The QMS used in this instrument is a HAL 2 (Hiden Analytical Ltd., Warrington, UK.). Gases in the QMS are ionised using a tungsten filament. The mass resolution is approximately 1 atomic mass unit. The ion beam is intensified by a secondary electron multiplier, rather than faraday collectors as used in most stable isotope instruments.

2.6.3. Nitrogen static mass spectrometer.

The mass spectrometer is a modified version of a Dennis Leigh Technology Magnetic Sector analyser (DLT, Winsford, Cheshire, U.K.), with a 110mm radius flight tube and a 90° magnetic sector.

2.6.3.1. The ionisation source.

The ionisation source is a traditional "nude" Nier type design as described by Wright et al (1988). The ionising electrons are emitted by a tungsten filament (DLT, Winsford, Cheshire, U.K.), operating at 3.5-4.0 A, with an ionising energy of 76eV, producing an operating trap current of 125μA. A tungsten filament is preferred to others such as rhenium, because it has been observed to be more durable, although initially it takes longer to degas (Wright et al., 1983). This ensures that the mass spectrometer is operational for longer periods of time as the filament has a greater life expectancy. Ionisation source parameters are controlled by a source control box (DLT IOS 5001, Winsford, Cheshire, U.K.).

2.6.3.2. The collector assembly.

The ion beam is focused into the collectors by means of a 90° sector magnet generating a flux density of 0.4 T. The total volume of the mass spectrometer, including source and collector housing is estimated to be $\sim 0.5 \times 10^{-3} \text{ m}^3$. The collector assembly utilised on this instrument is a modification of that described by Carr *et al.* (1986) for carbon isotopic analysis. The system uses three separate Faraday collectors, one each for mass 28 ($^{14}\text{N}^{14}\text{N}^+$), mass 29 ($^{15}\text{N}^{14}\text{N}^+$) and mass 30 ($^{15}\text{N}^{15}\text{N}^+$). In previous instruments (Wright *et al.* 1983), the impinging ion beams were scanned over the collector in order to allow abundance and isotopic measurements to be made, whereas in this instrument the collectors are fixed and the ion beams are focused directly into the correct collector. The two major advantages of this procedure are: (i) it has allowed the abundance of mass 30

within the mass spectrometer to be ascertained, and hence correction made for the contributions of CO and any hydrocarbons to the nitrogen analyses (see section 2.10.1.4); (ii) it minimises the length of time for each analysis and increases the number of data points measured during this period. The importance is obvious, when dealing with an element such as nitrogen with a relatively short half-life against destruction in the mass spectrometer. The increased number of measurements can only enhance the precision of the final results and reduce the errors associated with the measurements. For comparison, the instrument described by Wright *et al.* (1988) would make only 15 scans of the ion beam, each scan taking 20-30 seconds, whereas the instrument documented in this paper makes 100 measurements on each collector in two minutes.

2.7. Carbon abundance measurements

Carbon abundances are measured on a capacitance manometer (MKS Baratron, model 390HA, Massachusetts, U.S.A.), connected to a metal liquid nitrogen trap, where CO₂ released from the sample is usually frozen down after the end of nitrogen isotopic analysis (see section 2.5) and then can be released in the baratron volume (between valves 21 and 23, fig. 2.2). The CO₂ pressure in the baratron is displayed on a digital meter with a saturation pressure of 1 torr; if the baratron is saturated an appropriate splitting procedures are used. Subsequently CO₂ can be transferred into a take off vessel attached to the manifold (fig. 2.2) and eventually analysed using an off line dynamic mass spectrometer.

2.8. Reference gas aliquotting systems.

2.8.1 Nitrogen reference gas aliquotter.

The nitrogen reference gas consists of 99.998% pure nitrogen (White Spot Grade, British Oxygen Corporation, Ipswich, U.K.) which is stored in a metal cylinder behind valve 29 (Fig. 2.1). In order to accurately calculate the correct isotopic composition of any sample gas analysed on this instrument, the reference gas has to be initially calibrated

with respect to AIR or another known nitrogen standard (section 2.10).

Previous mass spectrometers have utilised two reference gas systems: a fixed volume and a variable volume aliquotting system (Wright et al ., 1988; Wright *et al.*, 1983; Carr et al ., 1986). However, this method of reference gas metering proved to be too restrictive in dealing with a large variety of nitrogen abundances and it is also difficult to automate.

For the instrument described herein, sample and reference are matched by means of a capillary gas pipette (between reference gas volume REF1 and valve 29, fig. 2.1) capable of delivering picomole quantities of reference gas into the inlet with a reproducibility of 0.5% once the instrument has stabilised (Pillinger, 1992). Using this technique, the quantity of reference gas to be admitted into the mass spectrometer is determined, not by adjusting the volume of the aliquotter, but by altering the length of time that reference gas is bled into the constant volume contained by valves 27, 28 and 29. This is known as the bleed time. Initial testing of the capillary aliquotter was carried out by Russell (1992) using the carbon static vacuum mass spectrometer described by Carr *et al.* (1986) to ensure there was no fractionation effects from the capillary. In order to ensure that any sample gas can be matched with an equal pressure of reference gas, the capillary is set to a bleed rate of ~ 1 pmol/s. The accuracy of the aliquotting is discussed in Appendix 1 (fig. A1-1 and table A1-1).

After the reference gas has been bled into the inlet volume for the desired length of time, valve 29 is closed, and the gas is expanded up to the inlet valve of the mass spectrometer. Before being admitted into the analyser, any trace contaminants e.g. CO₂ are removed by a liquid nitrogen cold trap (CF1, fig. 2.1) placed between the inlet and the mass spectrometer.

2.8.2 Noble gas reference gas aliquotter.

An aliquotter of a similar design is used for noble gas reference gas analysis, but the cylinder is filled with air to provide a mixture of noble gases. It consists of reference vessel filled with air at about 3 atm pressure and connected to the vacuum system via a

capillary through which a continuous flow of the air is bleeding. The system makes it possible to take any necessary aliquot of the air. The noble gas reference aliquots are purified prior to analysis using Ti-Al getter (GT2 fig. 2.1); some of the noble gases can be trapped on activated charcoal (AC, fig. 2.1), if necessary. Relative abundance of He in the reference gas was found to be different from the expected value for air i.e. $(\text{He}/\text{Ar})_{\text{ref}}/(\text{He}/\text{Ar})_{\text{AIR}} \approx 17.5$ (the effect is possibly due to fractionation at constant rate by passage through the capillary); the He/Ar ratio was found to be unchanged over the 1 year period of time. The capillary is set to a bleed rate of 1.77×10^{-11} and 1.5×10^{-9} for He and Ar respectively, and the dependence between the bleed time and the intensity of the signal measured by QMS were found to be linear (Appendix 1: fig. A1-2, A1-3 and A1-4) as in the case of nitrogen reference.

2.9. Automation of the analysis.

All analytical procedures including extraction, purification and actual analysis are controlled by a Opus Technology 486 PC together with Labview Graphical Programming Language version 4.0. The latter was chosen specifically for its intuitive programming style, allowing access for maintenance and upgrading to those with an interest in the mass spectrometer who do not have formal programming skills. The computer communication configuration is illustrated in fig. 2.5.

2.9.1. Inlet system.

The valves, which are used routinely during analyses, are pneumatically operated utilising compressed air generated in the two lines by two compressors. Valves and relays are controlled using the valves control device which is a product made at the Open University (four of these devices are currently being used). It is designed to latch data regarding up to 12 valve or relay settings in or out upon being addressed and strobed by the computer. A key safety feature is that the controllers also allow manual control of the valves, in the event of computer failure.

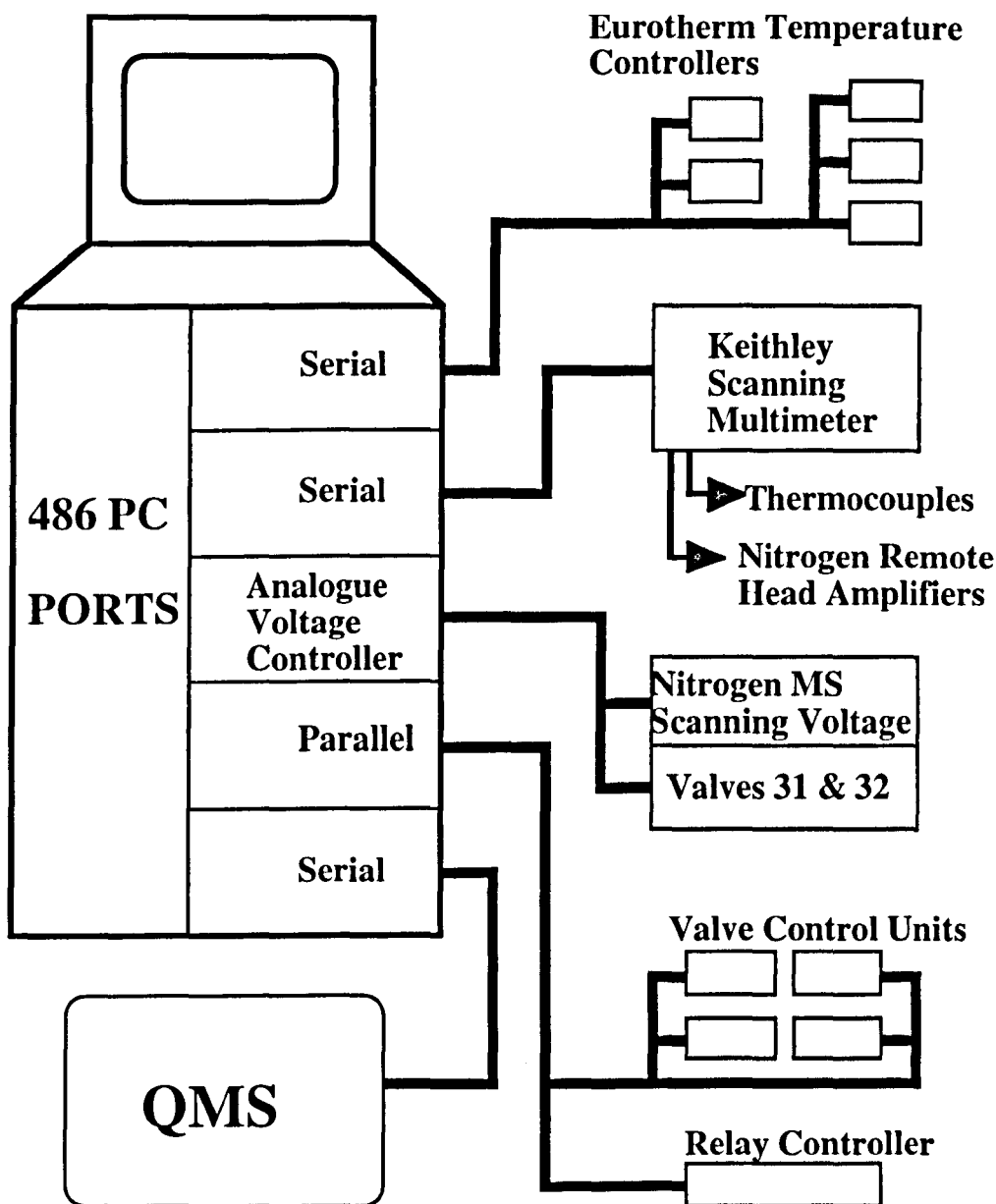


Figure 2.5. Configuration of the computer communications.

2.9.2 Control of temperature.

Analyses performed by the instrument require various accurately controlled temperature states to be achieved in different parts of the system (the furnaces, cryo-trap, Cu/CuO fingers etc.). Eurotherm 808 series temperature controllers (Eurotherm Controls Ltd., UK) are used to monitor and maintain these temperatures, by adjusting the internal heater power consumption for each device. The PC is able to read current status and write

target these temperatures via the serial link.

For complete automation of the system is necessary to be able to control the cooling of the cryogenic trap, cold fingers and molecular sieve. One of the simplest methods, adopted here, is to use a network of pipes and valves and simply pump nitrogen taken from a liquid nitrogen reservoir dewar flask through a metal jacket surrounding each device to be cooled, as and when required. Computer control is achieved by use of the valve control devices operating the valves and switching the pumps on and off.

The molecular sieve also contains an internal heating element, this is switched on as a time saving measure for rapid degassing during the clean up procedure. For the cryogenic trap, the internal heater and Eurotherm 808 temperature controller, operating in conjunction with “pulsed” nitrogen cooling enables the cryogenic trap to acquire and maintain any temperature between liquid nitrogen temperature and 200°C as necessary.

2.9.3. QMS control.

The controller unit, supplied with the QMS, performs the manipulation of the quadrupole r.f. field and allows the user full control of masses detected and sensitivity of the detector, within certain parameters, performing several modes of scanning. This controller is operated by the PC in its turn, thus it acquires results of mass scans generated by QMS and for subsequent processing.

2.9.4. Nitrogen MS control.

The Analogue Voltage Card is used to set the scanning voltage for the nitrogen mass spectrometer. The m/z 28, 29 and 30 intensities are read using a Multimeter with Scanning Card (Keithley Instruments Inc., USA) connected to the mass spectrometer remote head amplifiers. Each amplifier has a different sensitivity. The major (mass 28) uses a $1\text{G}\Omega$ resistor, with a sensitivity of 10^{-8} A at full scale deflection (f.s.d). The minor 1 ($m/z=29$) uses a $100\text{G}\Omega$ resistor with 10^{-10} A f.s.d and minor 2 ($m/z=30$) uses a $100\text{G}\Omega$ resistor with 10^{-11} A f.s.d.. The PC is then able to acquire data from the

multimeter for producing the intercept values of intensity of m/z 28, and 28/29, 30/29 ratios and errors.

2.9.5. Pressure and Temperature Monitoring.

The Keithley Multimeter is used for more than the mass spectrometer. It also monitors pressure by reading the baratron (BAR, fig. 2.1) output voltage and reads temperatures in other parts of the system via thermocouples.

2.10. Instrumental appraisal and calibration.

Prior to the analysis of samples, the instrument needs to be stringently assessed. The internal precision, sensitivity and reproducibility of the mass spectrometer is calculated from repeated reference gas analyses until a suitable operational level is achieved. In respect to the accuracy of N analysis correction for the presence of non-nitrogen components is also essential. Full system blanks are necessary, both during recovery of the instrument after maintenance and routinely thereafter to ensure the instrument operates with its optimum blank level. The instrument also requires calibration, in order that the yield and isotopic composition data obtained can be considered as quantitative and comparable both within, and between laboratories.

2.10.1. Instrumental appraisal.

2.10.1.1.Nitrogen.

The precision of the $\delta^{15}\text{N}$ measurements can be ascertained from the analysis of aliquots of reference gas. In this paper, two types of experiments have been undertaken to achieve this. The first experiment is a zero enrichment test, in which repeat analyses on equal sized aliquots of gas have been measured, in order to determine both the precision for the aliquot size and to monitor instrumental drift during the course of the experiment. The second requires the analysis of several aliquots at a variety of reference gas pressures, such that the precision for different sized aliquots can be calculated, and it is

also yields information about the absolute variation of the 28/29 ratio with increasing size of the aliquot.

For the zero enrichment experiment 48 analyses of 0.1 nmol aliquots of nitrogen reference gas were made using a 10 minute pumping out time for the mass spectrometer. The zero enrichment study gave a standard deviation (1σ) of $\pm 0.21\text{‰}$ (Appendix 2: table A2-2, fig. A2-1)).

For the second experiment, analyses of reference gas were made for 12 different sized aliquots from 0.01 nmol to 0.12 nmol, each using a 10 minute pumping out time between measurements. The $\delta^{15}\text{N}$ values and the associated errors were calculated from the mean 28/29 ratios. The results obtained are given in Table 2 and shown graphically in Figure 2.6.

From Table 2.2 and Figure 2.6., it can be seen that the precision improves with increasing bleed time and that this instrument can routinely measure isotopic compositions with a precision of $+0.4\text{‰}$ over a wide range of sample sizes from 0.5 nmol to 0.12 nmol; larger samples would have to be split to provide an aliquot of the correct size for study so there is no advantage in going to larger specimens. For small amounts of reference gas (<50 pmol), the precision lies between $+1.0$ and $+2.4\text{‰}$.

Table 2.1. Standard deviations for nitrogen isotopic measurements of different aliquots of reference gas (Appendix 2: table A2-1).

Size, (nmol)	Mean 28/29 \pm st.dev	St.dev, ‰
0.02	131.52 \pm 0.32	2.43
0.03	133.49 \pm 0.21	1.60
0.04	134.59 \pm 0.14	1.02
0.05	135.20 \pm 0.09	0.64
0.06	135.64 \pm 0.08	0.63
0.07	135.84 \pm 0.08	0.58
0.08	136.13 \pm 0.09	0.64
0.09	136.29 \pm 0.07	0.51
0.12	136.74 \pm 0.05	0.38

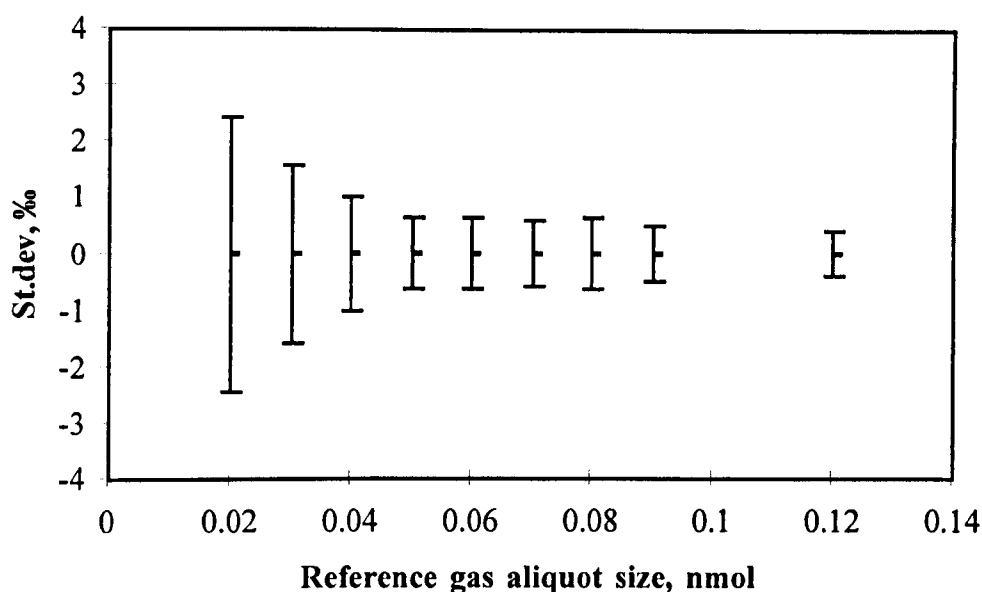


Figure 2.6. Variations of error in $\delta^{15}\text{N}$ against reference gas aliquot size (table 2.1.).

2.10.1.2. "Mass 30" effect on nitrogen isotope measurements and correction of nitrogen isotopic composition.

From Table 2.2 it can be seen that the 28/29 ratio varies as a function of sample size. To investigate the dependence of 28/29 ratio on aliquot size a three isotope plot 28/29 ratio vs. 30/29 ratio was considered. For variable amounts of reference nitrogen a reproducible 28/29-30/29 linear correlation is usually obtained (fig. 2.7). Large aliquots (> 0.1 nmol) of nitrogen have high 28/29 and low 30/29 ratios and the ratios are not variable; however, points for aliquots smaller than 0.1 nmol move towards low 28/29 and high 30/29, indicating the presence of an increasing proportion of contaminant from the system and thus producing a mixing line. The slope of the mixing line seen in fig. 2.7. changes over a long period of time indicating that the isotopic composition of the inlet contaminant varies. Therefore, it appears to be that inlet contaminant is a mixture of several components in constant proportion over at least short periods of time; candidate species are most likely to be CO and hydrocarbons released from valves and metal pipeline. It is not surprising that a metal inlet, and especially metal valves, could release CO and hydrocarbons.

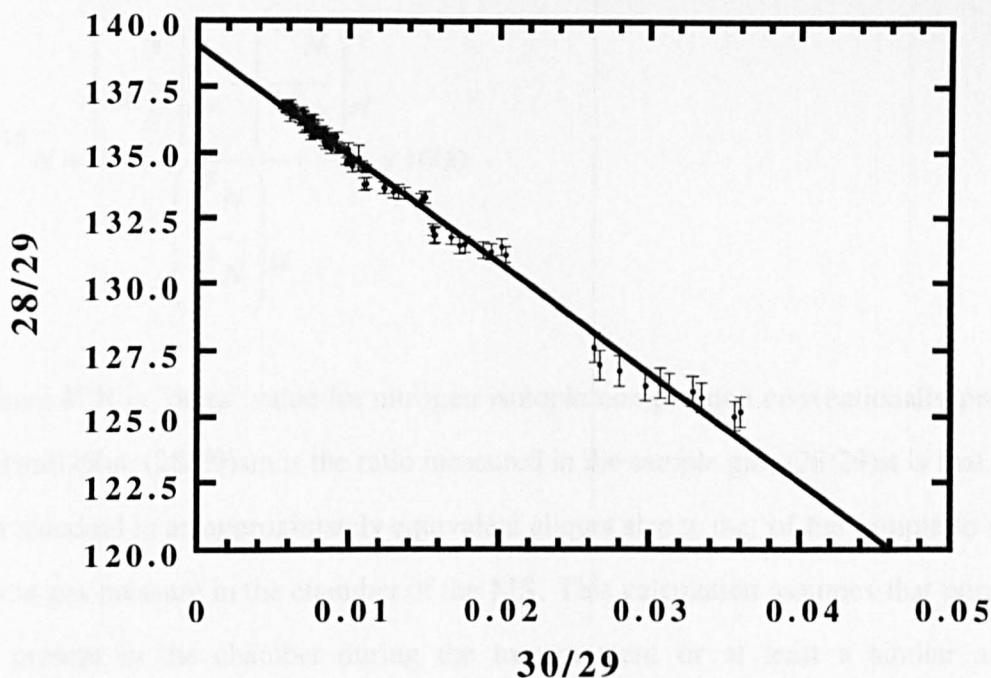


Figure 2.7. Reference gas calibration line: 28/29 vs. 30/29 ($R^2=0.989$ for the line).

Assuming the same effects are present in the case of samples analysis, the 28/29-30/29 reference-gas correlation can be used for correction for the non-nitrogen components. This assumption has been supported by experiments with sample gas. Nitrogen released from the samples was split into a few aliquots of different sizes which were separately measured; the same 28/29-30/29 dependence as for the reference nitrogen was obtained.

2.10.1.3. Mass 30 correction.

The conventional way of representing N isotopic data is the "delta" format. The "delta" value in ‰ for N can be calculated using formula:

$$\delta^{15}N = \frac{\left(\frac{28}{29}\right)_{st} - \left(\frac{28}{29}\right)_{sm}}{\left(\frac{28}{29}\right)_{sm}} \times 1000. \quad (2.1)$$

which is equivalent to commonly known "delta" notation:

$$\delta^{15}N = \frac{\left(\frac{^{15}N}{^{14}N} \right)_{sm} - \left(\frac{^{15}N}{^{14}N} \right)_{st}}{\left(\frac{^{15}N}{^{14}N} \right)_{st}} \times 1000$$

where $\delta^{15}N$ is "delta" value for nitrogen isotopic composition conventionally presented in permill (‰); $(28/29)_{sm}$ is the ratio measured in the sample gas; $(28/29)_{st}$ is that measured for standard in an approximately equivalent aliquot size to that of the sample to obtain the same gas pressure in the chamber of the MS. This calculation assumes that pure nitrogen is present in the chamber during the measurement or at least a similar amount of contaminant with similar composition is present in the reference and sample gases, which implies that ratio 30/29 in each pair of measured gases should be affected in the same way. However since this may not be always the case (especially when aliquot size is lower than 0.1 nmol) the correction procedure can be used. The correction also produces a better error estimation since it is based on the stability of reference gas measurements during the experiment.

The calculation of $\delta^{15}N$ using "mass 30" is based on the fact that there is a linear correlation between different aliquots of reference gas and the assumption that each sample gas measurement lies on a similar mixing line. For series of reference gas measurements the slope, intercept and their 1σ errors are calculated using a York fit. From these the 28/29 ratio of pure nitrogen and its error can be estimated assuming that 30/29 ratio of it is 0.0018. Assuming that the CO-hydrocarbons mixture on the reference mixing line, the value for pure nitrogen of the sample gas can be calculated; the error of 28/29 for nitrogen of the sample gas is also estimated. The geometrical illustration of the correction is shown on fig. 2.8. Using 28/29 ratios for reference and sample gases the $\delta^{15}N$ can be calculated in accordance with the formula (2.1). For each sample gas 1σ error is estimated separately.

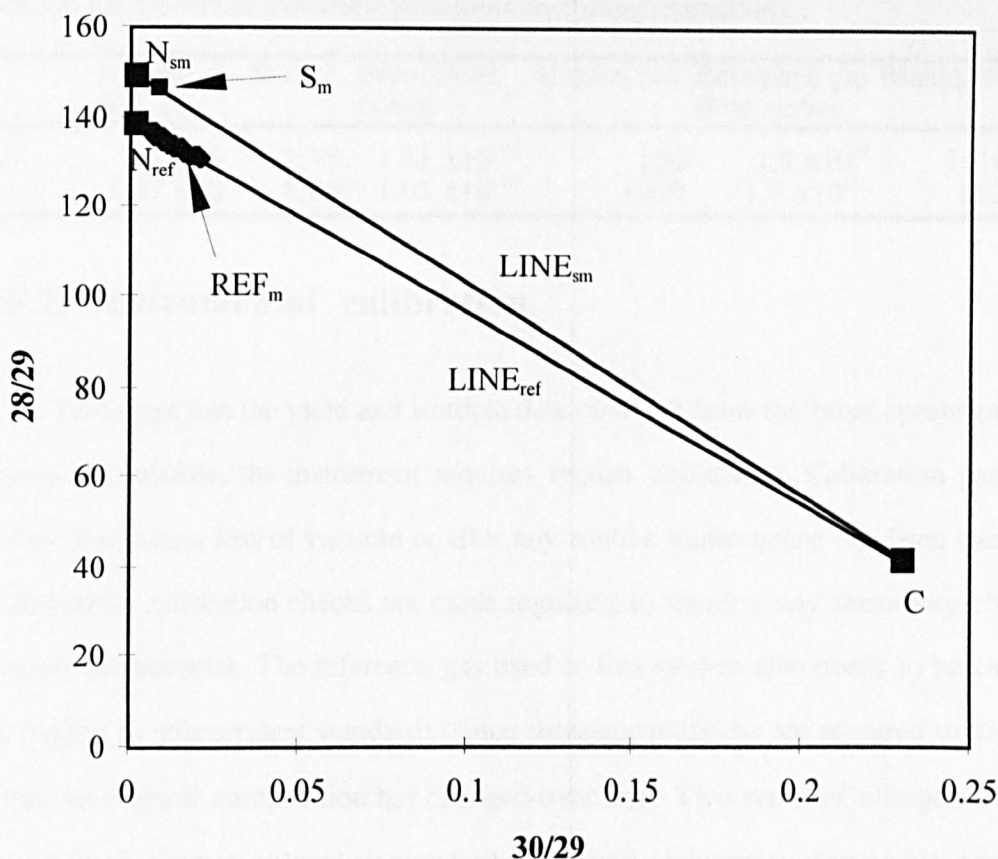


Figure 2.8. Geometrical illustration of “mass 30” correction (REF_m and S_m are experimentally obtained data for reference gas and sample gas respectively; $LINE_{sm}$ and $LINE_{ref}$ are mixing lines between nitrogen of the sample (N_{sm}) reference gas (N_{ref}) on the one hand and contaminant (C) on the other; 28/29 corresponded to the N_{ref} and N_{sm} are used for the calculation of the $\delta^{15}N$).

2.10.1.1. He, Ar and Ne measurements.

The precision of He and Ar abundance is determined from the repeated analysis of aliquots of reference gas (Appendix 3) (table 2.1.). It should be noted however, that use of an electron multiplier enables significant changes of the QMS sensitivity; the main limitations of the analysis by QMS are the blank levels (table 2.1). Precision of Ar isotope measurements has been determined for the range of aliquots of AIR standard from $1.5 \times 10^{-9} \text{ cm}^3$ to $7.2 \times 10^{-8} \text{ cm}^3$ (^{40}Ar); the $^{40}\text{Ar}/^{36}\text{Ar}$ ratio is 283 ± 12 and $^{38}\text{Ar}/^{36}\text{Ar}$ is 0.18 ± 0.02 (Appendix 3). Both ratios are very close to the Ar ratios of atmospheric air ($^{40}\text{Ar}/^{36}\text{Ar}=296$; $^{38}\text{Ar}/^{36}\text{Ar}= 0.185$).

Table 2.2. Precision, sensitivity and blanks of ^{40}Ar and ^4He measurements (the blanks are measured for the whole analytical procedure including extraction) .

	Aliquot size, cc	St.dev.	Sensitivity, cc/cps	Aliquot, sec	Reference gas flow, cc/sec	Blanks, cc/g
^{40}Ar	1.80×10^{-7}	2.7%	1.31×10^{-10}	120	1.5×10^{-9}	3×10^{-10}
^4He	1.47×10^{-8}	8.8%	1.05×10^{-12}	1000	1.5×10^{-11}	1×10^{-9}

2.10.2. Instrumental calibration

To ensure that the yield and isotopic data obtained from the mass spectrometer are accurate and reliable, the instrument requires regular calibration. Calibration parameters are reviewed after a loss of vacuum or after any routine maintenance has been carried out and thereafter, calibration checks are made regularly to monitor any sensitivity change in the mass spectrometer. The reference gas used in this system also needs to be calibrated with respect to independent standards, since subsequent checks are required to determine whether its isotopic composition has changed over time. Two types of nitrogen standards are used for this purpose: local air standard (AIR) and a laboratory diamond standard.

2.10.2.1. AIR standard.

Several studies have proved that the atmosphere is a homogeneous reservoir (Dole *et al.* 1954, Junk and Svec 1958, Mariotti 1985), therefore air nitrogen is the simplest absolute standard. AIR can be used to monitor sensitivity of mass spectrometer and stability of N isotopic composition of nitrogen and noble gas reference gas.

The AIR was stored in a 300ml metal cylinder with two modified valves (40 and 41, fig. 2.2) acting as an aliquotting system to provide a aliquots of 0.5ml for routine calibrations of MS. The aliquot of required size can then be transferred in the clean up section and after purification the quantity of nitrogen in the aliquot is measured using the baratron (note the baratron is calibrated for CO_2 , see 2.10.2.5). Now the intensity of m/z 28, measured by MS, can be calibrated using known amounts of nitrogen. From the results shown in the Appendices 4 and 5, it can be seen that local AIR provides an accurate and reproducible means of obtaining a value for the nitrogen conversion factor

and for measurement of the isotopic composition of the reference gas.

AIR standard can also be used as an independent isotopic standard to control isotopic compositions of Ar and relative ^4He abundance in the noble gas reference.

2.10.2.2. Diamond standard.

Neither reference gas nor AIR standards reproduce the whole experimental procedure applied to the samples during analysis including extraction and purification, hence they do not necessarily reflect the reproducibility of the combustion experiments. Therefore it is essential to introduce a standard which can evaluate reproducibility of the whole procedure used from extraction to analysis. This is most important in the case of N and C since they can be involved in various chemical reactions during preparation of the sample gas for analysis. Therefore a laboratory diamond standard was introduced for routine measurements to investigate the reproducibility of N and C isotopic compositions and N abundances. Since the majority of diamonds can be heterogeneous in terms of N and C isotopic compositions and N content (e.g. Boyd 1988), a diamond powdered to 10-15 μm was chosen assuming that even in the case of possible isotopic difference between grains it is not likely that different aliquots of diamond powder would show isotopic heterogeneity. A typical sample consists from ≈ 6000 to ≈ 100000 grains from the reservoir of $\approx 10 \times 10^9$ grains of diamond.

Preparation, extraction, purification and analysing procedures used to obtain N and C isotopic composition and N content in the diamond standard are exactly the same as routinely performed for samples. The results obtained were blank corrected and the $\delta^{15}\text{N}$ calculation included "mass 30" correction. Summaries of N and C isotope and N abundance data are shown in table, Fig 2.9 and 2.10 ($\delta^{15}\text{N} = -0.23 \pm 0.99\text{‰}$, $\delta^{13}\text{C} = -9.7 \pm 0.5\text{‰}$, nitrogen abundance = 1103 ± 79 ppm (see Appendix 5)).

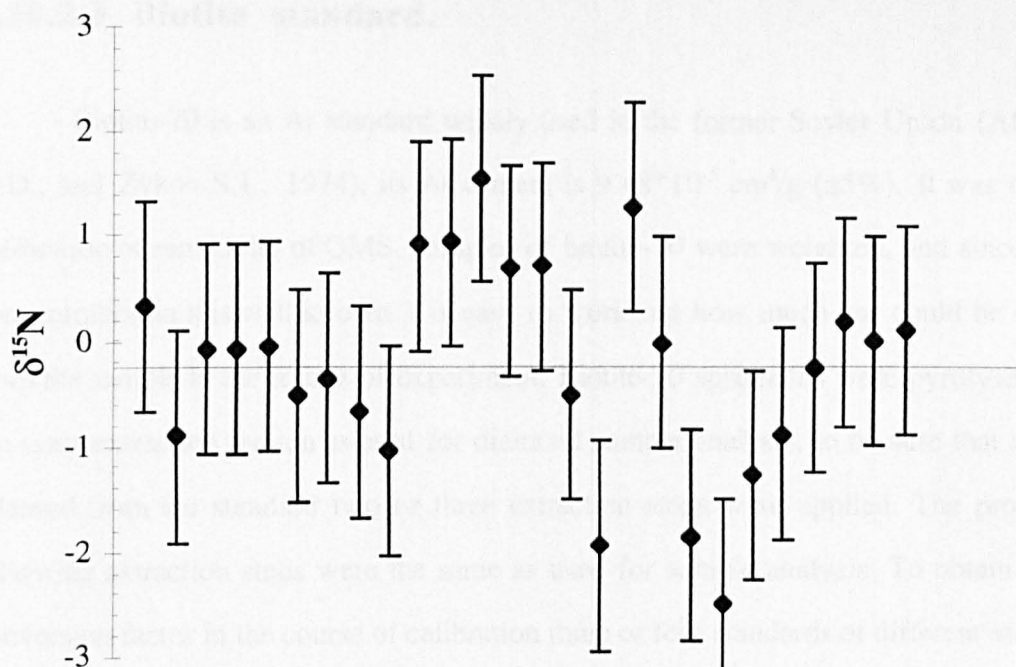


Figure 2.9. Reproducibility of experiments in terms of N isotopic composition, based on measurements of laboratory standard diamond.

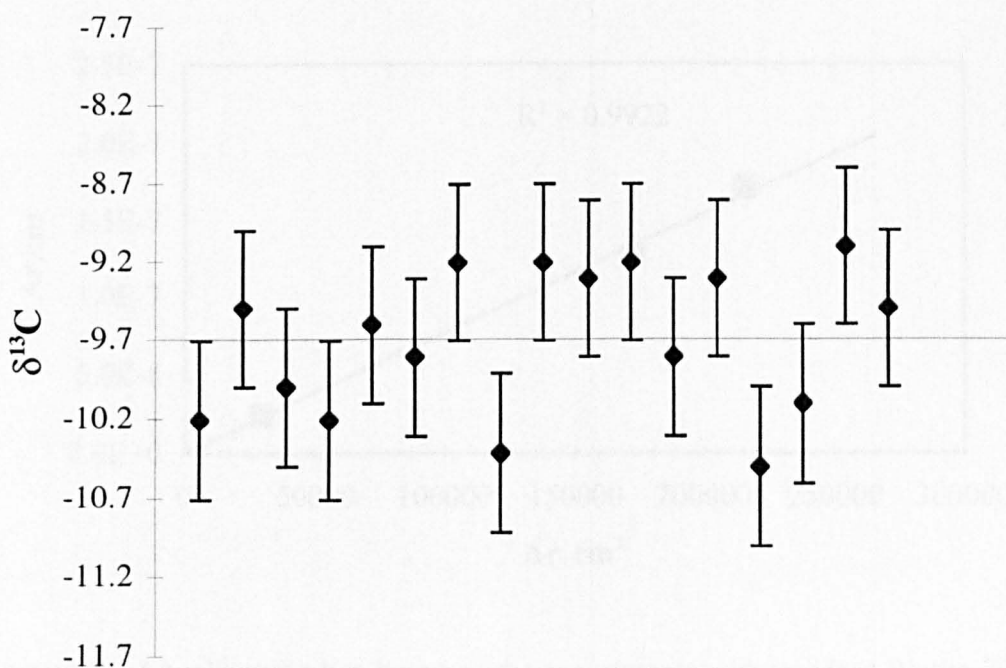


Figure 2.10. Reproducibility of experiments in terms of C isotopic composition, based on measurements of laboratory standard diamond.

2.10.2.3 Biotite standard.

Biotite-70 is an Ar standard widely used in the former Soviet Union (Afanas'ev G.D., and Zykov S.I., 1974); its Ar content is $9.48 \cdot 10^{-5} \text{ cm}^3/\text{g}$ ($\pm 5\%$). It was used for calibration of sensitivity of QMS. Samples of biotite-70 were weighted, and since the Ar concentration in it is well known it is easy to work out how much gas could be released from the sample in the course of experiment. Biotite-70 specimens were pyrolysed using the same extraction section as used for diamond sample analysis; to be sure that all Ar is released from the standard two or three extraction steps were applied. The procedures following extraction steps were the same as used for sample analysis. To obtain reliable conversion factor in the course of calibration three or four standards of different size were analysed. The conversion factor is calculated as the gradient of the graph — measured ^{40}Ar (intensity) vs. calculated ^{40}Ar from the weight of the sample (fig. 2.11).

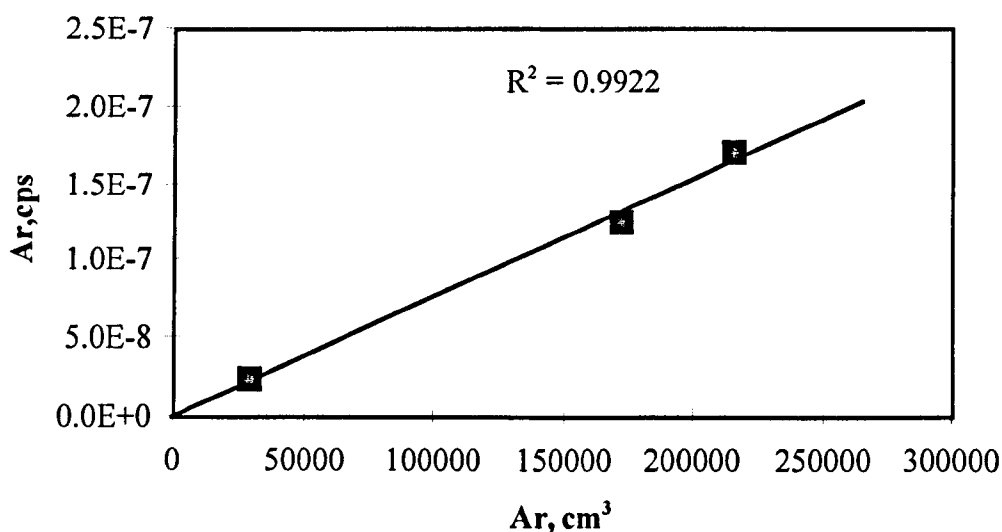


Figure 2.11. Ar calibration line based on the experiments with standard Biotite-70 (Ar, cps is intensity of Ar signal measured by QMS in counts per second; Ar, cm³ is amount of Ar released from each sample of standard calculated from known concentration of Ar in Biotite-70).

2.10.2.4. Baratron calibration

The baratron can be calibrated either using known quantities of CO₂ gas, measured on a separate instrument and transferred via evacuated glass take off vessels or by combustion of diamond crystals of known weight. The conversion factor is calculated from the gradient of the graph — measured C content (baratron pressure) vs. carbon content (diamond weight). The usual precision of carbon measurements is $\pm 5\%$ as could be determined from the calibrations; the combustion experiments involving diamond samples have also indicated that the deviation of the carbon content measured using the baratron from the diamond weight is not higher than 5-10% .

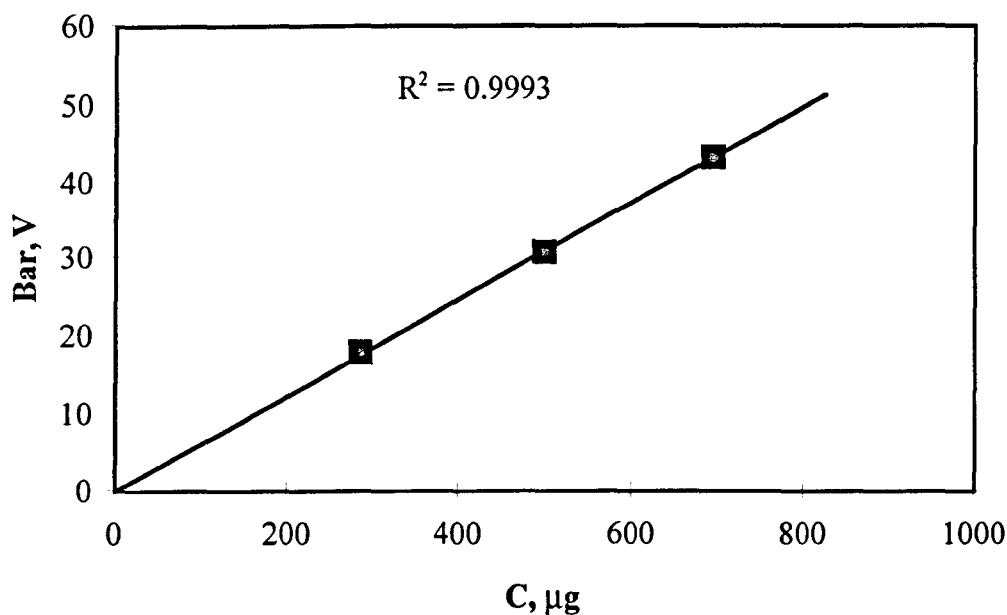


Figure 2.12. Calibration of Capacitance manometer (Baratron) using diamond (Bar, V is pressure measured by baratron in volts; C, mg is weight of diamond crystals).

2.11. Blank measurements.

In order to obtain precise abundance and isotopic composition data using the combined instrument, it is imperative that the magnitude and isotopic composition of the full system blank is accurately known. Such blanks are carried out before and in some

cases after experiments, in order to correct the measured abundance and isotopic values for the sample. These blank measurements are usually performed for the extraction temperatures of 1100-1200°C since it is the highest extraction temperature used in the course of experiments and blanks at this temperature are supposed to represent worse possible cases during the experiments.

The nitrogen combustion blank was found to be quite constant for a series of experiments during a single day (variations being within 20% for quantities of nitrogen and within 3‰ for isotopic composition). In absolute terms and over longer periods blanks could vary from 0.02 to 0.05 nmol in terms of nitrogen abundances with $\delta^{15}\text{N}$ shifting from 0 to -12‰ in terms of isotopic composition. The pyrolysis blank is generally slightly lower than the combustion blank i.e. typically <0.02 nmol. Isotopically, the pyrolysis blank tends towards even lighter values of $\delta^{15}\text{N}$ between -15‰ and -25‰.

The nitrogen blank measured from the purification section alone, is usually ≈ 5 pmol with a $\delta^{15}\text{N}$ composition of between -25‰ to -35‰ due to the small size of the blank. The nitrogen blank from the inlet section (including the extraction section) will vary slightly between each experiment but generally ranges from 0.01 nmol to 0.04 nmol. The $\delta^{15}\text{N}$ values usually range from -10‰ to -20‰.

2.12. Concluding remarks and further developments.

The main advantages of the instrument are ability (i) to perform simultaneous analysis of a number of gases, (ii) to analyse isotopic composition of nitrogen on nmol sized samples with high precision; (iii) to perform bulk and step heating (combustion) experiments in automatic mode.

Currently carbon isotope analysis of extracted CO_2 can only be possible off line, and therefore it does not provide results with the highest precision. The technique does not allow to study carbon isotopic composition with high resolution during stepped extraction, because of limited number of ports in the manifold and sample size requirements for analysis by conventional dynamic mass spectrometer. Therefore

introduction of an integrated carbon isotope instrument particularly for small sample analysis is an obvious step forward.

Chapter 3. Carbon and nitrogen isotopic composition of mantle diamonds and their implications for the Earth's evolution model.

Where so many hours have been spent in convincing myself that I am right, is there not some reason to fear I may be wrong?

Jane Austen

Abstract.

Many studies of the carbon isotopic composition of diamonds have been made during last 20-30 years. Variations of $\delta^{13}\text{C}$ from +2.5 to -35‰ with a major peak of ≈ -5 ‰ were observed for diamonds from kimberlitic sources; carbon isotopic compositions of CO_2 in the MOR basalts and carbonatites have also been found to be of ca. -5‰, suggesting that mantle carbon is about this value. However, reasons why the diamond data scatter away from this value remain in dispute. Two major views on this question propose either an influence of subducted crustal material on diamond formation or processes of carbon isotope fractionation. Several efforts have been made to combine the study of carbon isotopic composition in terrestrial diamonds with that of nitrogen, but so far only diamonds from kimberlites with unknown paragenesis have been considered.

The current study considers diamonds of known paragenesis as well as diamonds with unusual carbon isotopic signatures from various sources. As a result I obtained preliminary conclusions about $\delta^{15}\text{N}$ variations in diamonds of eclogitic (-3 to +23‰) and peridotitic (-34 to +9.5‰) types. I also characterised for $\delta^{15}\text{N}$ diamonds with a wide spread of $\delta^{13}\text{C}$ from +2.8‰ to -30‰ and found the main peak of the $\delta^{15}\text{N}$ distribution to be ≈ -1 ‰ suggesting that subcontinental mantle must have almost been equilibrated with the atmosphere in respect of nitrogen isotopic composition before the majority of diamonds were formed. Herein I confirm the suggestion, made on the basis of different studies, that subduction plays a significant role in diamond formation, and that diamonds may trap gases delivered into mantle regions by subducted plates. Our data also confirm an important role for enstatite chondrite type of material in the formation of the Earth, since I found $\delta^{15}\text{N}$ and $\delta^{13}\text{C}$ of one diamond ($\delta^{15}\text{N}$ of -34‰, $\delta^{13}\text{C}$ of -4.2‰) within the range of enstatite chondrites, and obtained signs of evolution of mantle $\delta^{15}\text{N}$ from -34‰ to the values close to the modern atmosphere.

3.1. Introduction.

Diamonds have long attracted scientists of many kinds and the remarkable properties of the mineral have made it an important source of information for mantle geochemistry in particular. In the first place most diamonds are xenocrysts in kimberlites and lamproites, having merely been transported to the Earth's surface by kimberlitic (or lamproitic) melt; petrologically they link with mantle xenoliths. Therefore using diamonds we can probe deep levels of subcontinental mantle, especially for carbon and nitrogen isotopic signatures, since no other minerals formed in the deep mantle normally have carbon and nitrogen concentrations comparable with those in diamond. In the second place different methods have indicated the antiquity of diamond; studies of mineral inclusions have shown that diamonds could be as old as 3 to 3.3 Ga. (Richardson *et al.*, 1993), whereas estimations of diamond ages based on noble gas studies have been taken to suggest that some diamonds are almost as old as the Earth (Ozima *et al.*, 1983, Ozima, 1989). Therefore, diamond may sample ancient mantle, and due to its high resistance to secondary processes, may preserve the signatures of the processes in which it was formed during the early stages of Earth's evolution.

3.1.1. $\delta^{13}\text{C}$ in diamonds.

After pioneer work by Craig (1953), who first analysed six octahedral diamonds from the South African kimberlite mines and obtained values between -2.4 and -4.7‰ with one exception of +2.4‰, huge amounts of data have been acquired for diamonds localities world wide (Wickman, 1956; Vinogradov *et al.* 1966; Koval'skiy *et al.* 1972; Galimov *et al.* 1978; Kravtsov *et al.* 1978; Gurkina *et al.* 1979; Sobolev *et al.* 1979; Smirnov *et al.*, 1979, Deines *et al.* 1984, 1987, 1991, 1992; Kirkley *et al.*, 1991; Boyd *et al.*, 1987; 1988, 1994; Milledge *et al.*, 1983). The $\delta^{13}\text{C}$ values obtained for diamonds were found to be spread over the range from +2.8‰ to -35‰ with the main peak of the distribution at -5‰. There have been some attempts to find correlations between $\delta^{13}\text{C}$

and different properties of diamonds, such as inclusion type and morphological varieties as determined by Orlov's classification (Orlov, 1973). Some such relationships were indeed observed for different morphological varieties of diamond (Vladimirov *et al.*, 1989): octahedra have $\delta^{13}\text{C}$ ranging from -25‰ to +1‰, which covers almost the whole range of $\delta^{13}\text{C}$ observed for diamonds; cubic monocrystals tended to the $\delta^{13}\text{C}$ values lighter than those for the majority of diamonds ($-15 \pm 4\text{‰}$); fibrous cubes, coated diamonds and octahedra with syngenetic graphite inclusions do not appear to be distinguishable from one another in this respect ($\delta^{13}\text{C}$ of $-7 \pm 2.5\text{‰}$), but cores of coated diamonds could be outside the common range, with lower values of $\delta^{13}\text{C}$. The above conclusions were arrived via diamonds obtained mainly from Yakutian kimberlites, but, the $\delta^{13}\text{C}$ ranges observed were confirmed by Boyd and Pillinger (1994) for fibrous cubes and coated diamonds from other localities. Clear relationships between carbon isotopic composition and the paragenesis of mineral inclusions were first identified by Sobolev *et al.* 1979: the $\delta^{13}\text{C}$ value for most diamonds containing peridotitic inclusions or obtained from peridotitic xenoliths range between -1‰ and -10‰ (peak $\approx -5\text{‰}$), in contrast to the diamonds of eclogitic suite which show $\delta^{13}\text{C}$ variations from -35‰ to +2.5‰ (major peak $\approx -6\text{‰}$), covering the whole range of $\delta^{13}\text{C}$ for diamonds. Such variations were also observed for Type II diamonds (Milledge *et al.*, 1983).

3.1.2. $\delta^{15}\text{N}$ in diamonds.

The first six analyses of nitrogen isotopic composition in diamonds were reported by Wand *et al.* (1980) and Becker and Clayton (1977) and $\delta^{15}\text{N}$ was found to be in the range 0 to +5‰. Shortly afterwards several crystal aggregates of diamonds from Mbuji Mayi, Zaire were studied for nitrogen isotopic composition by Javoy *et al.* (1984), who found wider variations from +5 to -5‰. A significant number of data for diamonds from kimberlites world-wide were provided by Boyd (1988) in the first systematic research of nitrogen isotopes in diamonds. Diamonds of different varieties, from different kimberlite pipes were analysed for $\delta^{13}\text{C}$ and $\delta^{15}\text{N}$, and internal variations of $\delta^{15}\text{N}$ within single diamond crystals were demonstrated. The octahedral diamonds were

characterised by wide variations of $\delta^{15}\text{N}$ values from +16‰ to -11‰ (Boyd and Pillinger, 1994) which appeared to be correlated with $\delta^{13}\text{C}$ in some respects: low $\delta^{13}\text{C}$ diamonds ($\delta^{13}\text{C}$ lower than -10‰) contain nitrogen within the range -2.5‰ to +16‰, whereas high $\delta^{13}\text{C}$ diamonds ($\delta^{13}\text{C}$ from -2‰ to -10‰) contain nitrogen ranging from +6‰ to -11‰ (Boyd and Pillinger, 1994). Nitrogen carbon isotopic compositions of fibrous diamonds (coats and fibrous cubic diamonds of variety IV according the classification of Orlov(1973)) were proved to lie in a rather narrow range ($\delta^{15}\text{N} = -5 \pm 4\text{‰}$ and $\delta^{13}\text{C} = -6.5 \pm 3\text{‰}$) (Boyd *et al.*, 1987). Based on these data Boyd *et al.*(1994) suggested a model of formation for this particular type of diamond. According to this model, the growth of fibrous diamonds occurred when kimberlitic magma invaded continental lithosphere, but failed to move the whole way up to the surface. The magma released a significant amount of fluid which was saturated with carbon, so that rapid crystallisation of diamond could occur.

3.1.3. Interpretations of $\delta^{13}\text{C}$ and $\delta^{15}\text{N}$ variations in diamonds.

It is generally accepted that the isotopic composition of the carbon reservoir in the Earth's mantle is about -5‰. Peaks in $\delta^{13}\text{C}$ distribution for diamonds, carbonatites, carbonates from kimberlites, and MORB, along with OIB are in good agreement with each other and point to the existence of a homogeneous reservoir of carbon (Mattey, 1987; Javoy *et al.*, 1986); no difference was observed for suboceanic (basalts) and sub-continental (kimberlites, carbonatites) mantle. However, the reason for the rather wide variations of $\delta^{13}\text{C}$ within diamonds of the eclogitic suite is still problematical. The most popular idea suggests the variations of $\delta^{13}\text{C}$ in E-type diamonds are due to the subduction of crustal carbon and its effect on diamond formation in eclogites (see Kirkley *et al.*, 1991). However, some scientists appeal to processes of high temperature fractionation occurring deep within the mantle to rationalise $\delta^{13}\text{C}$ variations obtained for diamonds (Galimov, 1984, 1991; Javoy *et al.* 1986); there have also been several approaches which generally invoke Rayleigh distillation, which are either at variance with new data or difficult to envisage (Kirkley *et al.* 1991). Variations of $\delta^{13}\text{C}$ in the

mantle arising as a result of heterogeneity of the Earth from the very beginning with the time of diamond genesis were also discussed (Deines *et al.* 1987). However, Boyd(1988) and Kirkley *et al.*(1991) point out the difficulty of preserving primordial isotope heterogeneity. The situation regarding the understanding of isotopic geochemistry of nitrogen within the mantle remains even more complicated (Boyd and Pillinger 1994; Boyd, 1988; Exley *et al.*, 1987; Javoy *et al.*, 1984, 1986). On the basis of $\delta^{15}\text{N}$ variations in fibrous diamonds and also in high- $\delta^{13}\text{C}$ octahedral diamonds, Boyd and Pillinger (1994) concluded that $\delta^{15}\text{N} \approx -5\text{‰}$ represents the subcontinental mantle nitrogen reservoir in agreement with earlier suggestion of Javoy *et al.*, 1986, based on the study of diamonds and basalts. However, the whole range of variations found in diamonds from -11‰ to $+13\text{‰}$ could not be explained unambiguously.

3.1.4. Aims of the study.

As was noted above, previous combined studies of carbon and nitrogen isotopic composition in diamonds have already indicated certain differences in the distribution of $\delta^{15}\text{N}$ for isotopically light and isotopically heavy $\delta^{13}\text{C}$ diamonds. However, nitrogen isotope data for diamonds with heavy carbon ($\delta^{13}\text{C}$ -2‰ to $+2.5\text{‰}$) and with very light carbon ($\delta^{13}\text{C}$ -15‰ to -35‰) are either not statistically representative or absent which might be explained by the rarity of such specimens as compared with the majority of diamonds which have $\delta^{13}\text{C}$ $-5 \pm 4\text{‰}$. Therefore I decided to pay more attention to diamonds from sources which contain diamonds with unusual $\delta^{13}\text{C}$ values. In this work I also started to measure for both carbon and nitrogen isotopic composition for diamond samples of known paragenetic varieties, since differences observed by others in $\delta^{13}\text{C}$ distribution for eclogitic and peridotitic diamonds may be reflected in the $\delta^{15}\text{N}$ distribution as well. Here I report preliminary results of this study of samples with known paragenesis.

3.2. Samples.

3.2.1. Diamonds with known paragenesis.

Diamonds from one eclogitic xenolith and four peridotitic xenoliths from the Roberts Victor kimberlite pipe (central part of Kaapvaal craton) were studied. Carbon and nitrogen isotopic composition and nitrogen content have been measured for several fragments of diamond crystalline aggregates from eclogitic xenolith RV124. The xenolith itself had been studied by others and was found to be Type A, according to the classification of Jagoutz *et al.*, (1984) or Type I according to classification of MacGregor and Carter (1970) (Jacob and Jagoutz, 1991). The age of this xenolith, as estimated using Sm-Nd isotopic systematics by Jacob and Jagoutz *et al.*, (1994), is 2.7 ± 0.2 Ga.

Peridotitic xenoliths, from which diamonds have been extracted, were classified according to the CaO content in the garnets as lherzolites (RV161,167) and harzburgites (RV180, 175)(Viljoen *et al.*, 1991). One fragment of a crystal from xenolith RV161 was analysed. A single octahedral crystal from lherzolite RV167 was broken and fragments of rim and core have been studied. Five fragments of a diamond polycrystalline aggregate from the harzburgitic xenolith RV175 have been studied as well as the five fragments of an aggregate of octahedral diamonds from the harzburgitic xenolith RV180.

Inclusion-bearing diamonds came from four Yakutian kimberlite pipes (Appendix 6): Udachnaya, Mir, 23d Party Congress and Aikhal. Udachnaya (376 ± 3 My, Kinny *et al.*,1995) and Aikhal kimberlite pipes belong to the Daldyn-Alakit kimberlite field. Mir (358 ± 6 m.y. Ilupin *et al.*, 1990) and 23d Party Congress kimberlite pipes are located in the Malo-Botuobiya kimberlite region. All these kimberlites have late Devonian emplacement age (Davis,1977). Available samples were divided into E (eclogitic) and P (peridotitic) types on the basis of a detailed mineralogical study of inclusions. For isotope analysis I have used chips of the samples; in some cases it was

known that the fragments came either from core or from rims of the original crystals. All original crystals, except for one sample, were classified as octahedra. One sample from Aikhal was classified as a coated diamond, but only the external coat was available for analysis. Polycrystalline aggregates (boart) were also present in this sample set (Appendix 6).

3.2.2. Diamonds with unusual $\delta^{13}\text{C}$ and $\delta^{15}\text{N}$ isotope signatures.

Several diamond fragments from New South Wales (Australia) placers, where diamonds with heavy carbon have been reported before (Sobolev *et al.*, 1989; Vladimirov *et al.*, 1989), were selected for analysis. Diamonds usually occur in Tertiary alluvial stream gravels in the region of Inverell and northern New South Wales. The New South Wales samples were from two distinct but adjacent areas: Copeton and Bingara. Samples from this area were analysed previously for carbon isotopic composition only, inclusions in those samples were found to be of the calc-silicate (suggested to be specific eclogitic subtype; Vladimirov *et al.*, 1989) only one sample contained minerals of eclogitic affinity commonly described in majority of kimberlites (Meyer *et al.*, 1995).

Several framesites from Orapa and Jwaneng kimberlite pipes have been selected for this research since framesites from these pipes, as indicated by previous studies, consist of a large proportion of samples having light carbon isotopic composition (Kirkley *et al.*, 1991, Deines *et al.*, 1993). Both Orapa and Jwaneng are located within the Kaapvaal craton. The kimberlite diatreme Orapa is located 250 km west of Francistown, north-eastern Botswana. The pipe is among the largest kimberlite diatremes of the world. The age of intrusion has been established by the U-Pb method in zircons (93.1 Ma; Davis, 1977) and by fission track methods (92 ± 6 Ma, 87 ± 6 Ma; Raber, 1978). The Jwaneng kimberlite belong to the south part of Botswana, being of late Permian age (235 Ma according to a zircon study, Kinny *et al.*, 1986).

A few fragments of single octahedral crystals from the North Queensland area (Australia) were analysed to confirm the presence of extremely light nitrogen measured

in the diamonds by van Heerden (1994). Unfortunately the exact locality is unknown for these samples.

3.3. Experimental technique (see also chapter 2).

Samples of 0.05 to 1 mg were prepared prior to analysis by preheating (1150°C - 2-4 hours) under vacuum to remove any possible atmospheric or organic nitrogen contamination. After the high temperature treatment samples were transferred under vacuum into a combustion reactor. Extraction of carbon and nitrogen was carried out by a bulk combustion technique at 1150°C in a quartz reactor connected with Cu/CuO reservoir 9horizontal combustion section, see 2.4.1). One-stage purification was applied to separate N and CO₂, and CO₂ from other gases using either CaO or a cryogenic technique (Boyd *et al.*, 1988). Measurements of blank were carried out before and in some cases after experiments. The blank was found to be quite constant for a series of experiments during a single day (variations being within 20% for quantities of nitrogen and within 3‰ for isotopic composition) but over longer periods absolute blanks could vary from 0.5 to 2.5 ng. Data presented in this paper are blank corrected, and in all cases the blank was less than 10% of the gas released from the samples.

3.4. Results.

Twenty eight fragments of peridotitic diamonds from all sources (diamonds from xenoliths and diamonds with inclusions) indicated, as expected, small variations in respect of $\delta^{13}\text{C}$ from -3.4‰ to -7.6‰ (av. -5‰), being consistent with previously reported $\delta^{13}\text{C}$ data on peridotitic diamonds. Variations of $\delta^{15}\text{N}$ in peridotitic diamonds ranged from -6‰ to +9.5‰. nitrogen concentrations in these diamonds were from 15 to 1360 ppm (fig. 3.1., Appendix 7). Nineteen fragments of eclogitic diamonds, also from all sources, spread over a $\delta^{13}\text{C}$ range of 11‰ from -4.5‰ to -15.1‰ (av.-7.4‰). The difference in $\delta^{13}\text{C}$ distributions of eclogitic and peridotitic diamonds is generally in agreement with conclusions arrived at by Sobolev *et al.*, (1979). The $\delta^{15}\text{N}$ values for eclogitic diamonds range from -2.5‰ to +6.5‰ and nitrogen content varied from 38 to

2290 ppm. However, I should note that most of the eclogitic diamonds I analysed are within the range of $\delta^{13}\text{C}$ from -4.5‰ to -10‰. The coat of the eclogitic diamond studied here had $\delta^{15}\text{N}$ of -6.1‰ and $\delta^{13}\text{C}$ of -5.8‰, which is outside the range of $\delta^{15}\text{N}$ obtained for octahedral eclogitic diamonds (fig. 3.1., Appendix 7), but in agreement with previously reported data for fibrous diamonds and coats of coated diamonds (Boyd *et al.*, 1987).

Samples from New South Wales, as expected, gave $\delta^{13}\text{C}$ in the range between -3.9‰ and +2.9‰. Nitrogen isotopic composition was found to be enriched in ^{15}N (heavy)*, being variable from +6‰ to +23‰ (NSW fig.3.1., appendix 7). No previously analysed diamonds indicated nitrogen isotopic composition as heavy as +23‰. Nitrogen concentrations were also variable from 30ppm to 2300 ppm.

Our framesites gave $\delta^{13}\text{C}$ within the narrow range of ca. -21 ± 2.5 ‰. I did not encounter any of the framesites with higher $\delta^{13}\text{C}$ values measured by others (Kirkley *et al.*, 1991, Deines *et al.*, 1993). The nitrogen isotopic composition of the sample set showed a larger range of variation than that of carbon, being between -2.9‰ and +11.5‰ (Frm fig.3.1., Appendix 8)). For most of the specimens the nitrogen content was $\approx 100 \pm 50$ ppm, only four out of twelve samples showed higher nitrogen concentration, one being as high as 1230 ppm.

North Queensland diamonds showed a range in respect of $\delta^{13}\text{C}$ from -2.5‰ to -6.9‰, while $\delta^{15}\text{N}$ was between -10‰ and -34‰. All nitrogen contents appear to be rather high, being in the range from 550 to 1700 ppm (NQL fig. 3.1., Appendix 7).

* in heavy is used to define enrichment in ^{15}N or ^{13}C and light enrichment in ^{14}N and ^{12}C isotopes relative to the well known international standards.

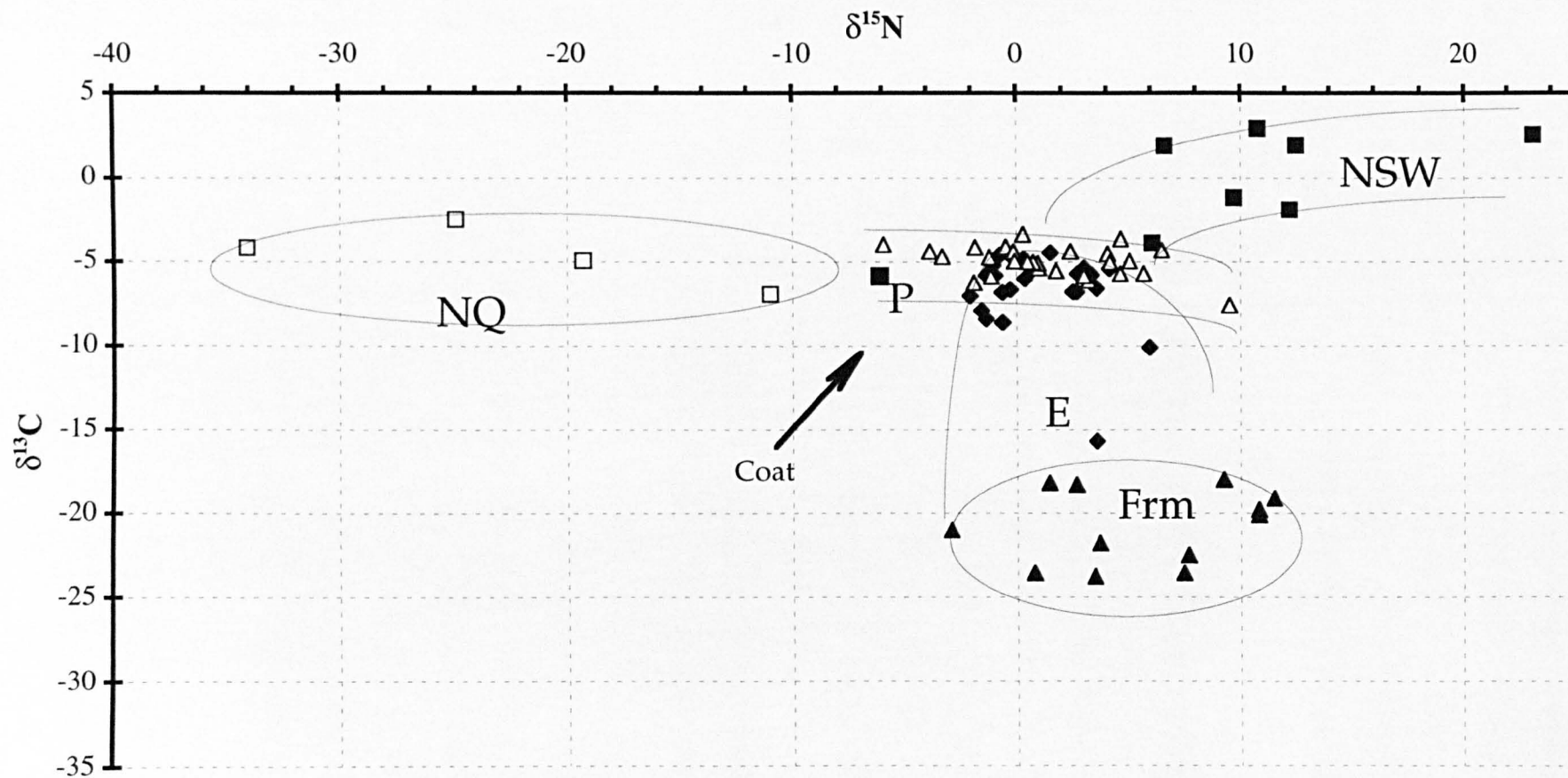


Fig.3.1 Results of experimental study of C and N in diamonds of different paragenesis and diamonds with C and N isotopic extremes (empty triangulars — peridotitic diamonds (P); filled rhombus — eclogitic diamonds (E); filled triangulars — framesites (Frm); filled squares — diamonds from New South Wales (NSW); empty squares — diamonds from North Queensland(NQ)).

3.5. Discussion.

As a preliminary to the discussion, I would like to emphasise that this paper is targeted on the understanding of general variations of $\delta^{13}\text{C}$ and $\delta^{15}\text{N}$ in diamonds of mantle origin, and on their significance for modelling the carbon and nitrogen isotopic evolution of the Earth's mantle. Therefore, I am not concerned here with the interpretation of local isotopic variations in diamonds from each particular source, this will be discussed elsewhere.

3.5.1. $\delta^{15}\text{N}$ and $\delta^{13}\text{C}$ in diamond of peridotitic and eclogitic paragenesis.

Peridotitic diamonds in general showed a larger range of $\delta^{15}\text{N}$ variations than eclogitic ones, although eclogitic and peridotitic diamond areas overlap on the $\delta^{13}\text{C}$ - $\delta^{15}\text{N}$ isotopic plot (fig. 3.2.). In addition to diamonds with paragenesis determined directly, I use diamonds for which the paragenetic type can be suggested both on the basis of their $\delta^{13}\text{C}$ values and on known frequencies of distribution of diamonds of peridotitic or eclogitic paragenesis from well known sources. If I suppose that no peridotitic diamonds have carbon with isotopic composition lighter than -10‰ (Sobolev *et al.*, 1979), then I may assume our framesites, significantly enriched in ^{12}C , to be of eclogitic type like the Argyle diamonds studied for nitrogen and carbon by Boyd and Pillinger(1994) (fig.3.2.). To strengthen the assumption concerning Argyle diamonds, I may note that the majority of diamonds from Argyle lamproites are of eclogitic type. Samples from New South Wales which are significantly enriched in the ^{13}C isotope might also be related to diamonds of eclogitic type, since inclusions in the diamonds with this carbon isotopic signature were previously identified as a specific variety of the eclogitic affinity. Although, the total range of $\delta^{15}\text{N}$ for eclogitic diamonds can be taken as from -3‰ to +13‰ (with the exception of one

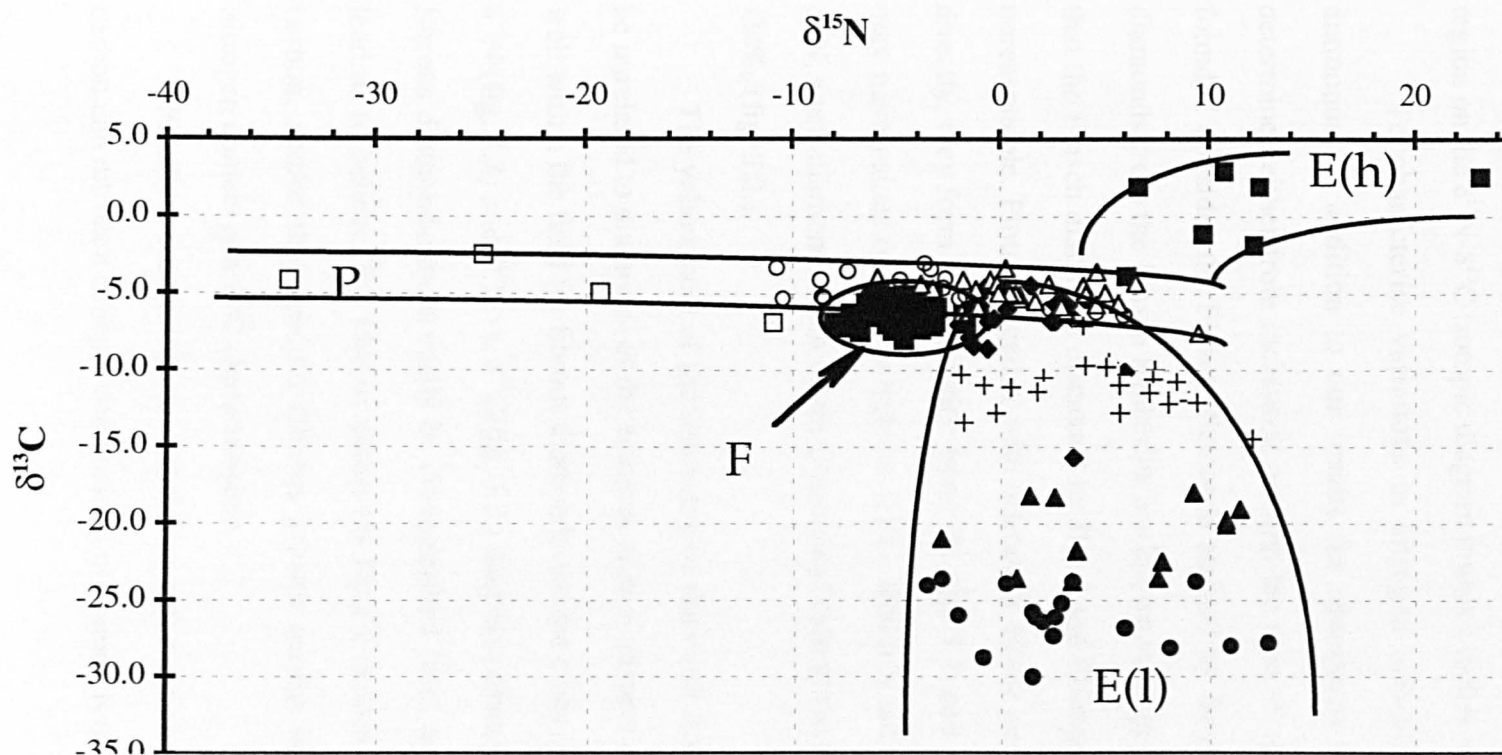


Fig.3.2 The $\delta^{13}\text{C}$ - $\delta^{15}\text{N}$ plot for diamonds of different paragenesis and fibrous diamonds. We should note that N and C isotopic data obtained by Boyd, 1988 would be plotted within the fields determined (empty triangulars — diamonds with directly determined peridotitic paragenesis; empty circles — Finsch diamonds (Boyd and Pillinger, 1994); filled rhombus — diamonds of directly determined eclogitic paragenesis; filled triangulars — framesites; filled squares — diamonds from New South Wales; empty squares — diamonds from North Queensland; filled circles — carbonado diamonds (see Chapter 5); large filled squares — cores of eclogitic diamonds; crosses — fibrous diamonds; E(l) and E(h) — eclogitic fields included either isotopically light(E(l)) or isotopically heavy(E(h)) diamonds; P — peridotitic trend; F — fibrous diamonds (Boyd et al., 1987).

sample from New South Wales which has $\delta^{15}\text{N}=+23\text{‰}$), the field of eclogitic diamonds in $\delta^{13}\text{C}$ vs. $\delta^{15}\text{N}$ co-ordinates is shown on fig. 5, where E(l) is eclogitic field for diamonds with light carbon and E(h) is the eclogitic field for diamonds with heavy carbon isotopic composition. Carbonado diamonds, which in many ways resemble some types of framesites or eclogitic diamonds, show the same range of $\delta^{15}\text{N}$ variations as I proposed for eclogitic diamonds (Shelkov *et al.*, 1995), though they extend the E(l) region on the $\delta^{15}\text{N}$ - $\delta^{13}\text{C}$ isotopic diagram towards lighter values of $\delta^{13}\text{C}$ (fig. 3.2).

To characterise variations in nitrogen isotopic composition for peridotitic diamonds, in addition to our results for specimens whose paragenesis had been determined either from inclusions or from the type of xenolith in which samples were found, I consider the Finsch diamonds studied by Boyd and Pillinger, (1994). Most diamonds from the Finsch kimberlite are known to be peridotitic, hence the assumption that the Finsch diamonds discussed by Boyd and Pillinger, (1994) are peridotitic is not unreasonable. Plotted together with diamonds whose paragenesis has been determined directly, they form the peridotitic trend (P) (fig. 3.2) and show that peridotitic diamonds may have values of $\delta^{15}\text{N}$ as light as -11‰ , which is not necessarily the lower limit for $\delta^{15}\text{N}$, since diamonds from North Queensland extend the P trend towards a $\delta^{15}\text{N}$ value of -34‰ (fig. 3.2.).

The yellow coat of the one eclogitic diamond studied from Aikhal was found to be unrelated to diamonds of the eclogitic suite in respect of carbon and nitrogen, but it is well within the field for fibrous diamonds and the coats of coated diamonds on the N vs. $\delta^{15}\text{N}$ (fig. 3.3) and $\delta^{15}\text{N}$ vs. $\delta^{13}\text{C}$ (fig. 3.2.) diagrams (data from Boyd *et al.*, 1987), where fibrous diamonds could easily be distinguished from octahedral diamonds. Such data lead us to believe that fibrous diamonds have a certain exotic source of nitrogen and carbon, and/or that specific fibrous growth results in diamond with distinct $\delta^{15}\text{N}$, nitrogen content and $\delta^{13}\text{C}$ characteristics.

Finally I would like to summarise information now available concerning the carbon and nitrogen isotopic composition of diamonds of mantle origin:

- a) The peak of the $\delta^{15}\text{N}$ data distribution for octahedral diamonds world wide is ca. -1‰ , although the total range is of ca. 50‰ (from -34‰ to $+23\text{‰}$) (fig. 3.4. A); Given that the $\delta^{13}\text{C}$ distribution diagram for the samples discussed here (fig. 3.4. B) resembles the world wide distribution of $\delta^{13}\text{C}$ for diamonds reported in the literature (Galimov, 1991), $\delta^{15}\text{N}$ distribution is also likely to be broadly characteristic for diamonds world wide.
- b) The available $\delta^{15}\text{N}$ data for eclogitic diamonds with $\delta^{13}\text{C}$ of ca. -5‰ varies from -2‰ to $+5\text{‰}$ with a distribution peak of $\approx -1\text{‰}$ (fig. 3.5. A);
- c) The $\delta^{15}\text{N}$ of isotopically light diamonds ($\delta^{13}\text{C}$ lower than -10‰) in respect of carbon isotopic composition ranges from -2‰ to $+11\text{‰}$ (fig. 3.5. B);
- d) Diamonds of P-trend show variations of $\delta^{15}\text{N}$ from -34‰ to $+11$ (fig. 3.5. C);
- e) Diamonds of P-trend and E diamonds with both $\delta^{13}\text{C}$ of ca. -5‰ and light $\delta^{13}\text{C}$ signatures have peaks close to the -1‰ (fig. 3.5.);
- f) The $\delta^{15}\text{N}$ range for isotopically heavy diamonds in respect of carbon isotopic composition overlaps with the eclogitic diamond range, being from $+6\text{‰}$ to $+23\text{‰}$ but the number of analyses is still small for this type of diamonds;
- g) Fibrous diamonds exhibit a tightly restricted range for both $\delta^{13}\text{C}$ and $\delta^{15}\text{N}$ with peaks at -6.5‰ e.s.d. 1.5‰ for carbon and -5‰ e.s.d. 2.5‰ for nitrogen, and also lie within a well defined field on the $\delta^{15}\text{N}$ vs. N content diagram (fig. 3.3.).

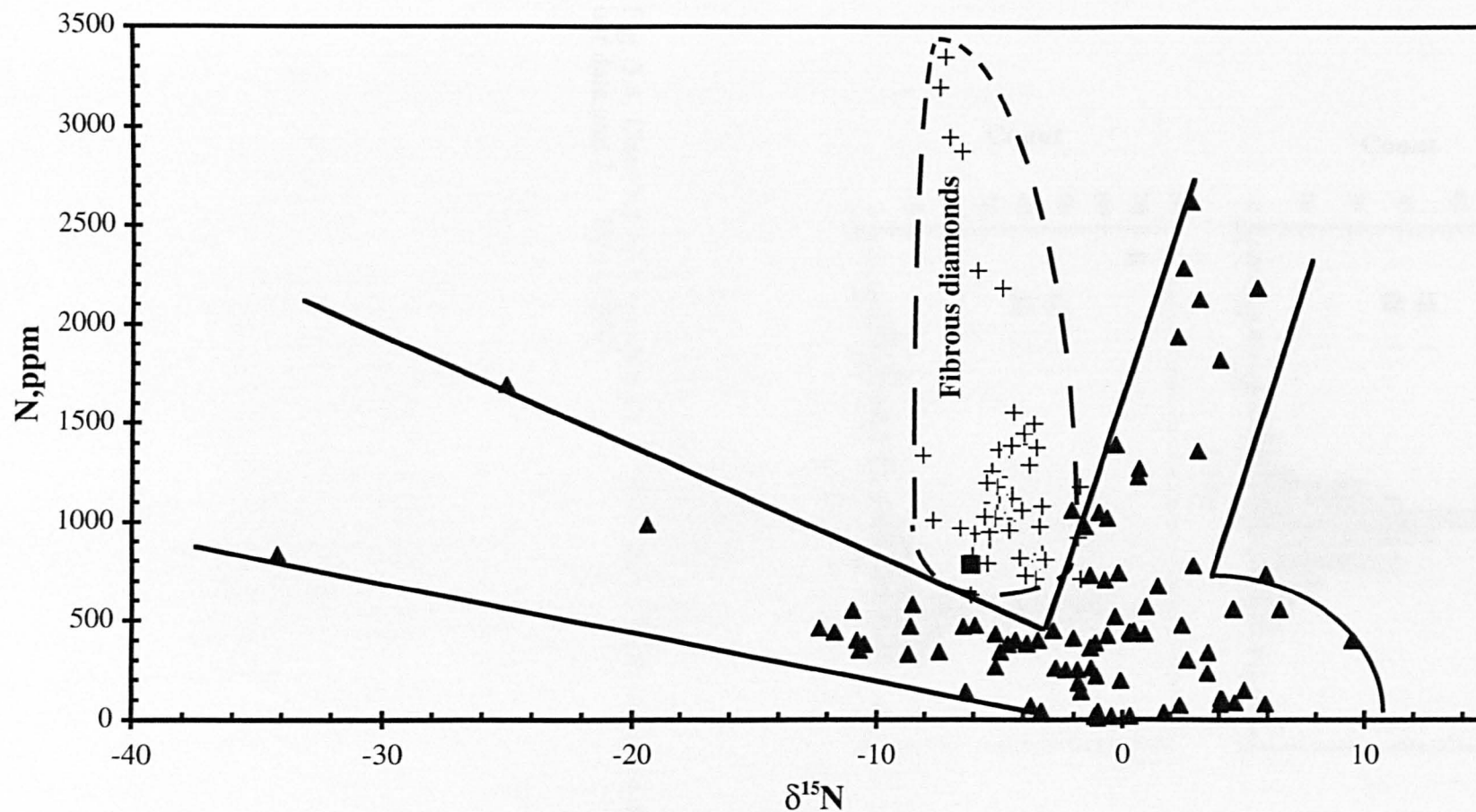


Fig. 3.3 N vs. $\delta^{15}\text{N}$ plot for octahedral diamonds having $\delta^{13}\text{C}$ in the range from -3‰ to -9‰ and fibrous diamonds (black triangulars - octahedral diamonds (our data and Boyd and Pillinger, 1994) , crosses - fibrous diamonds (Boyd et al., 1987), black square - coat of eclogitic diamond from Aikhal kimberlite).

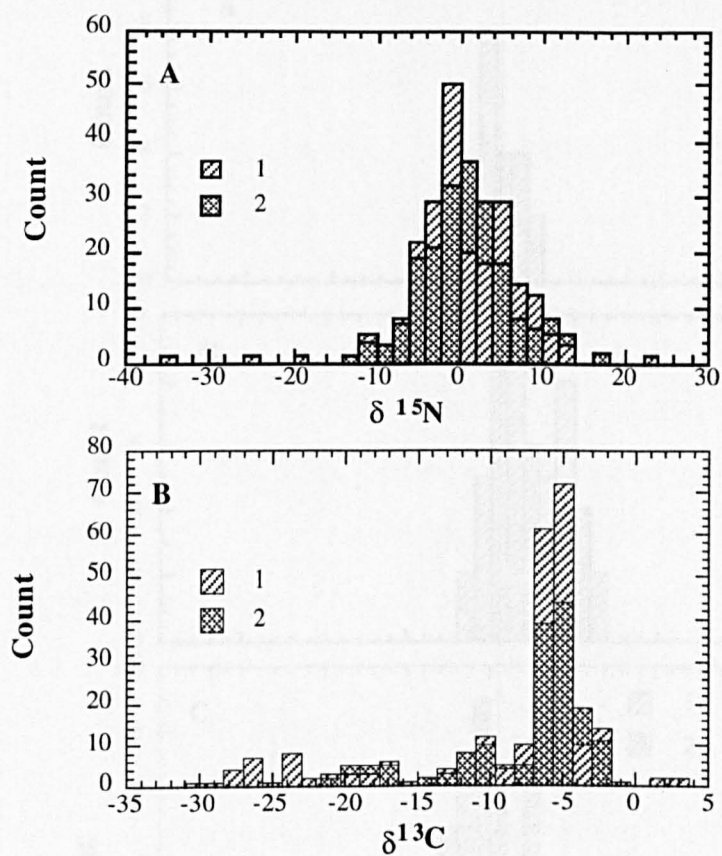


Fig. 3.4. Distribution histogram for $\delta^{15}\text{N}$ (A) and $\delta^{13}\text{C}$ (B) in octahedral diamonds (1—our data and 2 — Boyd,1988).

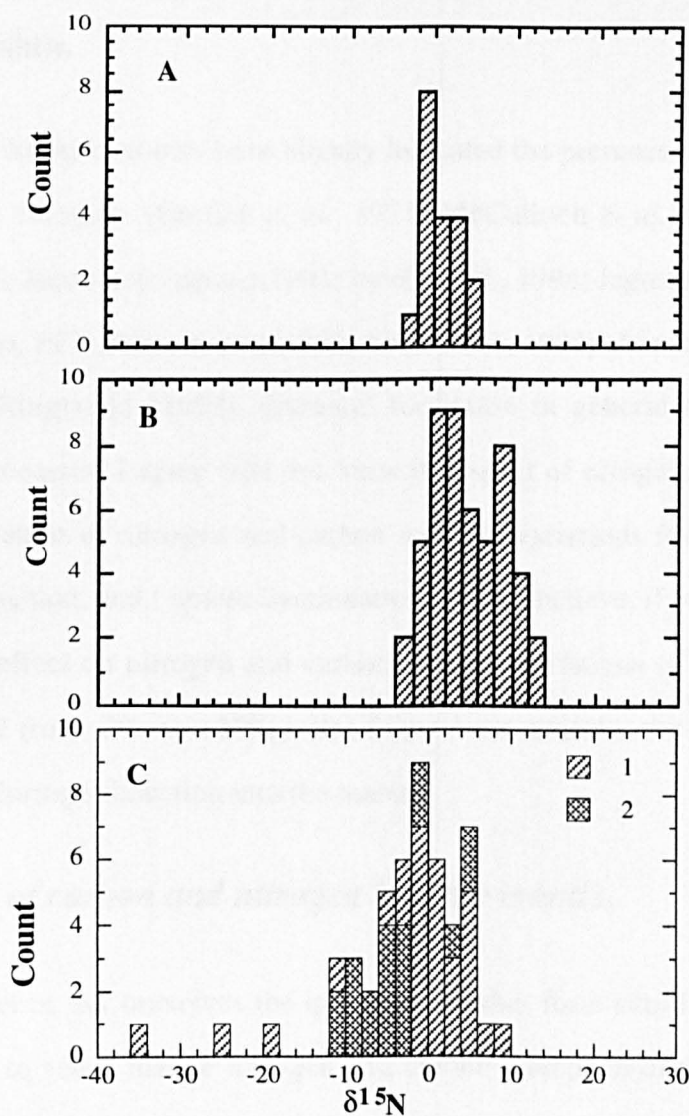


Fig.3.5. Distribution histogram for $\delta^{15}\text{N}$ of: A — eclogitic diamonds with $\delta^{13}\text{C}$ of ca. -5‰; B — eclogitic diamonds with $\delta^{13}\text{C}$ lower than -10‰, including carbonado and framesites; C — peridotitic diamonds (1 — our data; 2 — Finsch diamonds (Boyd and Pillinger, 1994)).

3.5.2. Eclogitic diamonds in relation to the carbon and nitrogen in the subducted slab.

Many isotopic studies have already indicated the presence of subducted material in the mantle eclogites (Garlick *et al.*, 1971; McCulloch *et al.* 1981; MacGregor and Manton, 1986; Jacob and Jagoutz, 1991; Jacob *et al.*, 1994; Jagoutz *et al.*, 1984; Manton and Tatsumoto, 1971, Pearson *et al.* 1995; Jerde *et al.*, 1993). According to the model by Kesson and Ringwood (1989), diamond formation in general is closely related to subduction processes. I agree with this view in respect of eclogitic diamonds since our own interpretation of nitrogen and carbon isotopic variations for eclogitic diamonds involves subduction, and I ignore fractionation which I believe, if present, does not have a significant effect on nitrogen and carbon isotopic variations ($\delta^{13}\text{C}$ from +2.9‰ to -35‰ and $\delta^{15}\text{N}$ from -3‰ to +23‰). But first I must consider the behaviour of carbon and nitrogen during subduction into the mantle.

Subduction of carbon and nitrogen into the mantle.

First let us ask ourselves the question: in what form could nitrogen and carbon be subducted to affect mantle nitrogen and carbon isotope systematics in general and those of diamonds in particular? The major part of any subducted slab consists of basalts since it is built up from oceanic crust, and carbon and nitrogen of this material would carry mantle carbon and nitrogen significantly contaminated by atmospheric gas, and I suppose the resulting carbon and nitrogen isotopic signatures to be close to the R1 reservoir (fig. 3.6.). Metasediments would be also involved, carrying carbon and nitrogen in the form of organics, carbon in marine carbonates and nitrogen in the NH_4^+ form in clay minerals (micas). In a clay, the NH_4^+ ion may easily be substituted in the K^+ position. The isotopic composition of nitrogen in subducted potassium clay minerals is close to atmospheric or slightly heavier (Wada *et al.*, 1975, Haendel *et al.*, 1986, Bebout and Fogel, 1992) being also close to the R1 reservoir. Depending on the stability

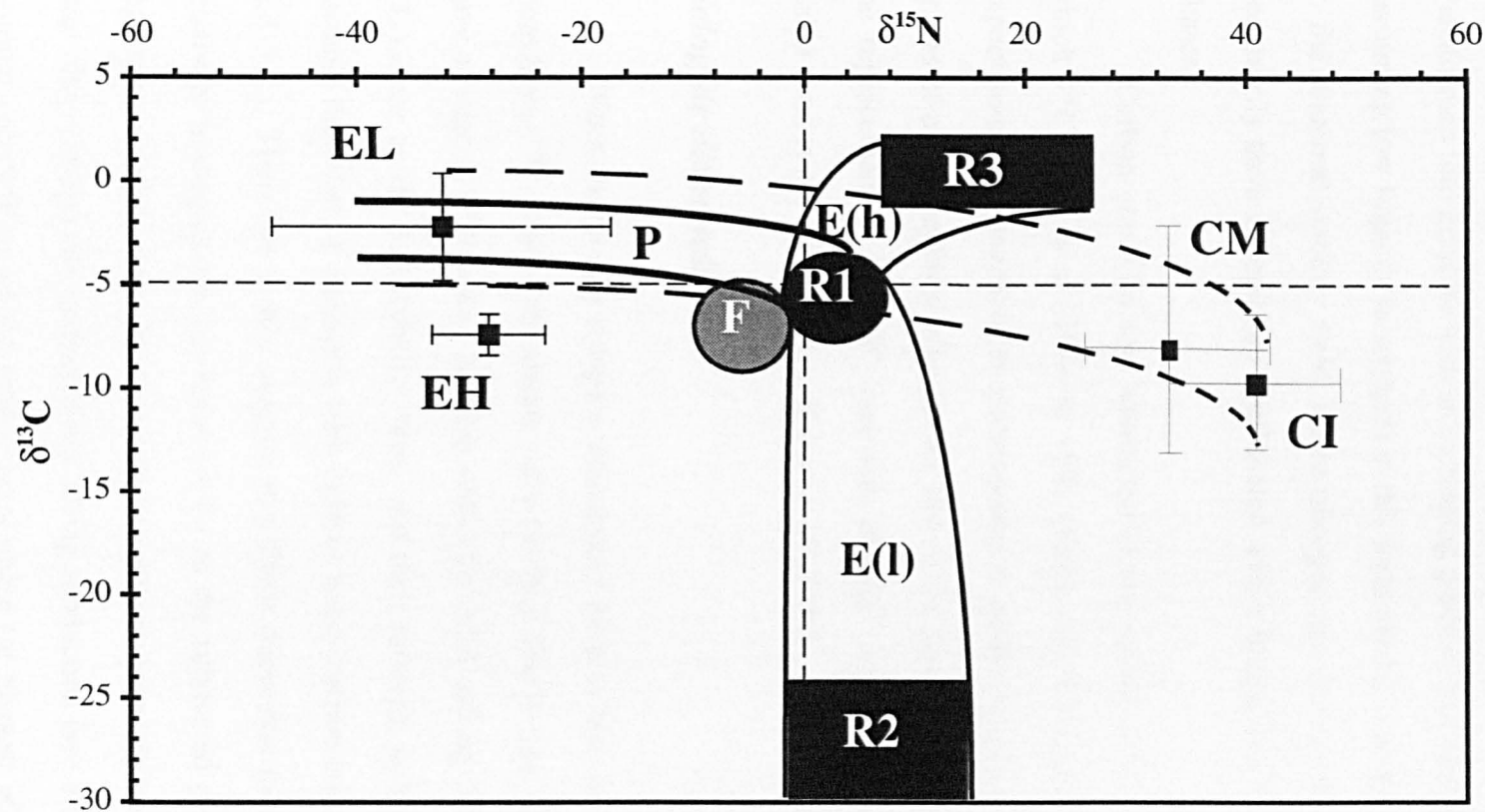


Fig.3.6. Schematic $\delta^{13}\text{C}$ vs. $\delta^{15}\text{N}$ diagram indicating different diamond fields and possible reservoirs which mixing can provide diamonds with variations of C and N isotopic composition (see text for details). R1,R2,R3 — possible reservoirs provided eclogitic diamonds with variable isotopic compositions of C and N; F — fibrous diamonds; P — "peridotitic" trend; E(h) and E(l) — eclogitic trends.

of these minerals and on metamorphic reactions in the descending slab, nitrogen may be released at different depths. Unfortunately the behaviour of NH_4^+ in the metamorphic reactions is not well understood due to lack of experimental data. Organic matter, having wide isotopic variations with respect to carbon and nitrogen would be transformed into graphite with an increasing grade of metamorphism, and may be stable (assuming low fugacity of oxygen) in this form until it reaches the depth corresponding to the diamond stability field, hence nitrogen and carbon in this graphite would not necessarily have isotopically equilibrated with nitrogen and carbon contained by other phases.

Carbon could be also subducted in the mantle in the form of carbonates for which $\delta^{13}\text{C}$ range is of -10‰ to +5‰ (Keith and Weber, 1964). In general I would expect some carbonates to be decomposed in metamorphic reactions at relatively low grades of metamorphism, whereas the rest of the carbonates would just be experiencing the replacement of the Ca^{2+} ions with the Mg^{2+} ions with increasing pressure being stable even at great depths (e.g. Huang *et al.*, 1980).

Eclogitic diamonds.

When discussing eclogitic diamonds I have to bear in mind that a majority of them have $\delta^{13}\text{C}$ close to the mantle value (≈ -5 ‰). The E-type diamonds with $\delta^{13}\text{C} = -5 \pm 3$ have a range of $\delta^{15}\text{N}$ of ca. -2.5‰ to +5‰ (fig. 3.5A and fig. 3.6., R1), with a peak (≈ -1 ‰) close to the atmospheric value, and their nitrogen isotopic composition is less variable than that of diamonds with light or heavy carbon isotopic signatures (fig. 3.5 and 3.2.). Therefore I may suggest that these diamonds indicate the presence of a relatively homogeneous gas reservoir R1 in the subducted plate. This reservoir may represent nitrogen and carbon of different phases (possibly basalts and micas formed after clay) isotopically homogenised during subduction (see above), or may reflect the isotopic composition of the predominant phase (or phases) which transported carbon and nitrogen into the regions of eclogitic diamond formation. Diamonds with either

heavy (E(h) fig. 3.2. and fig. 3.4.B) or light (E(l) fig. 3.2. and 3.4.B) isotopic signatures ($\delta^{13}\text{C}$ lower than -10‰) are relatively rare among the specimens so far examined (fig. 3.4.B), and may have been formed from material locally unequilibrated with the main subduction reservoir (R1 fig. 3.6.), or from some minor phase which was originally isotopically distinct in respect of nitrogen and carbon from phases represented by R1. Large variations of $\delta^{15}\text{N}$ in the isotopically light diamonds support the presence of local heterogeneity in the slab, and could also be assigned to the minor mineral phases unequilibrated with major reservoir R1 in respect to carbon and nitrogen isotopes. As noted above, crustal organic matter, having light carbon and heavy nitrogen (both are variable with the total ranges from $\approx -10\text{‰}$ to $\approx -50\text{‰}$ for carbon and from $\approx -2.5\text{‰}$ to $\approx +20\text{‰}$ for nitrogen (Drechsler and Stiehl, 1977; Stiehl and Lehmann, 1980, Cline and Kaplan, 1975; Saino and Hattori, 1980; Sweeney and Kaplan, 1978; Hoefs and Schidowski, 1967 and others)), which had been subducted, would be transformed into graphite at high pressure and temperatures (if the oxygen fugacity was low); hence it would not necessarily be equilibrated completely with the slab environment in terms of carbon and nitrogen. Therefore, the E(l) field (fig. 3.6.) may be produced either because of heterogeneity of organic matter in the slab, or because of formation of diamonds at different stages of equilibration between the major gas reservoir R1 present in the slab and the carbon solid phase R2 representing the most usual variations for terrestrial organic material, which can be subducted (fig. 3.6.). The interpretation of the E(h) trend is more difficult due to the lack of adequate statistics; however, assuming that heavy carbon in these eclogitic diamonds is a signature of subducted carbonates containing heavy nitrogen (possibly also due to presence of minor amounts of organic matter) the E(h) trend could be interpreted in a similar way to the E(l) by involving a different degree of equilibration of the main nitrogen and carbon reservoir (R1) with diamond source material (in this case carbonates R3).

I may note here, that even though I have not encountered any eclogitic diamonds with $\delta^{15}\text{N}$ lighter than -3‰ , these diamonds may well exist, since subducted reservoir R1 could be contaminated in different proportions by pure mantle nitrogen which at the

early stages of the mantle evolution (discussed below) might have had a $\delta^{15}\text{N}$ as light as $\approx -34\text{‰}$.

3.5.3. Peridotitic diamonds.

Whereas the carbon isotopic composition of peridotitic diamonds in general is not very variable ($\delta^{13}\text{C} \approx -5 \pm 4$) and is consistent with the $\delta^{13}\text{C}$ value accepted as the mantle isotope signature for carbon, the nitrogen isotopic composition for these diamonds ranges from -34‰ to $+9.5\text{‰}$ ($\delta^{15}\text{N}$). The first and the simplest interpretation of this fact is that isotopic fractionation occurred either in the reservoir or during diamond growth, does not involve carbon and affects only the nitrogen isotopic system. It is a fact that the behaviour of nitrogen in sectioned synthetic diamond is highly variable, whereas the carbon does not appear to be affected (Boyd *et al.*, 1988); however, lack of evidence proving unambiguously that significant fractionation effects may occur in connection with diamond growth in the mantle, makes extensive fractionation unrealistic at least at present.

The second possible interpretation of the wide range of $\delta^{15}\text{N}$ variations within the P trend suggests that mixing of the nitrogen reservoirs with different nitrogen isotopic compositions subsequently affected the isotopic signatures of diamonds. If I agree with the suggestion made by Deines (1991) that total subducted carbon has $\delta^{13}\text{C}$ almost indistinguishable from that of the mantle ($\delta^{13}\text{C}$ of -7‰), then mixing it with mantle carbon ($\delta^{13}\text{C} \approx -5\text{‰}$) would leave the carbon isotopic system almost unchanged. Nitrogen which can be subducted is either close to atmospheric isotopic composition or heavier (metasediments indicated $\delta^{15}\text{N}$ from $\approx -2\text{‰}$ to $\approx +15\text{‰}$ (Wada *et al.*, 1975; Haendel *et al.*, 1986; Bebout and Fogel, 1992). If subducted nitrogen could be one component of the mixture, then a second component is required to have $\delta^{15}\text{N}$ of -34‰ or lower to account for the observed variations of $\delta^{15}\text{N}$ in diamonds. However, the nitrogen reservoir of suboceanic modern mantle having $\delta^{15}\text{N}$ of -4.5‰ (Marty *et al.*, 1996), would not supply diamonds with light enough nitrogen. On the other hand diamonds in general represent old mantle (harzburgitic diamonds from Finsch were formed $\approx 3\text{Ga}$

ago according to Richardson, 1993), which would have had lighter nitrogen, possibly as light as -34‰ assuming that primitive mantle was formed from enstatite chondrite type of material (Javoy *et al.*, 1986 and below in the text). Therefore light nitrogen incorporated in some of the diamonds would indicate the presence of a significant proportion of old mantle nitrogen component, and the lightest values are the closest to the primitive mantle nitrogen isotopic signature. Subducted nitrogen (either atmospheric or heavier) mixing with light mantle nitrogen in different proportions may provide the whole range of nitrogen isotopic variations obtained for peridotitic diamonds. This conclusion is consistent with the petrological model of subduction slab processes by Kesson and Ringwood (1989) showing that some of the mantle peridotites could be closely related to eclogites and hence affected by slab gases. The process of global nitrogen isotopic evolution (discussed further below) may also have affected the nitrogen isotopic signature of the mantle, and hence also of peridotitic diamonds.

3.5.4. Fibrous diamonds.

The areas on the $\delta^{15}\text{N}$ - $\delta^{13}\text{C}$ and N - $\delta^{15}\text{N}$ diagrams occupied by fibrous diamonds (F fig. 3.6. and fig. 3.3.) are distinct from the fields of octahedral diamonds (P and E on fig.3.6.), although they slightly overlap. Fibrous diamonds are considered to have grown at a later stage than the growth episodes involved for octahedral diamonds, on which fibrous diamonds frequently appear as a coat. This was suggested because fibrous diamonds are only found in the young pipes (350-71 My) and contain nitrogen in the low aggregation state (Boyd *et al.*, 1994). Hence, the growth of these diamonds may be unrelated to the formation of the other diamond types, which accords with their distinct isotopic signatures (fig. 3.3. and 3.2.). The difference between carbon and nitrogen isotopic signatures of fibrous diamonds and diamonds of octahedral shape, including the cores of the coated stones, could be due to the presence of a different sources of nitrogen and carbon. Fibrous diamonds could be crystallised from fluid in a kimberlite melt (Boyd *et al.*, 1994) which possibly contained nitrogen from the same source as MOR basalts ($\delta^{15}\text{N}$ of fibrous diamonds is consistent with that proposed for suboceanic

mantle by Marty,1996). On the other hand, it is possible that nitrogen acquired by these diamonds was fractionated during outgassing from the melt, resulting in a slight enrichment of light isotopes in the fluid (1.5‰ for carbon and 4‰ for nitrogen, i.e. the difference between $\delta^{13}\text{C}$ and $\delta^{15}\text{N}$ peaks of distribution for fibrous and octahedral diamonds).

3.5.5. Earth's origin as deduced from carbon and nitrogen isotope variations in diamonds.

As source material for the accretion of the Earth, two types of meteorites were previously suggested: enstatite chondrites (Javoy *et al.*, 1986) and carbonaceous chondrites (Ringwood, 1975; Zindler and Hart, 1986). In 1986 Javoy *et al.*, discussed the importance of the enstatite chondrite model based on the carbon and nitrogen data obtained from diamonds. Although, this group suggested that the primitive nitrogen of the Earth's mantle have a $\delta^{15}\text{N}$ of ca. -40‰ as in enstatite chondrites, they had not encountered diamonds or any other mantle phases with $\delta^{15}\text{N}$ lower than -11.2‰.

In modelling carbon and nitrogen isotopic systematics of the Earth's source material, I am using carbon and nitrogen isotopic and content data by Grady *et al.*, (1986) for enstatite chondrites (EH and EL). These nitrogen and carbon data were obtained by step heating and combustion experiments, and for our purposes I rejected steps lower than 700°C, being aware of terrestrial contamination which may often be observed in lower temperature steps; bulk $\delta^{13}\text{C}$, $\delta^{15}\text{N}$, N and carbon contents calculated from high temperature steps were found to be less variable than bulk values calculated without rejection of low temperature steps. Data for carbon and nitrogen in carbonaceous chondrites (CI and CM) were summarised by Kerridge (1985). For our models I used average values for EL,EH, and CI,CM chondrites.

On the basis of observations made on carbon and nitrogen isotopic compositions of diamonds, two possible routes for Earth's evolution will be discussed. The first scenario of carbon and nitrogen evolution of the Earth based on the homogeneous accretion model, is as follows. Since carbon and nitrogen isotopic data for the EL type

of meteorites lies on the continuation of peridotitic(P) trend (fig. 3.6.) and $\delta^{15}\text{N}$ and $\delta^{13}\text{C}$ for a few diamonds were found within the range for $\delta^{15}\text{N}$ and $\delta^{13}\text{C}$ of this type of meteorite, I assume the bulk of the Earth has isotopic signatures of $-32\pm 15\text{‰}$ ($\delta^{15}\text{N}$) and of $-2.2\pm 2.6\text{‰}$ ($\delta^{13}\text{C}$) with respect to nitrogen and carbon, which is the average for EL chondrites. Degassing of carbon and nitrogen into the primitive atmosphere most probably did not cause any fractionation, but significant losses of the gas phase from the primitive atmosphere would have changed the nitrogen isotopic signature towards enrichment by heavy isotopes, and so the atmospheric nitrogen would become heavier than that of the mantle. Soon after the main degassing events, subduction started the process of equilibrating the mantle and the crustal nitrogen, subsequently introducing significant amounts of atmospheric nitrogen and heavy fractionated nitrogen, resulting from biogenic processes, into the mantle via subduction slabs. Since subduction could transport crustal material into Earth's deep levels, the signature of primitive nitrogen ($\delta^{15}\text{N} \approx -32 \pm 15\text{‰}$) might be detected only in the oldest diamonds. However, the P trend (fig. 9) confirms the process of the evolution of the mantle nitrogen reservoir towards the atmospheric isotopic composition. Two facts: (i) the peak in the distribution for $\delta^{15}\text{N}$ in octahedral diamonds $\approx -1\text{‰}$, indicating nitrogen isotopic composition for subcontinental mantle, and (ii) the $\delta^{15}\text{N}$ of MOR basalts suggested to be of $\approx -4.5\text{‰}$ (Marty *et al.*, 1996), corresponding to that of suboceanic mantle,— support the suggestion that mantle nitrogen isotopic composition had almost been equilibrated with nitrogen of the atmosphere.

The second scenario is mainly based on the assumption of heterogeneous accretion discussed by Javoy *et al.*, (1984). These authors suggested that carbonaceous chondrite material was mainly concentrated in the uppermost layers of the Earth while enstatite chondrite type of material constituted the primitive mantle. Fig. 3.7. shows the mixing line between EL ($\delta^{15}\text{N} = -32\pm 15\text{‰}$; $\delta^{13}\text{C} = -2.2\pm 2.6\text{‰}$; N=77 \pm 17 ppm; C=3620 \pm 1400 ppm) and CI meteorites ($\delta^{15}\text{N} = +42\pm 9\text{‰}$; $\delta^{13}\text{C} = -10\pm 2.9\text{‰}$; N=1480 \pm 260 ppm; C=35300 \pm 6300 ppm); the diamond peak distribution value lies on this line and requires the relative proportion of EL and CI type material to be $\approx 96:4$ (the use of CM

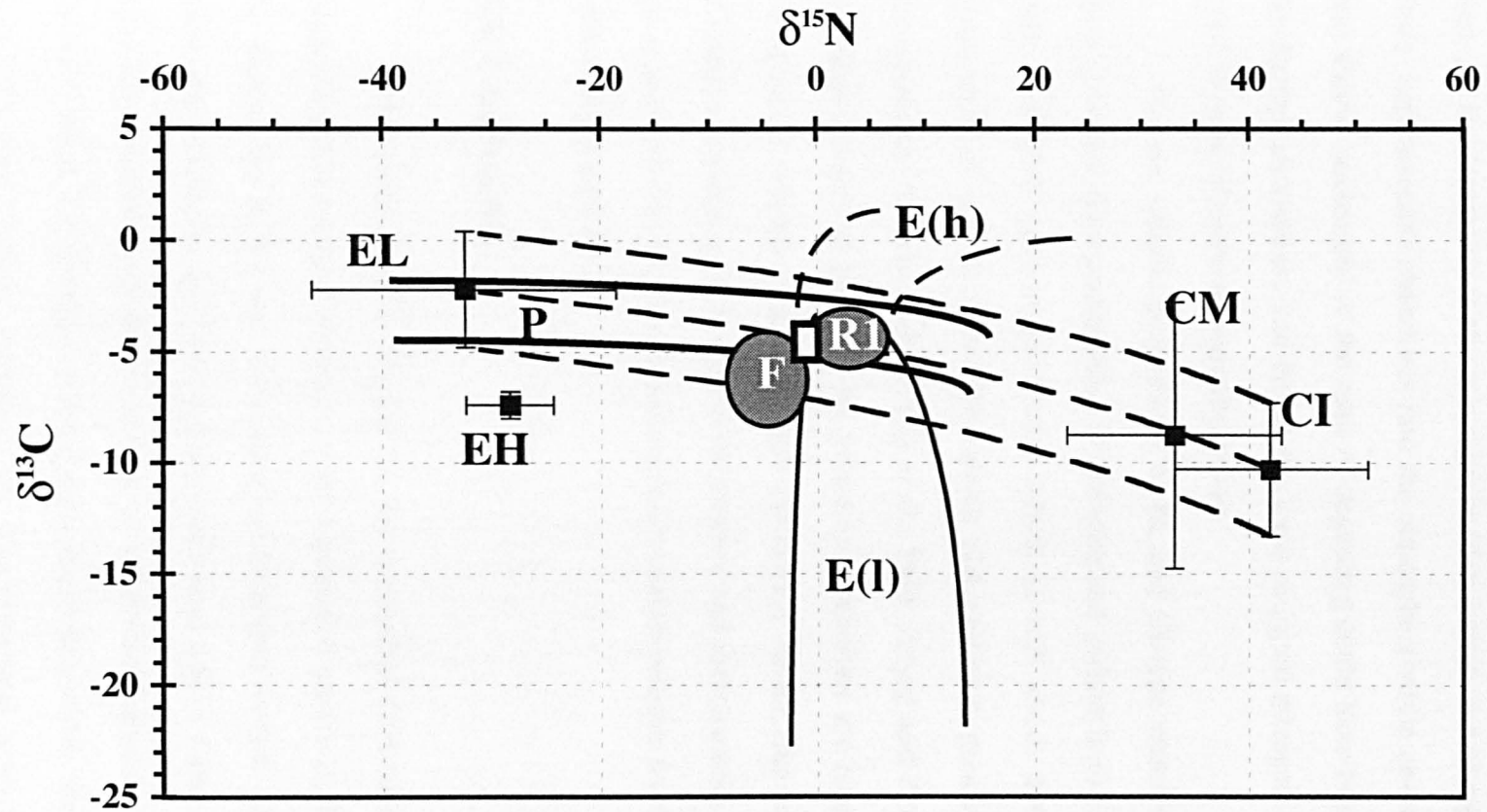


Fig.3.7. Schematic $\delta^{13}\text{C}$ vs. $\delta^{15}\text{N}$ diagram showing different diamond fields along with CI, CM, EH and EL chondrites (see text for details, error bars corresponds to the std. of calculated average values for the meteorite types). Dashed lines are mixing trend between CI and EL chondrites; empty white squares distribution peak for octahedral diamonds; P — "peridotitic" trend; E(h) and E(l) — eclogitic trends; F — fibrous diamonds; R1 — homogeneous subducted C and N reservoir).

type of material instead of CI would not change the situation significantly). The fields of fibrous diamonds and the composition of the homogeneous subducted component (R1) are crossed by this mixing line (fig.3.7). The peridotitic trend (P) also follows the line. As an alternative to the two-layer model, carbon and nitrogen could be degassed from carbonaceous chondrites into the atmosphere while enstatite chondrite material was almost unchanged or the rates of degassing could have been different; as a result the Earth's atmosphere and hence the crust acquired nitrogen and carbon signatures close to those of carbonaceous chondrites.

For the relative proportions of EL and CI type materials (96:4) used for the mixing model, the concentration of nitrogen and carbon in the mixture would be 130 ppm and 4900 ppm respectively, which is still about 260 times the nitrogen concentration and 90 times the carbon concentration greater than concentrations calculated for the bulk Earth (Trull *et al.*, 1993; Zhang and Zindler, 1993). Therefore, substantial losses of gas from the primitive atmosphere are required, which in its turn could lead to fractionation of nitrogen and carbon. Hence, this model is acceptable only if losses of carbon and nitrogen from enstatite and carbonaceous chondrites were in the same proportion as they had been originally, and no isotopic fractionation had occurred, which seems unlikely.

3.6. Conclusions.

The peak of $\delta^{15}\text{N}$ distribution for octahedral diamonds appears to be $\approx -1\text{‰}$ suggesting that nitrogen reservoir of subcontinental mantle is almost equilibrated with the atmosphere by the time the majority of diamonds formed, although, $\delta^{15}\text{N}$ variations show that this reservoir is less homogeneous than that of carbon, and had experienced more complicated evolution. In contrast to octahedral diamonds, fibrous diamonds have distinct carbon and nitrogen isotopic signatures being within the narrow ranges of $\delta^{15}\text{N}$ and $\delta^{13}\text{C}$; these isotopic signatures are also consistent with those for MOR basalts (Marty *et al.*, 1996), suggesting that they both may have been influenced by a common reservoir, though, the difference between the diamond types could be produced by

fractionation, since it is assumed that fibrous diamonds were growing rapidly from a carbon saturated fluid phase (Boyd *et al.*, 1994).

Eclogitic diamonds have revealed the presence of nitrogen with isotopic signatures suggesting the involvement of subducted material in their formation. Diamonds of this type with $\delta^{13}\text{C}$ of ca. -5‰ have relatively small variations of $\delta^{15}\text{N}$, possibly indicating the presence of a homogeneous subducted nitrogen reservoir in the plate (main reservoir), while diamonds with either light ($\delta^{13}\text{C}$ lower than $\approx -10\text{‰}$) or heavy ($\delta^{13}\text{C}$ higher than $\approx -2\text{‰}$) carbon isotopic signatures exhibit wide $\delta^{15}\text{N}$ variations, suggesting that some phases may have been isotopically unequilibrated with the predominant phase which carried nitrogen and carbon in subducted plate.

Peridotitic diamonds having a wide spread of $\delta^{15}\text{N}$ values from -34‰ to +9.5‰ show a possible trend of nitrogen isotopic evolution in the subcontinental mantle, also resulting from subduction. It confirms the suggestion of Javoy *et al.*, (1984) that the primitive nitrogen signature of the mantle reflects a contribution from enstatite chondrites, since among our samples I encountered few diamonds consistent with $\delta^{15}\text{N}$ values of enstatite chondrites (EL) (no other Earth's reservoir known may provide such a light nitrogen isotopic signature). Although, the P trend was defined for peridotitic diamonds, I am aware of the possibility that some eclogitic diamonds could be present in it due to the influence of mantle nitrogen, which could have significant effects especially during the early stages of Earth's evolution while mantle nitrogen had a very distinct isotopic signature.

Extremely light nitrogen isotopic composition measured in the diamond specimens from North Queensland (the lightest $\delta^{15}\text{N}$ is -34‰) strongly supports the hypothesis proposing involvement of enstatite chondrite type of material in the formation of the Earth. Even though no geological information on the exact primary source of these diamonds is currently available, they make a strong case, since no terrestrial material has indicated existence of such values so far. The additional information, which is required for further understanding of evolution of nitrogen reservoir of the mantle, is the age of diamonds with light nitrogen isotopic signature.

Chapter 4. The radial distribution of implanted and trapped ^4He in single diamond crystals and implications for the origin of carbonado.

Plato is dear to me, but dearer is truth.

Aristotle

Abstract.

I have investigated variations of ^4He content in the different zones of single natural diamond crystals using a step combustion technique. The results indicate that some diamonds may be strongly irradiated during their residence in the Earth's crust, since concentrations of ^4He in the 30 μm outer layer were found to be as high as 0.014 cm^3/g . The observation leads to a conclusion that similarly high ^4He concentrations in carbonado diamonds do not necessarily demand an exotic origin. Previous theoretical estimates of the magnitude of He implantation in diamonds, which use normal U-Th concentrations of ca. 30 ppm in the surrounding rocks (Green et al., 1979), do not agree with experimentally obtained results. The He concentrations actually found in the "skins" (outer ≈ 30 μm layer of the crystals) of the samples, I studied, require concentrations of U and Th in the host rock from 160 ppm to 1000 ppm. The interiors of the samples have also been analysed and exhibited ^4He concentrations from 3×10^{-7} cm^3/g to 2×10^{-5} cm^3/g , indicating heterogeneity even within single diamond crystals and arguing for the changes in the growth environment. From ^4He zoning within a diamond from the Finsch kimberlite, a maximum ^4He diffusion coefficient was estimated to be $\approx 4 \times 10^{-21}$ cm^2/sec , lower than previous estimates, indicating that diamond may retain indigenous ^4He in the structure during its residence under mantle P,T conditions.

4.1. Introduction.

For well over fifteen years now, diamonds have attracted the attention of mantle geochemists interested in using them to probe the primitive $^3\text{He}/^4\text{He}$ isotopic signature of the Earth. The first recognition that diamonds trapped helium was made by Takaoka and Ozima in 1978. Since that time many studies have been undertaken, and a considerable scatter of ^4He concentrations from 10^{-8} to 10^{-1} cm^3/g have been observed with $^3\text{He}/^4\text{He}$ ratios varying by a factor of 1000 either side of the atmospheric ratio (1.38×10^{-6}) (Takaoka and Ozima 1978; Ozima M. and Zashu, 1983; Ozima *et al.*, 1983; Ozima *et al.*, 1985; McConville *et al.*, 1991; McConville and Reynolds, 1989; Kamenskiy and Tolstikhin, 1992; Kurz *et al.*, 1987; Wiens *et al.*, 1990; Lal *et al.*, 1989; Lal, 1989; Lal, 1994; Verchovsky *et al.*, 1993; Shukolyukov *et al.*, 1993). A number of mechanisms and various sources (mantle, cosmogenic and crustal) may have been involved in the accumulation of He in the diamond structure.

One of the processes, identified as having a profound effect on abundance and isotopic make-up of helium in diamonds, is the implantation of α -particles (^4He) into the structure to modify the abundance of gas already trapped during growth within the mantle (Lal, 1989; Lal, 1994; Verchovsky *et al.*, 1993). Theoretical treatments have found that the amounts of helium, suggested to be of implantation origin, were consistent with U-Th concentrations in kimberlite rocks and diamond residence times (McConville and Reynolds, 1989; Lal, 1989; Lal, 1994). Verchovsky *et al.* (1993) have shown experimentally the presence of implanted He in microdiamonds from Kochetav Massif, in which ^4He abundance is inversely proportional to crystal size, providing circumstantial evidence for surface concentrations of gas. The high helium concentrations observed for Kochetav diamonds, are rationalised on the basis of their being in the crust for a long time or even having originated within the crustal rocks, where average concentrations of radioactive elements are much greater than in the mantle. Verchovsky *et al.*, (1993) used a step combustion technique (raising the temperature slowly during the experiment) to show helium enrichment in the early stages. However, the change in helium concentration was

not uniform, probably because the samples had rough surfaces and contained a range of grain sizes. Here I apply step combustion for the first time to single diamonds having a well-defined surface and extracted from mantle sources, *i.e.* kimberlites and lamproites, to investigate the actual extent of α -particle implantation.

4.2. Samples and experimental technique.

Long before noble gas geochemists invoked implantation of α -particles to explain their data, investigators, examining diamonds by microscopic techniques, suggested that damage seen along sample edges and around various inclusions and cracks could be due to α -radiation (Vance and Milledge, 1972; Vance *et al.*, 1973). These features appeared to be the result of α -damage after kimberlite emplacement, since they could be annealed (a green colour changing to brown) by heat treatment at temperatures above 600°C (Vance and Milledge, 1972). In 1972 Vance *et al.* confirmed the suspicion by experiments demonstrating that colourless diamonds artificially exposed to α -particles acquired a green colour similar to that encountered in the natural stones. Thus, relatively high ^4He concentrations might be expected in samples with a green colour in their margins. Such diamonds are often found in kimberlitic rocks, particularly in the uppermost parts of pipes affected by ground water, as well as within alluvial deposits, where the radiation damage is usually much greater (Vance *et al.*, 1973; Harris *et al.*, 1977; Harris, 1987).

Accordingly three single diamond crystals (two, F1 and F4 from uppermost parts of the Finsch kimberlite and one, A1, from the Argyle lamproite) with opaque green coloured skins were selected. F1 and A1 had relatively intense green colour, but irregular shapes, though A1 appeared to be more spherical than F1. F4 had a weaker colour, but it was almost an ideal rhombic dodecahedron. To investigate whether I could obtain ^4He concentrations as depth profiles, step combustion experiments (within the range 500°C-850°C) were carried out, ^4He analysis was achieved using a Quadrupole Static mass spectrometer. The resulting data are blank corrected (^4He blank is $2 \times 10^{-9} \text{cm}^3$) and the experimental error for the values reported is ca. 10%. For each step the yield of carbon was measured (precision of $\approx 1\%$) by a high sensitivity capacitance manometer (see

chapter 2) and converted to an equivalent thickness of diamond skin R (in microns) using a simple spherical model. The experiments were made using routine procedure under computer control after desired temperature sequence was entered.

4.3. Results.

The data in fig. 1 demonstrate that stepped combustion makes it possible to obtain ^4He concentration profiles for diamond crystals as a function of their radius, progressively destroying the diamond on a layer by layer basis. After multiple combustion steps (11 for F4, 10 for A1, 10 for F1) each sample was removed from the combustion apparatus to examine the shape of the crystals. One specimen (F1) was found to have broken at an unknown point during combustion, and hence its ^4He profile (fig.4.2 F1) is anomalous because the resulting chips had combusted separately after breaking. Nevertheless the very first combustion steps release amounts of ^4He similar to the other stones. Our model to explain the ^4He profiles obtained for the other two samples is valid, since after combustion of outer layers (30 μm for F4 and 80 μm for A1) the specimens had retained their original shapes. After examination of the crystal shape the samples were re-loaded into the vacuum system again and stepped combustion was continued. The results of all the experiments are summarised in fig.4.1 (see also Appendix 8).

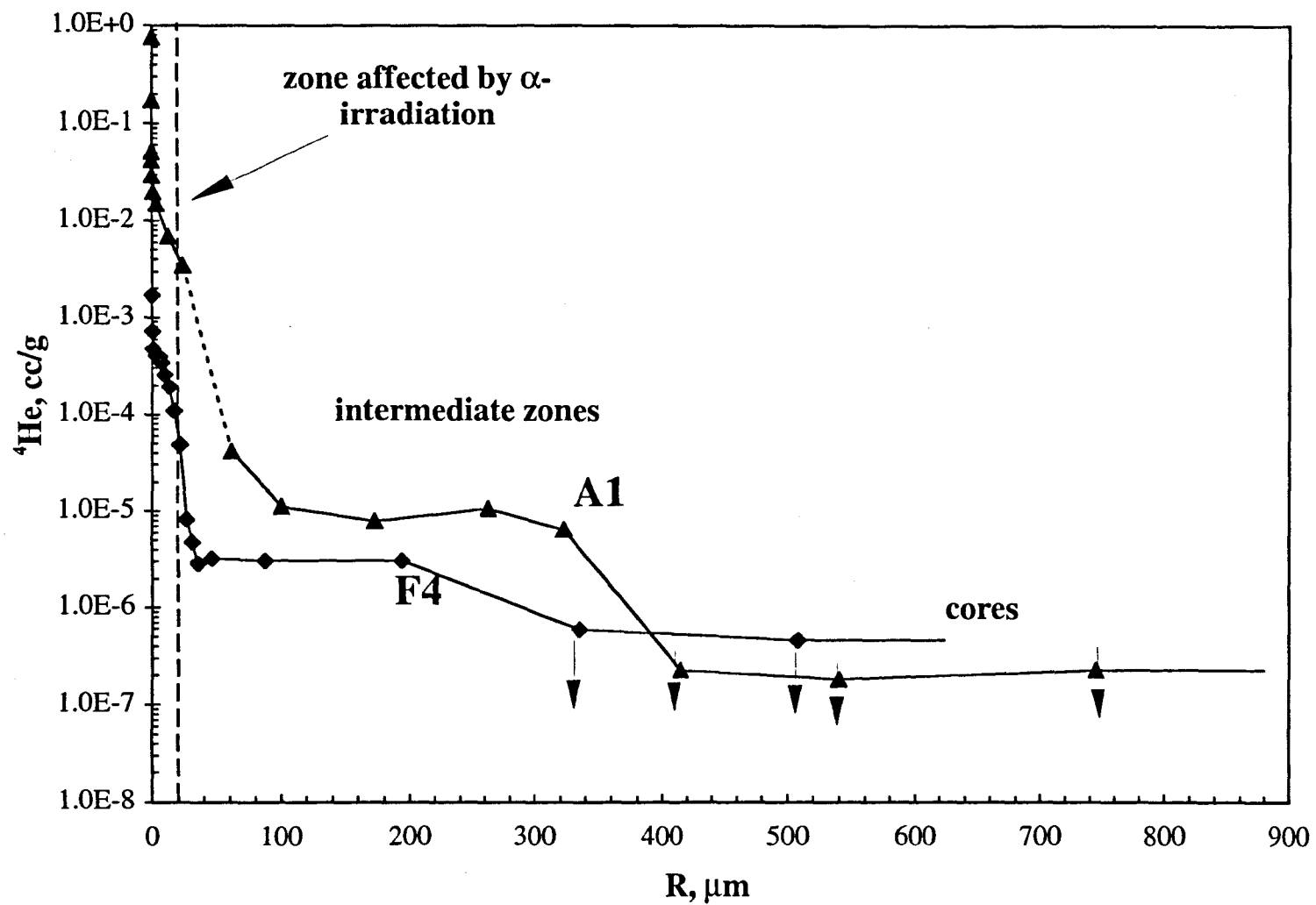


Figure 4.1. Complete ^4He content depth profiles for two diamond crystals (A1 -triangles, F4 - rhombus).

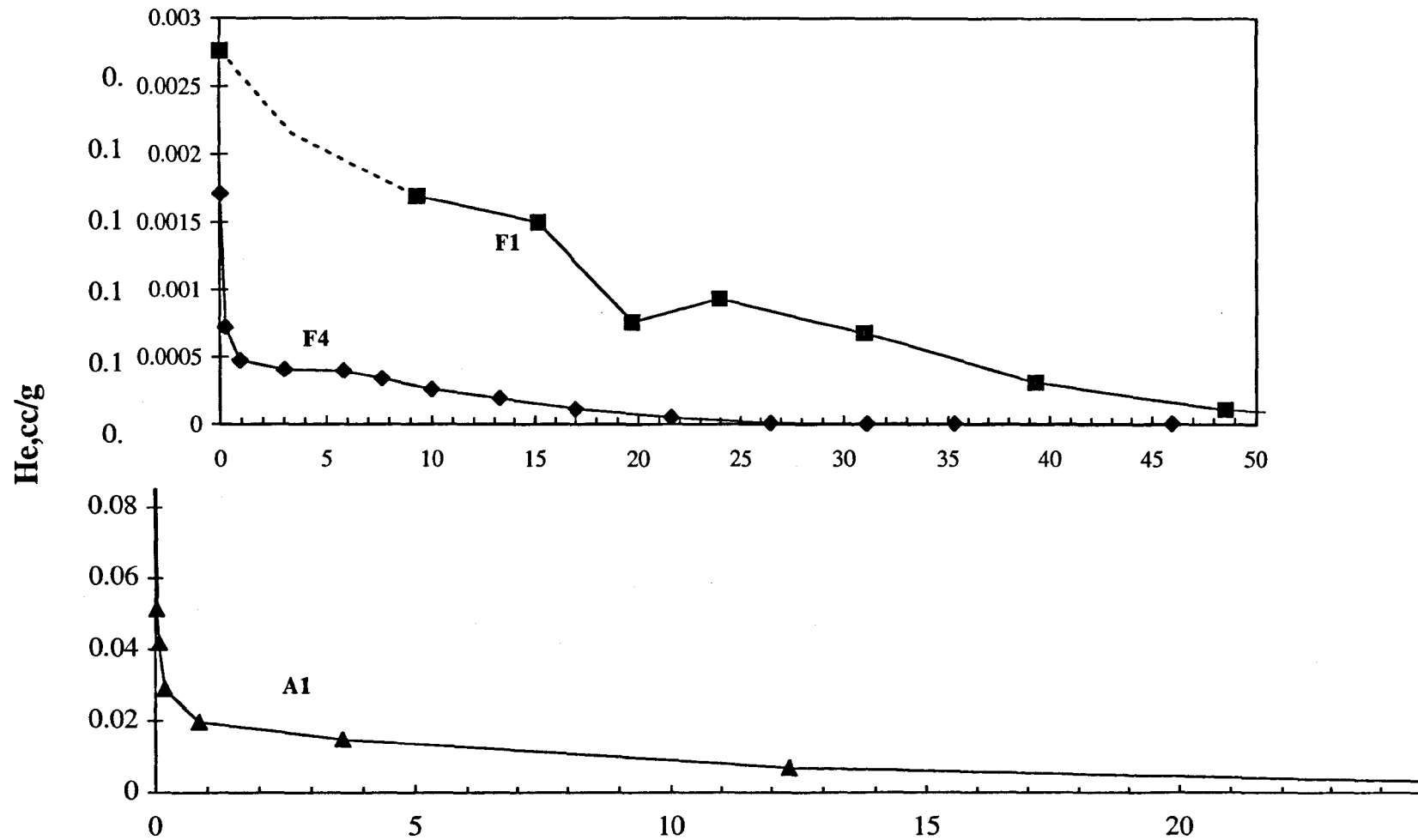


Figure 4.2. Detailed ^4He content profiles corresponded to the skins of the samples F4, F1 and A1 (A1 -triangles, F4 - rhombus, F1 - cubes). F4 had been broken during the experiment and the profile does not reflect natural zoning; the profile for sample A1 starts from the second point.

Table 4.1. ^4He concentrations in the diamonds studied and U-Th concentrations in the host rocks required to produce excess of ^4He (see Appendix 9).

Sample and mass in mg	^4He ,cc/g in the first step (0.3-0.4 μm)	^4He ,cc/g in the 30 μm crust	α -radiation dose, α/cm^2	^4He in the intermediate zone	^4He in the core*	^4He ,cc/g total	U-Th,ppm
A1 (10.5)	0.76	$1.4 \cdot 10^{-2}$	$2.8 \cdot 10^{16}$	$1.2 \cdot 10^{-5}$	$<4 \cdot 10^{-7}$	$1.4 \cdot 10^{-3}$	1560
F1 (1.9)	$2.2 \cdot 10^{-3}$	$9 \cdot 10^{-4}$	$2.8 \cdot 10^{15}$	nm	nm	$1.7 \cdot 10^{-4}$ (calc)	1150
F4 (3.3)	$1.7 \cdot 10^{-3}$	$2 \cdot 10^{-4}$	$5.1 \cdot 10^{14}$	$3 \cdot 10^{-6}$	$<5.5 \cdot 10^{-7}$	$2.9 \cdot 10^{-5}$	248

Comments: U-Th concentrations (last column) in the rocks surrounding diamond crystals correspond to the He concentrations in the diamonds "skins" assuming homogeneous distribution of α -particle emitters in the host rock, spherical geometry of the crystals and the residence time of diamond in the crust equal to the age of kimberlite (1.2Ga age of Argyle lamproite (Pidgion et al., 1989); 0.12 Ga. age of Finsch kimberlite (Nixon, 1987)). nm - non measured, calc - calculated without analysing whole sample completely, * - the values are the maximum estimation from the blank variations, since the released gas was in the limits of error of blank.

4.4. Discussion.

4.4.1. Bulk concentrations of implanted ^4He and the ^4He implantation profiles.

The observed ^4He concentration profiles, especially in the case of sample F4 (the closest to the spherical geometry), demonstrate that ^4He excess in the crystal edge is in general agreement with an irradiation implantation scenario, since high ^4He contents have been observed down to the depth of around 31 μm (fig. 4.1. and 4.2, 4.3) which is close to the maximum range of α -particles produced by decay of U, Th and their daughter elements (30 μm for the diamond structure (Mendelssohn *et al.*, 1978)). The absolute concentrations of ^4He in the sample skins are remarkably high (0.014 cc/g, 0.0009 cc/g and 0.0002 cc/g (table 4.1)); to achieve such levels of concentrations of implanted ^4He , U-Th concentrations in the diamond bearing rock would have to have been much greater than 20-30 ppm (the U-Th concentrations usually observed in the kimberlitic rocks (Green *et al.*, 1979)). The matrix U-Th concentrations, which are necessary to explain the observed excess of ^4He in the sample edges (assuming Th/U=3, homogeneous distribution of U and Th, and exposure times equivalent to the age of the Argyle lamproite (1.2 Ga (Pidgeon *et al.*, 1989) and Finsch kimberlite (0.12Ga (Nixon, 1987))), are from 248 ppm to 1560 ppm (table 1). Thus, the existence of a diamond host environment exceedingly enriched in U and Th at some stage of the geological history of our samples is implied by the new experimental work. The actual process responsible for this does not necessarily need to result in an overall increase of U and Th in the whole volume of kimberlite or lamproite, but could constitute a local micron size U and Th rich layer around diamond, and possibly also around other grains. The redistribution and concentration of U and Th around diamond grains can be, for example, attributed to the influence of groundwaters on the diamond host rocks which resulted in thin layer mineralisation around some of the mineral grains. In support of this hypothesis I note that green coated diamonds were abundant at high levels of Finsch and Premier kimberlites affected by groundwater (Vance *et al.*, 1973, Harris, 1987; Green *et al.*, 1980).

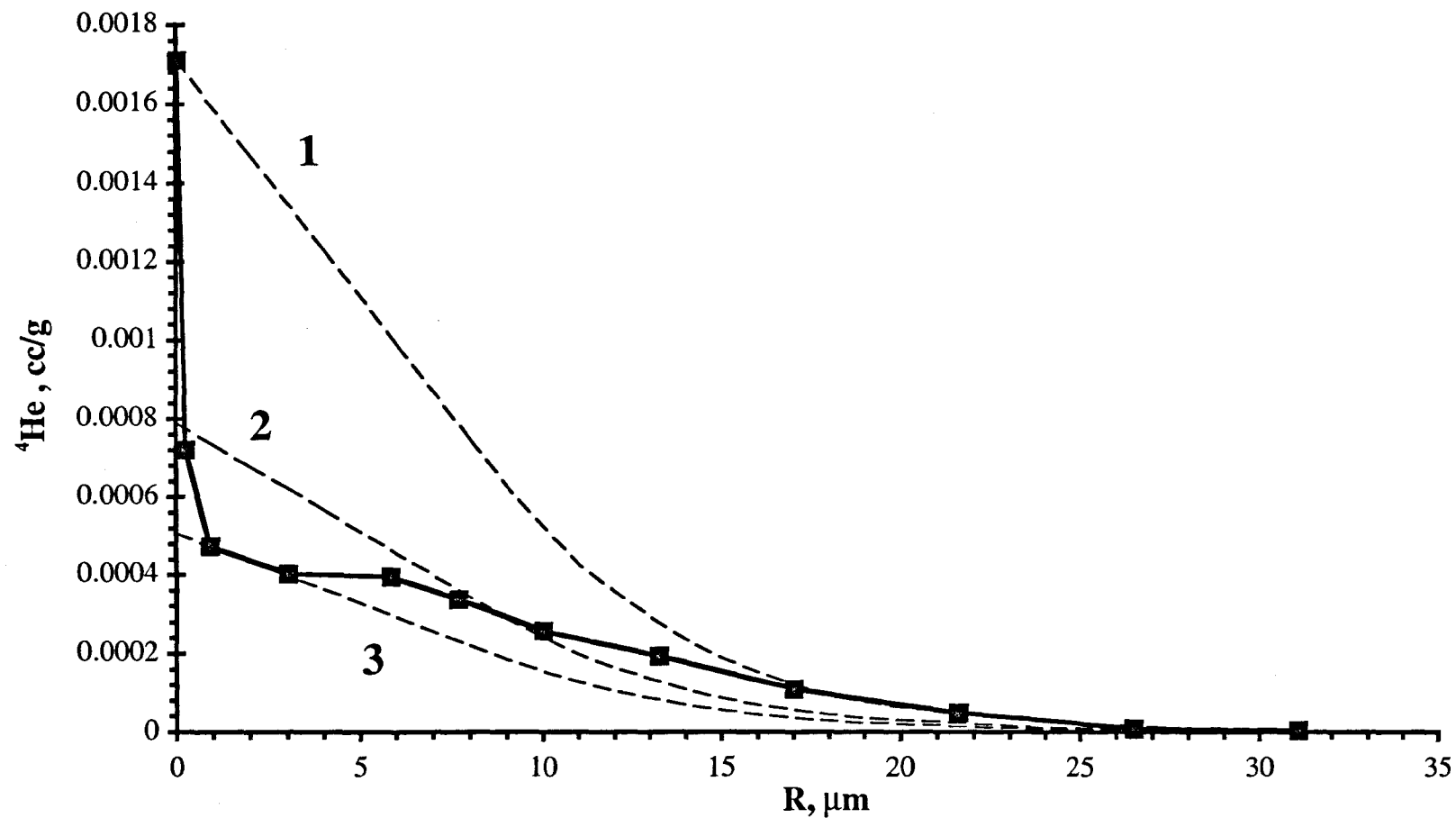


Figure 4.3. A comparison between theoretical and experimentally obtained ^4He implantation depth profiles (solid line - ^4He concentration curve for the skin of the diamond F4 from Finsch kimberlite, dashed lines - ^4He concentration curves calculated for implantation from the model assuming $\text{U}/\text{Th}=3$, homogeneous distribution of α -particle emitters (Verchovsky et al., 1993) and exposure time equal to the age of Finsch kimberlite (1 — for $\text{U}+\text{Th}=540\text{ppm}$; 2 — for $\text{U}+\text{Th}=248\text{ ppm}$; 3 — for $\text{U}+\text{Th}=160\text{ppm}$).

Although the concentration profiles observed are generally similar to those expected from implantation (see Appendix 10), they do not exactly follow the theoretical curves (fig. 4.3.) derived for implantation from a matrix with homogeneously distributed α -emitters and equal yield of α -particles of different energies (Th/U=3) (Verchovsky *et al.*, 1993). In particular at the very surface i.e. the outermost of 2-3 μm the ^4He concentrations drop much faster than predicted. The phenomenon requires further detailed investigation in order to be completely understood, but some of the suggestions which might explain the discrepancy are: (1) inhomogeneous distribution of U and Th in the matrix; for example concentrated in the small mineral grains which may lodge in surface imperfections, as is the case when discrete haloes are visible (Mendelssohn *et al.*, 1978); (2) radioactive disequilibrium of U and Th series elements resulting in variations in the yield of α -particles with different energies; (3) preferential diffusion of He during the experiment along defects created by α -implantation. The latter was checked experimentally for one of the samples which was pyrolysed before combustion at the temperature higher than all the following combustion steps. No difference in the He profiles was found for the sample compared to the others.

It is important to emphasise here that whatever the reasons for the difference between theoretical and experimental He concentration profiles it does not change the most important conclusion that an implantation mechanism has led to origin of the very high ^4He concentrations in 30 μm edge of the samples.

4.4.2. Implications of the results for the origin of carbonado.

The high ^4He concentrations in the skins of the diamonds studied here suggest a possible explanation for the controversy related to the origin of carbonado diamonds (polycrystalline type of diamonds usually recovered from the placer deposits in Brazil and Central African Republic (see Chapter 5)). Among the unusual features related to this diamond type are the extremely high concentration of radiogenic noble gases particularly ^4He (up to $10^{-1} \text{ cm}^3/\text{g}$). Such high values have even allowed consideration of a formation mechanism for involving carbonado transformation of coal into diamond under influence

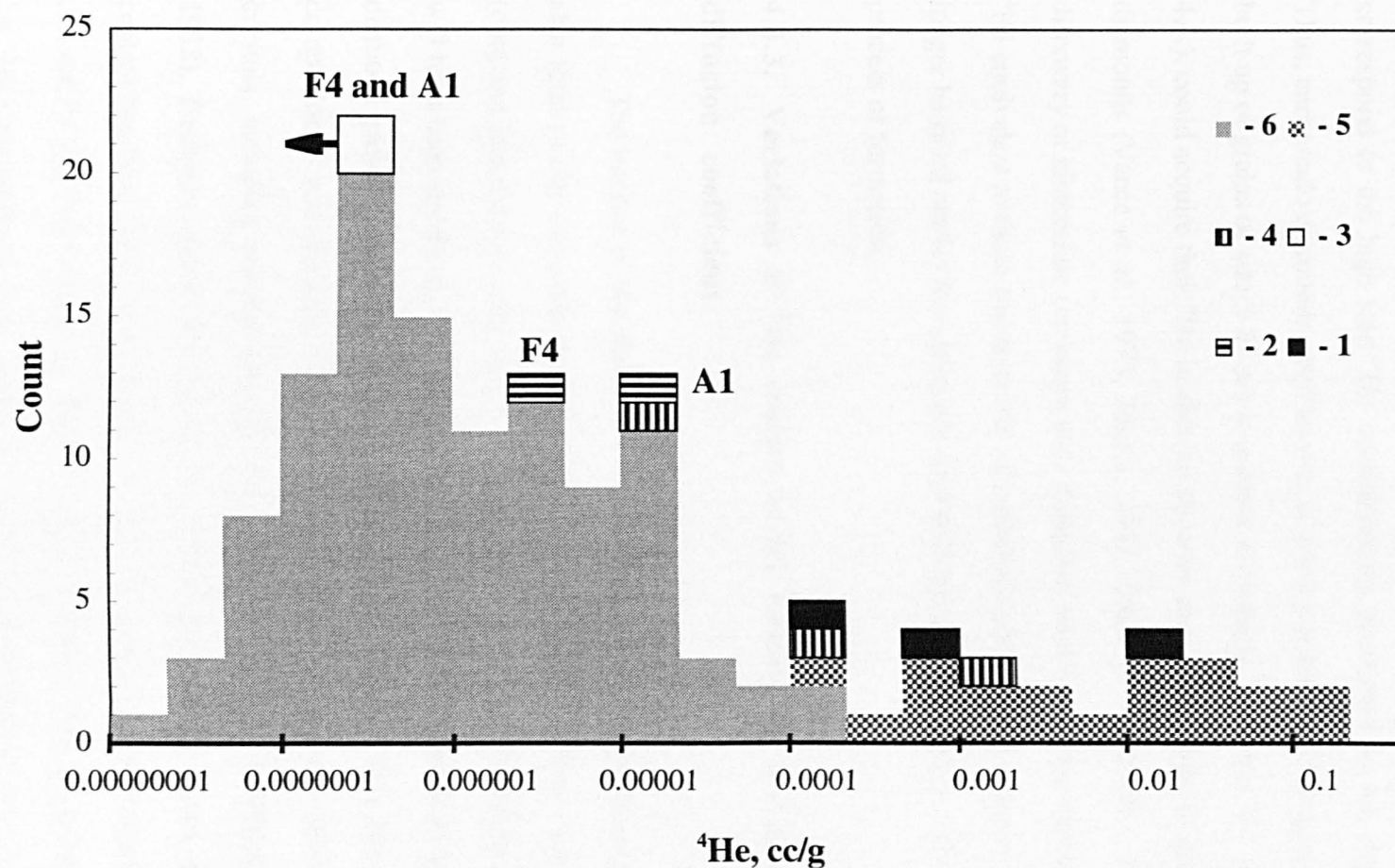


Figure 4.4. ^4He concentrations of mantle diamonds, carbonado and different zones of diamond crystals of mantle origin. (1 - concentrations within the skins of A1, F1, F4; 2 - concentrations within the medium zone of F4 and A1; 3 - concentration within the core of F4 and A1; 4 - total concentrations of A1, F1, F4; 5 - ^4He concentrations of carbonado, including data reported previously by Ozima et al. (1991); 6 - ^4He concentrations of mantle diamonds reported by others (summarised by Verchovsky et al., 1993)

of U-Th irradiation (Ozima *et al.*, 1991; Kaminsky, 1987; Daulton and Ozima, 1996). However, if a porous diamond aggregate with a grain size of ca. 60 μm or less were to experience the same dose of α -irradiation as the samples studied here, the high ^4He concentrations observed in the outer 30 μm layers of our diamonds (table 1) would correspond to the high total ^4He concentrations encountered in the diamond aggregate. Thus, carbonado diamonds, well known as porous polycrystalline aggregates, which are built up of grains of size 5-20 μm in general, containing ^4He from 10^{-4} to 10^{-1} cm^3/g (fig. 4.4.), could acquire their ^4He in alluvial deposits in a similar way to green coloured skin diamonds (Vance *et al.*, 1973, Harris, 1987; Green *et al.*, 1980) studied here. The discovery of kimberlitic (or lamproitic) diamonds with local concentrations of radiogenic ^4He equivalent to those characteristic of carbonado means that a kimberlite origin can no longer be ruled out for the carbonado diamond type, which need not involve any unusual process of formation.

4.4.3. Variations of ^4He content in the interior of the diamonds and He diffusion coefficient.

The interior of the diamond crystals (deeper than 30 μm from the surface) were also found to be non-uniform with respect to ^4He concentrations, indicating two zones (core and intermediate zone on fig.4.1, 4.4. and table. 4.1). It is assumed that these zones will have been unaffected by implantation, and therefore contain only He trapped during diamond growth. Diamond zoning in respect of different carbon and nitrogen isotopic compositions and nitrogen concentrations has been frequently observed in diamond crystals, including samples from Finsch kimberlite (Boyd and Pillinger, 1994; Boyd, 1988). Therefore, although reported here for the first time, it is not surprising that He content has been found to be variable within the diamond crystals studied. The cores of A1 and F4 (fig. 4.1) contain so little He that I was only able to establish an upper limit for ^4He concentration; these values are within the main peak of ^4He content distribution for mantle diamonds analysed using bulk extraction (fig. 4.4.). The intermediate zones

have relatively high ^4He content in comparison to the ^4He concentration range known from studies of kimberlite diamonds (fig. 4.4.), indicating that such high ^4He contents can be trapped by diamonds during their growth in the mantle and is not necessarily the result of implantation, as was assumed by Lal (1989,1994). Variations of ^4He concentration may indicate changes in P,T, time and/or partial pressure of He and further experiments would be necessary to investigate these possibilities. However, using the present data from the core and the intermediate zone of the Finsch diamond (F4) limits of a ^4He diffusion coefficient may be estimated, assuming from the ^4He concentration profile the maximum diffusion distance of 140 μm (fig.1). If the shortest residence time of the intermediate zone is taken as 0.87 Ga (the time difference between the eruption of Finsch kimberlite (0.12 Ga, Nixon, 1987) and the youngest probable growth event of octahedral diamonds of Kaapvaal craton, which is the age of eclogitic diamonds from Orapa (0.99 Ga, Richardson *et al.*, 1990)), then the diffusion coefficient is $\approx 4 \cdot 10^{-21} \text{ cm}^2/\text{sec}$. However, if the longest residence time was 3.08 Ga (the time difference between eruption of Finsch kimberlite (0.12 Ga, Nixon, 1987) and the age of Finsch harzburgitic diamonds (3.3Ga, Richardson *et al.*, 1993)), then the diffusion coefficient is $\approx 1.1 \cdot 10^{-21} \text{ cm}^2/\text{sec}$. The value of upper limit for ^4He diffusion coefficient ($\approx 4 \times 10^{-21} \text{ cm}^2/\text{sec}$) at the temperatures of diamond residence in the mantle (1000°C-1300°C) is less than the estimates by Ozima and Zashu (1988) of $10^{-18} - 10^{-20} \text{ cm}^2/\text{sec}$, and much lower than diffusion coefficients suggested by Zashu and Hiyagon (1995) and Wiens *et al.*, (1994) of $10^{-16} - 10^{-17} \text{ cm}^2/\text{sec}$.

4.5. Conclusions.

1. The very high ^4He content at the surface of single diamond crystals can be considered as a main result of this work. It suggests that implanted radiogenic ^4He may constitute a considerable part of the total ^4He in diamonds of mantle origin; its contribution might be sometimes greater than 99%. Therefore, bulk analysis of diamond crystals may give misleading information about trapped ^4He and hence about He isotopic composition. Thus, the only certain way to obtain reliable information on trapped He and its isotopic

ratio in diamonds is to remove a 30 μm skin from them before analysis. In this respect I suggest that a preliminary combustion step should be applied before extraction by any other technique. If helium released by combustion can be analysed as here it will allow the implanted He as well, as He originally trapped in the diamond interior, to be quantified. The use of multiple combustion steps would allow helium (and another noble gases) variations to be considered along with measurements of N and C isotopic compositions and contents, which are important indicators of changes in the inventory of mantle volatiles.

2. The concentrations of U and Th, required to explain the contents of implanted ^4He reported here, are much greater than those which were actually encountered in the host rocks (assuming uniform distribution), imply that U and Th can be concentrated in the direct vicinity of diamonds during their residence in the crust. Localised high U and Th concentrations should be sought to verify such a conclusion.

3. It follows from above that carbonado might have acquired high ^4He contents in a similar way to diamonds from kimberlitic rocks, so that the high ^4He (and high fission Xe) contents reported for carbonado (e.g. Ozima *et al.*, 1991) cannot be considered as a sign of an exotic origin.

4. The maximum ^4He diffusion coefficient at the mantle PT conditions has been estimated at a new lower limit of $\approx 4 \times 10^{-21} \text{cm}^2/\text{sec}$ on the basis of ^4He zoning obtained for the interior of the diamond crystal from the Finsch kimberlite. However, in order to provide precise determination of the He diffusion coefficient in diamond more samples with better age estimations should be analysed.

Chapter 5. Carbonado origin: a comparison with other forms of microcrystalline diamond based on C, N, He data and inner morphology.

The more alternatives the more difficult the choice.

Abbe D'Allainval

Abstract.

The origin of Carbonado remains a controversial topic in spite of many studies focused on this unusual type of polycrystalline diamond. A number of observations contradict to each other and do not coincide with facts concerning polycrystalline diamonds of known origin. However, none of the previous investigations involved a combination of various methods applied for the same samples, therefore in this work different approaches were combined to address the problem, including isotope analysis of N and C, abundance of N and He, infrared spectroscopy and microscopic structural analysis. A comparison between carbonado and other types of diamond polycrystalline aggregates was carried out.

The ^4He concentrations of 17 carbonado samples from Brazil and Ubangui (Central Africa) were in the range from 2.4×10^{-4} to 1.6×10^{-1} cc/g, which appeared to be a wider range than reported previously by Ozima et al. (1991). In seven framesite samples from Orapa and Jwaneng the ^4He content (7.8×10^{-6} cc/g to 6.4×10^{-5} cc/g) was higher than the one would usually expect from kimberlite diamonds basing on data reported previously. However, three single diamond grains from top parts of Finsch and Argyle pipes had concentrations of ^4He in 30 mm "skin" (2×10^{-4} cc/g to 1×10^{-2} cc/g)(see Chapter 4) within carbonado range of helium suggesting that carbonado could acquire their He in a similar environment.

Nitrogen contents and isotopic compositions of the carbonado samples studied here are well within the ranges for diamonds of mantle origin. Two measurements of

infrared spectra for rather large diamond crystallites (150-200 μm in size) located in two carbonado specimens from Brazil had indicated IaA type of nitrogen aggregation state, which required a significantly long residence time of these samples at mantle temperatures.

As revealed by study of microstructure, carbon isotopic composition and nitrogen content carbonado seems to be different to shock produced diamonds of Popigai crater, whereas nitrogen content distribution and microscopic structure of carbonado samples had indicated a certain similarity with those of framesites; $\delta^{13}\text{C}$ of some framesites was also in the range of that identified for majority of carbonado. Carbon isotopic composition for most of the samples analysed is in agreement with previous data ($\delta^{13}\text{C}$ from -24‰ to -30‰), however one carbonado sample from Ubangui has indicated $\delta^{13}\text{C}$ and $\delta^{15}\text{N}$ values of -5.8‰ and -5‰ respectively, which would seem to point to a relationship with diamonds of mantle origin.

The results of this study suggest that there is nothing which distinguishes carbonado from eclogitic diamonds and framesites in particular. None of the observations contradict to the mantle origin of carbonado provided crustal material is available as a carbon source.

5.1. Introduction.

Carbonado has been known as a polycrystalline form of diamond at least since the 1840's (Trueb and de Wys, 1971). It was first discovered and mined as a placer mineral in Sincoro county in Brazil. Subsequently it has been found in the States of Bahia, Parana and Minas Gerais (Trueb and de Wys, 1969; Kaminsky, 1991) and is known from other areas particularly in Venezuela (Gran Sabana region) and from Ubangui region (Berberati, Carnot, Nola (West Ubangui) and Ouadda, N'Dele (East Ubangui)) of the Central African Republic, where the name "carbon" (Trueb and de Wys, 1971) is more common. In the previous studies of carbonado a number of microscopic, physico-chemical and isotope methods were involved and the most significant observations are summarised below: (i) carbonado is porous polycrystalline aggregate of microdiamonds; crystallites are 5-20 μm in size (ii) all carbonados were found in placers only; (iii) the composition of mineral inclusions in carbonados is quite different from those found in kimberlite diamonds (Trueb and Buttermann, 1969; Trueb and de Wys, 1969); (iv) the range of C isotopic composition for carbonados from Brazil (Vinogradov *et al.*, 1966; Galimov *et al.*, 1978, 1985) and for two samples from Central Africa (Ozima *et al.*, 1991, Kaminsky, 1987) is $\delta^{13}\text{C} = -23$ to -30‰ ; (v) concentrations of radiogenic isotopes of noble gases in carbonados are much higher than in any other terrestrial diamonds indicating an association with U and Th rich environments during their geological history (Ozima *et al.*, 1991). This was confirmed by photoluminescence study stating the presence of considerable radiogenic damage in carbonado (Kagi *et al.*, 1994); (vi) results for REE abundance are contradictory showing in one study (Kagi *et al.*, 1994) a pattern similar to that seen in kimberlite, while in the other (Kaminsky *et al.*, 1994) it is like that in the crust. While most of the facts can be reasonably understood from traditional point of view on diamond formation within the mantle: (i) crustal minerals could be secondary, since the majority of them are present as infill in pores and cracks between diamond crystallites (Trueb and de Wys, 1971); (ii) some eclogitic diamonds have isotopically light carbon similar to that of carbonado

(Galimov,1991); (iii) fine grained polycrystalline aggregates of diamond are known in kimberlites as bort, framesite, stuartite etc., but extremely high concentrations of radiogenic noble gases appears to be highly unusual for diamonds of mantle origin. To account for such concentrations by implantation from surrounding rocks concentrations of more than hundred ppm of U-Th are required a very considerable time (for carbonado with the highest He content reported by Ozima *et al.*(1991) 240 ppm of U-Th would be necessary for 4.5 Gy or 1800 ppm for 1 Gy). Whereas, kimberlitic rocks usually contain only about 20-30 ppm of U-Th and average crust concentration is about 10 ppm. Therefore the radiogenic noble gas data seem to be a key argument for the origin of carbonado.

On the basis of the observations outlined above several hypotheses for the formation of carbonado have been put forward including: (i) impact origin (Smith and Dawson, 1985); (ii) mantle formation followed by a long crustal history (Kagi *et al.*, 1994); (iii) formation in the crust by the transformation of carbon rich material under the influence of radiation (Kaminsky *et al.*, 1987). The impact hypothesis has been proposed on the basis of the facts that mineral inclusions in carbonado and the carbon isotopic signature can be considered as crustal and could be easily reconciled with an impact origin. However Kaminsky (1991) showed a number of differences between shock produced diamonds and carbonado arguing against any relation between carbonado and impact diamonds (as stated above crustal minerals in carbonado can be secondary and some of kimberlite diamonds can have $\delta^{13}\text{C}$ similar to that of carbonado). The hypothesis of mantle origin (Kagi *et al.*, 1994) does not seem very strong either, particularly as the facts involved are too contradictory: REE data obtained in different studies do not agree with each other, and IR spectra are too uncertain to recognise the presence of platelets as indicator of a rather long residence time within the mantle. As to the last hypothesis, it is known that organic rich sediments often have a high U-Th content and therefore may provide extremely high implantation levels (Ozima *et al.*, 1991). Recent discoveries of nanometre sized diamonds in acid-resistant residues of carburanium of Precambrian age (Daulton *et al.*, 1994) might have been conclusive

proof that irradiation processes were involved in carbonado formation but crystallites of micron size have not been found yet (Trueb and de Wys, 1971, Trueb and de Wys, 1969).

The current study was aimed at testing the various hypotheses of carbonado formation on the bases of comprehensive comparison of carbonado with polycrystalline diamonds of known origin and in particular to find out whether carbonado is a distinct type of diamond, or merely a variety of polycrystalline diamond related to others of less controversial provenance. It was hoped that $\delta^{15}\text{N}$, $\delta^{13}\text{C}$, N and ^4He abundances might become a means of separating the samples of interest into well defined groups of different origin.

5.2. Samples.

Nitrogen and helium abundance and carbon and nitrogen isotopic composition for a series of carbonado samples from Ubangui and Brazil has been studied together with framesites from the Jwaneng and Orapa kimberlite pipes (Botswana) and shock diamonds from the Popigai crater. Specimens from Ubangui and several framesites have been polished to study microscopic morphology of the aggregates (table 5.1). Grain size, shape of crystallites and interstitial spaces were determined using light and electron microscopy. Two samples from Brazil consisted of large crystallites (100-150 μm according to surface observations) with a high N concentrations allowed reliable IR spectra to be obtained (table 5.1).

5.3. Experimental technique.

Nitrogen and carbon from the samples of 0.03 to 0.8 mg were analysed in accordance to the analytical procedure described in the section 3.3 (see also chapter 2).

^4He abundance analysis were carried out in separate experiments to the ones in which C and N were analysed. ^4He has been analysed using the Quadrupole Static mass spectrometer. To reduce ^4He blank to the level of $2 \times 10^{-9} \text{ cm}^3$ double wall quartz combustion and CuO reactors were used (see section 2.4.1).

Table 5.1. Methods involved in the research.

Sample	N (ms)	C(ms)	He(ms)	Microscopic	IR
Carbonado Ubangui					
JJG4105.C	X	X	X	X	
JJG4105D	X	X	X	X	
JJG4105A	X	X	X	X	
JJG4105E	X	X	X	X	
JJG4105B	X	X	X	X	
JJG4105(?)	X	X	X		
Carbonado Brazil					
Br-34	X	X	X		
Br32	X	X			
Br-4	X	X	X		
BMCB	X	X	X		
BRCB1	X	X	X		
BRCB2	X	X	X		
BRCB5	X	X	X		
CB5	X	X	X		
CB11	X	X	X		
CB20	X	X	X		X
CB					X
BRCB4	X	X			
BRCB6	X	X			
BRCB7	X	X	X		
BRCB3	nm	X			
Framesites					
ORF121.484	X	X	X	X	
PHN/25.484	X	X	X		
PHN/26.479	X	X	X		
JWF-6.479	X	X	X		
JWF-11.479	X	X	X		
JWF-10.479	X	X	X	X	
JJG-4104.488	X	X			
JJG-4103.484	X	X		X	
FRM1.487	X	X			
GPF3	X	X	X		
GPF2	X	X			
GPF1	X	X			

ms - mass-spectrometric study: N - nitrogen content and isotopic composition; C- carbon isotopic composition; He - helium content). Diamond from Popigai crater have been studied for N and C isotopic composition and N content (see Chapter 6).

5.4. Results

5.4.1. N abundance and N and C isotopic composition

The results are tabulated in table A8-1 (Appendix 11). There is essentially no difference between our $\delta^{13}\text{C}$ values for individual Brazilian carbonados and the results obtained by Vinogradov *et al.*, 1966, Galimov *et al.*, 1978, 1985, Kaminsky, 1991. Based on the data, carbonados from Ubangui are indistinguishable from those collected in Brazil in respect of $\delta^{13}\text{C}$ and $\delta^{15}\text{N}$ (figure 5.1 and 5.2). However, one sample (JJG4105A) from Ubangui turned out to be so different from all the others ($\delta^{13}\text{C} = -5.8\text{‰}$ (repeated measurements), $\delta^{15}\text{N} = -5\text{‰} \pm 5$) that it may belong to a different category altogether.

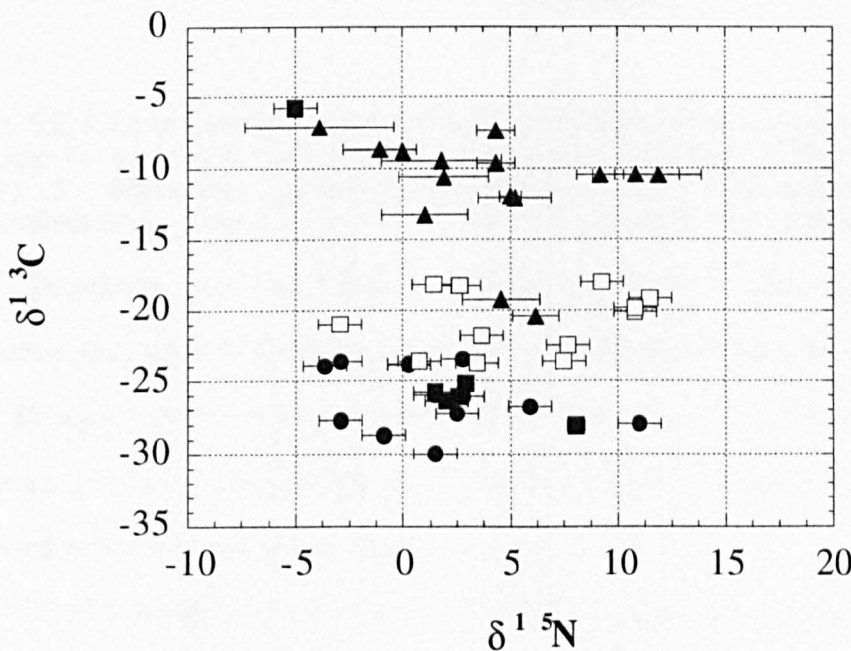


Figure 5.1. N-C isotope plot for different types of polycrystalline diamonds (filled circles - Brazilian carbonado; filled squares - Ubangui carbonado; filled triangles - shock diamonds from Popigai crater and other localities (see Chapter 6); empty squares - framesites).

Whereas Brazilian and Ubangui carbonados are similar, they can easily be distinguished from most framesites which are enriched in ^{13}C (fig. 5.2). The N abundance and $\delta^{15}\text{N}$ do not show significant differences (figures 5.1, 5.3, 5.4). A small

number of carbonados and framesites have the same C isotopic composition (fig. 5.1, 5.2). Both the Jwaneng and Orapa pipes contain normal single crystal diamond with isotopic compositions similar to the framesites studied here (Deines *et al.*,1993; Kirkley *et al.*, 1991).

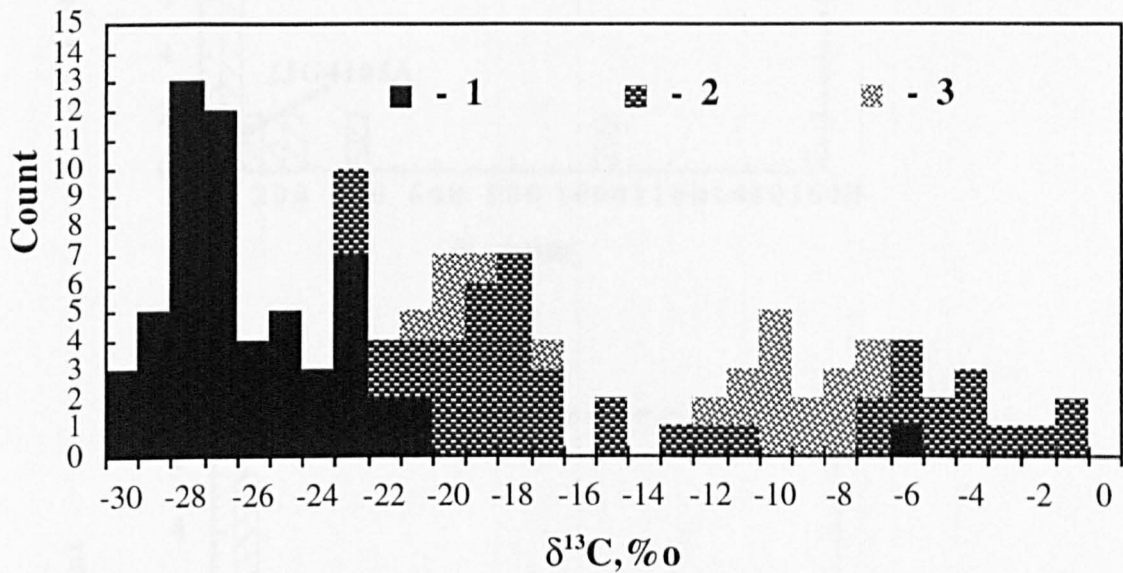


Figure 5.2. Carbon isotopic composition of carbonado, framesites and shock produced diamonds (1- carbonado, including data reported by Kaminsky (1991), and Ozima *et al.*, (1991); 2 - framesites, including data from previous studies(Deines *et al.*,1993; McCandless *et. al.*, 1989; Kirkley *et al.*, 1991); 3 - shock produced diamonds this study.

Diamonds from the Popigai crater are even more ^{13}C enriched than analysed framesites, they have $\delta^{13}\text{C}$ similar to many other specimens measured by Galimov *et al.*, 1978. Popigai samples were extremely low in nitrogen; in two of them it could not be measured, giving an estimated maximum limit of 5 ppm. Diamonds of impact origin are discussed in more details in the Chapter 6.

The N isotopic composition of carbonado, framesites and diamonds of impact origin are in the same range, -2‰ to +15‰, and are in fact indistinguishable at this point.

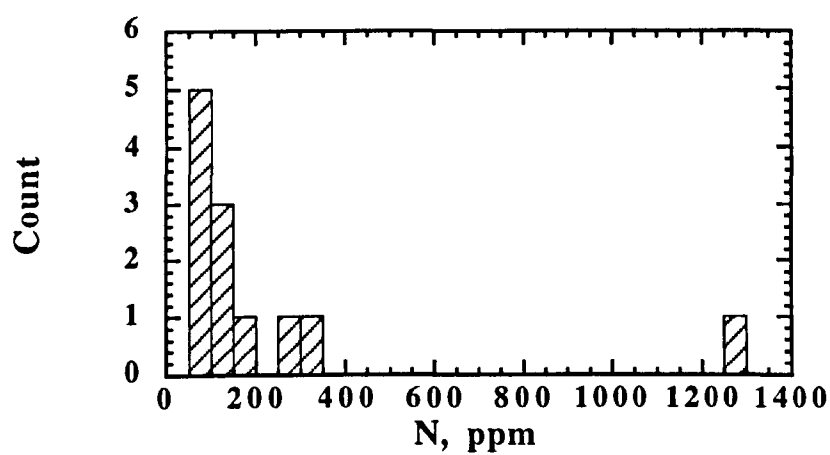
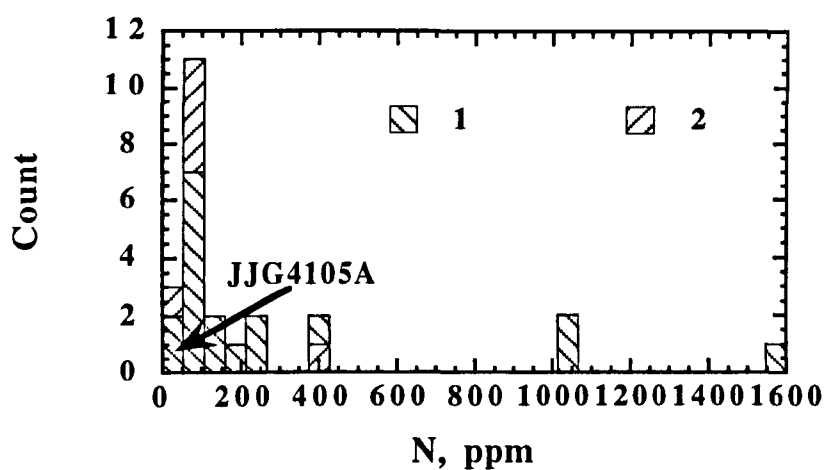


Figure 5.3 and 5.4. Distribution of N content in carbonado top (1 - Brazilian carbonado, 2 - Ubangui carbonado) and bottom in framesites.

5.4.2. Morphology and inner structure of carbonado

Although this research was based on a limited number of samples only it was possible to observe several structural varieties. A few samples contain aggregates which were full of rounded holes and consist of crystallites with size less than 5 microns. This is probably a major type, as it is consistent with observations made previously (Trueb and de Wys, 1971; Trueb and de Wys, 1969; Trueb and Buttermann, 1969). Another specimen (JJG4105E) was different from all the others due to the abnormally big size of some crystallites (several of them being as large as 200 microns) observed within a 1-10 μm grain size matrix. The sample could be described as of "porphyritic" structure. One of the large crystallites has a squared cross section (similar to cross section of octahedral crystal) which appeared to be zoned. However, the observed holes in the sample were shaped similar to those in the carbonados which described as a major type. The sample JJG4105C is uniformly crystallised and crystallites varied from 40 to 70 microns. The holes in this specimen appeared to be interstitial spaces left after the resorption of other minerals.

Some, but not all, carbonados have a smooth surface which resembles the ablated surface of meteorites. Only one of the samples (JJG4105B) with the smooth coat shows a significant difference between the rim and interior when viewed orthogonally: the 200 μm rim did not have any holes and the crystallites were probably smaller. The boundary between the rim and the rest of the sample was sharp and indicates either an extreme change in the conditions of growth, or a rapid transformation of the structure of the diamond aggregate close to the surface.

It should be noted that no distinguishable difference in terms of N and C isotopes were found between carbonados with different internal structures. The sample JJG4105A, which differs by C and N isotopes from the others, consists of 5-10 μm crystallites and interstitial space between them is unrecognisable. Several framesites were also polished and studied. Crystallite size was found to be variable, and cover the

total range observed for carbonado. I have not observed any of rounded holes similar to those common for most of the carbonado samples. The interstitial space in fine grain framesites are rather similar to those observed in the sample JG4105C.

5.4.3. IR study of carbonado

Infrared (IR) spectroscopy is used routinely to assess the quantity and hence aggregation state of nitrogen in diamond and hence to provide important information about mantle residence time for a given temperature (or vice versa). It is known that the nitrogen is present in single substitutional form (IR spectral type Ib) when the diamond is formed. Aggregation is a second-order process and to change the N aggregation state in diamond to produce IR spectral types IaA or IaB, high temperatures (higher than 800°C) prevailing for a significant length of time (dependent on N content) are required.

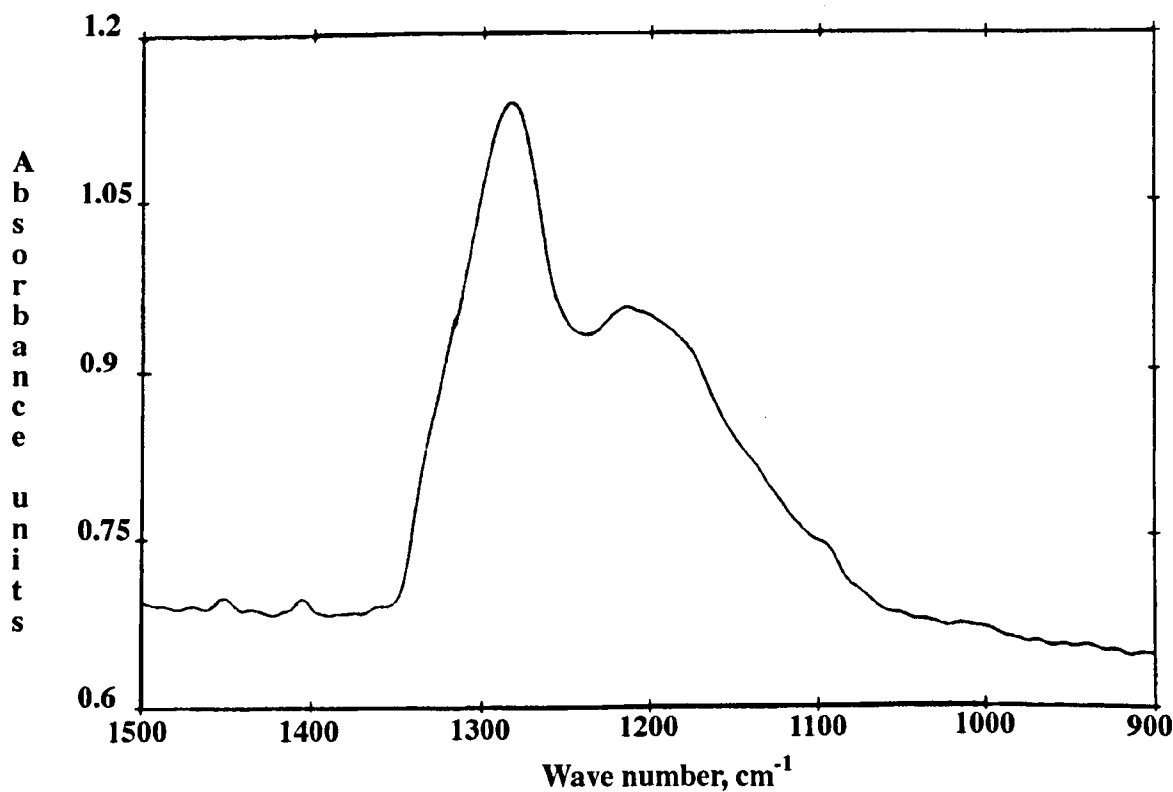


Figure 5.5. IR spectra of carbonado (CB20) crystallite indicating IaA aggregation state of N.

In two carbonados from Brazil individual grains were large enough for IR spectroscopy and showed fully developed IaA spectra. The N concentration of

fragments from one of the carbonados (CB20) was measured by mass spectrometry (1590 ppm) and in the other, not studied by mass spectrometry, may be even higher, as estimated from the IR spectrum (fig. 5.5). It is not yet clear whether the overall N content of N-rich carbonados is governed by the presence of a few type IaA N-rich crystals or whether all the diamond crystals are N-rich. The temperature required for complete conversion of N from the Ib to the IaA aggregation state in diamond is about 1000°C for a mantle residence time of about 3 Gy. It is difficult to contemplate such a long residence time for carbonado at such temperatures for times as long as 3Gy in any place in the crust, and these two crystals must have experienced normal mantle residence conditions similar to those experienced by many natural diamond monocrystals.

5.4.4. He abundances.

Helium data for carbonado from both sources and framesites obtained during the current investigation are summarised on fig.5.6. (see Appendix 11). No significant difference was obtained for the two populations of carbonado although Brazilian samples show higher scattering which might be a result of poor statistical representation for the South African group. The results reported by Ozima *et al* (1991) for carbonado are within the same range, however the greater number of samples included in the present study indicate significantly larger scatter of the ^4He content. Framesites from Orapa and Jwaneng have the highest ^4He concentrations among the diamonds of mantle origin, which are however lower than those in carbonado (fig. 5.6.).

Three carbonado specimens have a unique combination of the isotope signatures. The sample JG4105A has mantle carbon isotopic composition ($\delta^{13}\text{C} = -5.8\text{‰}$) and light nitrogen ($\delta^{15}\text{N} = -5\text{‰}$). Its He content ($0.00086 \text{ cm}^3/\text{g}$) is higher than in any of kimberlite diamonds and falls within the range for other samples of carbonado. The CB20 which exhibited an IR spectrum, indicating a rather long mantle history prior to the diamond emplacement into the crust has one of the lowest He concentration (0.00059 cc/g) observed in carbonado so far. However, carbon isotopic composition of

the sample ($\delta^{13}\text{C}=-23.8\text{‰}$) is well within in the carbonado range. The third specimen JIG4105C with the distinct microstructure (see above) also has relatively low ^4He content (0.00071 cc/g) but $\delta^{13}\text{C}$ value (-25.2‰) is not different from other carbonados with higher He concentrations.

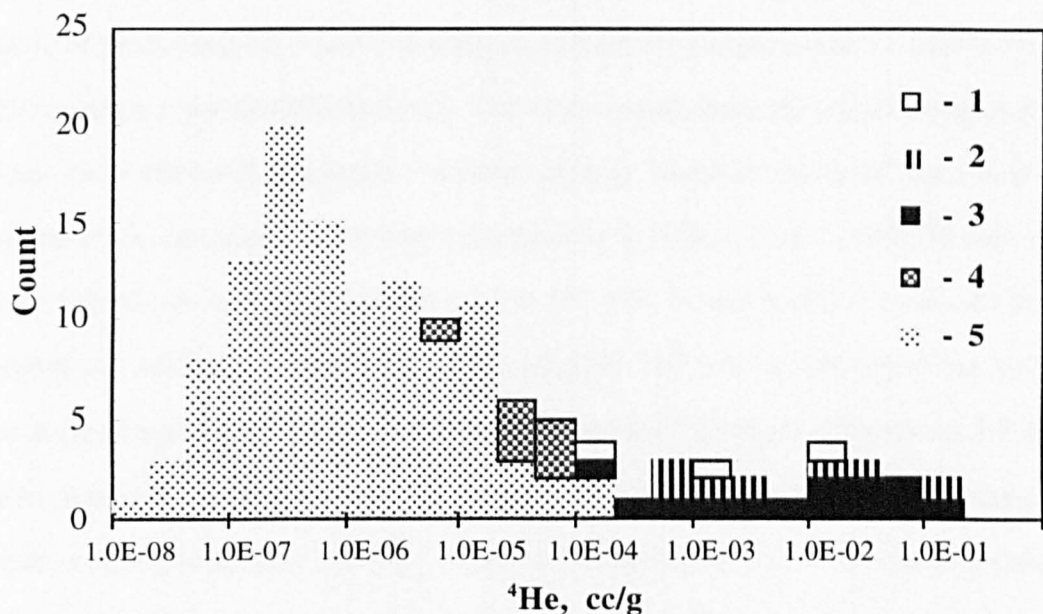


Figure 5.6. Distribution of ^4He concentrations in diamonds. (1 -concentrations within the rims of A1, F1, F4 (see Chapter 4); 2 - Ubangui carbonado; 3 - Brazil carbonado; 4 - framesites; 5 - ^4He concentrations in kimberlitic diamonds reported by others, summarised by Verchovsky and Begemann, 1993. Plot includes data for carbonado reported previously by Ozima *et al.* (1991))

5.5.Discussion.

5.5.1. Carbonado and diamonds of impact origin.

During the work leading to this thesis ideas concerning the formation of carbonado have evolved in respect of the impact origin. Shelkov *et al.*, (1994), Shelkov *et al.*, (1995) Milledge *et al.*, (1995) have suggested that Brazilian and Ubangui carbonados might have a common provenance, the link being a giant crater, proposed to explain the magnetic anomaly spread over 700,000 km² of Central Africa (Girdler *et al.*,

1992). If this feature is of Precambrian age, plate tectonic processes may have subsequently separated the resulting carbonados when the Atlantic opened. At the moment the best evidence that carbonados could be related to an impact event may be morphological appearance of the specimen (JJG4105B) mentioned above and by Shelkov *et al.*, 1995. The specimen has a surface layer explicable only in terms of highly unequilibrated processes. Impact is one of the few naturally known processes capable of producing the P and T conditions needed for the formation or transformation of diamond in a non-equilibrium way. The latter could cause the transformation of the surface of a diamond aggregate structure (plastic transformation of diamonds was experimentally modelled in the shock process by Novikov *et al.*, 1993). However, an impact hypothesis is argued against by several other observations: (i) samples with a "porphyritic" structure contain octahedral crystal of 200 micron size which are unlikely to be formed rapidly; (ii) the differences in N content between carbonado and impact-related diamonds studied here (see also chapter 6); (iii) the IR spectra of two carbonado samples also argue against a process which is almost instantaneous on a geological time scale. Taking into account that explanations other than an impact event might account for Central African magnetic anomaly, and that the observed surface layer of the sample (JJG4105B) could have resulted from rapid change in the diamond growth environment while diamond was in a mantle or crustal region, the evidence for impact hypothesis is far from conclusive.

5.5.2. Relations to the diamonds derived by kimberlites

Helium

According to Ozima *et al.* (1991) the radiogenic noble gases, including ^4He , cannot be produced in carbonado *in situ* as it would require time scale longer than the age of the Earth. Therefore, the only reasonable explanation for their occurrence is implantation from surrounding diamond matrix. This process has been discussed for other types of terrestrial diamonds before by Verchovsky *et al.*, 1992, Lal, 1989, etc. As

carbonado is found on Earth over a wide area, it would not be unreasonable to expect a large variations of U and Th content in the carbonado bearing placer deposits. Therefore carbonados with a wide range of ^4He contents would be expected as well. Variations in the grain size of crystals would also lead to the variations of He content as a result of surface implantation effect. Such ideas could be tested by looking for correlations between ^4He content and grain size or porosity. There is a qualitative correlation between grain size of diamond crystallites and concentration of ^4He for some specimens. For example, two samples with the lowest He concentrations (CB20 and JIG4105C) have the largest grain size.

However, an important question about He in carbonado is whether or not it needs a very special mechanism to be produced and implanted. In other words does the difference in the distribution of the He content in kimberlite diamonds and carbonado (fig.5.6) arises because of the difference in the grain size of kimberlite and carbonado diamonds. The results for framesites from kimberlites suggest that they are tending towards the He content of carbonados, although the framesites were extracted from primary kimberlites and therefore have not been exposed to irradiation in the placer deposits. This might suggest that crystallite size is a very important consideration. Given that I have found kimberlite diamonds with high skin helium concentrations approaching those for carbonado which are essentially a much higher proportion of surface it is possible that carbonados were irradiated in the same environment (see Chapter 4), which was thought to be within the surface region of the kimberlite pipe after emplacement. So, kimberlitic origin of carbonado does not seem now as unrealistic at least from their noble gas concentration point of view as was first thought. In other words the radiogenic noble gases can not be considered as a specific genetic feature for carbonado any more.

Carbon and nitrogen isotopic composition

It is known that the variations of $\delta^{13}\text{C}$ from -23‰ to -32‰ is unusual for terrestrial diamonds apart from some eclogitic diamonds (Galimov, 1991) or IR type II diamonds (Milledge *et al.*, 1983) which themselves may be eclogitic. Although framesites from Orapa and Jwaneng kimberlites have carbon isotopic composition which approach the above range, the overlap with carbonado is only minor. According to recent data (Mathez *et al.*, 1995), moissanite from kimberlites has a similar $\delta^{13}\text{C}$ range to carbonado which shows that in some cases kimberlites could contain other minerals with the same carbon isotopic signature as carbonado.

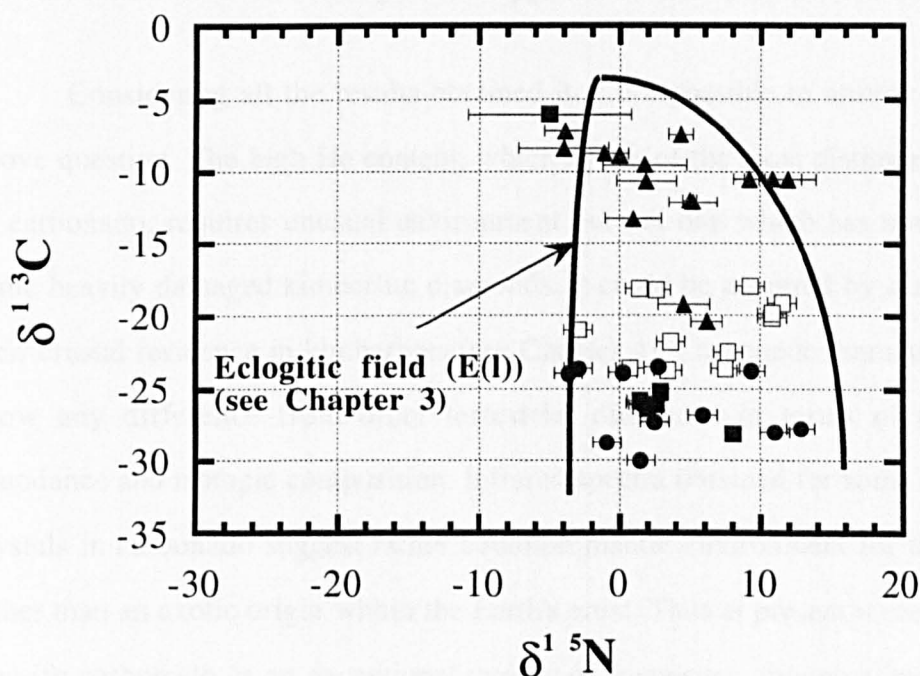


Figure 5.7. N and C isotope variations in polycrystalline diamonds(filled circles - Brazil carbonado; filled squares - Ubangui carbonado; filled triangles - shock diamonds from Popigai crater and other localities; empty squares - framesites).

Investigation of the C isotopic composition of diamonds derived from kimberlites has shown differences in the distribution of $\delta^{13}\text{C}$ values for diamond associated with eclogitic or with peridotitic minerals. Whereas peridotitic diamonds

show $\delta^{13}\text{C}$ of the range -2 to -10‰ (peak -5‰), eclogitic ones spread from +2.5 to -35‰ although the peak value is not much altered (-6‰) (Sobolev, 1979). Nitrogen isotope systematics are not as well established as for carbon and current study began to consider N and C isotopic composition of diamonds of known paragenesis. In Chapter 3 the approximate range of $\delta^{15}\text{N}$ for eclogitic diamonds was suggested to be -2 to +15‰ (fig.5.8.) as seen for carbonados (and framesites).

Thus, the suggestion that carbonado relates to kimberlite derived diamonds with a supposed subducted crustal component does not contradict our observations. The IR spectra which shows IaA type of N aggregation in two crystals are much more easily reconciled with such an origin.

5.6. Is carbonado an exceptional type of terrestrial diamonds?

Considering all the results obtained it is not possible to answer positively the above question. The high He content, which is one of the most distinguishing features of carbonado, requires unusual environment but not one which has not been seen by some heavily damaged kimberlite diamonds. It could be acquired by diamonds during their crustal residence in kimberlites (see Chapter 4). Carbonado diamonds also do not show any difference from other terrestrial diamonds in terms of their nitrogen abundance and isotopic composition. Infrared spectra obtained for some coarse grained crystals in carbonado suggest rather common mantle environment for their formation rather than an exotic origin within the Earth's crust. Thus at present it seems possible to classify carbonado as an exceptional variety of framesites, though some difference of their microstructure is observed. The other distinguishing difference between carbonado and other diamonds concerns their carbon isotopic composition: it is in general isotopically lighter than in any other types of diamonds, though it is fully within the range for eclogitic diamonds. Carbonados could be eclogitic diamonds which all come from closely related if not the same reservoir - the situation which is similar to that observed sometimes for carbon isotope variations for eclogitic diamonds from the same region: it could be different from general distribution. However, in one carbonado

sample from Ubangui I found $\delta^{13}\text{C} = -5.8\text{‰}$, which is exhibiting perfectly mantle signature to be present in some of carbonado, arguing against $\delta^{13}\text{C}$ range being restricted to the low values only.

5.7. Conclusions.

1. Carbon and nitrogen isotope data show no significant difference between two populations of carbonado (Brazilian and Central African) so they could be formed as a single population or in very similar geological events.
2. Variations of $\delta^{15}\text{N}$ and $\delta^{13}\text{C}$ for carbonado are in the range for crustal organics and metasediments. However, it does not necessarily mean that carbonado formed in crust, as subducted crustal material, could be involved in diamond formation in the mantle.
3. Diamonds from the Popigai crater are different from other types of polycrystalline diamonds studied according to $\delta^{13}\text{C}$, N.
4. One specimen of carbonado has a very distinct unequilibrated rim (although others also have a kind of coat) which could be explained by fast changing of growth conditions or partial transformations in the process which affected the edge of the sample only. The latter could be caused by shock although a undetermined mantle process could be responsible.
5. Conversely two diamonds, crystals in N-rich carbonados, with an infrared spectrum suggestive of long slow equilibration at temperatures and pressures akin to mantle residence were found.
6. It appears to be that high concentrations of implanted radiogenic noble gases detected in carbonado are not distinguishable from those which can be implanted into single diamond crystals in kimberlites.
7. None of the parameters previously suggested as distinct carbonado feature were able to uniquely distinguish carbonados from framesites or from eclogitic diamonds.

Chapter 6. C, N, Ar and He study of shock diamonds from Ebeliakh alluvial deposits and Popigai crater.

*There are more things in heavens and
earth Horatio,
Than are dreamt of in your philosophy.
William Shakespeare*

Abstract.

Nineteen diamond aggregate specimens (1-2 mm size) and two graphites from Popigai crater shock transformed rocks, two diamond aggregates from Pechug-Katun crater and six diamond samples (5-7 mm size) from Ebeliakh river placers were studied. X-ray investigation has confirmed that samples from Ebeliakh were involved in an impact event with exception of one specimen where no lonsdaleite was detected.

The carbon isotopic composition of diamonds from Popigai varies within the previously reported limits ($\delta^{13}\text{C}$ -10 to -22‰) whereas diamonds from the placer produced heavier values of $\delta^{13}\text{C}$ (-7 to -10‰). All the specimens studied contain very low amounts of nitrogen, mostly <20 ppm, but a few up to 60 ppm were detected. One exceptional sample from Ebeliakh in which no lonsdaleite has been identified contains 800 ppm of nitrogen and together with distinct $\delta^{13}\text{C}$ of -27.6‰. It suggests the sample to be unrelated to the main group of samples. For specimens, where the quantity of nitrogen allowed reliable analysis, $\delta^{15}\text{N}$ values were found to range from -3.9 to +11.9‰. On the basis of combined Ar and N study of shock diamonds from Ebeliakh placers it was concluded that these aggregates can be a mixture of at least two types of gas carriers. A possible explanation would be involvement of CVD type of process in addition to the direct graphite-diamond shock transformation.

6.1. Introduction.

The term yakutite was introduced in 1991 by Kaminsky for diamonds of impact origin. Such samples were previously known as "hexagonal diamonds" (Bundy and Kaspar, 1967; Hanneman *et al.*, 1967), "carbonado-like diamonds" (Bartoshinsky *et al.*, 1980), "lonsdaleite-bearing polycrystalline diamond" (Rumyantsev *et al.*, 1980), "carbonado with lonsdaleite" (Orlov and Kaminsky, 1981).

In 1966, in alluvial deposits of Northern Yakutia, diamonds of a unique nature were discovered. They were shapeless, frequently of dark-brown to steel-grey colour. Taking into account their unusual appearance, these diamonds were named yakutites after the where they were found — Yakutia. Similar polycrystalline diamond aggregates were later encountered in alluvial deposits in Ukraine (Polkanov *et al.*, 1973, 1978). Eventually the hexagonal modification of carbon (lonsdaleite) was recognised in the polycrystalline aggregates of diamond (Krajnyuk and Bartoshinsky, 1971; Kaminsky *et al.*, 1978, 1985; Klyuev *et al.*, 1978, Valter *et al.*, 1990) and since lonsdaleite is a high pressure modification of carbon, which was already found in meteorites (Hanneman *et al.*, 1967), the formation of yakutites was suggested to be linked with meteorite impact events. In 1972, Masaitis *et al.*, reported first finds of diamonds with lonsdaleite in impactites of the Popigai crater which confirmed an impact origin for polycrystalline diamonds with lonsdaleite. Currently impact produced diamonds of smaller size range were reported to be found in deposits of KT-boundary (e.g. Gilmour I. *et al.* 1992), Ries crater (e.g. Hough *et al.*, 1995) and many others (e.g. Masaitis 1990, Veshnevsky *et al.*, 1995).

6.1.1. Properties of diamonds formed in the impact craters.

Impact diamonds are mainly 0.1 to 0.5 mm in size (rarely up to 1 to 5 mm), being an aggregates of crystallites of 0.1-1 μm (Kaminsky, 1991). The colour of these diamond aggregates is variable from colourless through yellow to grey and black (yellow and black are the most ordinary). The total range of carbon isotopic composition was reported to be from -9‰ to -25‰ (Kaminsky *et al.*, 1977; Galimov *et al.*, 1978; Kaminsky 1994,

Masaitis *et al.*, 1990), although, specimens from different areas of sampling show bi-modal distribution of $\delta^{13}\text{C}$ being either -9.9‰ to -20.1‰ or -22.3 to -24.6‰ (Veshnevsky *et al.*, 1995). Several other features of the diamonds have also indicated a dual nature: the density of impact diamonds was reported to be in the two ranges 3.44 to 3.55 g/cm³ and 2.5 to 3.1 g/cm³, colour of photoluminescence was either yellow-orange or yellow-green; the combustion temperature range was either 580-760°C or 520-650°C. Based on the above differences, two major source materials have been proposed to explain the differences in the properties of shock diamonds: graphite and organics (coal) (Veshnevsky *et al.*, 1995).

6.1.2. Formation of shock diamonds.

Diamond/lonsdaleite in impact craters was assumed to be the result of the direct shock conversion of graphite (or coal) to diamond/lonsdaleite (some of diamond aggregates resemble the morphological shape of graphite), however, the recent finding of diamond in close relations with silicon carbide suggests that extremely high pressure is not necessarily required for diamond formation in the Ries crater (Hough *et al.*, 1995). By analogy with CVD (carbon vapour deposition) diamonds grown on Si substrates, where inter-growth of SiC and diamond occurs, diamonds in the Ries crater could have originated in the vapour or even in plasma within a fireball, which might have been produced by impact explosion (Hough *et al.*, 1995).

6.1.3. Noble gases in shock produced diamonds.

No specific study has previously been made to determine noble gas isotopic composition and their distribution in natural impact diamonds. However, noble gas fractionation within shock and CVD diamonds produced under laboratory conditions has been studied in relation to the formation processes (direct shock transformation and CVD) discussed above. Two types of CVD diamonds and diamonds formed by shock transformation indicated three different noble gas abundances patterns (Matsuda *et al.*, 1991). Noble gas abundance patterns for both types of CVD diamonds appeared to be

distinguishable from those of shock produced diamonds, since insignificant noble gas fractionation occurred in direct shock transformation of graphite into diamond (Matsuda *et al.*, 1989, 1995).

Only one natural diamond from the Popigai crater has been analysed to obtain noble gases data (Verchovsky *et al.*, 1991). The elemental abundance pattern was found to be consistent with that obtained for artificial shock diamonds. However, the sample showed at the same time unusually high concentrations of radiogenic ^{40}Ar and ^4He which appearance have not been unambiguously explained (Verchovsky *et al.*, 1991).

6.1.4. Aims of the study.

Since neither noble gases nor nitrogen had been systematically studied in natural diamonds of shock origin, it was decided to analyse shock diamonds from two geological sites (Popigai crater and Ebeliak river placers) for Ar, N, C isotopic composition and for Ar, N, He content. It should be noted, however, that as no connection with primary rocks is known for the diamonds from Ebeliak it is not entirely clear whether their formation took place in the same or in a similar impact event to Popigai. Therefore, a secondary goal for this work was to compare the diamonds from the two sources. In addition distribution of Ar and N within the diamond aggregates was studied using step combustion technique.

6.2. Samples.

Within the study yakutites from Popigai crater (71°30'N, 111°0'E, diameter of 100 km, age of 35 ± 5 My Grieve *et al.*, 1995) and Ebeliak river placers (Northern Yakutia) have been analysed. One suite of samples is a set of 19 diamonds (the largest aggregate was 1.5mm in diameter) extracted from the impactites of the Popigai crater, which is along with distinct morphological features indicating the relation to the shock. Another set of samples consisted of 7 polycrystalline diamonds (the sizes of these aggregates were between 3 and 5 mm in diameter) came from Ebeliak river placer deposits (Northern Yakutia, about 200-300 km on the East from Popigai crater). Ebeliak river placers are known to be diamond rich deposits and especially for the presence of

polycrystalline diamond aggregates quite dissimilar from kimberlite diamonds in morphology. Since lonsdaleite has previously been reported in these aggregates (Kaminsky *et al.*, 1985), there is no doubt that they relate to an impact event.

The Popigai crater is on the slope of the Anabarskii shield, where the crystalline Archean rocks are overlapped by terrigenous and carbonate formations of Proterozoic, Cambrian and Permian age and penetrated by dikes and sills of Triassic dolerites. The parameters of the Popigai crater are determined on the basis of morphological and structural observations, geophysical data also show presence of negative magnetic and gravity anomalies. The crater seems made of two funnels, placed one inside the other. Breccias are developed in the inner funnel and also locally distributed in the confines of the outer funnel and beyond the rims of the crater. The visible thickness of impactites of about 200 m.

In all the diamond aggregates from the Ebeliakh river placer deposits, except sample Y7, X-ray diffraction data has been able to relate the samples to an impact event. These aggregates also fit the descriptions of yakutites from Siberian placers reported before (Kaminsky *et al.*, 1985), with exception of Y7 again, which is rather like carbonado specimens in appearance.

In addition to shock diamonds from Ebeliakh and Popigai, two diamond samples from the Puchezh-Katun (57°6'N, 43°35'E, age of 175 ± 3 My Grieve *et al.*, 1995) crater and two specimens of graphite from the Popigai crater were studied. Graphite and the diamonds from Puchezh-Katun crater were analysed for $\delta^{13}\text{C}$ only.

6.3. Experimental technique.

Samples of 0.05 to 1 mg were analysed for C and N isotopic composition in accordance with the analytical procedure described in the section 3.3 (see also chapter 2).

Either a bulk or a step combustion technique was used for the gas extraction in the range of temperatures from 500°C to 850°C (1100°C for bulk experiments); a double wall quartz combustion reactor (the inter-space between the walls was under vacuum) was designed to lower He and Ar blank down to $1 \times 10^{-9} \text{ cm}^3$ and $3 \times 10^{-10} \text{ cm}^3$ respectively (see

chapter 2). Helium was analysed for ^4He content using a Quadrupole Mass-spectrometer in the static mode. Then after purification procedures (section 2.5) either Ar and N isotope analyses were performed (N by static mass spectrometer, Ar by quadrupole static mass spectrometer) or the Ar isotopic composition and N content were analysed in static regime by Quadrupole Mass spectrometer in separate aliquots, depending on the aims of the experiment.

The fragment of sample Y18 and fragment of Y14 have been step combusted with different resolutions in addition to the bulk experiments discussed above. Instead of the high temperature treatments two pyrolysis steps (1000°C and 1100°C) were applied to the samples before combustion. Since Ar release in these steps was insignificant, the high resolution experiment with Y18 (Y18(2) in further discussion) was carried out without high temperature pyrolysis at all, which resulted, however, in a large contribution of nitrogen contaminant in the first two steps (Appendix 12 table A12-2).

6.4. Results

6.4.1. N, C, He and Ar in the bulk experiments.

It has previously been suggested on the basis of infrared (IR) and electro-paramagnetic resonance (EPR) studies that diamonds of shock origin have low nitrogen content (Kl'uev *et al.*, 1978, Kaminsky *et al.*, 1985). The quantitative analysis performed herein has confirmed the suggestion for both sets of samples studied; in a few experiments reliable measurements could not be obtained as N levels were too low (Appendix 12). For those specimens where the amount of N was sufficient to apply reliable isotope measurements the variations of $\delta^{15}\text{N}$ were found to be between -3.8‰ ($\pm 4\%$) and +11.9‰ ($\pm 2\%$) (Fig. 6.1.). Carbon isotopic composition was analysed for the all samples, and ranged from -7.2‰ to -20.4‰ (Fig. 6.1, 6.2), although, yakutites from Ebeliak have exhibited the more limited range of $-8.35 \pm 1.15\%$. Only three out of nineteen Popigai samples fell into the range obtained for diamonds from Ebeliak (Fig. 6.6.2). The diamonds from the Popigai crater indicate a bi-modal distribution of $\delta^{13}\text{C}$ which does not correlate with either N content or N isotopic composition.

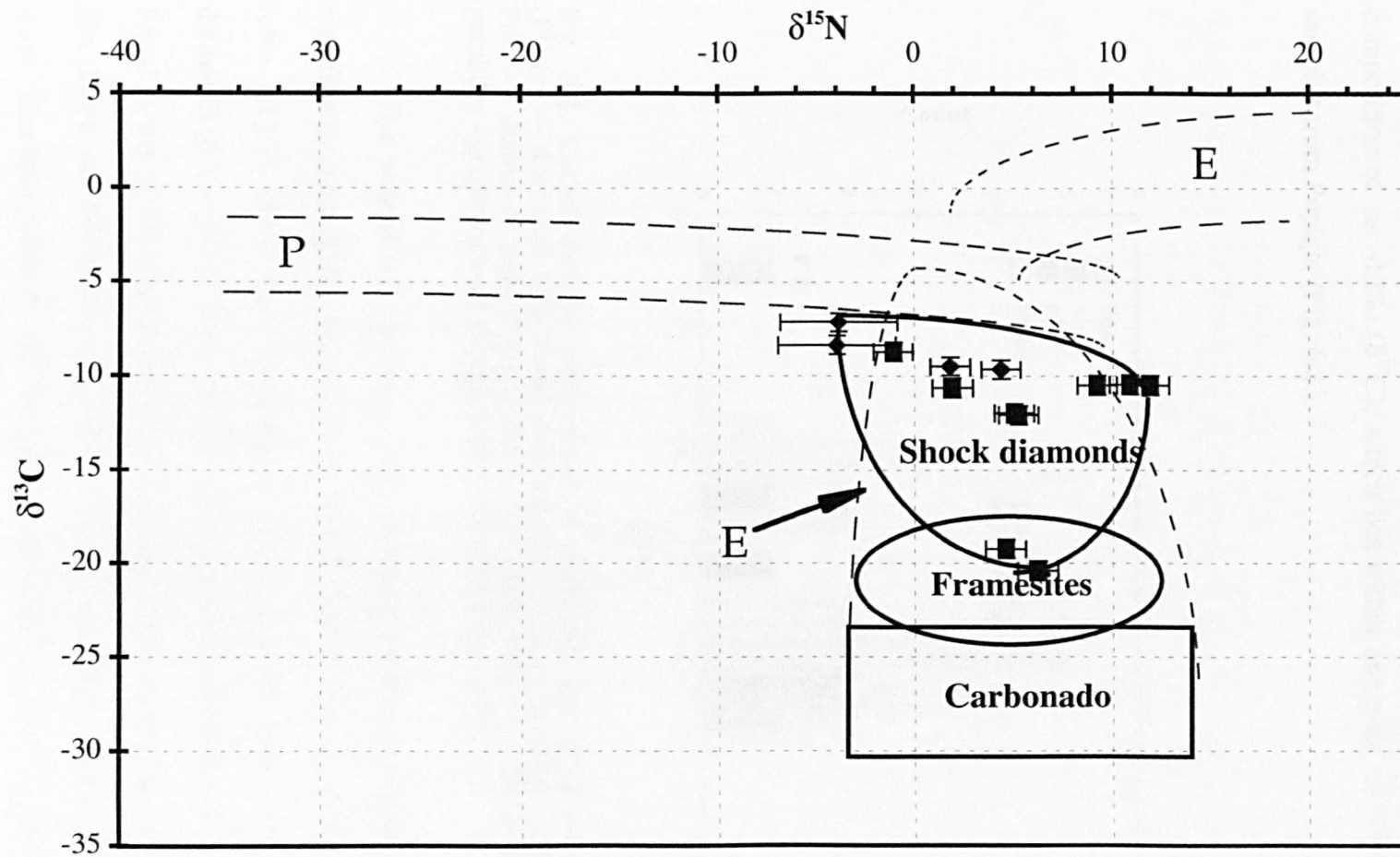


Figure 6.1. C and N isotopic composition of shock diamonds (rhombus — diamonds with lonsdaleite from Ebeliak, squares — diamonds from Popigai impactites; dashed lines show the fields proposed for peridotitic (P) and eclogitic diamonds (E) (see Chapter 3)).

Specimens of graphite show $\delta^{13}\text{C}$ within the range reported previously for graphite from the crater (Masaitis *et al.*, 1990) (fig.6.2), although the range for graphites reported previously together with our samples does not in fact overlap with either of the peaks for $\delta^{13}\text{C}$ distribution of analysed diamonds from Popigai (Fig. 6.2).

Diamond samples from Pechug - Katun crater contain carbon with an isotopic composition of ca. -12‰ ($\delta^{13}\text{C}$), which lies within one peak of $\delta^{13}\text{C}$ distribution for samples from Popigai (Fig. 6.2.).

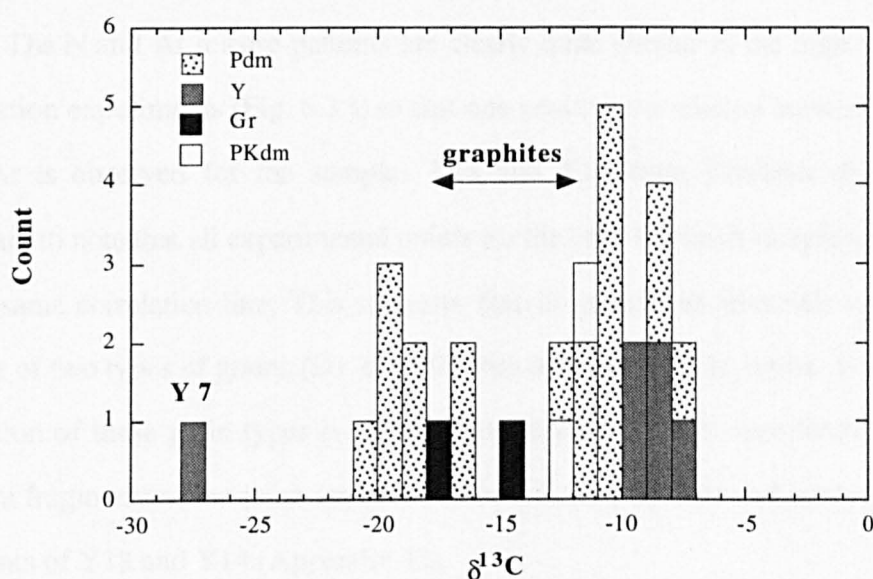


Fig. 6.2. Carbon isotopic composition of diamonds and graphites from impactites. (PKdm — diamonds from Puchezh-Katun crater; Gr — graphites from Popigai crater; Pdm — diamonds from Popigai crater; Y — diamonds from Ebeliak River deposits; graphites - graphites from Popigai crater (Masaitis *et al.*, 1990)

The exceptional specimen from Ebeliak (without lonsdaleite - Y7) differs significantly from all the others in terms of $\delta^{13}\text{C}$ and N content (Fig. 6.2., Appendix 12 table. A12-1). The $\delta^{13}\text{C}$ of the sample (-27.6‰) is in the range of that for carbonado diamonds ($\delta^{13}\text{C} = -20$ to -30‰) and the N concentration of 800 ppm is far higher than that found in any of the other diamonds studied here, also being in the range for carbonado (Shelkov *et al.*, 1995). Since Y7 differs from the main Ebeliak sample group in several ways other than purely by the absence of lonsdaleite, I must conclude that the sample cannot be genetically related to the others.

The argon content and isotopic composition have been studied in nine samples from the Popigai crater and in all of the samples from Ebeliakh. The Ar content was found to be variable from 1.7×10^{-6} to 3×10^{-4} cc/g and the $^{40}\text{Ar}/^{36}\text{Ar}$ ratio changes from atmospheric (≈ 296) to extremely radiogenic (>1000) (Appendix 12).

Helium concentrations have only been measured for specimens from Ebeliakh and were found to vary between 1×10^{-6} and 2×10^{-4} cc/g (Appendix 12) and do not correlate with either Ar, or total Ar, N contents.

6.4.2. N and Ar release patterns and correlations.

The N and Ar release patterns are clearly quite similar in the high resolution step combustion experiments (Fig. 6.3.), so that one positive correlation between release of N and ^{36}Ar is observed for the samples Y18 and Y14 from Ebeliakh (Fig. 6.5). It is important to note that all experimental points for the bulk Ebeliakh sample turned out to be on the same correlation line. This suggests that in general all Ebeliakh samples are the mixture of two types of grains (D1 and D2) with different N/ ^{36}Ar ratios. It seems that the proportion of these grain types is variable not only in different samples but even within different fragments of the same sample as it is indicated by repeated analysis of different fragments of Y18 and Y14 (Appendix 12).

Similar correlation between N and ^{36}Ar is also observed for the samples from Popigai crater. The corresponding correlation line is, however, different from that for Ebeliakh samples indicating that in this case the both components have lower N/ ^{36}Ar ratios.

6.4.3. Ar components.

The total variations of $^{40}\text{Ar}/^{36}\text{Ar}$ ratio in the sample Y18 were found to be from 376 to 2148 and those in the sample Y14 were from 336 to 681 (including bulk analyses). Argon appears to be released from diamond grains (fig 6.3.) because any other potential Ar carriers (e.g. silicates) should release their Ar during pre-combustion pyrolysis steps at 1100°C performed for the most of the samples.

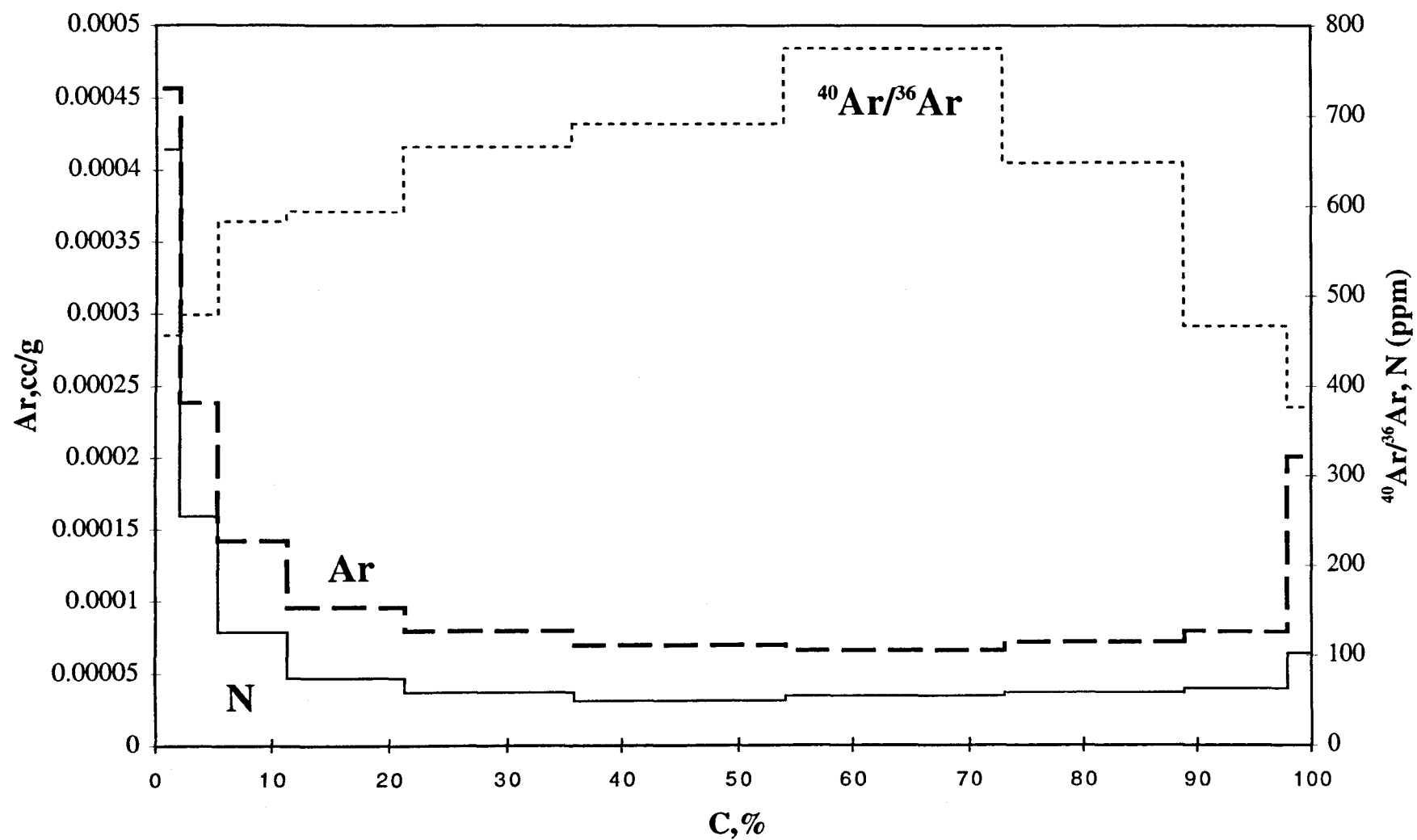


Figure 6.3. Step combustion experiment Y18(2).

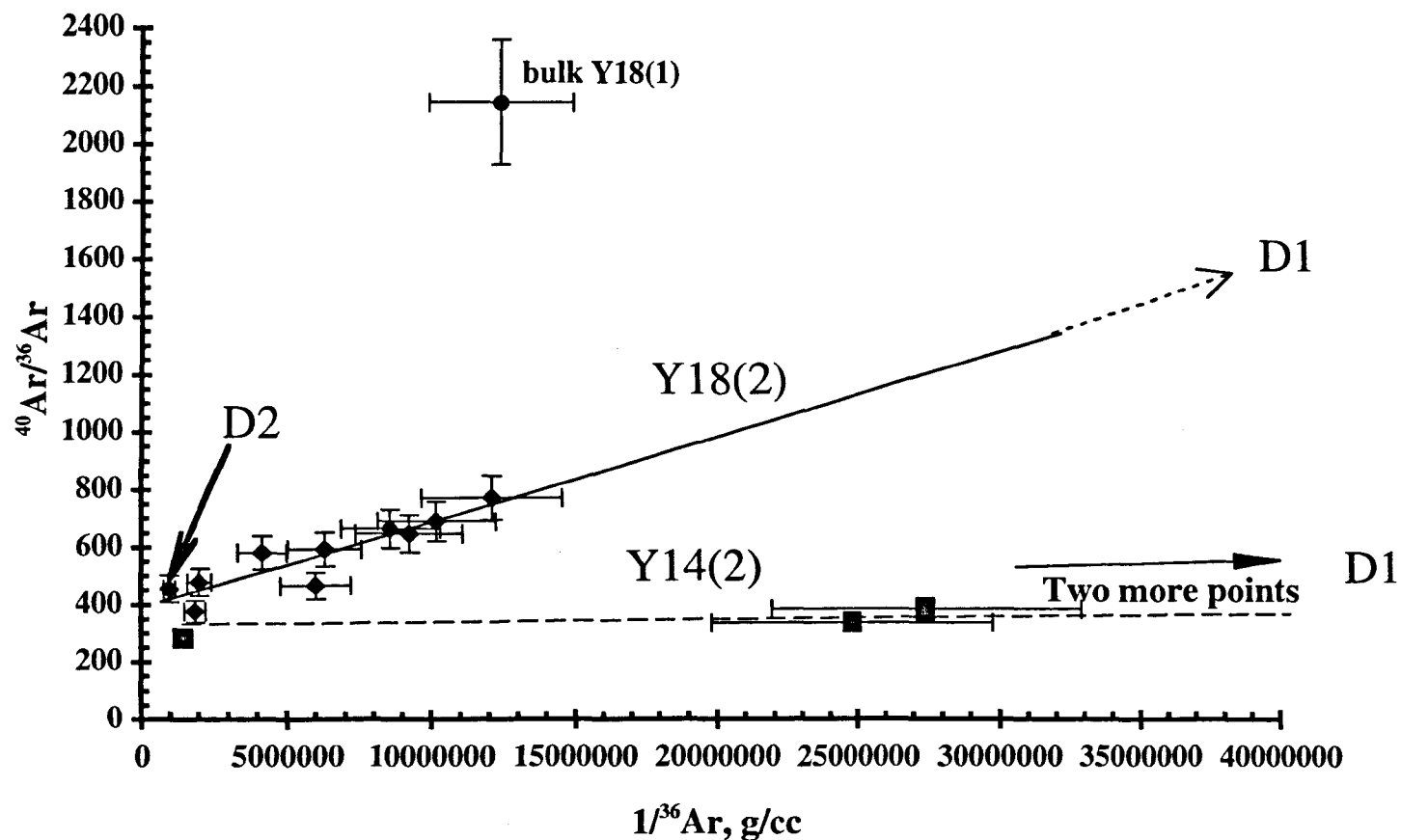


Figure 6.4. $^{40}\text{Ar}/^{36}\text{Ar}$ - $1/^{36}\text{Ar}$ correlations based on results of step combustion experiments Y18(2) (solid line) and Y14 (dashed line) (filled rhombus - single steps of experiment Y18(2); filled squares - single steps of experiment Y14(2) two point including bulk (Y14(1)) used for calculation of the correlation line are not on the picture; filled circle - result of bulk experiment Y18(1); D1 and D2 - two types of diamond grains suggested to be responsible for the mixing line).

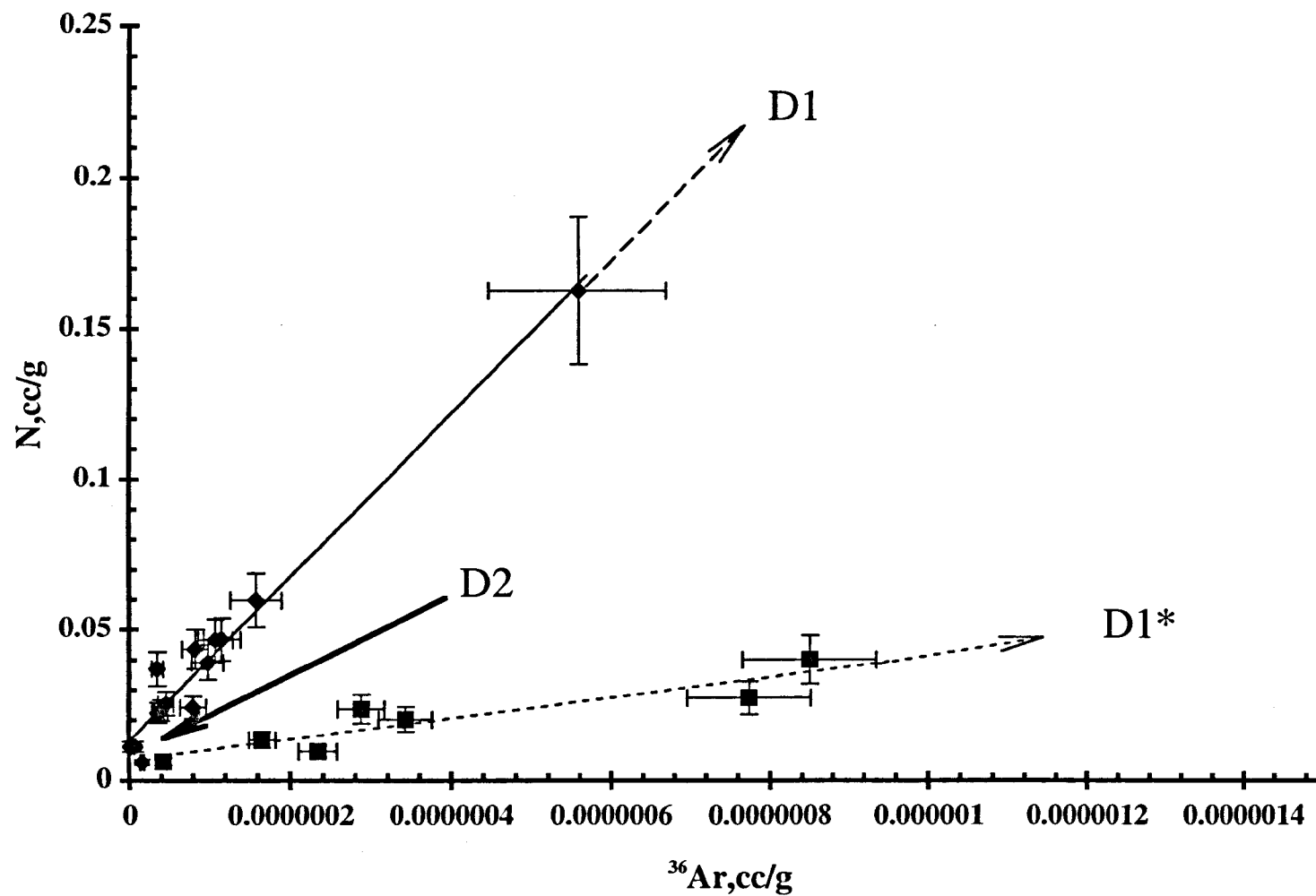


Figure 6.5. Comparison of N — ^{36}Ar correlations of samples from Ebeliak deposits with lonsdaleite and samples from Popigai creator (squares — Popigai samples; rhombus — Ebeliak measurements; D1 and D2 - two types of diamond grains suggested to be responsible for the mixing lines).

All combustion steps in the experiment Y18(2) show linear correlation in coordinates ($^{40}\text{Ar}/^{36}\text{Ar}$) - ($1/^{36}\text{Ar}$) (fig 6.4., Appendix 13 table A13-3). The correlation may indicate a mixture of two types of carriers with different $^{40}\text{Ar}/^{36}\text{Ar}$ ratios and concentrations of ^{36}Ar if these carriers have different but overlapping combustion temperatures. Correlation between concentrations of Ar_{rad} and Ar_{atm} indicates that just this mixing model is valid in this case. Correlations between ^{36}Ar and N, $^{40}\text{Ar}(\text{rad})$ and N (Appendix 13 table A13-1 and A13-1) also confirm the interpretation.

The results of experiments Y18(2) and Y14 plotted on the same $^{40}\text{Ar}/^{36}\text{Ar}$ vs. $1/^{36}\text{Ar}$ plot indicate the presence of two mixing lines with almost the same intercepts but with different slopes (Fig. 6.5, Appendix 13 table A13-3), suggesting the component D2 to be the same in both samples with an almost atmospheric $^{40}\text{Ar}/^{36}\text{Ar}$ ratio, while the other component D1 has distinguishable $^{40}\text{Ar}/^{36}\text{Ar}$ ratios in these two samples. Since there is only one correlation line for N vs. ^{36}Ar measurements (Ebeliak samples), indicating only two types of different carriers, I may assume one of these carriers (D1) to have variable $^{40}\text{Ar}/^{36}\text{Ar}$ ratio. The fact, that bulk Y18 measurement does not belong to the correlation line $^{40}\text{Ar}/^{36}\text{Ar}$ vs. $1/^{36}\text{Ar}$ (fig. 6.4) identified for the step combustion experiment of Y18(2), although it does lie on the line N vs. ^{36}Ar (fig. 6.5), shows that even in the different fragments of the same sample the $^{40}\text{Ar}/^{36}\text{Ar}$ ratio in the carrier D2 could be very variable i.e. the sample is extremely heterogeneous in terms of ^{40}Ar content.

6.5. Discussion.

6.5.1. Two component mixture.

Assuming the presence of two diamond components representing different gas carriers, the interpretation of the gas release patterns for the samples studied by step combustion is as follows: the first (D1) component represents diamond grains with more restricted range of combustion temperatures ($\approx 650\text{-}800$) than the second component (D2) having range of combustion temperatures $\approx 550\text{-}850^\circ\text{C}$. Compared to D1 grains, D2 grains have (i) lower, but a slightly higher than atmospheric $^{40}\text{Ar}/^{36}\text{Ar}$ ratio; (ii) lower

N/³⁶Ar ratio being closer to atmospheric one for Popigai diamonds, (iii) higher Ar and N concentrations. Because of the difference in the combustion temperatures the first component (D1) is almost undetectable at the beginning and at the end of the experiments. These grains have much higher than atmospheric N/³⁶Ar and ⁴⁰Ar/³⁶Ar ratios and ⁴⁰Ar/³⁶Ar ratio can be variable for different samples and even within the same sample.

All diamonds from Ebeliakh are in the narrow range of $\delta^{13}\text{C}$ ($-8.35 \pm 1.15\text{‰}$) suggesting that, despite the fact that all of them have been extracted from placer deposits, they are rather a result of a single (impact) formation event. The above conclusion is supported by the grouping of all the samples on the same N - ³⁶Ar correlation line (fig. 6.5). The diamonds from Ebeliakh seem also to be distinguishable from the diamonds from Popigai with respect to their $\delta^{13}\text{C}$ distributions (fig. 6.2) and to N vs. ³⁶Ar correlations (fig. 6.5).

The nitrogen isotopic composition does not suggest any distinction between diamonds of shock origin on the one hand and carbonado, framesites or diamonds of eclogitic suite (Fig. 6.1.) on the other hand. All these diamonds are known to contain a fraction (sometimes significant) of crustal N, which is expected to be a principal component for diamonds formed by impact. Given that impact transformation of graphite (or another solid state carbon phase) into diamond is extremely fast and unequilibrated process, I may suggest that N and Ar can be partially inherited from the source material and the N/³⁶Ar ratios in diamonds, which are higher than that of atmosphere, could be rationalised on the basis of the fact that N can be a structural impurity in diamonds or other pre-existing carbon phases, can create chemical bonds with C and therefore can be trapped with higher efficiency than Ar.

Helium in the samples from Ebeliakh is variable and does not correlate with any of the other gases studied. Therefore the nature of He in these diamonds is probably a post impact phenomenon resulting from implantation from U and Th decay in the diamond host rocks, and the variations in the He contents can be simply a result of corresponding variations in the U and Th concentrations. Assuming that the samples were affected by implantation from average crustal concentrations of U and Th, the age of implantation,

calculated for the average He content for all Ebeliak samples, turns out to be about 40 My, which is close to the age of Popigai crater. Of course there are many uncertainties in such age estimation, although a much greater age is not very probable since it would require U-Th concentrations to be much lower than average crustal values.

Finally attention should be drawn to the fact that the $\delta^{13}\text{C}$ distribution for Popigai diamonds does not exactly correspond to that for graphites (Fig. 6.2). This observation might mean that, during or before the shock event, graphite was mixed with other carbon phases with isotopic composition which can be lighter as well as heavier than that for graphite. It is also possible that diamond has not been a result of direct solid state carbon phase transformation only, but has been accomplished by growing from a gas phase (CVD like process, Hough *et al.*, 1995) as well. However, the sampling statistic for graphites and diamonds is poor and the inconsistency in distributions of $\delta^{13}\text{C}$ of graphites and diamonds can vanish when more representative sets of samples would be studied.

6.5.2. The model.

From the above considerations I can suggest two models based on the N and Ar data. Both models assume the mixture of two diamond populations having different oxidation temperatures: D1 with high and variable $^{40}\text{Ar}/^{36}\text{Ar}$ ratio, low N and ^{36}Ar concentrations, but high N/ ^{36}Ar ratio and D2 with low close to the atmospheric $^{40}\text{Ar}/^{36}\text{Ar}$ ratio and high concentrations of N and ^{36}Ar and low N/ ^{36}Ar ratio. The differences in oxidation temperature might be due to differences in the grain size distributions of the two diamond populations (Wright and Pillinger, 1989), to zonation of single grains, to the presence of two phases with different temperature ranges of combustion, or to a combination of all three.

The first version of the model assumes the presence of the two diamond types to be the result of two processes operating during impact. Graphite or/and other solid state carbon phases are the source material for component D1: hence it contains inherited radiogenic Ar with a high $^{40}\text{Ar}/^{36}\text{Ar}$ ratio and N enriched relatively to ^{36}Ar in comparison to the atmosphere. It has been reported before that carbon phases from ancient

metamorphic complexes can have high concentrations of radiogenic Ar (Roskamp and Schultz, 1985), so that diamond resulting from direct shock transformation of such phases may inherit Ar with high $^{40}\text{Ar}/^{36}\text{Ar}$ ratios and reflect all the variations in $^{40}\text{Ar}/^{36}\text{Ar}$ ratios present in the primary material. The diamond component (D2) then crystallised from gas phase (CVD like process) trapping N and Ar from the gas mixture locally presented. The argon isotopic composition of the mixture is supposed to be close to that in the atmosphere. The diamonds were precipitated in the form of relatively large crystal grains and formed at the same time a thin layers on the already existing relatively small diamond grains D1. Therefore, performing a step combustion experiment with such a mixture of D1 and D2 diamonds, the D2 component is observed to be dominant at the beginning and at the end of the experiment with a mixture of D1 and D2 in variable proportions in the middle.

Another version of the same model suggests lonsdaleite and diamond to be the two principal components. In this case it is unnecessary to appeal for two different processes during the impact, i.e. the graphite-diamond phase transformation and CVD-type diamond synthesis, to produce two components with different geochemical signatures. Different amounts of gases could be inherited from the source material and different trapping efficiency of the surrounding atmosphere might result from distinction in the crystal structures of diamond and lonsdaleite. Therefore, supposing the same grain size relationship and crystal intergrowing as it is suggested for the above model the observed release patterns of N and Ar can be explained.

6.5.3. Sample Y7

The sample did not show any signs of a relating to an impact on the basis of X-ray diffraction study and other features (N=800ppm, $\delta^{13}\text{C}=-27\text{‰}$). In fact everything measured indicated a distinction from all the other samples. The appearance of the diamond aggregate along with the C isotopic composition suggest that it is very similar to carbonado, although that does not rule out the possibility the sample being an eclogitic diamond (the same might be also proposed for carbonado in general as the diamond type

(see Chapter 5)). However, the concentration of Ar with isotopic composition close to the atmospheric distinguishes the specimen from kimberlitic diamonds previously analysed by the others (Fig. 6.6), but no comparative results for carbonado are available. Considering that high nitrogen concentrations are unlikely to be present in the diamonds formed by shock, and high atmospheric Ar contents have not been found in kimberlitic diamonds, I might consider the possibility of the effect of impact on the pre-existing diamond. The atmospheric Ar in which case have been implanted into the diamond structure during the impact. However, due to the similarity of the sample with carbonado it might be an example of carbonado from Siberia.

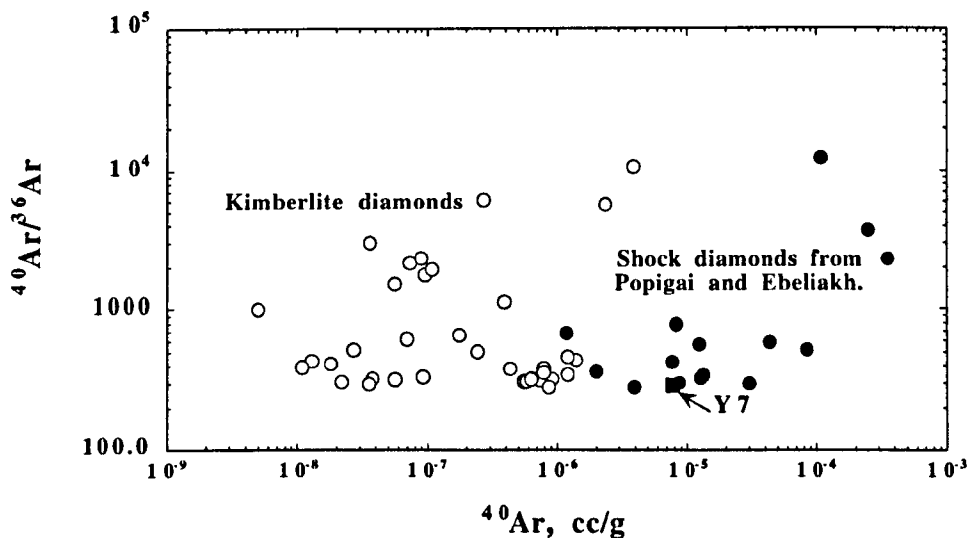


Fig.6.6. Comparison of Ar in shock diamonds from Popigai and Ebeliakh with kimberlitic diamonds (Ozima *et al.*, 1985; Kamenskiy and Tolstikhin, 1992; McConvill and Reynolds, 1989).

6.6. Conclusions.

1. Polycrystalline diamonds from the Ebeliakh placer, excluding Y7, seem to be formed in the same impact event.
2. According to Ar and N study shock diamonds from Ebeliakh and Popigai consist of a mixture of at least two different types of diamond grains; one of which contains a highly radiogenic Ar acquired during pre-impact history of the source material.

3. Diamonds from Ebeliakh are distinguishable from Popigai samples by the $\delta^{13}\text{C}$ and different N- ^{36}Ar correlations, therefore they could be considered as the result of the separate impact event.
4. Difference in $\delta^{13}\text{C}$ distribution between Popigai diamonds and graphites makes it doubtful that graphite is the only source material for diamonds of the Popigai crater.
5. Diamonds formed by shock exhibit enrichment in atmospheric Ar and depletion in N by comparison with diamonds derived from kimberlites.

Chapter 7. Conclusions and further research.

Various problems concerning carbonado provide a link in the research carried out for this thesis. Resolution of the controversy, concerning the origin of carbonado required a wide spectrum of investigations including: 1) detailed study of C and N systematics of mantle diamonds, including polycrystalline diamond varieties; 2) investigation of geochemical signatures of diamonds produced in meteorite impact events; 3) and characterisation of possible modifications of the He isotopic system in diamonds after their emplacement, due to U-Th decay in the diamond surrounding environment.

7.1. Conclusions.

7.1.1. C and N systematics of terrestrial diamonds and their implications.

Different types of terrestrial diamonds were characterised for C and N isotopic composition; only one genetic variety has not been studied (diamonds from metamorphic rocks of Kokchetav Massif). Different fields were identified for various diamond types in a $\delta^{13}\text{C}$ vs. $\delta^{15}\text{N}$ diagram on the basis of data presented in this work and data reported previously by the others (Boyd, 1988; Javoy, et al., 1984). The distinction between octahedral and fibrous diamonds was confirmed on the basis of $\delta^{15}\text{N}$ vs. N abundance plot supporting the suggestion that these diamond types are genetically different (Boyd et al., 1994). The field occupied by octahedral diamonds in its turn was subdivided into P and E (peridotitic and eclogitic) fields. Variations of N isotopic composition in eclogitic diamonds appeared to be the same as those in carbonado, yakutites, and in crustal rocks and organic matter, suggesting that crustal material was involved in the formation of these diamond types. In the case of yakutites, the carbon phase was transformed into diamond at the surface due to an impact, and hence trapped N with a crustal isotopic signature. For eclogitic diamonds and carbonado crustal C and N may have been involved in diamond

formation due to subduction processes. Such a hypothesis has already been suggested to explain genesis of eclogitic xenoliths and carbon isotopic signatures of some diamonds (Gregory and Taylor, 1981; McCulloch et al. 1981; Jacob and Jagoutz, 1991; Jagoutz et al., 1984; Manton and Tatsumoto, 1971; Pearson et al. 1995; Kirkley et al., 1991; Boyd and Pillinger, 1994). Whereas the N isotopic variations from -2.5‰ to +11‰ (isotopically heavy diamonds ($\delta^{13}\text{C}$ from -2‰ to +2.5‰) can have $\delta^{15}\text{N}$ as heavy as +23‰) of eclogitic diamonds are consistent with the variations observed in the crust, some of peridotitic diamonds have $\delta^{15}\text{N}$ values lower than -2.5‰ (the total $\delta^{15}\text{N}$ range is from -34‰ to +9.5‰) which is highly unusual for any terrestrial materials. The N isotopic composition for modern mantle, as revealed by MORB studies, is ca. -4‰ (Marty et al., 1996), therefore it is difficult to explain any N isotopic compositions lighter than -4‰ present in diamonds. Possibly diamonds are as old as 3.3 Gy or more and their nitrogen isotopic signature could reflect the ancient mantle whose composition in respect of N may have been different from that obtained for the modern basalts. This conclusion supports the suggestion of Javoy et al., (1986), that nitrogen in the primitive mantle had a signature similar to enstatite chondrite type material, because several diamonds with C and N isotopic values consistent with those of enstatite chondrites (EL) were encountered in this work. Thus, the P trend on the $\delta^{15}\text{N}$ vs. $\delta^{13}\text{C}$ diagram may be interpreted as a sign of the N isotopic evolution of the Earth's mantle from -34‰ to -4‰ for sub-oceanic mantle, and to -1‰ for sub-continental mantle.

A reasonable mechanism of the evolution is as follows: a) nitrogen in the primitive Earth's atmosphere was enriched by heavy isotope due to massive losses of gas; b) subduction initiated the process of evolution of the mantle nitrogen due to exchange between the mantle and subducted crustal rocks, which contained the heavy nitrogen trapped from atmosphere and even heavier nitrogen resulting from biogenic processes. Subsequently nitrogen in the mantle evolved forwards the $\delta^{15}\text{N}$ value of the modern atmosphere.

7.1.2. The origin of carbonado.

A comparison of the geochemical signatures and inner morphology of carbonado with those of framesites and yakutites suggests that carbonado is closely related to framesites and eclogitic diamonds in general, suggesting a common origin. The main carbonado field in the $\delta^{13}\text{C}$ vs. $\delta^{15}\text{N}$ plot could be continuation of the eclogitic field, and may suggest that carbonado is an extreme variety of eclogitic diamond. The inner morphology of some carbonado and IR spectra of a few crystallites in the specimens of carbonado studied here have make it very unlikely that these diamonds could have been formed in metastable conditions or in any kind of unequilibrated processes such as shock (Smith and Dawson 1985; Shelkov et al., 1994, 1995) or the transformation of coal under influence of U-Th irradiation as suggested by Kaminsky, 1987. However, the presence of the outer unequilibrated rim in one of the samples can be is easier reconciled as a result of an impact than as a result of the rapid changes of diamond growth conditions in the mantle environment.

As already stated the main carbonado field in the $\delta^{13}\text{C}$ vs. $\delta^{15}\text{N}$ overlaps with that of framesites but one carbonado specimen had $\delta^{13}\text{C}$ (-6.5‰) and $\delta^{15}\text{N}$ (-5‰) values which do not require any involvement of crustal material, revealing that carbonado samples are not necessarily restricted to the previously suggested range of $\delta^{13}\text{C}$: -22‰ to -31‰ (Kaminsky, 1991). Range of nitrogen concentrations in carbonado was found to be consistent with variations found in framesites, while all yakutites showed very low N content. A very important observation concerns concentrations of noble gas isotopes resulting from U-Th fission: any diamonds can acquire high concentrations of the radiogenic ^4He (and hence fission Xe) during residence in the crust after formation and therefore high abundance of ^4He is not diagnostic of the provenance of carbonado. The single diamond crystals from Finsch kimberlite and Argyle lamproite studied here showed He concentrations corresponding to the same α -particle implantation rate as that required for carbonado to explain isotopic composition of noble gases. Thus, all data for carbonado can be understood without invoking any unusual process of diamond

formation by assuming that carbonado diamonds were formed within the mantle from subducted carbon and nitrogen and were then emplaced into the crust by kimberlitic melt (single diamond crystals are also found in the alluvial deposits containing carbonado).

7.1.3. ^4He content in the single diamond crystals.

Inner zonation of ^4He in single diamond crystals was investigated, using, for the first time, a step combustion technique; several distinct zones were shown to be present covering almost the whole range of ^4He content variations previously reported for terrestrial diamonds, including carbonado. The outer zone resembles a theoretically calculated ^4He implantation profile, for the first time experimentally confirming the presence of ^4He implanted in the outer layers of diamond crystals extracted from kimberlites and lamproites. The outer layers had concentrations of ^4He as high as those in carbonado, suggesting that U-Th can be redistributed in the exposed areas of diamond bearing rocks due to alterations by ground water apparently concentrating around diamond crystals. Hence the attempts to estimate the contribution of ^4He implanted, due to U-Th decay, on the basis of the average U-Th concentrations in the rock (Lal 1989; McConville et al., 1991) are needed to be treated with caution. Internal regions of both diamond crystals, which could not be affected by U-Th due to the low penetration range of α -particles ($<30\mu\text{m}$), were found to consist of two zones in respect of He concentration, suggesting that diffusion coefficients of He in diamond at mantle temperature is $\approx 4 \times 10^{-21} \text{ cm}^2/\text{sec}$ and is lower than it was estimated by some other workers (Zashu and Hiagon, 1995; Wiens et al., 1994) confirming the suggestion by Ozima and Zashu, 1988, that diamond would be able to preserve its original He isotopic signature.

7.1.4. C, N, Ar and He in diamonds of shock origin.

C, Ar, and N study in diamonds of shock origin from two geological sites (Popigai impact crater and Ebeliak river placer deposits) suggests that they resulted from separate impact events or source materials; the He study, though, suggests that diamond formation episodes did not occur at significantly different time.

In diamond aggregates from Ebeliakh two different diamond components were identified as defined by N and Ar study, suggesting that either two types of formation process (shock transformation and CVD) or two types of source material have been involved. One of the two components, present in the diamond aggregates, contains Ar with $40/36$ isotopic ratios much higher than that of air, possibly reflecting the signature of pre-impact ancient graphites.

7.1.5. Experimental technique.

In the course of the study the original instrument designed for nitrogen isotopic analysis has been considerably modified to enable analysis of argon, nitrogen and carbon isotopic compositions and He content in the same experiments. Many significant changes were implemented to establish a system which can perform an entire analysis in automatic mode.

A number of changes were specifically required to achieve analysis of noble gas by the instrument. First, a quadrupole mass spectrometer has been introduced into the system. Second, double wall combustion vessels for combined nitrogen and noble gas analysis have been designed. Third, the purification procedure has also been modified to satisfy needs of noble gas analysis and new section including a getter and activated charcoal has been attached to the inlet. Fourth, the gas flow capillary reference gas system, similar to the one used for nitrogen, has been introduced (air is used as a reference gas) to provide reference material for routine measurements of noble gases.

A bulk combustion section was designed to achieve high sample throughput. An internal laboratory diamond standard has been introduced to control precision and sensitivity of entire analytical procedure used for analysis of C and N isotopic composition and N content in diamond samples. Although not yet done, a standard for noble gases could be chosen.

7.2. Suggestions for further research.

7.2.1. C and N isotope study of diamonds.

Even though the fields of C and N isotopic variations in diamonds of eclogitic and peridotitic varieties were described here, further research on the subject is necessary, since the conclusions were based on a limited number of specimens. In respect of diamonds with heavy C isotopic signature (Copeton diamonds) very few were available, although these diamonds may be considered as an important object of further research due to their unique C and N isotopic composition.

As mentioned above, diamonds from metamorphic complexes have not been characterised in this study, while new discoveries of such diamonds in geological localities other than Kokchetav Massif have been reported suggesting other processes of diamond formation may be geologically important. The studies of diamonds from the Kokchetav massive indicated an unusual isotopic composition in comparison to other diamonds types. Thus, the isotopic study of this diamond type can also lead to the important conclusions regarding the particular diamond formation processes occurred in the metamorphic complexes.

7.2.2. Diamonds formed by an impact.

The further geochemical characterisation of yakutites from different localities may also be of great importance. As revealed from Ar and N study of yakutites, the formation of these aggregates is not a simple process, and further investigation of Ar and N isotopic system of yakutites may shed more light on the diamond formation during meteorite impacts. A number of researchers have already suggested a possible involvement of CVD type of process in diamond formation during meteorite impact, but this is still a controversial subject. Possibly the study of noble gas abundance patterns in shock produced diamonds can be effective way of identifying diamonds formed in CVD process if they are present (the noble gas abundance pattern of diamonds formed directly by shock

were shown to be distinguishably different to that of diamonds formed in various CVD experiments (Masuda et al., 1991, 1995)).

The Popigai diamonds studied here show signs of differences in the distribution of $\delta^{13}\text{C}$ in diamonds and graphites which were proposed previously as a source material for the diamonds. Therefore, better characterisation of $\delta^{13}\text{C}$ distribution in diamonds and graphites extracted from different rocks of the impact crater can be sufficient in order to test previously proposed mechanism for diamonds formation

7.2.3. Applications of step combustion technique for the study of mantle diamonds.

As a result of a number of investigations it has been suggested that ^4He and ^3He isotopes could be acquired by diamonds during their post-emplacement history. Some of these effects may have only influence on the diamond surface and resulting He could in principle be separated from indigenous component, but since only bulk analysis (high temperature pyrolysis commonly used for noble gas studies in diamonds) were previously applied, the possibility to separate different He components experimentally has not been explored. There were several attempts, though, to correct the data using theoretical estimations, but the actual experimental results showed the unreliability of that approach. The new data obtained on He zoning in diamond using step combustion technique, which allowed us to separate secondary implanted and originally trapped components, has shown the potential of the technique to provide reliable information about indigenous He isotopic composition and about the involvement of He into early mantle evolution. Therefore, further research in this direction would undoubtedly lead to the better understanding of He isotope systematics of diamonds.

Previous measurements of $^{40}\text{Ar}/^{36}\text{Ar}$ in diamond are also difficult to interpret unambiguously because of the difficulty of distinguishing the various competing sources when gases extracted by bulk pyrolysis. On the contrary the step combustion method has the capability to discriminate between Ar released from inclusions (it will be more radiogenic than that of the diamond matrix), surface-bound atmospheric Ar (removed in

initial combustion steps) and indigenous trapped Ar. Furthermore, the step combustion with high resolution can possibly be used as a variation of the ^{40}Ar - ^{39}Ar method instead laser technique. It might prove a valuable way of recognising diamonds of different generations.

There are some other important advantages of step combustion technique gas extraction from diamond as compared with a technique utilising graphitisation of diamond. One of them is that it enables to extract nitrogen, carbon and noble gases simultaneously for further analysis. Therefore, diamond zoning can be characterised using abundances and isotopic composition of these elements and possibly identify an important links between them. It is obvious, hence, that such complex information can resolve a number of problems of diamond geochemistry and geochemistry of mantle volatiles in general.

APPENDIX 1: ACCURACY OF NITROGEN AND NOBLE GAS REFERENCE ALIQUOTTING SYSTEM.

Fig. A1-1 and A1-2 show a plot of $I(28)$ (i.e. a nitrogen abundance in the reference gas aliquot) versus bleed time and a plot ^4He intensity vs. bleed time of noble gas reference. The both graphs display a good linear relationship and pass close to the origin. ^{40}Ar and ^{36}Ar intensities plotted vs. noble gas reference gas bleed time are also in a good agreement with linear correlation dependence, however the intercepts for the lines are noticeably higher than zero suggesting that Ar blank of the noble gas clean up section has to be considered. The greater scatter of ^{36}Ar data around the correlation line than that of ^{40}Ar is believed to be due to lower abundance.

The results discussed above suggest that highly accurate amounts of reference gas can be metered out and analysed using this pipette/capillary system.

Table A1-1. The intensities of the signal for N and ^4He abundance analysis in reference gases.

N	Time, sec	$I(28)$, volts	N	Time, sec	^4He , counts
0	5	0.971	0	300	4641.09
1	10	1.570	1	600	9460.558
2	15	2.469	2	900	14184.95
3	20	3.088	3	1200	18641.41
4	25	3.806	4	1500	23030.23
5	30	4.649	5	1800	27589.15
6	35	5.280	6	2100	32059.91
7	40	6.026	7	2400	36739.09
8	45	6.784	8	2700	42000.00
9	50	7.440	9	3000	45523.12
10	55	8.318			

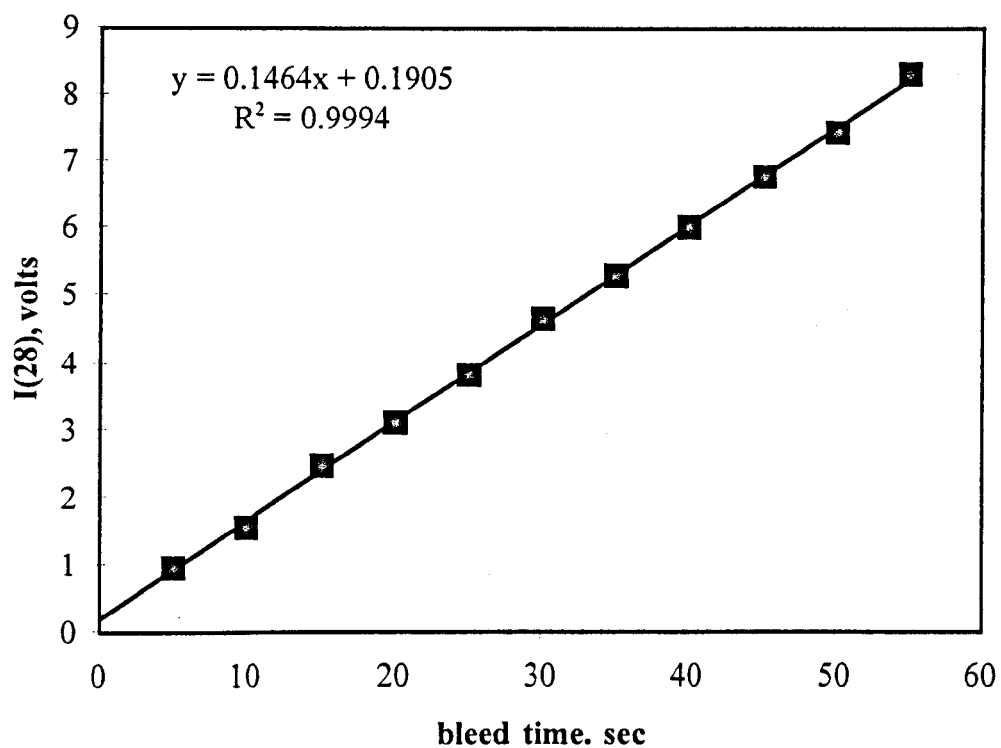


Figure A1-1 Measurements of m/z 28 (nitrogen) in reference gas vs. bleed time (table A2-1).

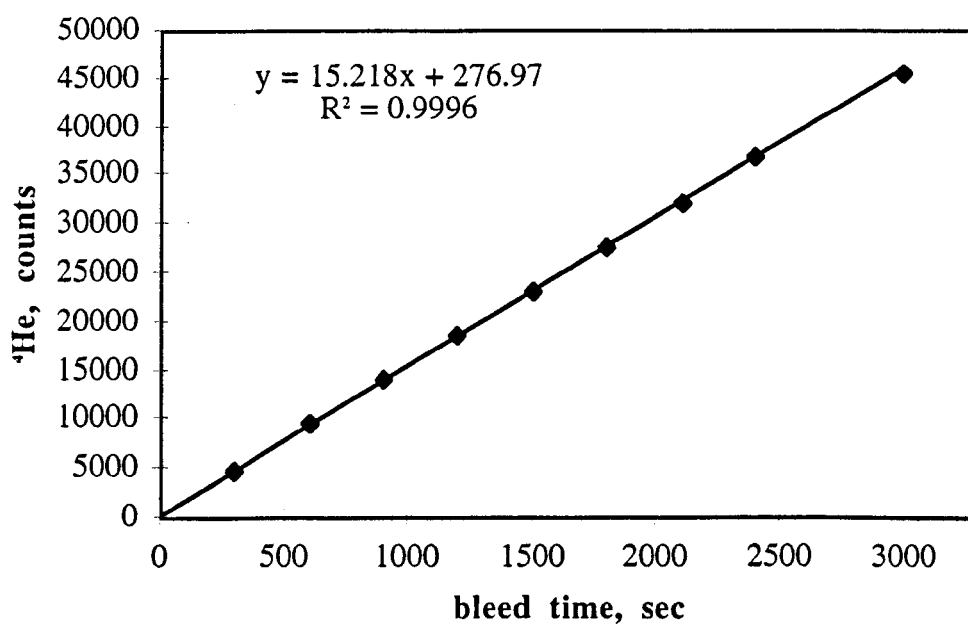


Figure A1-2. ^4He measurements in reference gas vs. bleed time (table A2-1).

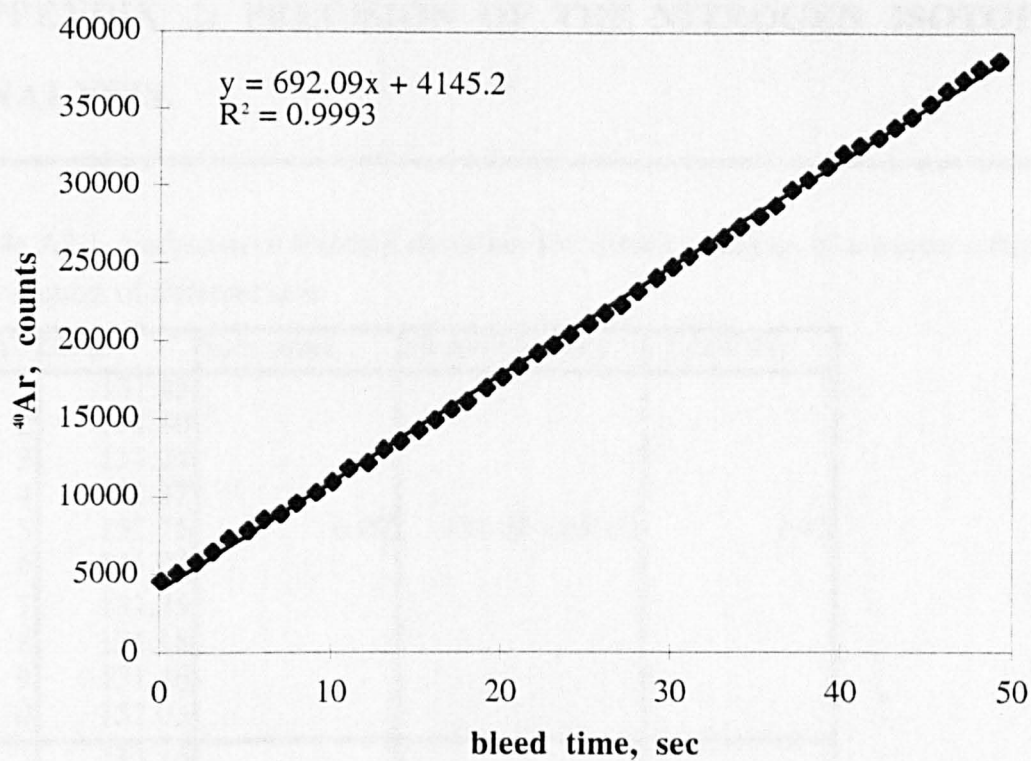


Figure A1-3. ^{40}Ar measurements in reference gas vs. bleed time (table A3-1).

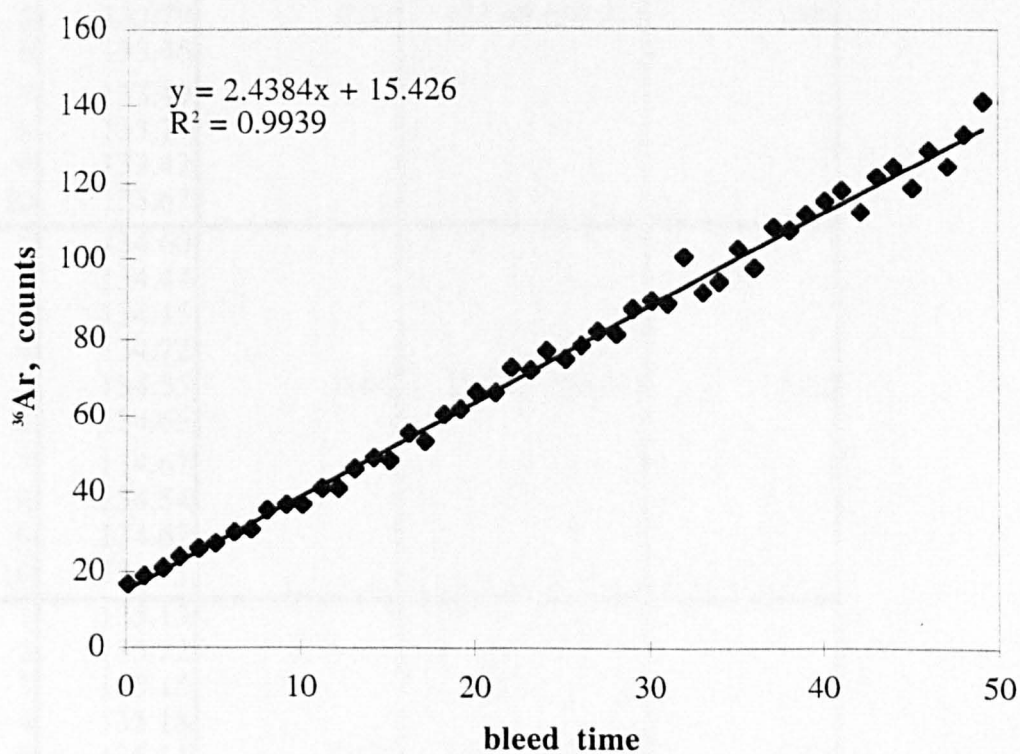


Figure A1-4. ^{36}Ar measurements in reference gas vs. bleed time (table A3-1).

APPENDIX 2: PRECISION OF THE NITROGEN ISOTOPIC ANALYSIS.

Table A2-1. Variations of standard deviation for isotopic analysis of nitrogen reference gas aliquots of different size.

Run	28/29	Size, nmol	Mean (\pm St.dev)	St.dev(‰)
1	131.43	0.02	131.52 (\pm 0.32)	2.43
2	131.80			
3	131.24			
4	131.37			
5	131.75			
6	131.07			
7	131.85			
8	131.18			
9	131.46			
10	132.03			
1	133.16	0.03	133.49 (\pm 0.21)	1.60
2	133.28			
3	133.63			
4	133.27			
5	133.79			
6	133.46			
7	133.49			
8	133.77			
9	133.42			
10	133.62			
1	134.60	0.04	134.59 (\pm 0.14)	1.02
2	134.44			
3	134.45			
4	134.72			
5	134.35			
6	134.65			
7	134.67			
8	134.54			
9	134.67			
10	134.77			
1	135.13	0.05	135.20 (\pm 0.09)	0.64
2	135.22			
3	135.15			
4	135.18			
5	135.11			
6	135.25			
7	135.29			
8	135.10			
9	135.38			
10	135.21			

1	135.50	0.06	135.64 (± 0.08)	0.63
2	135.57			
3	135.78			
4	135.61			
5	135.57			
6	135.67			
7	135.72			
8	135.60			
9	135.72			
10	135.65			
1	135.92	0.07	135.84 (± 0.08)	0.58
2	135.77			
3	135.90			
4	135.89			
5	135.82			
6	135.76			
7	135.96			
8	135.79			
9	135.72			
10	135.84			
1	136.13	0.08	136.13 (± 0.09)	0.64
2	136.12			
3	135.99			
4	136.02			
5	136.13			
6	136.15			
7	136.09			
8	136.13			
9	136.24			
10	136.28			
1	136.23	0.09	136.29 (± 0.07)	0.51
2	136.42			
3	136.33			
4	136.25			
5	136.25			
6	136.24			
7	136.36			
8	136.36			
9	136.28			
10	136.21			
1	136.77	0.12	136.74 (± 0.05)	0.38
2	136.70			
3	136.75			
4	136.79			
5	136.72			
6	136.80			
7	136.74			
8	136.72			
9	136.78			
10	136.63			

Table A2-2. Repeated measurements of 0.1 nmol aliquots of nitrogen reference gas (fig. A2-1).

run	28/29	1σ	δ ¹⁵ N	run	28/29	1σ	δ ¹⁵ N
1	138.05	0.06	0.33	25	138.12	0.08	-0.22
2	138.13	0.10	-0.24	26	138.12	0.05	-0.17
3	138.14	0.07	-0.35	27	138.08	0.06	0.08
4	138.11	0.05	-0.11	28	138.09	0.06	0.01
5	138.15	0.04	-0.37	29	138.09	0.04	0.06
6	138.13	0.04	-0.27	30	138.10	0.05	-0.01
7	138.10	0.08	-0.04	31	138.08	0.06	0.10
8	138.11	0.08	-0.15	32	138.07	0.09	0.14
9	138.10	0.11	-0.03	33	138.01	0.03	0.61
10	138.12	0.06	-0.20	34	138.04	0.06	0.37
11	138.14	0.12	-0.30	35	138.05	0.06	0.34
12	138.09	0.05	0.01	36	138.08	0.06	0.10
13	138.10	0.05	-0.07	37	138.06	0.08	0.27
14	138.07	0.08	0.20	38	138.07	0.03	0.15
15	138.11	0.05	-0.15	39	138.07	0.06	0.19
16	138.10	0.08	-0.05	40	138.06	0.07	0.27
17	138.10	0.03	-0.04	41	138.06	0.07	0.22
18	138.09	0.05	0.03	42	138.09	0.05	0.05
19	138.12	0.06	-0.17	43	138.06	0.08	0.21
20	138.14	0.06	-0.32	44	138.07	0.05	0.19
21	138.13	0.05	-0.25	45	138.10	0.05	-0.07
22	138.10	0.04	-0.04	46	138.08	0.05	0.08
23	138.11	0.07	-0.12	47	138.08	0.09	0.07
24	138.12	0.08	-0.21	48	138.11	0.05	-0.12
Average for 28/29 ratio is 138.09							
St.dev. for 28/29 ration is 0.03							
St.dev. in ‰ is 0.21							

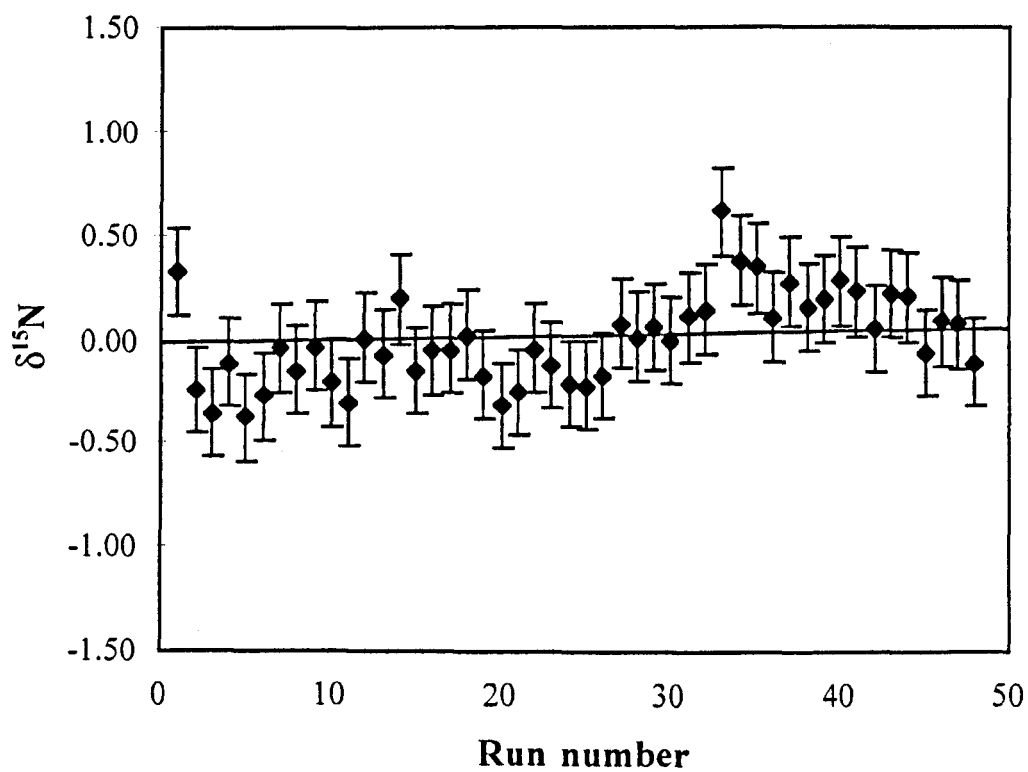


Figure A2-1. Zero enrichment on consecutive aliquots of 0.1 nmol of nitrogen reference gas (table A2-2).

APPENDIX 3: PRECISION OF THE AR ISOTOPIC ANALYSIS BASED ON THE MEASUREMENTS OF DIFFERENT ALIQUOTS OF REFERENCE GAS.

Table A3-1. Ar measurements of different aliquots of the reference gas (fig. A3-1 and A3-2).

N	Time,	³⁶ Ar	⁴⁰ Ar	⁴⁰ Ar, cc	³⁶ Ar, cc	³⁶ Ar/ ³⁶ Ar	+/-	⁴⁰ Ar/ ³⁶ Ar	+/-
5	1	18.69	5175	1.47E-09	5.29E-12	0.16	0.02	288.37	12.85
6	2	21.43	5815	2.93E-09	1.08E-11	0.18	0.02	276.18	9.78
7	3	24.22	6633	4.40E-09	1.60E-11	0.23	0.02	293.74	12.44
8	4	25.90	7353	5.86E-09	2.06E-11	0.19	0.02	321.75	17.87
9	5	27.70	7988	7.33E-09	2.54E-11	0.20	0.01	282.57	6.76
10	6	30.63	8546	8.79E-09	3.15E-11	0.15	0.01	280.31	8.54
11	7	30.99	8970	1.03E-08	3.54E-11	0.20	0.02	297.01	8.00
12	8	35.60	9705	1.17E-08	4.30E-11	0.15	0.01	270.80	8.15
13	9	37.35	10400	1.32E-08	4.73E-11	0.20	0.02	284.31	7.47
14	10	37.05	11083	1.47E-08	4.90E-11	0.19	0.02	301.73	8.64
15	11	41.45	11835	1.61E-08	5.64E-11	0.16	0.01	288.88	5.50
16	12	41.78	12233	1.76E-08	6.00E-11	0.19	0.01	289.50	6.35
17	13	46.80	13180	1.90E-08	6.76E-11	0.15	0.01	282.11	6.41
18	14	49.56	13672	2.05E-08	7.44E-11	0.20	0.01	277.27	5.57
19	15	48.94	14313	2.20E-08	7.51E-11	0.21	0.01	307.34	9.24
20	16	55.99	14922	2.34E-08	8.80E-11	0.17	0.01	268.84	4.59
21	17	53.55	15605	2.49E-08	8.55E-11	0.18	0.01	288.22	7.59
22	18	60.64	16260	2.64E-08	9.83E-11	0.18	0.01	270.77	6.48
23	19	62.36	17009	2.78E-08	1.02E-10	0.16	0.01	270.38	5.10
24	20	66.26	17826	2.93E-08	1.09E-10	0.16	0.01	266.71	5.65
25	21	66.13	18454	3.08E-08	1.10E-10	0.20	0.01	286.31	6.81
26	22	72.34	19266	3.22E-08	1.21E-10	0.18	0.01	263.75	4.60
27	23	71.61	19810	3.37E-08	1.22E-10	0.18	0.01	277.68	5.28
28	24	76.78	20448	3.52E-08	1.32E-10	0.19	0.01	269.30	4.69
29	25	74.64	21189	3.66E-08	1.29E-10	0.18	0.01	279.61	4.54
30	26	77.91	21884	3.81E-08	1.36E-10	0.18	0.01	279.67	5.49
31	27	81.44	22380	3.96E-08	1.44E-10	0.17	0.01	278.78	6.86
32	28	81.14	23314	4.10E-08	1.43E-10	0.20	0.01	289.36	5.01
33	29	87.34	24149	4.25E-08	1.54E-10	0.21	0.01	280.37	4.58
34	30	89.74	24742	4.40E-08	1.59E-10	0.17	0.01	280.76	3.44
35	31	88.70	25569	4.54E-08	1.58E-10	0.19	0.01	290.34	4.63
36	32	100.5	26181	4.69E-08	1.80E-10	0.16	0.01	260.43	4.46
37	33	91.53	26770	4.83E-08	1.65E-10	0.20	0.01	297.39	5.59
38	34	94.15	27425	4.98E-08	1.71E-10	0.18	0.01	294.05	4.61
39	35	103.1	28080	5.13E-08	1.88E-10	0.17	0.01	272.29	4.74
40	36	98.12	28767	5.27E-08	1.80E-10	0.18	0.01	292.80	4.19
41	37	108.36	29869	5.42E-08	1.97E-10	0.16	0.01	274.18	4.72
42	38	107.58	30461	5.57E-08	1.97E-10	0.18	0.01	280.39	4.69

43	39	112.01	31358	5.71E-08	2.04E-10	0.17	0.01	277.69	5.58
44	40	115.47	32244	5.86E-08	2.10E-10	0.19	0.01	277.05	3.33
45	41	118.15	32722	6.01E-08	2.17E-10	0.18	0.01	279.29	4.26
46	42	112.67	33210	6.15E-08	2.09E-10	0.19	0.01	291.49	5.78
47	43	121.83	33956	6.30E-08	2.26E-10	0.18	0.01	280.25	4.38
48	44	124.64	34571	6.45E-08	2.32E-10	0.17	0.01	273.01	3.11
49	45	119.16	35589	6.59E-08	2.21E-10	0.18	0.01	291.53	4.02
50	46	129.19	36360	6.74E-08	2.39E-10	0.18	0.01	280.79	4.11
51	47	125.05	37029	6.89E-08	2.33E-10	0.19	0.01	292.87	3.55
52	48	133.52	37837	7.03E-08	2.48E-10	0.17	0.01	284.43	3.68
53	49	141.62	38313	7.18E-08	2.65E-10	0.19	0.01	273.11	4.32
Average						0.18		282.77	
St.dev						0.02		11.47	

Table A3-2. Data table of Ar isotopic ratios measured in one aliquot of the reference gas (1.8*10⁻⁷ cc) (fig. A3-3 and A3-4) .

Run	³⁹ Ar, cps	³⁹ Ar/ ³⁶ Ar	+/-	⁴⁰ Ar/ ³⁶ Ar	+/-
1	77474.56	0.27	0.01	268.93	5.45
2	67738.82	0.24	0.01	251.60	5.51
3	66934.38	0.26	0.01	259.98	4.89
4	65993.23	0.29	0.01	274.87	4.75
5	64748.88	0.27	0.02	261.18	5.11
6	64414.64	0.28	0.01	268.77	5.48
7	63298.57	0.24	0.01	252.71	5.45
8	63560.24	0.26	0.01	254.38	5.16
9	63710.17	0.28	0.01	272.91	5.38
10	63564.30	0.26	0.02	260.07	4.93
11	63294.53	0.29	0.02	270.69	5.62
12	57391.34	0.33	0.02	262.68	5.48
13	63487.59	0.28	0.01	268.62	5.42
14	62357.17	0.26	0.01	262.31	5.94
15	62323.70	0.27	0.02	265.23	5.62
16	62147.76	0.27	0.01	265.62	5.55
17	62292.24	0.28	0.01	252.71	5.44
18	60908.68	0.27	0.02	260.92	5.87
19	63173.32	0.28	0.01	264.19	5.67
20	64686.04	0.30	0.02	265.60	5.37
21	64386.19	0.31	0.02	278.05	6.08
22	64580.46	0.24	0.01	260.08	5.20
23	65362.18	0.27	0.01	273.89	5.44
24	65247.25	0.26	0.01	256.05	5.52
25	64548.91	0.29	0.01	247.73	4.94
26	68830.20	0.27	0.01	272.77	5.13
27	69592.96	0.27	0.01	261.76	4.29
28	70707.98	0.27	0.01	265.85	4.48
29	69594.41	0.27	0.01	251.04	4.39
30	69832.76	0.28	0.01	265.81	5.39
31	69436.40	0.29	0.01	257.33	5.14
Mean	65046.58	0.27		263.14	
St.dev.	3684.72	0.02		7.89	

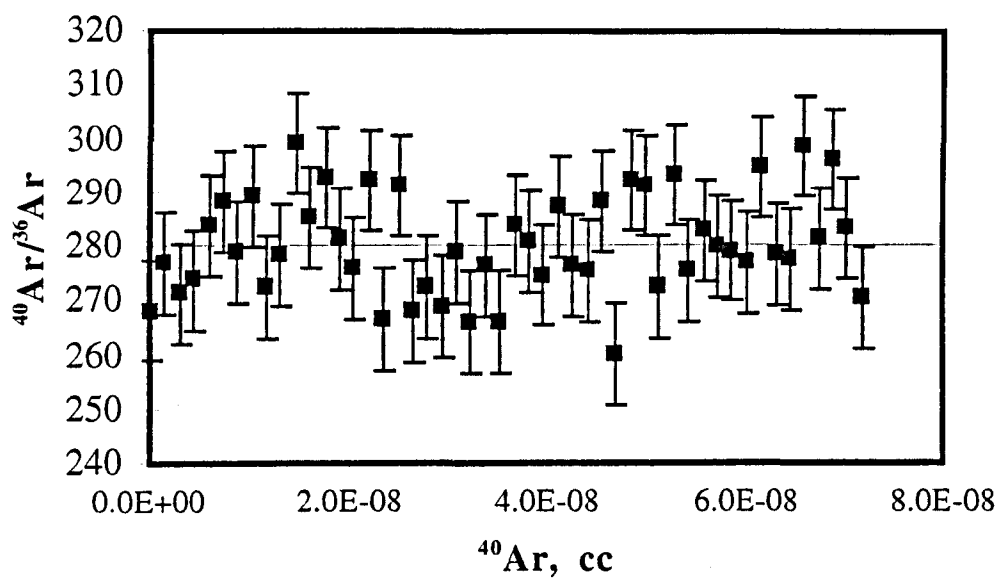


Figure A3-1. Variations of $^{40}\text{Ar}/^{36}\text{Ar}$ ratios in different aliquots of reference gas (table A3-1).

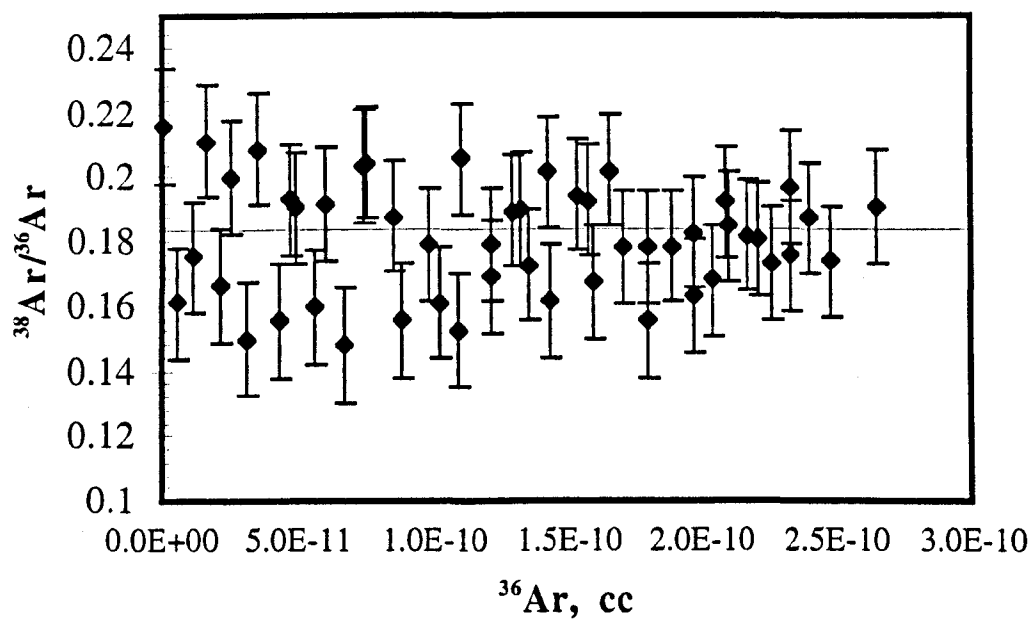


Figure A3-2. Variations of $^{38}\text{Ar}/^{36}\text{Ar}$ ratios in different aliquots of reference gas (table A3-1).

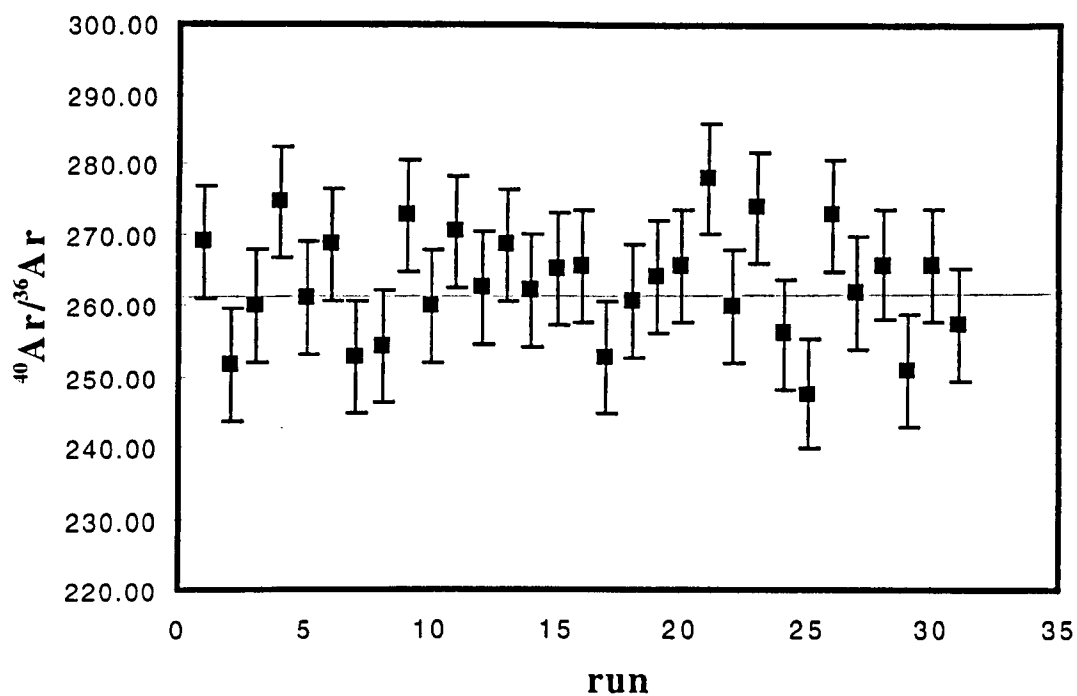


Figure A3-3. Repeated measurements of $^{40}\text{Ar}/^{36}\text{Ar}$ in Ar reference gas aliquot (1.8×10^{-7} cc) (table A3-2).

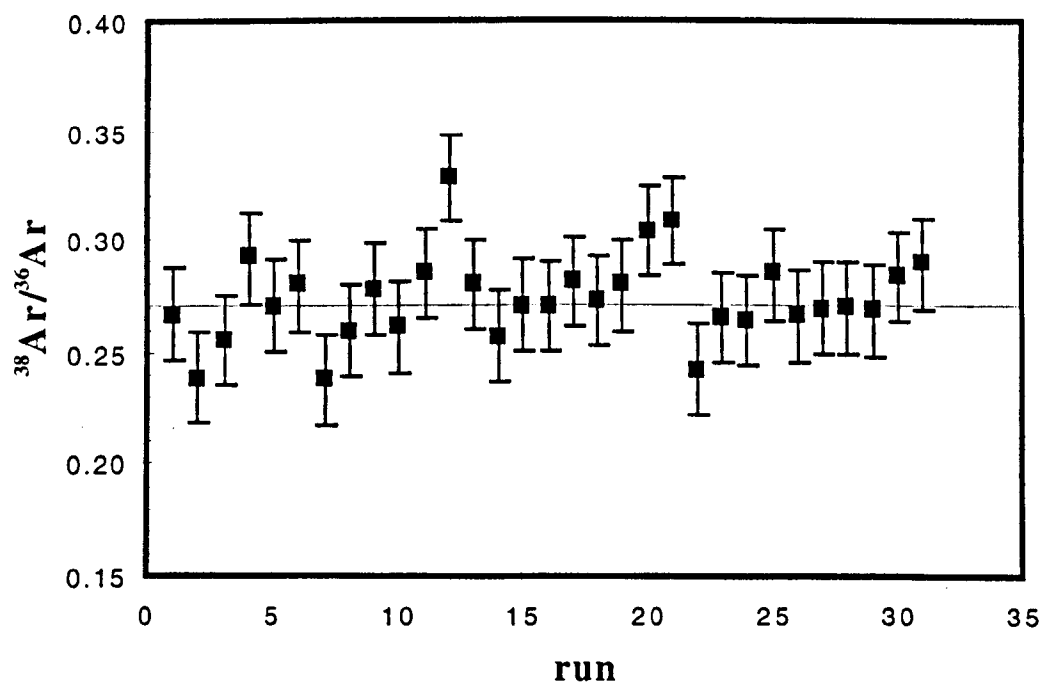


Figure A3-4. Repeated measurements of $^{38}\text{Ar}/^{36}\text{Ar}$ in the Ar reference gas aliquot (1.8×10^{-7} cc) (table A3-2).

APPENDIX 4: CALIBRATION OF THE NITROGEN MASS SPECTROMETER.

The mass spectrometer used for nitrogen analysis can be calibrated using AIR standard. The nitrogen abundance in the aliquot of the AIR can be measured by high sensitivity baratron, and in accordance with following measurements of nitrogen abundance by the MS the conversion factor between intensity of the m/z 28 and an actual nitrogen abundance can be calculated using the formula:

$$K = \frac{1.98 \times 3.402 \times P_{\text{bar}} \times \%}{I(28)},$$

where P_{bar} is the pressure of nitrogen measured by baratron measured in volts; $I(28)$ is intensity of the m/z 28 corresponded to the nitrogen abundance measured by MS in volts; 1.98×3.402 is the conversion factor between baratron pressure and nitrogen abundance; % is the percent of nitrogen which was let into the MS camera.

Table A4-1. Calibration of sensitivity of the MS.

P,bar	%	I(28)	K
9.88	0.016	3.362	0.342
6.06	0.055	7.272	0.310
1.75	0.13	4.946	0.329
1.06	0.239	5.509	0.309
11.45	0.016	3.772	0.333
6.66	0.055	8.395	0.296
1.97	0.13	5.675	0.304
1.16	0.13	3.275	0.329
0.77	0.339	6.239	0.299
Mean			0.317
St.dev			0.017

APPENDIX 5: EXPERIMENTAL REPRODUCIBILITY FOR N AND C.

Table A4-1 Reproducibility of experiments in terms $\delta^{15}\text{N}$, N content and $\delta^{13}\text{C}$ based on the study of the internal diamond standard and AIR standard.

N	$\delta^{15}\text{N}_{\text{dm}},\text{‰}$	$\delta^{13}\text{C}_{\text{dm}},\text{‰}$	$\text{N}_{\text{dm}}, \text{ppm}$	$\delta^{15}\text{N}_{\text{AIR}},\text{‰}$
1	0.34	-10.2	1169	-0.903
2	-0.89	-9.5	1092	0.003
3	-0.06	-10.0	1105	0.76
4	-0.06	-10.2	1196	0.28
5	-0.03	-9.6	1159	0.182
6	-0.51	-9.8	1101	0.67
7	-0.34	-9.2	1135	0.845
8	-0.66	-10.4	933	-1.36
9	-1.04	-9.2	1163	
10	0.92	-9.3	1108	
11	0.95	-9.2	969	
12	1.57	-9.8		
13	0.69	-9.3		
14	0.73	-10.5		
15	-0.49	-10.1		
16	-1.94	-9.1		
17	1.3	-9.5		
18	-0.003			
19	-1.84			
20	-2.49			
21	-1.26			
22	-0.87			
23	-0.24			
24	0.19			
25	0.02			
26	0.11			
Mean	-0.23	-9.7	1103	0.06
St.dev.	0.99	0.5	79	0.80

APPENDIX 6: TABLES OF SAMPLE DESCRIPTIONS FOR CHAPTER 3.

Table¹ A6-1. Short description of samples according to Dr G.P.Bulanova.

Sample	Type	Shape of crystal	Inclusions	Kimberlite pipe
3661	E	Octa	Omph	Udachnya
3662	E	Octa	Omph, Gar	Udachnya
3105r	E	Octa,rim	Cpx,Gar	Udachnya
3105c	E	Octa,core	Cpx,Gar	Udachnya
3694	P	Octa	Mss	Udachnya
3295c	P	Octa,core	Ol	Udachnya
3582	P	Octa	Ol	Udachnya
3588	P	Octa	Ol, Mss	Udachnya
3798c	P	Octa	Chr, Ol	Udachnya
4173r	E	Octa(rounded),rim	Cpx,Gar,Cs,Po	23d Party Congress
4173c	E	Octa(rounded),core	Cpx,Gar,Cs,Po	23d Party Congress
4240	E	Octa	Po	23d Party Congress
4160y	P	Octa,core	Ol	23d Party Congress
4160	P	Octa,rim	Ol	23d Party Congress
4143r	P	Octa	Po+Cpx	23d Party Congress
4147r	E	Octa	Po	23d Party Congress
2214	E	Octa, coated (coat)	Po	Aikhal
1169c	E	Cube-octa->octa		Mir
1169r	E	Cube-octa->octa	Gar	Mir
1153c(b)	E	cube->round->octa	Po	Mir
1153r	E	cube->round->octa	Po	Mir
1591c	E	Octa	Po	Mir
1591r	E	Octa	Po	Mir
3143	P	Octa	Ol,Mss	Mir
1558	P	Octa	Ol,Mss	Mir

* — shape of original crystals of diamonds from which the fragments studied were extracted, if several fragments were analysed the location within the crystal is specified (c-core, r-rim).

¹ Abbreviations used in the above tables: Cs — coesite; Gar — garnet; Chr — chlorite; Cpx — clinopyroxene; Mss — melt; Omph — omphacite; Ol — olivine; Phlg — phlogopite; Po — pyrrhotite; Octa — octahedra.

Table A6-2. Short description of boart specimens according to Dr G.P. Bulanova.

Sample	Type	Type of aggregate	Grain shape	Inclusions	Kimberlite pipe
B149	E	Coarse grain	Octa	Gar	Udachnya
B107	P	Coarse grain	Octa	Ol+Phlg	Udachnya
B159	P	Coarse grain	Octa	Chr	Udachnya
B5	E	Fine-coarse grain	Uncertain	Gar	Aikhal
B54	E	Coarse grain	Octa	Ru	Aikhal
B195	P	Coarse grain	Octa	Chr	Mir
B174	E	Fine-coarse grain	Uncertain	Gar	Mir
B196	E	Coarse grain	Octa	Gar	Mir

Table A6-3. Available information on diamonds from Archangels area (Dr O.V.Zaharchenko).

Sample	Type	Pipe
A8	P	Lomonsov
A2	P	Karpinsky
A11	P	Archangelskaya
A3	U*	Karpinsky
A10	U*	Pomorskaya
A12	E	Karpinsky
A20	U*	Pomorskaya
A14d	U*	Lomonsov

* — unspecified

APPENDIX 7: DATA TABLES FOR CHAPTER 3.

Table A7-1. C,N isotopic compositions and nitrogen contents in eclogitic diamonds from Yakutian and Archangelsk kimberlites.

Sample	$\delta^{15}\text{N}$	Err	N/C,ppm	Err	$\delta^{13}\text{C}$
3661	1.5	2.7	674	68	-4.5
3662	0.3	0.5	444	22	-4.8
3105r	-1.5	1.7	976	90	-7.9
3105c	2.5	1.4	474	45	-6.8
B149	5.9	1.1	734	71	-10.1
4173r	-2.0	1.2	1062	101	-7.0
4173c	-0.2	1.7	1392	135	-4.7
4240	3.5	1.5	232	23	-15.7
4147r	-0.3	1.3	530	30	-6.7
B5	-1.3	1.3	728	70	-8.4
B54	-0.6	1.7	1021	98	-6.8
B174	-1.0	2.1	38	4	-5.2
B196	3.0	1.1	778	75	-5.4
A12	-0.6	1.6	421	38	-8.6
1169c	1.3	1.3	290	30	-4.3
1169r	0.4	1.4	430	40	-6.0
1153 (b)c	3.5	1.5	338	50	-6.6
1153r	-4.0	1.5	289	50	-5.5
1591c	-1.3	1.5	360	50	-5.8
1591r	2.7	1.5	300	50	-5.7

Table A7-2. C, N isotopic compositions and nitrogen contents in peridotitic diamonds from Yakutian and Archangels kimberlites.

Sample	$\delta^{15}\text{N}$	Err	N/C,ppm	Err	$\delta^{13}\text{C}$
3694	-0.4	2.8	15	3	-4.1
3295y?	-1.2	4.0	15	4	-4.7
3582	4.6	1.5	555	56	-5.7
3588	-3.3	2.8	42	4	-4.7
B107	4.6	1.8	85	8	-3.6
B159	-5.9	1.7	475	46	-4.0
4160y	9.5	0.7	399	41	-7.6
4160	-0.1	1.0	740	75	-4.4
4143r	3.2	1.7	1361	130	-6.1
3143	1.7	1.7	33	3	-5.5
1558	1.0	1.0	568	54	-5.4
B195	1.0	1.0	432	42	-5.1
A8	3.0	0.4	2621	226	-5.9
A2	2.4	0.2	1942	168	-4.4
A11	0.3	1.2	15	2	-3.4
3798c	1.4	1.5	590	20	-4.2

Table A7-3. Peridotitic diamonds from Robert Victor peridotitic xenoliths .

Sample	$\delta^{15}\text{N}$	Err	N/Cppm	Err	$\delta^{13}\text{C}$
RV167	0.8	1	1270	100	-5.0
RV167.549	5.7	1	2190	200	-5.7
RV161	-1.8	1	252	25	-6.2
RV175A	-3.8	1	382	380	-4.4
RV175B	-1.1	1	218	22	-5.9
RV175C	0.5	1	446	440	-5.0
RV175E	-1.8	1	183	20	-4.1
RV175F	-0.1	1	195	20	-5.0
RV180A	4.0	1	75	10	-4.5
RV180B	4.1	1	102	10	-5.0
RV180C	6.5	1	556	50	-4.3
RV180D	5.0	1	149	15	-5.0

Table A7-4. Diamonds from Robert Victor eclogitic xenolith RV124.

Sample	$\delta^{15}\text{N}$	Err	N/Cppm	Err	$\delta^{13}\text{C}$
RV124.(24)	-0.9	1	1048	100	-5.8
RV124.1.3	3.3	1	2130	200	-5.8
RV124.1.5	2.7	1	2288	200	-6.8
RV124.3.1	0.7	1	1231	200	-5.5
RV124A	4.1	1	1823	280	-5.4
RV124B	-0.7	1	704	70	-4.6

Table A7-5. North Queensland exploration samples.

Sample	$\delta^{15}\text{N},\text{‰}$	Err	N/C,ppm(wt)	Err	$\delta^{13}\text{C},\text{‰}$
NQ12	-19.3	1.6	987	31	-4.9
NQ32d	-11.0	1.7	552	18	-6.9
NQ33	-34.1	0.3	835	34	-4.2
NQ25	-24.9	1.6	1700	300	-2.5

Table A7-6. Diamonds from New South Wales.

Sample	$\delta^{15}\text{N},\text{‰}$	Err	N/C,ppm(wt)	Err	$\delta^{13}\text{C},\text{‰}$
CO10/6	6.6	1.0	29	3	1.9
CO6/6	23.2	1.0	119	12	2.5
CO18/2	12.5	1.0	29	3	1.9
CO21/6	10.8	1.0	1670	167	2.9
CO5/6	12.2	1.0	147	15	-1.9
CH3d.555	9.7	1.0	817	82	-1.2
MRBI3.509	6.1	1.0	2363	236	-3.9

APPENDIX 8: DATA TABLES FOR CHAPTER 4.

Table A8-1. Sample F4: results of step combustion experiment.

Step	C, μg	$^3\text{He, cc}$	r, μm	$^3\text{He, cc/g}$
1	1.20	2.06E-09	0.04	1.71E-03
2	6.50	4.69E-09	0.26	7.22E-04
3	16.56	7.85E-09	0.94	4.74E-04
4	54.52	2.20E-08	3.03	4.04E-04
5	39.88	1.58E-08	5.83	3.97E-04
6	21.91	7.42E-09	7.68	3.39E-04
7	55.27	1.42E-08	10.01	2.57E-04
8	52.11	1.01E-08	13.27	1.94E-04
9	69.35	7.57E-09	17.01	1.09E-04
10	77.12	3.76E-09	21.57	4.88E-05
11	78.09	6.38E-10	26.48	8.17E-06
12	65.31	3.11E-10	31.09	4.76E-06
13	64.36	1.84E-10	35.33	2.86E-06
14	250.00	8.00E-10	45.97	3.20E-06
15	822.00	2.52E-09	86.93	3.06E-06
16	1216.00	3.69E-09	193.40	3.04E-06
17	500.20	2.98E-10	334.26	5.95E-07
18	161.20	7.41E-11	508.17	4.60E-07
Total	3551.59	1.04E-07		2.93E-05

Table A8-2. Sample F1: results of step combustion experiment.

Step	C, μg	$^3\text{He, cc}$	r, μm	$^3\text{He, cc/g}$
1	0.50	7.72E-10	0.02	2.21E-03
2	76.03	9.14E-08	3.43	1.72E-03
3	55.82	5.27E-08	9.35	1.35E-03
4	70.68	5.92E-08	15.18	1.20E-03
5	26.37	1.11E-08	19.73	6.04E-04
6	62.41	3.26E-08	24.00	7.47E-04
7	80.40	3.06E-08	31.02	5.45E-04
8	83.82	1.46E-08	39.34	2.50E-04
9	91.36	5.36E-09	48.55	8.39E-05
10	98.35	2.11E-09	58.97	3.07E-05
11	93.39	1.18E-09	70.00	1.81E-05
Total	739.13	3.02E-07		0.0004081

Table A8-3. Sample A1: results of step combustion experiment.

Step	C, μg	^3He ,cc	r, μm	^3He ,cc/g
1	0.18	1.33E-07	0.00259	7.57E-01
2	0.34	5.97E-08	0.01022	1.74E-01
3	1.26	6.46E-08	0.03379	5.13E-02
4	1.86	7.77E-08	0.07967	4.18E-02
5	5.43	1.57E-07	0.1869	2.89E-02
6	39.32	7.76E-07	0.84605	1.97E-02
7	147.22	2.19E-06	3.60784	1.49E-02
8	433.89	3.00E-06	12.353	6.91E-03
9	2140.00	7.44E-06	23.9578	3.48E-03
10	100.25	4.17E-09	61.5498	4.16E-05
11	320.30	3.57E-09	100.096	1.12E-05
12	2925.94	2.31E-08	232.455	7.89E-06
13	780.34	8.31E-09	262.116	1.06E-05
14	1004.00	6.49E-09	322.086	6.47E-06
15	1061.56	2.39E-10	414.31	2.25E-07
16	722.34	1.33E-10	540.176	1.84E-07
17	285.24	6.60E-11	745.014	2.31E-07
Total	9969.46	1.39E-05		1.40E-03

APPENDIX 9: CALCULATION OF U-TH CONTENT IN DIAMOND HOST ROCK.

^4He content in the diamond matrix formed due to U and Th α -decay can be calculated as (Verchovsky and Sukolukov, 1991):

$$^4\text{He} = 22.4 \cdot 10^3 \left\{ U \cdot \left[\frac{8}{238} \cdot \left(e^{\lambda_8 \cdot t} - 1 \right) + \frac{7}{235 \cdot 138} \cdot \left(e^{\lambda_5 \cdot t} - 1 \right) \right] + \frac{6\text{Th}}{232} \cdot \left(e^{\lambda_2 \cdot t} - 1 \right) \right\},$$

where ^4He is concentration (cc/g); U and Th are concentrations in g/g (ppm/ 10^6); λ_8 , λ_5 , and λ_2 are decay constants of ^{238}U , ^{235}U and ^{232}Th respectively ($1.6\text{E-}10$; $9.8\text{E-}10$ and $4.9\text{E-}11$). Hence, knowing ^4He concentration in the matrix and assuming U/Th ratio as ≈ 3 , U and Th concentrations can be calculated from the above equation. The concentration of He in the matrix can be worked out from the following equation (Verchovsky et al., 1993):

$$C_m = C_d \cdot \frac{4}{3} \cdot \frac{\rho_d}{\rho_m} \cdot \frac{r_o}{R} \cdot \left[1 - \frac{1}{12} \cdot \left(\frac{R}{r_o} \right)^2 \right],$$

where C_m is ^4He concentration(cc/g) in diamond bearing matrix; C_d is ^4He concentration(cc/g) implanted in diamond crystal (known from experimental data); ρ_d and ρ_m are densities of diamond and matrix respectively; R is the range of α -particles in diamond (assumed as $15.8 \mu\text{m}$ which is the an average α -particle range if U/Th ≈ 3 (Verchovsky et al., 1993)); r_o is radius of diamond crystal ($630 \mu\text{m}$ for F4, $510 \mu\text{m}$ for F1 and $895 \mu\text{m}$ for A1; the crystal radiuses are calculated from diamond weights in accordance with spherical model).

APPENDIX 10: CALCULATIONS USED TO PROVIDE THEORETICAL IMPLANTATION PROFILES FOR SAMPLE F4.

The implantation profiles (fig. 5.3) were derived for sample F4 from the model assuming that diamond is a sphere of radius r_0 (630 μm for sample F4) embedded in a matrix with uniform distribution of α -emitters. For mono-energetic α -particles the matrix normalised ^4He concentration at the distance x from the centre of diamond sphere can be calculated using the following equation:

$$\frac{C_d}{C_m}(x) = \frac{(R_i + x)^2 - r_0^2}{4 \cdot R_i \cdot x},$$

where C_d and C_m are ^4He concentrations in the diamond and matrix respectively; R_i is the range of α -particle of certain energy; r_0 is the radius of the diamond grain; x is the distance from the centre of the grain. In accordance with the model used by Verchovsky et al., 1993 U/Th ratio is assumed to be 3, which makes all α -decay energies equally abundant allowing us to calculate $C_d/C_m(x)$ ratio as an arithmetic mean of the ratios corresponded to the α -particles of all energies. Thus, the $^4\text{He}(x)$ concentrations can be calculated by simply multiplying $C_d/C_m(x)$ by ^4He concentrations in the matrix. The calculations are illustrated by the tables A10-1, A10-2 and A10-3, where the values under the heading R_i (the first row below contains the range for each α -particle produced by U-Th decay (the ^{235}U is neglected for calculations)) are the $C_d/C_m(x)$ ratios for mono-energetic α -particles; x is the co-ordinate relatively to the centre of the sphere (μm); C_d/C_m is the mean ratio calculated for α -particles of all energies; ^4He is the concentration in the diamond corresponding to the co-ordinate x or depth r (μm).

Table A10-1. Calculation of ^4He implantation depth profile for diamond crystal F4 (U-Th=540 ppm; U/Th=3)

x	R_i														C_d/C_m	$^4\text{He, cc/g}$	r
	8.9	9.5	11.1	11.1	11.6	13.7	14	15	16.1	17.6	18.3	19.8	23.9	30.2			
630	0.5035	0.5038	0.5044	0.5044	0.5046	0.5054	0.5056	0.506	0.5064	0.507	0.5073	0.5079	0.5095	0.512	0.5063	1.72E-03	0
629	0.4473	0.4511	0.4593	0.4593	0.4615	0.4689	0.4698	0.4726	0.4753	0.4786	0.4799	0.4826	0.4886	0.4954	0.4707	1.60E-03	1
628	0.391	0.3984	0.4142	0.4142	0.4183	0.4323	0.434	0.4392	0.4442	0.4501	0.4526	0.4573	0.4676	0.4789	0.4352	1.47E-03	2
627	0.3346	0.3455	0.369	0.369	0.375	0.3957	0.3982	0.4057	0.413	0.4216	0.4251	0.432	0.4466	0.4623	0.3995	1.35E-03	3
626	0.2781	0.2926	0.3237	0.3237	0.3317	0.359	0.3623	0.3722	0.3818	0.393	0.3977	0.4066	0.4256	0.4456	0.3638	1.23E-03	4
625	0.2215	0.2396	0.2783	0.2783	0.2883	0.3223	0.3263	0.3387	0.3505	0.3644	0.3702	0.3812	0.4045	0.429	0.3281	1.11E-03	5
624	0.1649	0.1865	0.2329	0.2329	0.2448	0.2855	0.2903	0.305	0.3192	0.3358	0.3426	0.3557	0.3834	0.4123	0.2923	9.90E-04	6
623	0.1081	0.1333	0.1874	0.1874	0.2012	0.2486	0.2542	0.2714	0.2878	0.3071	0.315	0.3302	0.3623	0.3956	0.2564	8.69E-04	7
622	0.0512	0.0801	0.1418	0.1418	0.1576	0.2117	0.2181	0.2376	0.2564	0.2783	0.2874	0.3046	0.3412	0.3788	0.2205	7.47E-04	8
621	0	0.0267	0.0961	0.0961	0.1139	0.1747	0.1819	0.2039	0.225	0.2496	0.2597	0.2791	0.32	0.3621	0.1849	6.27E-04	9
620	0	0	0.0504	0.0504	0.0702	0.1376	0.1456	0.17	0.1934	0.2207	0.232	0.2534	0.2987	0.3453	0.1548	5.25E-04	10
619	0	0	0.0046	0.0046	0.0263	0.1005	0.1093	0.1361	0.1619	0.1918	0.2042	0.2278	0.2775	0.3285	0.1266	4.29E-04	11
618	0	0	0	0	0	0.0633	0.0729	0.1022	0.1302	0.1629	0.1764	0.202	0.2562	0.3116	0.1056	3.58E-04	12
617	0	0	0	0	0	0.0261	0.0365	0.0682	0.0985	0.1339	0.1485	0.1763	0.2349	0.2947	0.0870	2.95E-04	13
616	0	0	0	0	0	0	0	0.0341	0.0668	0.1049	0.1206	0.1505	0.2135	0.2778	0.0692	2.34E-04	14
615	0	0	0	0	0	0	0	0	0.035	0.0758	0.0926	0.1246	0.1921	0.2609	0.0558	1.89E-04	15
614	0	0	0	0	0	0	0	0	0.0032	0.0467	0.0646	0.0988	0.1706	0.2439	0.0448	1.52E-04	16
613	0	0	0	0	0	0	0	0	0	0.0175	0.0365	0.0728	0.1492	0.227	0.0359	1.22E-04	17
612	0	0	0	0	0	0	0	0	0	0	0.0084	0.0469	0.1277	0.2099	0.0281	9.51E-05	18
611	0	0	0	0	0	0	0	0	0	0	0	0.0208	0.1061	0.1929	0.0228	7.74E-05	19
610	0	0	0	0	0	0	0	0	0	0	0	0	0.0845	0.1758	0.0186	6.30E-05	20
609	0	0	0	0	0	0	0	0	0	0	0	0	0.0629	0.1587	0.0158	5.36E-05	21
608	0	0	0	0	0	0	0	0	0	0	0	0	0.0412	0.1416	0.0131	4.43E-05	22
607	0	0	0	0	0	0	0	0	0	0	0	0	0.0196	0.1244	0.0103	3.48E-05	23
606	0	0	0	0	0	0	0	0	0	0	0	0	0	0.1072	0.0077	2.60E-05	24
605	0	0	0	0	0	0	0	0	0	0	0	0	0	0.09	0.0064	2.18E-05	25
604	0	0	0	0	0	0	0	0	0	0	0	0	0	0.0728	0.0052	1.76E-05	26
603	0	0	0	0	0	0	0	0	0	0	0	0	0	0.0555	0.0040	1.34E-05	27
602	0	0	0	0	0	0	0	0	0	0	0	0	0	0.0382	0.0027	9.24E-06	28
601	0	0	0	0	0	0	0	0	0	0	0	0	0	0.0208	0.0015	5.05E-06	29
600	0	0	0	0	0	0	0	0	0	0	0	0	0	0.0035	0.0002	8.42E-07	30

Table A10-2. Calculation of ^4He implantation depth profile for diamond crystal F4 (U-Th=248 ppm; U/Th=3).

x	R_i														C_d/C_m	$^4\text{He, cc/g}$	r
	8.9	9.5	11.1	11.1	11.6	13.7	14	15	16.1	17.6	18.3	19.8	23.9	30.2			
630	0.5035	0.5038	0.5044	0.5044	0.5046	0.5054	0.5056	0.506	0.5064	0.507	0.5073	0.5079	0.5095	0.512	0.5063	7.90E-04	0
629	0.4473	0.4511	0.4593	0.4593	0.4615	0.4689	0.4698	0.4726	0.4753	0.4786	0.4799	0.4826	0.4886	0.4954	0.4707	7.34E-04	1
628	0.391	0.3984	0.4142	0.4142	0.4183	0.4323	0.434	0.4392	0.4442	0.4501	0.4526	0.4573	0.4676	0.4789	0.4352	6.79E-04	2
627	0.3346	0.3455	0.369	0.369	0.375	0.3957	0.3982	0.4057	0.413	0.4216	0.4251	0.432	0.4466	0.4623	0.3995	6.23E-04	3
626	0.2781	0.2926	0.3237	0.3237	0.3317	0.359	0.3623	0.3722	0.3818	0.393	0.3977	0.4066	0.4256	0.4456	0.3638	5.68E-04	4
625	0.2215	0.2396	0.2783	0.2783	0.2883	0.3223	0.3263	0.3387	0.3505	0.3644	0.3702	0.3812	0.4045	0.429	0.3281	5.12E-04	5
624	0.1649	0.1865	0.2329	0.2329	0.2448	0.2855	0.2903	0.305	0.3192	0.3358	0.3426	0.3557	0.3834	0.4123	0.2923	4.56E-04	6
623	0.1081	0.1333	0.1874	0.1874	0.2012	0.2486	0.2542	0.2714	0.2878	0.3071	0.315	0.3302	0.3623	0.3956	0.2564	4.00E-04	7
622	0.0512	0.0801	0.1418	0.1418	0.1576	0.2117	0.2181	0.2376	0.2564	0.2783	0.2874	0.3046	0.3412	0.3788	0.2205	3.44E-04	8
621	0	0.0267	0.0961	0.0961	0.1139	0.1747	0.1819	0.2039	0.225	0.2496	0.2597	0.2791	0.32	0.3621	0.1849	2.88E-04	9
620	0	0	0.0504	0.0504	0.0702	0.1376	0.1456	0.17	0.1934	0.2207	0.232	0.2534	0.2987	0.3453	0.1548	2.42E-04	10
619	0	0	0.0046	0.0046	0.0263	0.1005	0.1093	0.1361	0.1619	0.1918	0.2042	0.2278	0.2775	0.3285	0.1266	1.98E-04	11
618	0	0	0	0	0	0.0633	0.0729	0.1022	0.1302	0.1629	0.1764	0.202	0.2562	0.3116	0.1056	1.65E-04	12
617	0	0	0	0	0	0.0261	0.0365	0.0682	0.0985	0.1339	0.1485	0.1763	0.2349	0.2947	0.0870	1.36E-04	13
616	0	0	0	0	0	0	0	0.0341	0.0668	0.1049	0.1206	0.1505	0.2135	0.2778	0.0692	1.08E-04	14
615	0	0	0	0	0	0	0	0	0.035	0.0758	0.0926	0.1246	0.1921	0.2609	0.0558	8.70E-05	15
614	0	0	0	0	0	0	0	0	0.0032	0.0467	0.0646	0.0988	0.1706	0.2439	0.0448	7.00E-05	16
613	0	0	0	0	0	0	0	0	0	0.0175	0.0365	0.0728	0.1492	0.227	0.0359	5.61E-05	17
612	0	0	0	0	0	0	0	0	0	0	0.0084	0.0469	0.1277	0.2099	0.0281	4.38E-05	18
611	0	0	0	0	0	0	0	0	0	0	0	0.0208	0.1061	0.1929	0.0228	3.56E-05	19
610	0	0	0	0	0	0	0	0	0	0	0	0	0.0845	0.1758	0.0186	2.90E-05	20
609	0	0	0	0	0	0	0	0	0	0	0	0	0.0629	0.1587	0.0158	2.47E-05	21
608	0	0	0	0	0	0	0	0	0	0	0	0	0.0412	0.1416	0.0131	2.04E-05	22
607	0	0	0	0	0	0	0	0	0	0	0	0	0.0196	0.1244	0.0103	1.60E-05	23
606	0	0	0	0	0	0	0	0	0	0	0	0	0	0.1072	0.0077	1.20E-05	24
605	0	0	0	0	0	0	0	0	0	0	0	0	0	0.09	0.0064	1.00E-05	25
604	0	0	0	0	0	0	0	0	0	0	0	0	0	0.0728	0.0052	8.11E-06	26
603	0	0	0	0	0	0	0	0	0	0	0	0	0	0.0555	0.0040	6.18E-06	27
602	0	0	0	0	0	0	0	0	0	0	0	0	0	0.0382	0.0027	4.26E-06	28
601	0	0	0	0	0	0	0	0	0	0	0	0	0	0.0208	0.0015	2.32E-06	29
600	0	0	0	0	0	0	0	0	0	0	0	0	0	0.0035	0.0002	3.88E-07	30

Table A10-3 Calculation of ^4He implantation depth profile for diamond crystal F4 (U-Th=160 ppm; U/Th=3).

	R _i																	
x	8.9	9.5	11.1	11.1	11.6	13.7	14	15	16.1	17.6	18.3	19.8	23.9	30.2	C _d /C _m	⁴ He, cc/g	r	
630	0.5035	0.5038	0.5044	0.5044	0.5046	0.5054	0.5056	0.506	0.5064	0.507	0.5073	0.5079	0.5095	0.512	0.5063	5.06E-04	0	
629	0.4473	0.4511	0.4593	0.4593	0.4615	0.4689	0.4698	0.4726	0.4753	0.4786	0.4799	0.4826	0.4886	0.4954	0.4707	4.71E-04	1	
628	0.391	0.3984	0.4142	0.4142	0.4183	0.4323	0.434	0.4392	0.4442	0.4501	0.4526	0.4573	0.4676	0.4789	0.4352	4.35E-04	2	
627	0.3346	0.3455	0.369	0.369	0.375	0.3957	0.3982	0.4057	0.413	0.4216	0.4251	0.432	0.4466	0.4623	0.3995	4.00E-04	3	
626	0.2781	0.2926	0.3237	0.3237	0.3317	0.359	0.3623	0.3722	0.3818	0.393	0.3977	0.4066	0.4256	0.4456	0.3638	3.64E-04	4	
625	0.2215	0.2396	0.2783	0.2783	0.2883	0.3223	0.3263	0.3387	0.3505	0.3644	0.3702	0.3812	0.4045	0.429	0.3281	3.28E-04	5	
624	0.1649	0.1865	0.2329	0.2329	0.2448	0.2855	0.2903	0.305	0.3192	0.3358	0.3426	0.3557	0.3834	0.4123	0.2923	2.92E-04	6	
623	0.1081	0.1333	0.1874	0.1874	0.2012	0.2486	0.2542	0.2714	0.2878	0.3071	0.315	0.3302	0.3623	0.3956	0.2564	2.56E-04	7	
622	0.0512	0.0801	0.1418	0.1418	0.1576	0.2117	0.2181	0.2376	0.2564	0.2783	0.2874	0.3046	0.3412	0.3788	0.2205	2.20E-04	8	
621	0	0.0267	0.0961	0.0961	0.1139	0.1747	0.1819	0.2039	0.225	0.2496	0.2597	0.2791	0.32	0.3621	0.1849	1.85E-04	9	
620	0	0	0.0504	0.0504	0.0702	0.1376	0.1456	0.17	0.1934	0.2207	0.232	0.2534	0.2987	0.3453	0.1548	1.55E-04	10	
619	0	0	0.0046	0.0046	0.0263	0.1005	0.1093	0.1361	0.1619	0.1918	0.2042	0.2278	0.2775	0.3285	0.1266	1.27E-04	11	
618	0	0	0	0	0	0.0633	0.0729	0.1022	0.1302	0.1629	0.1764	0.202	0.2562	0.3116	0.1056	1.06E-04	12	
617	0	0	0	0	0	0.0261	0.0365	0.0682	0.0985	0.1339	0.1485	0.1763	0.2349	0.2947	0.0870	8.70E-05	13	
616	0	0	0	0	0	0	0	0.0341	0.0668	0.1049	0.1206	0.1505	0.2135	0.2778	0.0692	6.92E-05	14	
615	0	0	0	0	0	0	0	0	0.035	0.0758	0.0926	0.1246	0.1921	0.2609	0.0558	5.58E-05	15	
614	0	0	0	0	0	0	0	0	0.0032	0.0467	0.0646	0.0988	0.1706	0.2439	0.0448	4.48E-05	16	
613	0	0	0	0	0	0	0	0	0	0.0175	0.0365	0.0728	0.1492	0.227	0.0359	3.59E-05	17	
612	0	0	0	0	0	0	0	0	0	0	0.0084	0.0469	0.1277	0.2099	0.0281	2.81E-05	18	
611	0	0	0	0	0	0	0	0	0	0	0	0.0208	0.1061	0.1929	0.0228	2.28E-05	19	
610	0	0	0	0	0	0	0	0	0	0	0	0	0.0845	0.1758	0.0186	1.86E-05	20	
609	0	0	0	0	0	0	0	0	0	0	0	0	0.0629	0.1587	0.0158	1.58E-05	21	
608	0	0	0	0	0	0	0	0	0	0	0	0	0.0412	0.1416	0.0131	1.31E-05	22	
607	0	0	0	0	0	0	0	0	0	0	0	0	0.0196	0.1244	0.0103	1.03E-05	23	
606	0	0	0	0	0	0	0	0	0	0	0	0	0	0.1072	0.0077	7.66E-06	24	
605	0	0	0	0	0	0	0	0	0	0	0	0	0	0.09	0.0064	6.43E-06	25	
604	0	0	0	0	0	0	0	0	0	0	0	0	0	0.0728	0.0052	5.20E-06	26	
603	0	0	0	0	0	0	0	0	0	0	0	0	0	0.0555	0.0040	3.96E-06	27	
602	0	0	0	0	0	0	0	0	0	0	0	0	0	0.0382	0.0027	2.73E-06	28	
601	0	0	0	0	0	0	0	0	0	0	0	0	0	0.0208	0.0015	1.49E-06	29	
600	0	0	0	0	0	0	0	0	0	0	0	0	0	0.0035	0.0002	2.48E-07	30	

APPENDIX 11: DATA TABLE FOR CHAPTER 5.

Table A8-1. $\delta^{15}\text{N}$, $\delta^{13}\text{C}$, N and He concentration in carbonado and framesites.

Sample	$\delta^{15}\text{N}$, ‰	$\delta^{13}\text{C}$, ‰	N, (ppm)	^4He , cc/g*10 ⁻⁴
Carbonado Ubangui				
JJG4105.C	2.9	-25.2	18	7.1
JJG4105D	8.05	-28.1	65	250
JJG4105A	-5.0	-5.8	4.2	8.6
JJG4105E	2.6	-26.1	392	55
JJG4105B	2	-26.4	58	15
JJG4105(?)	1.5	-25.8	80	120
Carbonado Brasil				
Br-34	2.5	-27.3	140	500
Br32	1.5	-30	33	nm
Br-4	11	-28	74	1640
BMCB	1.5	-26	258	85
BRCB1	5.9	-26.8	1040	2.4
BRCB2	-0.9	-28.8	63	760
BRCB5	2.8	-23.5	419	180
CB5	1.7	-26.1	50	48
CB11	12.8	-27.8	88	700
CB20	9.3	-23.8	1590	5.9
BRCB4	-2.9	-23.6	71	nm
BRCB6	0.3	-23.9	161	nm
BRCB7	-3.6	-24	103	17
BRCB3	nm	-26.8	66	nm
Framesites				
ORF121.484	7.7	-22.5	102	0.46
PHN/25.484	11.5	-19.1	96	0.64
PHN/26.479	9.26	-18	142	0.64
JWF-6.479	7.5	-23.6	112	0.49
JWF-11.479	10.8	-20.1	91	0.69
JWF-10.479	0.75	-23.6	190	0.36
JJG-4104.488	1.41	-18.2	251	nm
JJG-4103.484	3.44	-23.8	1294	nm
FRM1.487	3.66	-21.8	330	nm
GPF3	2.62	-18.3	100	0.078
GPF2	-2.9	-21	56	nm
GPF1	10.8	-19.8	77	nm

Standart deviation for $\delta^{15}\text{N}$ is 1‰, for $\delta^{13}\text{C}$ is 0.5‰. for N content 5% and for He content 10%.

APPENDIX 12: DATA TABLES FOR CHAPTER 6.

Table A12-1. Results of bulk analysis of polycrystalline diamonds from Ebeliakh.

Sample	$\delta^{15}\text{N}, \text{‰}$	Err	N, ppm	$\delta^{13}\text{C}, \text{‰}$	$^{40}\text{Ar}, \text{cc/g}$	$^{40}\text{Ar}/^{36}\text{Ar}$	$^{36}\text{Ar}, \text{cc/g}$	$^4\text{He}, \text{cc/g}$
Y7	nm	nm	800	-27.6	1.1E-05	307	3.6E-08	1.0E-05
Y17	nm	nm	29	-8.8	1.2E-05	301	3.5E-08	1.7E-05
Y14	-3.9	1.5	9	-7.2	1.7E-06	681	2.0E-09	2.0E-04
Y2	1.8	1.2	20	-9.5	1.8E-05	300	5.2E-08	4.0E-05
Y4	-3.96	4.7	4.9	-8.4	5.6E-06	299	1.6E-08	3.4E-05
Y18(1)	4.3	0.9	19	-9.7	1.7E-04	2148	8.0E-08	nm

Table A12-2. Results of bulk analysis of polycrystalline diamonds from Popigai crater.

Sample	$\delta^{15}\text{N}$	Err	N, ppm	$\delta^{13}\text{C}$	$^{40}\text{Ar}, \text{cc/g}$	$^{40}\text{Ar}/^{36}\text{Ar}$	$^{36}\text{Ar}, \text{cc/g}$
P3	nm	nm	<5	-20.0	nm	nm	nm
P7	nm	nm	<5	-19.3	nm	nm	nm
Pd336	5	0.5	36	-12.0	nm	nm	nm
Pd508/1	1.9	2.1	12	-10.6	9.9E-05	424	2.3E-07
Pd508/2	9.2	1.1	30	-10.5	8.6E-05	298	2.9E-07
Pd508/3	5.2	1.7	34	-12.1	2.8E-04	517	7.7E-07
Pd511	11.9	2	25	-10.5	1.2E-04	364	3.4E-07
Pd506/1	nm	nm	nm	-11.2	1.1E-04	12263	nm
Pd505/2	nm	nm	nm	-7.9	1.3E-05	342	nm
Pd532	10.9	2	2.4	-10.5	nm	nm	nm
PY-1	nm	nm	5	-16.1	nm	nm	nm
PB-5	nm	nm	8	-10.6	3.3E-05	781	4.2E-08
PY-2	6.2	1.1	50	-20.4	2.8E-04	326	8.5E-07
Pd535	4.6	1.8	17	-19.3	9.7E-05	585	1.7E-07
IG	-1.1	1.7	44	-8.7	nm	nm	nm
Pgr10*	nm	nm	nm	-17.6	nm	nm	nm
Pgr9*	nm	nm	nm	-14.1	nm	nm	nm
P8	nm	nm	nm	-16.5	nm	nm	nm
P4	nm	nm	nm	-8.1	nm	nm	nm
P2	nm	nm	nm	-18.1	nm	nm	nm
P1	nm	nm	nm	-18.4	nm	nm	nm
PK5 ⁺	nm	nm	nm	-12.6	nm	nm	nm
PK6 ⁺	nm	nm	nm	-11.1	nm	nm	nm

*- samples of graphite; ⁺-diamonds from Pechug-Katun crater

Table A12-3. Step combustion experiment Y18(2).

T,°C	N,ppm	⁴⁰ Ar,cc/g	⁴⁰ Ar/ ³⁶ Ar	³⁶ Ar,cc/g	⁴ He,cc/g	C,μg
625	663*	4.6E-04	456	9.9E-07	blank	3.9
650	255*	2.4E-04	479	4.9E-07	1.9E-06	9.3
675	125	1.4E-04	582	2.4E-07	1.0E-06	16.6
700	74	9.6E-05	594	1.6E-07	9.3E-07	28.4
725	59	7.9E-05	666	1.2E-07	1.0E-06	40.9
750	49	6.9E-05	691	9.8E-08	8.3E-07	51.9
775	54	6.6E-05	775	8.2E-08	9.3E-07	53.6
800	58	7.2E-05	648	1.1E-07	1.1E-06	44.5
825	63	7.9E-05	466	1.7E-07	1.3E-06	25.2
850	102	2.0E-04	376	5.3E-07	4.1E-06	6
Total	68	1.1E-04	540	2.0E-07	1.1E-06	282

Total N concentration was calculated from steps unaffected by N contamination

*-value affected by N contamination (see text for details)

Table A12-4. Step combustion experiment Y14.

T,°C	N,ppm	⁴⁰ Ar,cc/g	⁴⁰ Ar/ ³⁶ Ar	³⁶ Ar,cc/g	⁴ He,cc/g	C,μg
550	204	1.5E-04	269	5.6E-07	3.3E-05	3.2
600	29	1.6E-05	336	4.0E-08	3.4E-06	25
650	14	4.5E-06	516	7.3E-09	9.4E-06	79.3
700	28	1.7E-05	382	3.7E-08	1.9E-05	32.6
Total	24	9.2E-06	377	2.0E-08	1.1E-05	140.5

APPENDIX 13: STATISTICAL PARAMETERS OF LINEAR CORRELATIONS USED IN CHAPTER 6.

Table A13-1. Statistical parameters for linear correlation in co-ordinates N-³⁶Ar.

Line	Slope	Root MSWD	Intercept	Root MSWD	MSWD
Y	347303	103498	0.0060	0.0045	3.4
Y18(2)-14	311783	57850	0.0097	0.0032	0.9
Y14	310769	66162	0.0095	0.0019	0.3
P	38126.8	15211	0.0048	0.0034	1.7

Y - linear correlation by yakutites from Ebeliakh placers
 (results of bulk and step combustion experiments)
 P - linear correlation by diamonds from Popigai crater

Table A13-2. Statistical parameters for linear correlation in co-ordinates N-⁴⁰Ar (rad) for step combustion experiments with samples Y18 and Y14.

Line	Slope	Root MSWD	Intercept	Root MSWD	MSWD
Y18(2)	520	1108	0.0254	0.0451	2.1
Y14(1-2)	4012	1618	0.0027	0.0034	1.9

⁴⁰Ar(rad) - ⁴⁰Ar excess relative to the isotopic composition of the air.

Table A13-3. Statistical parameters for linear correlation in co-ordinates ⁴⁰Ar/³⁶Ar - 1/³⁶Ar, for samples studied by step combustion technique.

Line	Slope	Root MSWD	Intercept	Root MSWD	MSWD
Y18(2)	3.6E-05	1.0E-05	355	53	1.2
Y14(1-2)	1.2E-06	5.6E-07	309	43	4.6

Table A13-4. Statistical parameters for linear correlation in co-ordinates Ar_(rad)-Ar_(air) for step combustion experiments with samples Y18 and Y14.

Line	Slope	Root MSWD	Intercept	Root MSWD	MSWD
Y18(2)	0.50	0.13	2.7E-05	5.6E-06	2.0
Y14	0.37	0.21	9.6E-07	5.7E-07	2.8

References.

- Afanas'ev, G.D., and Zykov, S.I.,** (1974) Results of study of laboratory standards. *Izv. Akad. Nauk., ser. Geology*, 11, 5-17 (in Russian)
- Alvarez, L.W. Alvarez, W., Asaro, F., Michel, H.V.** (1980) Extraterrestrial cause for the Cretaceous Tertiary extinction. *Science*, 208, 4448, 1095-1108
- Bachman, P.K.,** (1994) General aspects of CVD growth of diamond and their correlation. in *Properties and growth of diamond* (ed. G. Davies)
- Barrie, A.,** (1991). New methodologies in stable isotope analysis. In: *Stable Isotopes in Plant Nutrition, Soil Fertility and Environmental Studies*, I.A.E.A., Vienna, 3-25.
- Becker, R.H., and Clayton, R.N.,** (1975). Nitrogen abundances and isotopic compositions in lunar samples. *Proc. Lunar Planet. Sci. Conf. 9th*, 2131-2149.
- Banno, S.,** (1970) Classification of eclogites in terms of physical conditions of their origin. *Phys. Earth Planet. Intern.*, 3, 405-421
- Bartoshinsky, Z.V., Bilenko, Yu.M., Zhikhareva, V.P., Koptil, V.I.,** (1980) On twins, intergrowths and polycrystalline species of natural diamond. *Mineralogicheskii sbornik L'vovskogo Universiteta*, 31/2, 53-55
- Bebout, G.E., and Fogel, M.L.,** (1992) Nitrogen-isotope composition of metasedimentary rocks in the Catalina Schist, California: Implications for metamorphic devolatilisation history. *Geochim. Cosmochim. Acta*, 56: 2839-2849.
- Becker, R. H., and Clayton, R.N.,** (1972) Carbon isotopic evidence for the origin of banded iron-formation in Western Australia. *Geochim. Cosmochim. Acta*, 36, 577-595.
- Becker, R. H. and Clayton, R.N.,** (1977) Nitrogen isotopes in igneous rocks. *Eos Trans. Am. Geophys. Union*, 58, 536 (abstr).

- Berman, R., Simon, F.** (1955) On the graphite-diamond equilibrium. *Z. Electrochem.*, 59, 333-345
- Boyd, S.R., Hall A., Pillinger, C.T.,** (1993) The measurement of $\delta^{15}\text{N}$ in crustal rocks by static vacuum mass spectrometer: application to the origin of the ammonium in the Cornubian batholith, S.W. England. *Geochim. Cosmochim. Acta*, 57, 1339-1347
- Boyd, S.R.,** (1988) A study of carbon and nitrogen isotopes from the Earth's mantle. Ph.D. Thesis, The Open University, Milton Keynes.
- Boyd, S.R., and Pillinger, C.T.,** (1994). A preliminary study of $^{15}\text{N}/^{14}\text{N}$ in octahedral growth form diamonds. *Chemical geology*, 116, 43-59.
- Boyd, S.R.,** (1988) A study of carbon and nitrogen isotopes from the Earth's mantle. Ph.D. Thesis, The Open University, Milton Keynes.
- Boyd, S.R., Mathey, D.P., Pillinger, C.T., Milledge, H.J., Mendelsohn, M.J. and Seal, M.,** (1987) Multiple growth events during diamond genesis: an integrated study of carbon and nitrogen isotopes and nitrogen aggregation state in coated diamonds. *Earth Planet. Sci Letters*, 86, 341-353
- Boyd, S.R., Pillinger, C.T., Milledge, H.J., Mendelsohn, M.J. and Seal, M.,** (1988) Fractionation of nitrogen in a synthetic diamond of mixed crystal habit. *Nature*, 331: 604-607
- Boyd, S.R., Pineau, F., and Javoy, M.,** (1994) Modelling the growth of natural diamonds. *Chemical geology*, 116, 29-42
- Boyd, S.R., Wright, I.P., Franchi, I.A., Pillinger, C.T.,** (1988) Preparation of sub-nanomole quantities of nitrogen gas for stable isotope analysis. *Sci. Instrum.*, 21, 876-885.
- Brandenberg E.** (1930) Röntgenuntersuchungen an Carbonados. *Schweiz. Mineral. Petrogr. Mitt.* 10, 490

Brookes S.T., Davies J.E., Scrimgeour C.M., Smith K. and Watt P.W. (1992). L Single cycle analysis of ^{15}N and ^{13}C enrichment in proteins. In: K.Takai (Editor), *Frontiers and New Horizons in Amino Acid Research*, Elsevier, Amsterdam, 411-415

Brown P.W. and Pillinger C.T. (1981). Nitrogen concentrations and isotopic ratios from separated lunar soils. *Meteoritics* 16, 298.

Bulanova, G.P., Barashkova, Yu.P., Tal'nikova, S.B., Smelova, G.B., (1993) *Natural diamond-genetical aspects.* "Nauka", Novosibirsk, 165

Bundy F.P., (1980) The P,T phase and Reaction Diagram for Element Carbon, *J.Geophys.Res.*, 85, 6930-6936

Bundy, F.R., Kasper, J.S. (1967) Hexagonal diamond- a new form of carbon. *Jornal Chem. Phis.*, 46, 3437-3446

Carswell, D.A., Clarke, D.B., Mitchell, R.H., (1979) The petrology and geochemistry of ultramafic nodules from Pipe 200, northern Lesotho. In Boyd F.R., Meyer H.O.A. (eds) *The mantle samples: inclusions in kimberlites and other volcanics.* Am. Geophys. Union., Washington, 127-144

Carr R.H., Wright I.P., Joines A.W. and Pillinger C.T. (1986). Measurement of carbon stable isotopes at the nanomole level: a static mass spectrometer and sample preparation technique. *J. Phys. E: Sci. Instrum.* 19, 798-808.

- Chang S., Lawless J., Romiez M., Kaplan I.R., Petrowski C., Sakai H. and Smith J.W.** (1974). Carbon, nitrogen and sulphur in lunar fines 15012 and 15013: abundances, distributions and isotopic composition. *Geochim Cosmochim. Acta* 46, 853-872.
- Chopin, C., and Sobolev, N.V.,** (1995) in *Ultrahigh Pressure Metamorphism*, R.G.Coleman, X.Wang eds., Cambridge University Press
- Chrenko, R.M., Tuft, R.E, Strong, H.M.** (1977) Transmission of the state of nitrogen in diamond. *Nature*, 270, 141-144
- Clayton, R.N., Onuma, N., and Mayeda, T.K.** (1976) A classification of meteorites based on oxygen isotopes. *Earth Planet. Sci. Lett.*, 30, 615-660
- Clement, C.R., Skinner, E.M.W., Scott Smith, B.H.** (1984) Kimberlite re-defined. *J. Geol.*, 32, 223-228
- Cline, J.D., Kaplan, I.R.,** (1975) Isotopic fractionation of dissolved nitrate during denitrification in the eastern tropical North Pacific Ocean. *Marine Chem.*, 3, 271
- Coleman, R.G., Lee, E.D., Beatty, L.B., Brannock, W.W.** (1965). Eclogites and eclogites: their differences and similarities. *Geol Soc. Am. Bull.*, 76, 483-508
- Craig, H.,** (1953) The geochemistry of the stable carbon isotopes. *Geochim. Cosmochim. Acta*, 3, 53-92.
- Darimont, A., Burke, E., Touret, J.** (1988) Nitrogen-rich metamorphic fluids in Devonian metasediments from Bastogne, Belgium. In: *Proceedings; 9th symposium on European current research on fluid inclusions. Bulletin de Mineralogie.* 111, 3-4, 321-330
- Daulton, T.L., Ozima, M., and Shukolyukov, Y.** (1995) Radiation-induced nano-diamond formation and its implications for interstellar diamonds. *Lunar and Planetary Science XXVI*, 313-314.

- Davidson, C.F.**, (1967) The kimberlites of the USSR. In Wyllie P.J. (ed) Ultramafic and related rocks. Wiley, New York, 251-256
- Davis, G.L.**, (1977). The ages and uranium contents of zircons from kimberlites and associated rocks. 2nd Kimberlite Conference, Santa- Fe (abstr)
- Dawson, J.B.**, (1980) Kimberlites and their xenoliths. Springer-Verlag, Berlin-Heidelberg-New York, 252
- Dawson, J.B., Smith, J.V., and Hervig, R.L.**(1980) Heterogeneity in upper-mantle lherzolites and harzburgites. Phil. Trans. R. Soc. Lond. Ser A 297, 323-331
- Dawson, J.B.**(1971) Advances of kimberlite geology. Earth. Sci. Rev., 7, 187-214
- Dawson, J.B.** (1968) Recent researches on kimberlite and diamond geology. Econ.Geol, 63, 504-511
- DeCarli, P.S., Jamieson, J.C.**, (1961) Formation of diamond by explosive shock. Science, 133, 3467, 1821
- Deines, P.**, (1989) Regularities in the C and nitrogen content of the mantle revealed through studies of diamonds and the chemistry of their inclusions. 28th International Geological Congress, extended abstr., 18-21
- Deines, P.**, (1991) Model simulations of carbon isotope variability in the mantle. 5th International Kimberlite Conference, 74-75 (abstr.).
- Deines, P., Gurney, J.J. and Harris, J.W.**, (1984) Associated chemical and carbon isotopic composition variations in diamonds from Finsch and Premier kimberlite, South Africa. Geochim. Cosmochim. Acta, 48, 325-342.
- Deines, P., Harris, J.W. and Gurney, J.J.** (1987) Carbon isotopic composition, nitrogen content and inclusion composition of diamonds from Robert Victor Kimberlite, South Africa Geochim. Cosmochim. Acta, 51, 1227-1243.

Deines, P., Harris, J.W. and Gurney, J.J., (1991) The carbon isotopic composition and nitrogen content of lithospheric and asthenospheric diamonds from the Jagersfontein and Koffiefontein kimberlite, South Africa. *Geochim. Cosmochim. Acta*, 55, 2615-2625.

Deines, P., Harris, J.W. and Gurney, J.J., (1993) Depth-related carbon isotope and nitrogen concentration variability in the mantle below the Orapa kimberlite, Botswana, Africa. *Geochim. Cosmochim. Acta*, 57: 2781-2796

Deuser, W.G., and Degens, E.T. (1967) Carbon isotope fractionation in the system CO (sub 2) (gas)-CO (sub 2) (aqueous)-HCO (sub 3) (aqueous). *Nature*, 215; 5105, 1033-1035

Drechsler, M., and Stiehl, G., (1977) Stickstoffisotopenvariationen in organischen Sedimenten, I. Untersuchungen an humosen Kohlen. *Chemie Erde*, 36: 126-138

Duit W, Jansen, J.B.H., Vanbreemen, A., Bos, A., (1986) Ammonium micas in metamorphic rocks as exemplified by Dome-de-Lagout (France). *Amer. Journ. of Sci.*, 286/9, pp.702-732

Emrich, K., Ehhalt, D.H., Vogel, J.C. (1970) Carbon isotope fractionation during the precipitation of calcium carbonate. *Earth and Planet. Sci. Lett.* 8/5, 363-369

Erd, R.C., White, D.E., Fahey, J.J., Lee, D.E. (1964) Buddingtonite, an ammonium feldspar with zeolitic water. *Amer. Mineral.*, 49, 831-850.

Evans T., Oi Z. (1982) The kinetics of the aggregation of nitrogen-atoms in diamond. *Proc. R. Soc.* vol 381, 159-178

Exley, R.A., Matthey, D.P., Pillinger, C.T., Sinton, J.M. (1986) Carbon isotope geochemistry of basalt glasses from the Lau and North Fiji marginal basins, *Terra Cognita*, 6, 324

Exley, R.A., Matthey, D.P., Clague, D.A., Pillinger, C.T. (1986) Carbon isotope systematics of a mantle "hotspot": a comparison of Loihi Seamount and MORB glasses., *Earth. Planet. Sci. Lett.*, 78, 189-199

- Exley, R.A., Boyd, S.R., Matthey, D.P., Pillinger, C.T.,** (1987) Nitrogen isotope geochemistry of basaltic glasses: implication for mantle degassing and structure. *Earth. Planet. Sci. Lett.*, 81, 163-179
- Fallick A.E., Gardiner L.R., Jull A.J.T. and Pillinger C.T.** (1980). Instrumental effects in the application of static mass spectrometry to high sensitivity carbon isotope measurements. *Adv. Mass Spectrum.*, 8, 309-317.
- Faure G.,** (1986) Principles of isotope geology. John Wiley and Sons, 589
- Fettke C.R. and Sturgis F.C.,** (1933) Note on the structure of carbonado or black diamond. *Amer.Mineral.*, 18, 172-174
- Franchi I.A., Wridht I.P. and Pillinger C.T.** (1986) Heavy nitrogen in Bencubbin — a light - element isotopic anomaly in stony-iron meteorite. *Nature*, Vol. 323, 6084, 138-140
- Frick U. and Pepin R.O.** (1981). Microanalysis of nitrogen isotope abundances: association of nitrogen with noble gas carriers in Allende. *Earth Planet. Sci. Lett.* 56, 64-81.
- Gabdiner L.R. and Pllinger C.T.** (1979). Stauc mass spectrometry for thz determination of active gases. *Anal. Chem.* 51, 1230-1236.
- Galimov, E.M.,Kaminsky, F.V. and Kodina, L.A.** (1985) New data on carbon isotopic composition of carbonado. *Geokhimia*, 5, 723-726. (Russian)
- Galimov, E.M,** (1984) The relation between formation conditions and variations in isotope composition of diamonds. *Geokhimia*, 8: 1091-1118 (reprinted in *Intl. Geochem.*, 118-141, 1985).
- Galimov, E.M,** (1991) Isotope fractionation related to kimberlite magmatism and diamond formation. *Geochim. Cosmochim. Acta*, 55: 1697-1708.
- Galimov, E.M., Kaminsky, F.V., Gricick, V.V. and Ivanovskaya, I.N.,** (1978) Study of carbon isotope composition of diamonds from Urals, Timan, Sayan, Ukraine and other regions. *Geokhimia*, 3, 340-349 (in Russian).

- Galimov, E.M.** (1968) Stable isotope geochemistry of carbon. Nedra, Moscow, 224
- Garlick, E.M., MacGregor, I.D., Vogel D.E.,** (1971) Oxygen isotope ratios in eclogites from kimberlites. *Science* 172, 1025-1027.
- Gerlach, V.W.,**(1924) Über die struktur des "schwarzen diamants". *Z. Anorg. Chem.*, 137,331 (German)
- Gilmour, I., Russell, S.S., Arden, J.W., Lee, M.R., Franchi, I.A., and Pillinger, C.T.** (1992) Terrestrial carbon and nitrogen isotopic-ratios from Cretaceous-Tertiary boundary nanodiamonds. *Science*, 258, 1624-1626
- Girdler, R.W., Taylor, P.T., Frawley, J.J.** (1992) A possible impact origin for the Bangui magnetic anomaly. *Tectonophysics*. 212, 45-58.
- Goresy, A.El., and Donnay, G.** (1968) A new allotropic form of carbon from the Ries crater. *Science*, 161, 363-364
- Grady, M.M., Wright, I.P., Carr, L.P. and Pillinger C.T.,** (1986) Compositional differences in enstatite chondrites based on carbon and nitrogen stable isotope measurements. *Geochim. Cosmochim. Acta*, 47: 2799 - 2813.
- Green P.F., Milledge H.J., Mendelssohn M.J., Nave E., Woods P.,** (1980) Fission-track studies in diamond and kimberlite. *Sol.State Nucl. Track Detect.* (10th Int. Conf., Lyon), Pergamon, 973-978
- Gregory R.T. and Taylor H.P.,** (1981) An oxygen isotope profile in a section of cretaceous oceanic crust, Samail ophiolite, Oman: Evidence for $\delta^{18}\text{O}$ buffering of oceans by deep (>5 km) sea-water-hydrothermal circulation at mid-ocean ridges. *J. Geophys. Res.*, 86, 2737-2755
- Grieve, R., Rupert, J., Smith, J., Terriault, A.,** (1995) The record of terrestrial impact cratering. *GSA TODAY*, 5/10, 194-196
- Gulbrandsen, R.A.** (1974) Buddingtonite, ammonium feldspar, in the Phosphoria Formation, southeastern Idaho. *Journal of Research of the U. S. Geological Survey*, 2/6, 693-697

Gurnay, J.J., Harris, J.W., Rickard, R.S. (1979) Silicate and oxide inclusions in diamonds from Finsch kimberlite pipe. in Kimberlites, diatremes and diamonds: their geology, petrology and geochemistry. Washington, 1,1-15

Gurney, J.J., Dawson, J.B., Harte, B., Lawless, P.J. (1975) The bulk chemical composition of peridotite facies rocks from Matsoku and Bultfontein pipes. Kimb. Symp. Cambridge, ext. abstr., 3-5

Haendel, D., Muhle, K., Nizsche, H., Stiehl, G. and Wand, U., (1986) Isotopic variations of the fixed nitrogen in metamorphic rocks. Geochim. Cosmochim. Acta, 50: 749-758.

Hannemen, R.E., Strong, H.M. and Bundy, F.R., (1967) Hexagonal diamonds in meteorites. Science, 1155, 995-997.

Harris, J.W. (1987) Recent physical, chemical and isotopic research of diamond. In Mantle Xenoliths (ed. P.H.Nixon), J. Willey & Sons, 471-500

Harris, J.W., Hawthorne, J.B., Osterveld, M.M. (1977) Regional and local variations in diamonds from some southern African kimberlites. Proc. 2nd Kimb. Conf, 27-41

Harte, B., Gurney, J.J., Harris, J.W. (1980) The formation of peridotite suite inclusions in diamonds. Contrib. Mineral. Petrol., 72, 181-190

Hashizume K. and Sugiura N. (1990) Precise measurements of nitrogen isotopic composition using a quadrupole mass spectrometer. Mass Spectroscopy, 38, 269-286

Hatton, C.J., (1978) The geochemistry and origin of xenoliths from Roberts Victor mine. PhD thesis, Univ. Capetown

Hauy R.J., (1882) Traite de mineralogie. Bachelier, Paris

Hoefs, J., and Schidowski, M., (1967) Carbon isotope composition of carbonaceous matter from the Precambrian of Witwatersrand system. Science, 155, 1096-1097

- Honma, H. and Itihara, Y.,** (1981) Distribution of ammonium in minerals of metamorphic and granitic rocks. *Geochim. Cosmochim. Acta*, 45/6, 983-988
- Hough, R.M., Gilmour, I., Pillinger, C.T., Arden, J.W., Gilkes, K.W.R., Yuan, J. and Milledg, H.J.,** (1995) Diamond and silicon in impact melt rock from the Ries impact crater. *Nature*, 378, 41-44.
- Huang, W.L., Wyllie, P.J., Nehru, C.E.,** (1980) Subsolidus and liquidus phase relationships in the system $\text{CaO-SiO}_2\text{-CO}_2$ to 30kb with geological applications. *Amer. Mineral.*, 65, 285-301
- Ilupin, I.P., Vaganov, V.I. and Prokopchuk, B.I.,** (1990) Kimberlites. *Nedra. Moscow*, 30-32 (in Russian)
- Irako M., Oguri T. and Kanomata I.** (1975). The static operation mass spectrometer. *Japan. J. Appl. Phys.* 14, 523-543.
- Ireland, T.R., Rudnick, R.L. and Spetsius, Z.** (1995) Trace elements in diamond inclusions from eclogites reveal link to Archean granites. *Earth Planer Sci. Lett.*, 128, 199-213
- Jacob, D. and Jagoutz, E.,** (1991) A diamond- graphite bearing eclogitic xenolith from Robert Victor (South Africa): indication for petrogenesis from Pb-, Nd-, and Sr-isotopes. *Proceed. of 5th International Kimberlite Conference*, 305-317.
- Jacob, D. Jagoutz, E., Lowry D., Matthey D., Kudrjavitseva G.,** (1994) Diamondiferous eclogites from Siberia: Remnants of Archean oceanic crust.. *Geochim. Cosmochim. Acta*, 58/23, 5191-5207.
- Jagoutz E., Dawson J.B., Hoernes S., Spettel B., Wanke H.,** (1984) Anorthositic oceanic crust in the Archean Earth. *15th Lunar Planet. Sci. Conf.*, 395-396
- Javoy, M. and Pineau, F.,** (1991) The volatiles record of a "popping" rock from the Mid-Atlantic ridge at 14°N; chemical and isotopical cdmposition of gas trapped in the vesicles, *Earth Planet. Sci.Lett.*, 107, 598-611

Javoy, M., Pineau, F. and Delorme, H., (1986) Carbon and nitrogen isotopes in the mantle. In: S.Deutsch and A.W. Hofmann (Editors), *Isotopes on Geology - Picciotto Volum. Chem. Geol.*, 57, 41-62.

Javoy, M., Pineau, F. and Demaiffe D., (1984) Nitrogen and carbon isotopic composition in the diamonds of Mbuji Mayi (Zaire). *Earth. Planet. Sci. Lett.*, 68, 399-412.

Jerde E.A., Taylor L.A., Grozaz G., Sobolev N.V., (1993) Exsolution of garnet within clinopiroxwene of mantle eclogites: Major- and trace-element chemistry. *Contrib. Mineral. Petrol.*, 114, 189-192

Kagi, H., Takahashi, K., Hidaka, H., Masuda, A. (1994) Chemical properties of Central African carbonado and its genetic implications. *Geochim. Cosmochim. Acta*, 58/12, 2629-2638.

Kamenskiy, I.L. and Tolstikhin, I.N. (1992) High $^3\text{He}/^4\text{He}$ in diamonds and constraints on the age of alluvium. *Geochem. Int.* 29, 94-102 .

Kaminsky, F.V. (1987) Genesis of carbonado - polycrystalline aggregate of diamond. *Dokl. Akad. Nauk USSR*, 291, 439-440(in Russian).

Kaminsky, F.V. (1991) Carbonado and Yakutite: properties and possible genesis. 5th Interan. Kimb. Conf., 136-143.

Kaminsky, F.V., Blinova, G.K., Galimov, E.M., Gurkina, G.A., Klyuev, Yu.A., Kodina, L.A., Kortil, V.I., Krivonos, V.F., Frolova, L.N. and Khrenov, A.Ya., (1985) Polycrystalline aggregates of diamond with lonsdaleite from placers of Yakutia. *Mineralogicheski*

Kaminsky, F.V., Galimov, E.M., Ivanovskaya, I.N., Kirikilitsa, S.I. and Polkanov, Yu.A., (1977) Carbon isotope composition of small diamonds from Ukraine. *Dokl. AN SSSR*, 236, 1207-1208 (in Russian).

Kaminsky, F.V., Klyuev, Yu.A., Prokopchuk, B.I., Tshaka, S.A., Smirnov, V.I. and Ivanovskaya, I.N., (1978) First carbonado finding and new balas finding in Soviet Union. Dokl. AN SSSR, 242. 687-689 (in Russian).

Kaminsky, F.V., Kulakova, I.I. and Oglobina, A.I., (1985) About polycyclic aromatic hydrocarbons in carbonado and diamonds. Dokl. AN SSSR, 283, 985-988 (in Russian).

Kaplan I.R. (1975). Stable isotopes as a guide to biogeochemical processes. Proc. R. Soc. Lond., B 189, 183-211.

Keith, M.L., and Weber, J.N., (1964) Isotopic composition and environmental classification of selected limestones and fossil. Geochim. Cosmochim. Acta, 28, 1787-1816

Kerr, P.F., Graf, D.L., Ball, S.H., (1948). Carbonado from Venezuela. Amer. Mineral., 33, 251-255

Kerridge, J.F., (1985) Carbon, hydrogen and nitrogen in carbonaceous chondrites: Abundances and isotopic composition in bulk samples. Geochim. Cosmochim. Acta, 49, 1707-1714

Kesson, S.E. and Ringwood A.E., (1989) Slab-mantle interactions (The formation of diamonds). Chem. Geol., 78, 97-118.

Kinny, P.D., Peter, D., Griffin, B.J., Brendon, J., Brakhfogel, F.F. and Felix, F., (1995) SHRIMP U-Pb ages of perovskite and zircon from Yakutian kimberlites. 6th International Kimberlite Conference, 275-276 (abstr.).

Kinny, P.D., Williams, I.S., Compston, W., and Bristow J.W., (1986) Archean zircon xenocrysts from the Jwaneng kimberlite pipe, Botswana. 4th International Kimberlite Conference, 267-269 (abstr.).

Kirkley, M., Gurney, J. and Rickard, R., (1991) Jwaneng framesites: carbon isotopes and intergrowth compositions. 5th International Kimberlite Conference, 127-135.

Kirkley, M.B., Gurney, J.J., Otter, M.L., Hill, S.L. and Daniels, L.R., (1991) The application of C isotope measurements to the identification of the sources of C in diamonds. *Appl. Geochem.*, 6, 477-494.

Klyuev, Yu.A., Nepsha, V.I., Epishina, N.I., Smirnov, V.I., Plotnikova, S.P., Prokopchuk, B.I. and Kaminsky, F.V., (1978) Structural peculiarities of natural polycrystalline diamonds. *Dokl. AN SSSR*, 240, 1104-1107 (in Russian).

Koval'skiy, V.V., Galimov, E.M. and Prokhorov, V.S., (1972) Carbon isotope composition of coloured Yakutian diamonds. *Dokl. AN USSR*, 203, 2, 440-443 (in Russian)

Krajnyck, G.G. and Bartoshinsky, Z.V., (1971) About electron paramagnetic resonance of diamonds from placers. *Mineralogicheskii sbornik L'vovskogo Universiteta*, 25/1, 70-75 (in Russian).

Kreulen R., and van Beek P.C.J.M., (1983) The calcite-graphite isotope thermometer; data on graphite bearing marbles from Naxos, Greece. *Geochim. Cosmochim. Acta*, 47/8, 1527-1530

Kroto H.W., Heath J.R., O'Brien S.C., Curl R.F., and Smalley R.E., (1985) C-60 - buckminsterfullerene. *Nature*, 318, 162-163

Kurz M.D., Gurney J.J., Jenkins W.J. and Lott III D.E. (1987) Helium isotopic variability within single diamonds from Orapa kimberlite pipe. *Earth Planet. Sci. Lett.*, 86, 57-68

Lal, D., (1989) An important source of ^4He (and ^3He) in diamonds. *Earth Planet. Sci. Lett.*, 96, 1-7

Lal, D., Craig H., Wacker J.F., and Poreda R., (1989) ^3He in diamonds: The cosmogenic component. *Geochim. Cosmochim. Acta* 53, 569-574

- Lal, D.**, (1994) Helium isotopic Information from deiamonds. in Noble Gas Geochemistry and Cosmochemistry, editor Masuda J., Terra Scientific Publishing Company Tokyo, 245-260
- Lee, D.C., Boyd, S.R., Griffin, B.J., and Reddickliffe, T.**, (1991) Coanjula diamonds, northern territory, Austalia. 5th International Kimberlite Conference, 51-68
- Leontyev L.N. and HadenskiiA.A.**, (1957) The nature of kimberlite pipes of Yakutia, Dokl. Akad. Nauk SSSR, 115, 368-371
- Letolle, R.**, (1980) Nitrogen-15 in the natural environment. In P. Fritz and J.Ch.Fontes, Handbook of Envitonmental Isotope Geochemistry, 1A, 407-434. Elsevier, Amsterdam, 545
- Lewis, H.C.**, (1887) On diamondiferous peridotite and the genesis of diamond. Geol. Mag. New Ser., 5, 22-24
- Lewis, H.C.**, (1888) The matrix of the diamond. Geol. Mag. New Ser., 5, 129-131
- Lewis R.S., Anders E., Wright I.P., Norris S.J. and Pillinger C.T.**, (1983). Isotopically anomalous nitrogen in primitive meteorites. Nature 305, 767-771
- Loughnan, F.C., Roberts, F.I., and Lindner, A.W.**, (1983) Buddingtonite (NH⁴-feldspar) in the Condor oilshale deposit, Queensland, Australia. Mineral. Mag., 47, 344, 327-334
- McCandless, T.E., Kirkley, M.B., Robinson, D.N., Gurney, J.J., Griffin W.L., Cousens, D.R., Boyd,F.R.**, (1989) Some initial observations on polycrystalline diamonds mainly from Orapa. Wokshop on Diamonds, 28th Intern. Geol. Congr., 47-51 (ext. abstr.)
- MacGregor, I.D. and Carter, J.L.**, (1970) The chemistry of clinopyroxenes and garnets of eclogite and peridotite xenoliths from the Roberts Victor mine, South Africa. Physics of the Earth and Planetary Interiors, 3, 391-397.
- MacGregor, I.D. and Manton W.D.**, (1986) Roberts Victor eclogites: ancient oceanic crust. J.Geophys.Res., 91, 14063-14079

- Macpherson, C., and Matthey D.P.,** (1994) Carbon isotope variations of CO₂ in Central Lau Basin basalts and ferrobasalts. *Earth Planet.Sci. Lett.*, 121, 263-276
- Manton W.D., and Tatsumoto, M.,** (1971) Some Pb and Sr isotopic measurements on eclogites from Roberts Victor mine, South Africa. *Earth Planet.Sci. Lett.*, 10, 217-226.
- Mariotti A.** (1984). Natural ¹⁵N abundance measurements and atmospheric nitrogen standard calibration. *Nature* 311, 251 -252.
- Marty B.** (1995) Nitrogen content of the mantle inferred from N₂-Ar correlation in oceanic basalts. *Nature*, 377, 326-329
- Marty, B., Zimmermann, L. and Humbert, F.,** (1996) Nitrogen isotopic composition of the silicate Earth and its bearing on the Earth-Atmosphere evolution. XXVII Lunar and Planetary Science Conference, 819-820.
- Masaitis V.L.** (1992) Impact craters - are they useful. *Meteoritics* 27, 21-27
- Masaitis, V.L., Futergendler, S.I. and Gnevushev, M.A.** (1972) Diamonds in the impactites of Popigai crater. *Zapiski Vsesoyuznogo Mineralogicheskogo Obshestva*, 1: 108-112 (in Russian).
- Masaitis, V.L., Gnevushev, M.A. and Shafranovsky, G.I.,** (1979) Mineral assemblages and mineralogical criteria of astrablems. *Zap. Vses. Mineral. obshestva*, 3, 257-273 (in Russian).
- Masaitis, V.L., Shafranovsky, G.I., Yezersky, V.A. and Reshetnyak, N.B.,** (1990) Impact diamonds in urelites and impactites. *Meteoritica*, 8: 180-195. (in Russian).
- Mathez, E.A., Fogel, R.A., Hutcheon, I.D., Marshintsev, V.K.,** (1995) Carbon isotopic composition and origin of SiC from kimberlites of Yakutia, Russia. *Geochim. Cosmochim. Acta*, 59/4, 781-792.

Matsuda J., Fukunaga K., and Ito K., (1991) Noble gas studies in vapor-growth diamonds: Comparison with shock-produced diamonds and the origin of diamonds in urallites *Geochim. Cosmochim. Acta*, 55, 2011-2023

Matsuda J., and Nagao K., (1989) Noble gas emplacement in shock-produced diamonds. *Geochim. Cosmochim. Acta*, 53, 1117-1121

Matsuda, J.I., Kazuya, F. and Keisuke, I., (1991) Noble gas studies in vapour-growth diamonds: Comparison with shock-produced diamonds and the origin of diamonds in ureilites. *Geochim. Cosmochim. Acta*, 55, 2011-2023.

Matsuda, J.I., Kusumi, A., Yajima, H. and Syono, Y., (1995) Noble gas studies in diamonds synthesised by shock loading in the laboratory and their implications on the origin of diamonds in ureilites. *Geochim. Cosmochim. Acta*, 59, 23, 4939-4949.

Mattey, D.P., Carr R.C., Wright, I.P., Pillinger, C.T., (1984) Carbon isotopes in submarine basalts. *Earth Planet.Sci. Lett.*, 70, 196-206

Mattey, D.P., (1987) Carbon isotopes in the mantle. *Terra Cognita*, 7, 31-37

McCandless T.E., Kirkley M.B., Robinson D.N., Gurnay J.J., Griffin W.L., Cousens D.R., Boyd F.R., (1989) Some initial observations on polycrystalline diamonds mainly from Orapa. Ext. abstr., Workshop on Diam., 28th Intern. Geol. Congr. Washington, 47-51

McConville P., and Reynolds J.H., (1989) Cosmogenic helium and volatile rich fluid in Sierra Leone alluvial diamonds. *Geochim. Cosmochim. Acta* 53, 2365-2375

McConville P., Reynolds J.H., Epstein S., and Roedder E. (1991) Implanted ^3He , ^4He and Xe in further studies of diamonds from Western Australia. *Geochim. Cosmochim. Acta* 55, 1977-1989

McCulloch M.T., Gregory R.T., Wasserburg G.J., Taylor H.P., (1981) Sm-Nd and $^{18}\text{O}/^{16}\text{O}$ isotopic systematics in an oceanic crustal section: evidence from the Samail ophiolite. *J. Geophys. Res.*, 86, 2721-2735

McCulloch, M.T., (1995) Sm-Nd systematics in eclogite and garnet peridotite nodules from kimberlites: Implications for the early differentiation of the Earth.. In: Kimberlites and Related Rocks (ed. J.Ross et al.); Geol.Soc.Austr. Spec.Publ., 14/2, 864-876.

McKirdy, D.M., and Powell, T.G., (1974) Metamorphic Alteration of Carbon Isotopic Composition in Ancient Sedimentary Organic Matter: New Evidence from Australia and South Africa. *Geology* (Boulder). 2/12, 591-595

Mendelssohn M.J., Milledge H.J., Vance E.R., Nave E., Woods P.A. (1978) Internal radioactive haloes in diamonds. in *Diamond research*: London, Industrial diamond information Bureau, p.31-36

Meyer, H.O.A. (1968) Mineral inclusions in diamond. *Car. Inst. Wash. Year Book* 66,446-450

Meyer, H.O.A. (1968) Chrome pyrope: an inclusion in natural diamond. *Science*, 160, 1446-1447

Meyer, H.O., Milledge, H.J., Sutherland F.L., (1995) Unusual diamonds and unique inclusions from New South Wales, Australia. 6th International Kimberlite Conference: 397-381 (abstr).

Milledge, H.J., Mendelssohn, M.J., Seal, M., Rous, J.E., Swart, P.K., and Pillinger, C.T., (1983) Carbon isotopic variations in spectral type II diamonds. *Nature*, 303, 791-792

Mitchell R.H. (1986) Kimberlites: mineralogy, geochemistry, and petrology. New York and London, Plenum Press, 442

Mitchell R.H. (1979) The alleged kimberlite-carbonatite relationship: Additional contrary mineralogical evidence. *Am. J. Sci.*, 279, 570-589

Mitchell R.H. and Crochet J.H., (1971) Diamond genesis — a synthesis of opposing views. *Mineral. Deposita*, 6, 392-403

Mitchell R.H., (1970) Kimberlite and related rocks— A critical re-appraisal. *J. Geol.*, 78, 686-704

- Nadeau, S., Pineau, F., Javoy, M. and Francis, D.,** (1990) Carbon concentrations and isotopic ratios in fluid inclusion-bearing upper mantle xenoliths along the northwestern margin of North America, *Chem. Geol.*, 81, 271-297.
- Nier A.O.** (1947). A mass spectrometer for isotope and gas analysis. *Rev. Sci. Instrum.* 18, 398-411
- Nixon, P.H.** (Editor), (1987) *Mantle Xenoliths* J. Wiley & Sons, 844
- Novikov, N.V., Maistrenko, A.L., Trefilov, V.I., Kovtun, V.** (1993) Structure and Properties of shock-wave sintered diamond composites. *Indus. Dia. Rev.*, 278-281
- O'Hara M.J., Saunders M., Mercy E.L.P.** (1975) Garnet peridotite, possible ultrabasic magmas and eclogite: interpretation of upper mantle process in kimberlite. *Phys. Chem. Earth.*, 9, 681-713
- Orlov Yu.L.,** (1973) The mineralogy of diamond. Nauka. Moscow (in Russian)
- Orlov Yu.L., Kaminsky F.V.** (1981) A new (IX) variety of polycrystalline diamond aggregates - "carbonado with lonsdalite" *Dokl. AN USSR*, 259, 459-461
- Ozima M, Zashu S Mathey D.P., Pillinger C.T.** (1985) Helium, argon and carbon isotopic compositions in diamonds and their implications in mantle evolution. *Geochim. J.* 19, 127-134
- Ozima M., and Zashu S.,** (1983) Primitive He in diamonds. *Science* 219, 1067-1068
- Ozima M., Zashu S., and Nitoh O.,** (1983) $^3\text{He}/^4\text{He}$ ratio, noble gas abundance and K-Ar dating of diamonds — An attempt to search for the records of early terrestrial history. *Geochim. Cosmochim. Acta* 47, 2217-2224
- Ozima, M.,** (1989) Gases in diamonds. *Ann Rev. Earth Planet. Sci.*, 17: 361-384.
- Ozima, M., Zashu, S., Tomura, K., Matsuhisa, Y.,** (1991) Constraints from noble-gas contents on the origin of carbonado diamonds. *Nature*. 351, 472-474.

Ozima, M., Zashu, S. and Niton, O., (1983) $^3\text{He}/^4\text{He}$ ratio, Noble gas abundance and K-Ar dating of diamonds - an attempt to search for the records of Early Earth's history. *Geochim. Cosmochim. Acta*, 47: 2217-2224.

Pang, P.C., and Nriagu, J.O., (1976). Distribution and isotope composition of nitrogen in Bay of Quinte (Lake Ontario) sediments. *Chem. Geol.*, 18, 93-105.

Pearson, D.G., Snyder, G.A., Shirey S.B., Taylor, L.A., Carlson, R.W., Sobolev, N.V. (1995) Re-Os isotope evidence for a mid-Archaean age of diamondiferous eclogite xenoliths from Siberia and constraints on Archaean tectonics. *Nature*, 374, 711-713.

Pidgeon R.T., Smith C.B., and Fanning C.M. (1989) Kimberlite and lamproite emplacement ages in Western Australia. *Proc. 4nd Kimb. Conf, Perth*, (eds. J.Ross et al.); *Geol.Soc. Australia, Spec. Publ. 14*, Vol 1,369-381 (1989)

Pillinger, C.T., (1984). Light element stable isotopes in meteorites—from grams to picograms. *Geochim. Cosmochim. Acta*, 48: 2739-2766.

Pillinger, C.T., (1992). New technologies for small sample stable isotope measurement: static vacuum gas source mass spectrometrys laser probes, ion probes and gas chromatography-isotope ratio mass spectrometry. *Int. J. Mass Spectrom. IOM processes*, 118, 477-501.

Pillinger C.T., (1993) Elemental carbon as interstellar dust. *Phil. Trans. of Roy. Soc.*, A343, 1667, 73-86

Polkanov, Y.A., Yeryomenko, G.K. and Sokhor, M.I., (1973) Impact diamonds in fine-grained placers in Ukraine. *Dopovidi AN URSR*, B11, 989-990 (in Ukrainian).

Polkanov, Yu.A., Khrenov, A.Ya. and Yeryomenko, G.K., (1978) Photoluminescence of carbonado from placers in Ukraine. *Dopovidi AN URSR*, B3: 216-220 (in Ukrainian).

- Raber, E.,** (1978) Zircons from diamond bearing kimberlites: Oxide reactions, fission track dating and mineral inclusion study. M.Sc. thesis, Univ. Massachusetts.
- Reynolds J.H.,** (1956). High sensitivity mass spectrometer for noble gas analysis. Rev. Sci. Instrum. 27, 928-934.
- Richardson S.H., Erlank A.J., Harris J.W., Hart S.R.,** (1990) Eclogitic diamonds of Proterozoic age from Cretaceous kimberlite. Nature, 246, 54-56
- Richardson, S.H., Harris, J.W. and Gurney, J.J.,** (1993) Three generations of diamonds from old continental mantle. Nature, 366, 256-258.
- Ringwood, A.E.,** (1975) Composition and Petrology of the Earth's Mantle. McGraw Hill, New York, 618.
- Robertson, R., Fox, J.J., and Martin, A.E.,** (1934) Two types of diamonds. Phil. Trans. Roy. Soc., A232, 463.
- Roskamp G. and Schultz L.,** (1985) Noble-gases in archean metasediments from Isua (Greenland) and the Pongola supergroup (South-Africa) Chem. Geol. 52, 111-117.
- Roth W.A., Neaser G., and Dopke O.,** (1926) Uber das spezifische Gewicht von Carbonado und von Glanzkohle. Chem. Ber. 59, 1397
- Rumyantsev G.S., Nadezhdina E.D., Malinovsky Yu.A.,** (1980) On lonsdalite-bearing polycrystalline diamonds. In Yu.L. Orlov and F.V. Kaminsky, Eds., Complexe investigation of diamond (Moscow), 3-19
- Russell, S.S.,** (1992). A carbon and nitrogen isotope study of chondritic diamond and silicon carbide. Unpublished PhD thesis, Open University.
- Saino, T., and Hattori, A.,** (1980) ^{15}N natural abundance in oceanic suspended particulate matter. Nature, 283: 752-754
- Sakai, H., Des Marias, D.J., Ueda, a. and Moore, G.J.,** (1984) Concentrations and ratios of carbon, nitrogen and sulfur in ocean-floor basalts, Geochim. Cosmchim. Acta, 48: 2433-2441.

Sellschop, J.P.F., (1979) Nuclear properties in physical and geochemical studies of natural diamonds. in *The properties of diamond.* (edit. Field J.E.), Academia Press, 107-164

Shelkov, D., Milledge, H.J., Verchovsky, A.B., Hutchison, R., Collinson, D.W., Pillinger, C.T., (1994) Do the Ubangi diamonds originated from a giant impact? *Meteoritics.*, 29, 532

Shelkov, D., Verchovsky, A.B., Pillinger, C.T., Hutchison, R., Milledge, H.J., (1995a) Carbonado: more clues to a common impact origin for samples from Brazil and The Central African Republic. *Lunar and Planetary Science XXVI*, 1281-1282.

Shelkov, D., Verchovsky, A.B., Milledge, H.J., Pillinger C.T., (1995b). Carbonado: a comparison between Brazilian and Ubangui sources based on carbon and nitrogen isotopes. 6th Int. Kimb. Conf., 518-520 (Ext. abstr.).

Shelkov. D., Verchovsky, A.B., Milledge, H.J. and Pillinger, C.T., (1998) Carbonado: a comparison between Brazilian and Ubangui sources with other forms of micro-crystalline diamond based on carbon nitrogen isotopes. *Proceedings of 6th Kimberlite Conferenc* (in press)

Shelkov, D.A., Milledge, H.J, Verchovsky A.B., Kaminsky, F.V., Pillinger, C.T., (1996). Preliminary C, N, He and Ar study of shock produced diamonds from the Popigai crater and Ebeliakh placer, Siberia. *Lunar and Planet., Sci., XXVII*, 1187-1188.

Shelkov, D.A., Verchovsky A.B., Milledge, H.J, Pillinger, C.T., (1998) The radial distribution of implanted and trapped ^4He in single diamond crystals and implications for the origin of carbonado. *Chem.Geol.*, (submitted)

Shibata, K., Kamioka, H., Kaminsky, F.V., Koptil, V.I., Svisero D.P., (1993) Rare earth element patterns of carbonado and yakutite: evidence for their crustal origin. *Mineral. Magazine*, 57, 607-611

- Shukolyukov Yu.A., Pleshakov A.M., Lavrova L.D.,** (1993) The unprecedentedly high $^3\text{He}/^4\text{He}$ ratio in diamonds from metamorphic rocks of Kokchetav Massif, Kazakhstan. *Petrology* 1, 95-102,
- Skinner E.M.W., and Clement C.R.,** (1979) Mineralogical classification of Southern African kimberlites. 2d Intern. Kimb. Conf., 1, 129-139
- Smirnov, G.I., Mofolo, M.M., Lerotholi, P., Kaminsky, F.V., Galimov, E.M. and Ivanovskaya, I.N.,** (1979) Isotopically light carbon from some kimberlite pipes in Lesotho. *Nature*, 366: 256-258.
- Smith, C.B.,** (1983) Pb, Sr and Nd isotopic evidence for sources of southern African Cretaceous kimberlites. *Nature*, 304, 51-55
- Smith, V.J., Dawson, J.B.,** (1985) Carbonado: Diamond aggregates from early impacts of crustal rocks? *Geology*, 13, 342-343.
- Smulikowski K.,** (1972) Classification of eclogites and allied rocks. *Kristallinikum*, 9, 107-130
- Sobolev N.V., Botkunov A.I., Kuznetsov I.K.,** (1969). Diamondiferous eclogite containing high-Ca garnet from Mir pipe, Yakutia. *Geology and Geophysics*, 4, 27-36
- Sobolev N.V.,** (1978) Mantle inclusions in kimberlites and problem of composition of the upper mantle. Novosibirsk, Science, Siberian division, 41-42
- Sobolev N.V., Har'kiv A.D., Pokhilenko N.P.,** (1986) Kimberlites, lamproaites and the problem of the upper mantle composition. *Geology and Geophysics*, 7, 18-28
- Sobolev, V.N., Taylor L.A., Snyder G.A.,** (1994) Diamondiferous eclogites from the Udachnaya Kimberlite Pipe, Yakutia. *International Geology Review*, 36, 12-64
- Sobolev, N.V., Galimov, E.M., Ivanovskaya, I.N. and Yefimova, E.S.,** (1979) Carbon isotope composition of diamonds containing crystalline inclusions. *Dokl. AN USSR*, 249, 1217-1220. (in Russian).

- Sobolev, N.V., Galimov, E.M., Smith, C.B., Yefimova, E.C., Maltsev, K.A., Hall, A.E. and Usova, L.V., (1989)** A comparative study of the morphology, inclusions and carbon isotopic composition of diamonds from alluvials of the King George River and Argyle lamproite mine (Western Australia), and of cube microdiamonds from northern Australia. *Soviet Geology and Geophysics*, 30/12, 1-49
- Sobolev, N.V., (1974)** Mantle nodules in kimberlites and the problem of composition of the upper mantle. Novosibirsk, Nauka, Sib. otd., 264
- Spray J.G Kelley, S.P., Reimold, W.U., (1995)** Laser probe ^{40}Ar - ^{39}Ar dating of coesite-bearing and stishovite-bearing pseudotachylytes and the age of the Vredefort impact event *Meteoritics*, 30/3, 335-343
- Stiehl, G., and Lehmann, M., (1980)** Isotopen-variationen des Stickstoffes humoser und bituminöser natürlicher organischer Substanzen. *Geochim. Cosmochim. Acta*, 44: 2737-1746
- Sturzer, O. (1931)** Die wichtigsten Lagerstätten der "Nicht-Erze" I Teil: Graphit, Diamant, Schwefel, Phosphat. 474 S. Berlin
- Sweeney, R.E., Liu, K.k., and Kaplan, I.R., (1978)** Oceanic nitrogen isotopes and their uses in determining the source of sedimentary nitrogen. In B.W. Robinson, ed., *Stable isotopes in earth science*, Dep. Sci. Ind. Res., New Zealand, Bull., 220, 9.
- Takaoka, N., and Ozima, M., (1978)** Rare gas isotopic composition in diamonds. *Nature*, 271, 45-46
- Taylor W.R., Canil, D., and Milledge, H.J., (1995)** Experimental determination of the kinetics of IbIaA nitrogen aggregation with application to natural Ib-IaA diamonds: 6th International Kimberlite Conference, extended abstr., 611-613.
- Taylor, W.R. and Milledge, H.J., (1995)** Nitrogen aggregation character, thermal history and stable isotope composition of some xenolith-derived diamond from Roberts Victor and Finsch: 6th International Kimberlite Conference, extended abstr., 620-622.

The kimberlites of USSR In:Wyllie P.J. Ultramaphic and related rocks. Wiley, NewYork, 251-256

Thompson R.N., (1974) Some high-pressure pyroxenes. *Min. Mag* 39, 768-787

Trofimov V.S., (1971) On the origin of diamandiferous diatremes. *Bull. Vulcanol.*, 24, 767-776

Trueb, L.F., and Buttermann, W.C., (1969) Carbonado: a microstructural study. *Amer. Mineral.*, 54, 412-425.

Trueb, L.F., de Wys, E.C., (1971) Carbon from Ubangi- a microstructural study. *Amer. Mineral.*, 56, 1252-1256.

Trueb, L.F., de Wys, E.C., (1969) Carbonado: natural polycrystalline diamond *Science*, 165, 799-802.

Trull, T., Nedeau, S., Pineau, F., Polve, M., Javoy, M., (1993) C-He systematics in hotspot xenoliths: Implications for mantle carbon contents and carbon recycling. *Earth and Planet.Sci. Lett.*, 118, 43-64.

Tsai H.M., Meyer H.O.A., Morean J., Milledge H.J., (1979) Mineral inclusions in diamonds: Premier, Jagersfontein and Finsch kimberlites, South Africa, and Williamson Mine, Tanzania. in *Kimberlites, diatremes and diamonds: their geology, petrology and geochemistry*. Washington, 1, 16-26

Vaganov V.I., Sokolov S.B., (1988) Thermometry of ultrabasic parageneses. Moscow, Nedra, 150

Valter, A.A., Kvasnitsa, V.N. and Eremenko, G.K., (1990) *Mineralogicheskii Journal*, 12/3, 3-116.

van Heerden, L.A., (1994) A nitrogen and carbon stable isotope study of some Western Australian diamonds. Ph.D. Thesis, The Open University, Milton Keynes.

van Heerden, L.A., Gurney, J.J., and Deines, P., (1995) The carbon isotopic composition of harzburgitic, lherzolitic, websteritic and eclogitic paragenesis diamonds from southern Africa: a comparison of genetic models. *S.Afr.J.Geol.*, 98/2, 119-125

Vance, E.R., and Milledge, H.J., (1972) Natural and laboratory α -particle irradiation in diamonds. *Mineralogical Magazine* 38, 878-881

Vance, E.R., Harris, J.W., and Milledge, H.J., (1973) Possible origins of α -damage in diamonds from kimberlite and alluvial sources. *Mineralogical Magazine* 39, 349-360

Verchovsky A.B., Ott, F., Begemann U., (1993) Implanted radiogenic and other noble gases in crustal diamonds from northern Kazakhstan. *Earth Planet. Sci. Lett.* 120, 87-102

Verchovsky, A.B., Valter, A.A. and Shukolyukov Yu.A., (1991) Noble gases in shock-produced diamond from Popigai meteorite crater. *Europ. Geophys. Union*

Veshnevsky, S. A., Afanas'ev, V.P., Koptil', V.I., (1995) Impact diamonds : their features, origin and significance. 6th Kimberlite Conference, Novosibirsk (abstr.) 657-659.

Viljoen, K.S., Robinson, D.N., Swash, P.M., Griffin W.L., Otter, M.L., Ryan, C.G. and Win, T.T., (1991). Diamond- and graphite- bearing peridotite xenoliths from the Roberts Victor kimberlite, South Africa. 5th International Kimberlite Conference, 285-303

Vinogradov, A.P., Kropotova, O.I., Orlov, Y.L. and Grinenko, V.A., (1966) Isotope composition of diamond crystals and carbonado. *Geokhimiya*, 12, 1395-1397 (in Russian).

Vladimirov, B.M., Zubarev, B.M, Kaminsky, F.V., Minorin, V.E., Odintsov, M.M., Orlov Y.L., Prokopchuk, B.I., Sobolev, E.V., Sobolev, N.V., Har'kiv, A.D., Cherniy, E.D., (1989) Geology and genesis of diamond deposits, Zubarev B.M.(editor), TsNIGRI, Moscow

- Vogel, J.C., Grootes, P.M. and Mook, W.G.,** (1970). Isotopic fractionation between gaseous and dissolved carbon dioxide, *Z.Phys.*, 230, 225-238.
- Wada, E., Kadonaga, T. and Matsuo, S.,** (1975). ^{15}N abundance in nitrogen of naturally occurring substance and global assessment of denitrification from isotopic viewpoint. *Geochem. J.*, 9, 139-148.
- Wagner, P.A.,** (1914) The diamond fields of Southern Africa. Transvaal Leader, Johannesburg
- Wand, E., Nitsche, H.M., Muhle, K. and Wetzel, K.,** (1980) Nitrogen isotope composition in natural diamond - first results. *Chem. Erde*, 39, 85-87.
- Wendt, I.,** (1968). Fractionation of carbon isotopes and its temperature dependence in the system $\text{CO}_2\text{-gas-CO}_2$ in solution and $\text{HCO}_3\text{-CO}_2$ in solution, *Earth Planet, Sci. Letters*, 4, 64-68.
- Westman B.J.,** (1982) Was Cullinan the largest diamond? *Californ. Min. J.*, 52, 64-68
- Wickman, H.,** (1956) The cycle of carbon and the stable carbon isotopes. *Geochim. Cosmochim. Acta*, 9, 136-153
- Wiens R.C, Lal D., and Craig H.,** (1990) Helium and carbon isotopes in Indian diamonds. *Geochim. Cosmochim. Acta* 54, 2587-2591
- Wiens R.C., Lal D., Rison W., Wacker J.F.,** (1994) Helium isotopic diffusion in natural diamonds. *Geochim. Cosmochim. Acta* 58, 1747-1757
- Wlotzka, F.,** (1972). Geochemistry of nitrogen. In Wedepohl, K.H., ed., *Handbook of Geochemistry*, Sections 7-B to 7-O, Springer-Verlag, Berlin and Heidelberg.
- Woods, G.S.,** (1994) Interconversion between the various forms of nitrogen in diamond. in *Properties and growth of diamond*. (G. Davies editor), 98-100
- Woods, G.S.,** (1994) The B aggregate of nitrogen in diamond. in *Properties and growth of diamond*. (G. Davies editor), 90-91

Woods, G.S., (1994) The "type" terminology of diamond. in Properties and growth of diamond. (G. Davies editor), 83

Wright I.P. (1984). $\delta^{13}\text{C}$ measurements of smaller samples. Trends Anal. Chem. 3, 210-215.

Wright, I.P., Boyd S.R., Franchi I.A., and Pillinger C.T., (1988) High precision determination of nitrogen stable isotope ratios at the sub-nanomole level. J.Phys.E: Sci. Instrum., 21, 865-875.

Wright, I.P., McNaughton, N.J., Fallick, A.E., Gardiner, L.R. and Pillinger, C.T., (1983). A high sensitivity high precision stable carbon isotope mass spectrometer. J. Phys. E: Sci. Instrum. 16, 497-504.

Wright, I.P. and Pillinger, C.T., (1989) Carbon isotopic analysis of small samples by use of stepped - heating extraction and static mass spectrometry. in New Frontiers in stable isotopic research: laser probes, ion probes and, small-sample analysis (W.C. Shanks III and R.E. Criss editors), 9-34

Zashu S. and Hiyagon H., (1995) Degassing mechanisms of noble gases from carbonado diamonds. Geochim. Cosmochim. Acta 59, 1321-1328

Zhang Y., and Zindler A., (1993) Distribution and evolution of carbon and nitrogen in Earth. Earth and Planet.Sci. Lett., 117: 331-345.

Zindler, A. and Hart, S., (1986) Ghemical geodynamics. Ann. Rev. Earth Planet. Sci., 14, 493-571.